KTeV Beam Systems
Design Report

Version 1.1
June 1994

KTeV Beam Systems Design Report

June 1994

R.Coleman,   V.Bocean,   S.Childress,   R.Ford,   W.Freeman,
G.Gutierrez, D.Jensen, T.Kobilarcik, A.Malensek, D.Pushka,
T.Sager,   W.Slater,   R.Tokarek,   J.Wrbanek

June 2, 1994

DRAFT

KTeV Beam Systems Design Report

KTeV Beams Group
Version 1.1 June 1994

Abstract

The primary and secondary beams for the KTeV experiments
E799-II and E832 are discussed. The specifications are presented
and justified. The technical details of the implementation of the
primary beam transport and stability are detailed. The target,
beam dump, and radiation safety issues are discussed. The
details of the collimation system for the pair of secondary beams
are presented.

INTRODUCTION

In this document, we present a discussion of the beams for the KTeV
experiments: E799-II and E832 [1,2]. The primary and secondary beam specifications
are closely related and are therefore discussed together.

Experiment E799-II is a study of rare K_L decays where the decays take place in
approximately 60 meters of vacuum decay pipe. Experiment E832 is a measurement
of ε'/ε in the neutral K system. A thick regenerator, located in the vacuum decay
region, will be moved spill-by-spill between the two neutral beams to produce K_S's.
The kaon decay products are detected, identified and measured using the charged
particle detection system and the CsI calorimeter that comprise the detector system.

---

[1] Fermi Lab Proposal E799.
[2] Fermi Lab Proposal E832.

A general feature of the beam system is a primary proton beam impinging on one interaction length of BeO to produce a pair of "identical" neutral beams side by side. The beams are rendered neutral by a set of sweeping magnets and collimators. A system of magnetic sweeping and shielding is designed to reduce the muon flux from both the target and beam dump sources. There is careful monitoring of the size, direction and intensity of the primary beam. The unspent primary must be dumped in such a manner as to not create excessive backgrounds. The secondary beam has five collimators: two of these are fixed-hole collimators (referred to as primary and defining collimators in this report); one is a slab collimator designed to prevent particles from scattering out of one beam (in the plan view) into the adjacent beam and hitting the calorimeter; and two are variable jaw collimators used to reduce the flux on the defining collimator if needed. The neutral beam must pass cleanly through the holes in the CsI.

The report is divided into 11 sections listed below:

1. Overview of KTeV beam specifications
2. Primary beam
3. Critical devices/interlocks
4. Beam dump/muon sweeping
5. Secondary beam
6. Radiation safety
7. Site and utility requirements
8. Installation
9. Alignment and long term stability
10. Budget and schedule
11. Unresolved issues/Continuing efforts

Where appropriate, other documents are cited and the results noted are only very briefly summarized in this document.

1. OVERVIEW OF KTeV BEAM SPECIFICATIONS

1.1 Intensity Parameters

A primary beam intensity of 5×10^{12} (3.5×10^{12}) protons per Tevatron cycle yields acceptable rates consistent with the proposal.[3,4] The K_L fluxes are calculated using the Malensek parameterization[5] which agrees well with measured K_L decay rates measured in E731.[6] These fluxes are discussed in more detail in the secondary beam section.

1.2 Stability Requirements

It is necessary, for experiment E832, that the sizes and positions of the two neutral beams be stable to 0.5 mm, that the areas be equal (to 1%), and that the kaon momentum spectra be equal (to 0.1%).[7] These conditions must be maintained during each spill and for the duration of the experiment, and also imply certain stability requirements on the primary beam, target, and collimators. Experience, particularly during E731, demonstrates that it is an important issue. The requirements on the primary beam are:

beam size on targets	< 0.25 mm in x and y
beam size stability	10%
beam positional stability	± 0.1 mm
angular stability	± 25 μrad

These requirements and how they were derived are discussed in section 5.3.

---

[3] Fermi Lab Proposal E799.

[4] Fermi Lab Proposal E832.

[5] A. J. Malensek, Fermi Lab FN-341.

[6] J.R. Patterson, "Determination of Re ε'/ε by the Simultaneous Detection of the Four $K_{L,S} \rightarrow \pi\pi$ Decay Modes", Dec. 1990, U. Chicago dissertation.

[7] D. Jensen, "On the Sensitivity of ε'/ε to Primary Beam Parameters", Feb.2, 1994, KTeV memo.

1.3 Backgrounds

1.3.1 Charged particles and photons

The magnetic sweeping of charged particles from the primary target must be sufficient to remove any noticeable effect from these charged particles relative to the number of charged particles from decays. In addition, copiously produced photons from the target must be removed by placing a lead filter in the beam.

1.3.2 Neutral kaon and lambda decays

Our goal is to keep background rates from the neutral beam comparable to the detector rate and trigger rate from neutral kaon decays. For example, the rate of single muons from $K_{\mu 3}$ decays occur at the rate of 40 (200) kHz for E832 (E799-II) at the CsI. The rate from lambda decays is about 10% of the rate of kaon decays in the detector.

1.3.3 Neutral beam (kaons, neutrons and a few lambda's)

a) Interactions with material in the beam path
Filters to reduce the photon and neutron products in the beam introduce a source of elastic and inelastic interactions.
In E832 the regenerator (100 cm of scintillator) is a significant source of background as well as trigger hodoscope (2 cm of scintillator) for both experiments.

b) Interactions with collimator/magnet apertures

Additional neutral beam background arises from the interaction of target spray and decay products which strike the inner walls of the neutral channel. In addition the filters introduce additional scattering of the beam which again strikes

the neutral channel walls or could leave the "beam hole" and strike the electromagnetic detector.

In previous experiments, radiation damage to the electromagnetic calorimeter near the neutral beam holes was a significant problem. A discussion of radiation damage and backgrounds are summarized in section 5.8. While KTeV is running at higher proton intensity (approximately three times higher), CsI is less sensitive to radiation damage than the previous Pb glass calorimeter.

1.4   Muon Rejection

The goal is to reduce the muon halo rate in the spectrometer from primary target and beam dump sources to 100 kHz at 5×10^{12} incident protons per spill. This is comparable to the projected inherent muon rate from $K_{\mu 3}$ decays of 40 (200) kHz for E832(E799II) at the CsI, of which about 1/4 remain in the beam channel. The radiation dosage at the experimental counting room should also be well within specified personnel safety levels, as should outdoor area muon rates.

1.5   KTeV Beam and Spectrometer System

The general description of the beam and spectrometer systems for KTeV is presented in this section. The KTeV primary beam follows the same initial trajectory to Enclosure NM1 as the previous NMUON beam line, and uses existing enclosures for primary beam transport and targeting. A pair of neutral beams, as defined by appropriate collimation, emerge into a large evacuated decay volume. This region is surrounded by an annular photon veto system. Decay products exit through a thin vacuum window to a detection apparatus consisting of a calorimeter, tracking and magnetic spectrometer, veto counters and particle identification systems. More detailed discussions of each system are presented below.

1.5.1   Beam elements

A plan view layout of the beam system is given in Figure 1.5.1. Shown in this figure are the relative location of components and their respective sizes. The KTeV primary beam follows the transport from the Tevatron along the current

Switchyard muon beam line. Existing dipoles in the upstream NM1 enclosure are utilized to raise the entrance beam height into enclosure NM2. The upstream section of the existing NM2 enclosure is utilized for the pretarget beam elements. These elements include a pair of B2 dipoles for establishing the final beam trajectory, final focus quadrupoles, AVB dipole string for control of the beam targeting angle, and instrumentation for beam position and intensity measurement.

The primary target, beam dump, muon sweeping magnets, initial neutral secondary beam collimation, and beam filters are positioned in the existing NM2 target hall.

Subsequent secondary beam elements are located in the downstream section of the existing NM2 enclosure, and in a new upstream extension to the existing NM3 enclosure. The function of these elements is to provide definition of the two horizontally separated kaon beams and to provide cleanup of charged and neutral particle backgrounds. It is important to note that since the beam can no longer be steered with magnets that the only control over the size, direction, and symmetry of the two beams is by collimation. This is the main reason alignment and stability play such an important role in the experiment. Beam transport between enclosures NM2 and NM3 is through a buried beam pipe as shown in the figure. Also shown is an offset alignment sight pipe which is used for referencing precision collimation elements between the two enclosures.

KTeV Beamline Layout
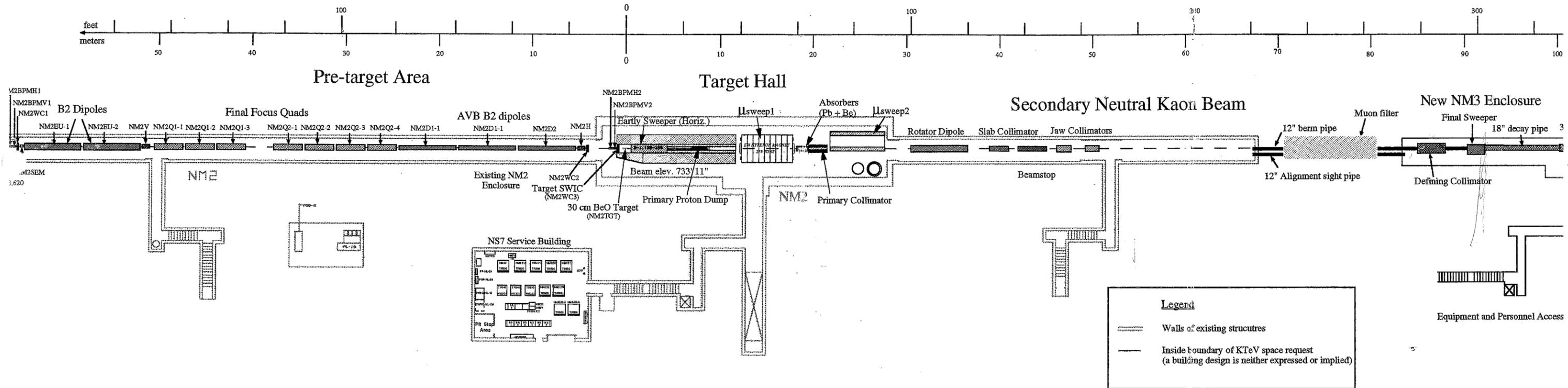
FIGURE 1.5.1.

1.5.2 The Spectrometer

A kaon decay region begins downstream of the final secondary beam collimation element and final sweeping magnet. The decay region opens into successively larger diameter pipes. For the rare decay experiment E799, the decay region begins at the 20 inch diameter pipe in the new NM3 extension, immediately downstream of the defining collimator and final sweeper magnet. This region provides a vacuum channel for particle decays and the neutral beam transport to the decay building and experimental hall. For E832, the decay region begins after a mask anti and active regenerator, elements which are removed for the E799 experiment. To house these components and the downstream decay region with instrumented veto ring counters, a new decay enclosure is required. This decay enclosure is located between NM3 and the new KTeV experimental hall.

The regenerator sits in vacuum and is moved to alternate beam positions between each beam spill. Its function is to provide a K_S beam from the incident K_L beams. This device is followed by a series of large vacuum vessels ranging in diameter from 200 cm to 240 cm. The vessels are connected together between successive ring veto counters to form a continuous vacuum region. The ring veto counters, labeled RC6-RC10, are designed to catch wide angle photons from background $3\pi^0$ decays and to eliminate other background events for rare decay modes. A 1.8 meter diameter thin window of Kevlar and aluminized Mylar terminates the vacuum volume.

The detector consists of drift chambers, veto counters, analysis magnet, transition radiation detectors, electromagnetic calorimeter, triggering hodoscope, and muon detection system. The four sets of drift chambers (labeled DC1-DC4), were used in the last experiment and are now being refurbished for KTeV. These chambers have resolutions of less than 100 microns. Each chamber has two horizontal planes (x and x') and two vertical planes (y and y'). These existing chambers will be used with fast chamber gas and new pre-amplifiers. The most upstream drift chamber, DC1, is placed at the end of the vacuum decay region. The other three chambers are supported by the spectrometer anti stands. Bags of helium gas are placed along the beam line downstream of the vacuum region to reduce the scattering of secondary particles in the spectrometer. The four sets of drift chambers

and the analyzing magnet will be used to measure the momenta and the decay vertex of the charged particles from kaon decays.

The "Spectrometer Anti" (SA) veto counters are lead and scintillator sandwich modules, rectangular in shape, which are used to detect and veto all particles within their active areas. There are four of these counters, including three (SA2-SA4) associated with a concordant numbered drift chamber and one (CIA) located near the CsI calorimeter. Each of these pairs will have a rigid aluminum and steel stand, supporting both a drift chamber and a veto module. They are located approximately equally spaced (relative to the magnet) after the decay region and before the calorimeter.

The SA, CIA and RC counters, together with the CsI and BA (see below) form a hermitic detector. All decay products with angles out to approximately 100 mrad with respect to the beam direction are detected with high efficiency.

The KTeV spectrometer magnet, in conjunction with the drift chambers, is used to measure the momenta of the charged particles from kaon decays. This magnet weighs 206 tons, with a 2.03 meters vertical by 2.90 meters horizontal gap. This device uses aluminum coils and, at a transverse momentum kick of 450 MeV/c, consumes approximately 400 kilowatts of power. The magnet is located between the SA2 and SA3 counters.

With a field integral of 400 MeV/c, for example, the momentum resolution is better than one percent up to 50 GeV/c, decreasing to 3 percent at 250 GeV/c.

Particle identification is achieved in part by using transition radiation detectors (TRD's). TRD1-TRD10 will be used to distinguish between pions and electrons. These detectors are located downstream of the last drift chamber. A scintillation trigger hodoscope system will also be placed in this region and used to form a fast trigger for charged particles.

The Cesium Iodide (CsI) array is the crucial detector for the KTeV experiments. It is located 1.5 meters downstream of the trigger hodoscope. This precision high-resolution electromagnetic (EM) calorimeter is the sole detector for reconstructing neutral mode kaon decays. This is accomplished by measuring the energy and position of photons from π^0 decays. The calorimeter consists of an array of 50 cm long blocks of pure CsI. Transverse dimensions of the array are 1.9 meters by 1.9 meters, with a total of 3100 CsI blocks. This electromagnetic calorimeter will

have an energy resolution of better than one percent and a position resolution of order 1 mm.

There will be two 15 cm square beam holes horizontally separated by 30 cm. center to center in the CsI calorimeter array for the neutral beams to pass through. Another instrumented defining aperture (the "Collar Anti") is located just upstream of the CsI calorimeter beam holes, and partially covers the CsI blocks surrounding the beam holes. The Collar Anti will also provide a well defined aperture for acceptance calculations.

Downstream of the calorimeter, a scintillator hodoscope behind a lead wall will serve as a hadron veto for purely electromagnetic decay triggers. There will be a beam hole in the hadron veto, and lead wall for the two beams to pass through. There will be a Beam TRD (bTRD) in the neutral beam to distinguish pions from protons (in hyperon decays) in the neutral beam downstream of the CsI. A beam hole veto calorimeter ("Back Anti") will be placed after the lead wall to tag forward decay photons and electrons that escape the calorimeter down the beam hole. A lead and scintillator stack will be used for the front electromagnetic section, and an iron scintillator stack will be used for the hadronic section.

The muon detection and veto systems downstream of the beam hole veto system consist of an iron muon filter instrumented with scintillator hodoscope planes. The purpose of the muon system will be to veto particle signals in particular decays, and serve as a muon identifier to reduce backgrounds in other decays. The muon filter also serves as the neutral beam dump.

2. PRIMARY BEAM

2.1 Primary Beam Requirements

The specifications for the primary proton beam are summarized in Table 2.1.1.

Table 2.1.1.

Primary Beam Specifications

Proton beam energy	800/900 GeV
Proton intensity	5×10^{12} protons per spill
Targeting angle	-4.8 mr (vertical) 0.0 mr (horizontal)
Targeting angle variability	-4.0 mr to -5.6 mr (vertical)
Beam size at the target (σ)	≤ 250 μm (horizontal and vertical)
Beam position stability	$\leq \pm 100$ μm (horizontal and vertical)
Beam angle stability	$\leq \pm 25$ μrad (horizontal and vertical)

Once the beam size at the target has been chosen the minimum beam divergence is given by the emittance. The emittance cannot be decreased after extraction because it is defined by the accelerator. The emittance values obtained by C.D. Moore et al.[8] will be used: $\varepsilon_H = 8\pi$ mm μrad horizontally, and $\varepsilon_V = 6\pi$ mm μrad vertically. The emittance is defined here as $\varepsilon = \sigma_x \sigma_\theta \pi$ mm μrad.

With a horizontal beam waist at the target, a beam size of about $\sigma_x \approx 150$ μm is expected. Using the above emittance a horizontal beam divergence of $\sigma_\theta \approx 60$ μrad is expected. Similar numbers are expected for the vertical beam size and divergence.

---

[8] "Tevatron Extraction Model," by C.D. Moore, R. Coleman, G. Goderre, M. Yang.

2.2   Magnets And Instrumentation Layout

For the KTeV beam line only modifications in enclosures NM1 and NM2 are needed. The modifications in enclosure NM1 are minor. The next fixed target run is expected to be at an energy of 800 GeV. The designed KTeV primary beam line will be able to run up to 900 GeV.

2.2.1   Enclosure NM1

Figure 2.2.1 shows the magnet and instrumentation layout in enclosure NM1. There are two EPB magnets (NM1U), a trim magnet (NM1H), two short BPMs (NM1BPH and NM1BPV), and a vacuum SWIC (NM1WC). These elements essentially fill all the available space.

The NM1U EPBs will be running at higher currents than in previous runs. This will be done to raise the beam at the KTeV target in order to meet the Ground Water Activation limits (in the Single Resident Well model). NM1U will bend up 3.433 mr. At 800 GeV/c this can be done with two EPBs running at 1660 amps. At 900 GeV/c the two EPBs would have to run at 2125 amps[9].

The BPMs and the vacuum SWIC will allow us to run with no material in the beam. Monte Carlo studies show that this is necessary in order to minimize the muon flux in the detector due to beam halo (see section 2.8).

---

[9]   Leon Beverly indicates that this is viable current with ramped EPBs. The EPBs could be replaced by a B2 for 900 Gev if reliability problems occur.

N01

NW1W

103,166

NM1U-1   NM1U-2   NM1H

NM1

NM1WC

103,184

NM1BPMV

NM1BPMH

0   5   25

SCALE   FEET
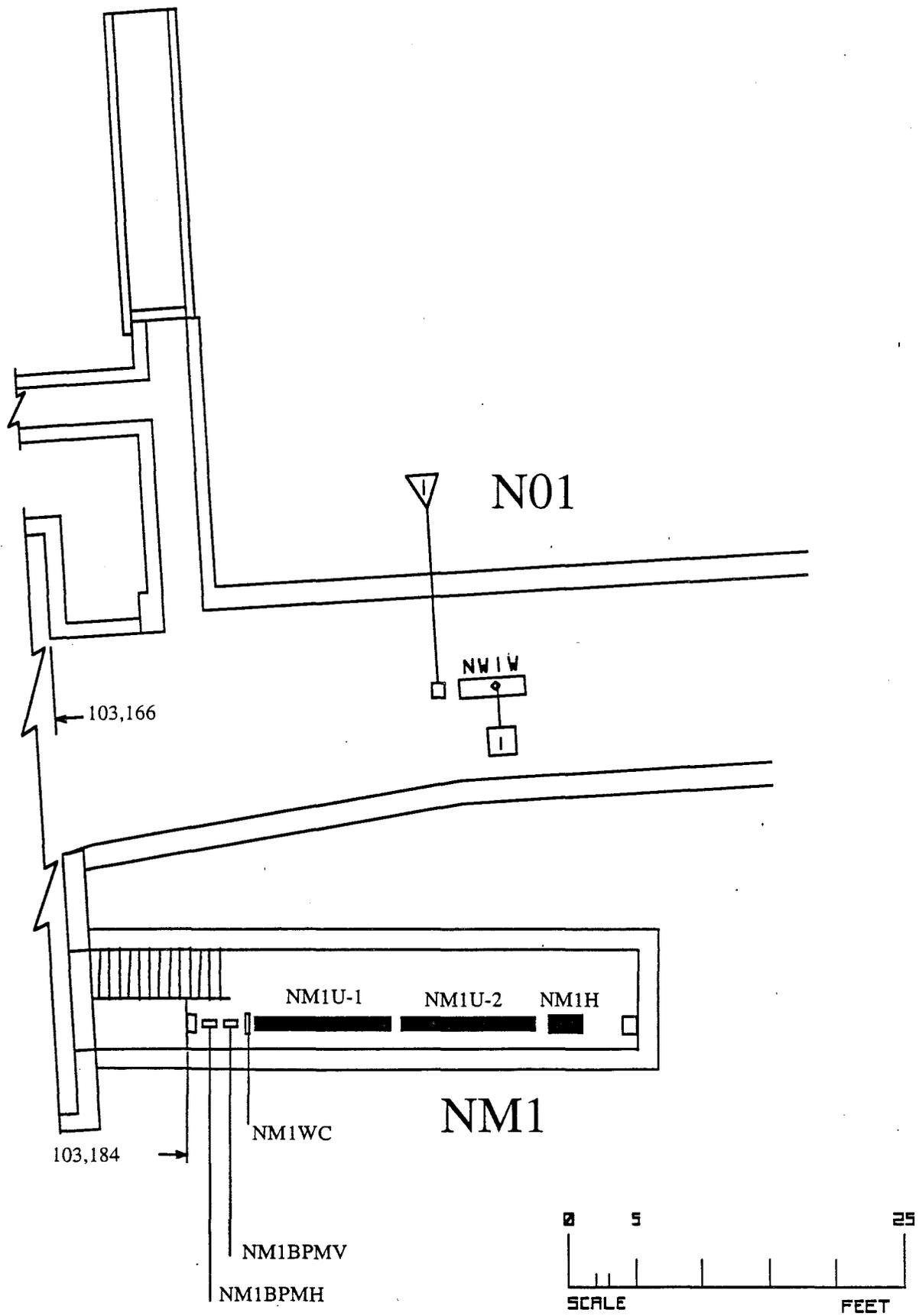
Beamline component layout of NM1

FIGURE 2.2.1.

2.2.2 NM1 to NM2 pipe

In order to raise the primary target as much as possible, the primary beam was placed two inches from the top of the NM1 to NM2 pipe. To see how much the beam could be raised, the pipe was surveyed. Figure 2.2.2 shows the results of the survey of the NM1 to NM2 pipe. This survey was done measuring the elevation of a target that was pulled from one end of the pipe to the other. In this way the bottom of the pipe was measured; the top was calculated using the pipe diameter (16 inches upstream, 24 inches downstream). The elevation of the low point on the top of the pipe was then verified by looking with an optical instrument from NM2 to NM1. The closest vertical point between the KTeV beam and the pipe is two inches. Horizontally the beam is centered in the pipe.
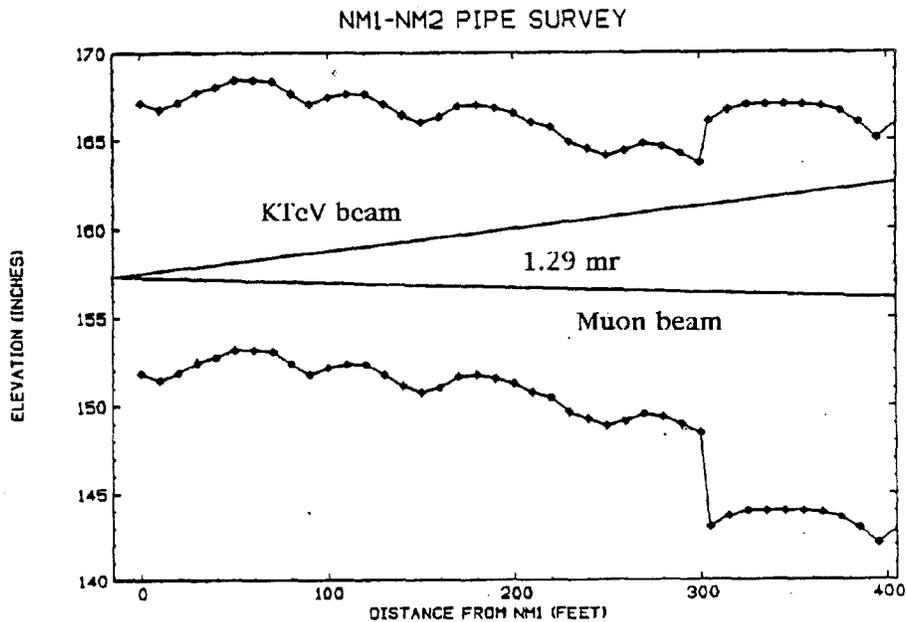
Figure 2.2.2.
NM1 to NM2 pipe survey. The pipe is 450 ft. long.
Also shown are the NM beamline (labeled "Muon beam) for past runs and the new KTeV beam.

2.2.3 Enclosure NM2

Figure 2.2.3 shows the magnet layout in enclosure NM2. Three conflicting issues have to be resolved: a) to increase the target height, the up bend in NM2 should be as far upstream as possible and the down bend as far downstream as feasible (also needed is an east bend to match the existing enclosure downstream of the target), b) to increase the accuracy of beam position and slope measurement, one position measuring device should be very close to the target and another one as far upstream as possible, and c) to maximize its range, the Angle Varying Bend (AVB) system needs to be close to the target. The conflict is resolved as follows.

At the upstream end, after leaving about 6 feet for instrumentation, the beam is bent east and up by NM2EU, a string of two B2s is rotated 30.4 degrees. A vertical trim (NM2V) follows NM2EU, allowing for independent adjustment in the horizontal and vertical planes. At the downstream end, one position measuring device (NM2WC3) is located two feet upstream of the target, and a second (NM2WC2) about 10 feet upstream of the previous one -- his allows extrapolation to the target with minimal loss in position resolution. The AVB system (NM2D1/NM2D2) is placed upstream of NM2WC2 (the horizontal trim NM2H is inserted here for fine control). The final focusing quadrupoles (NM2Q1/NM2Q2) are placed in the remaining space, between NM2EU and the AVB system.

The KTeV target is eleven inches higher than the previous muon target. This gain in elevation was achieved by positioning the beam two inches away from the top of the NM1 to NM2 pipe and by bending the beam up with NM2EU and back down with NM2D1 and NM2D2. If needed, the beam may be repositioned without changing the target position, although this would reduce the range of the AVB system[10].

---

[10] At 900 GeV/c, the beam can be lowered at the upstream end of NM2 by 2.6 inches by reducing the range of the AVB system from -4.0 to -5.6 mr to -4.0 to -4.8 mr. This will put the beam 4.6 inches away from the top of the pipe.

Figure 2.2.3 Magnet and instrumentation layout in enclosure NM2

2.3 The Angle Varying Bend (AVB) System

The vertical targeting angle can be changed using NM2D1 and NM2D2. Figure 2.3.1 shows a picture of the AVB system. The thicker line is the -4.00 mr beam trajectory; the thinner line is the -5.6 mr trajectory.
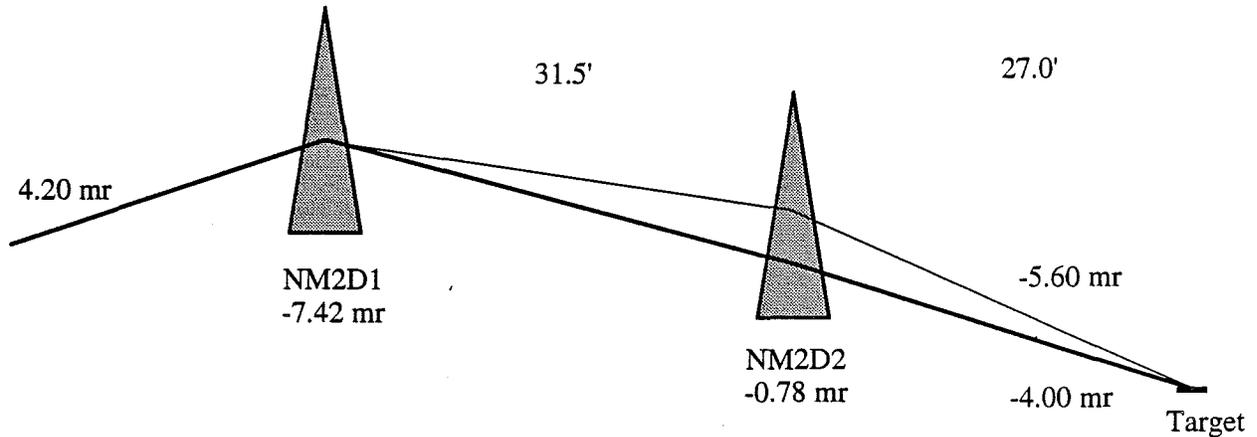
Figure 2.3.1.
AVB System Layout. The vertical and horizontal scales are different.

As can be seen in the figure, the angle is the smallest when NM2D2 is at its lowest field value. By increasing the NM2D2 field and at the same time decreasing NM2D1, the angle can be increased without changing the beam position at the target. The targeting angle is maximum when NM2D2 reaches its maximum. Then the bigger the NM2D2 range, the bigger the range in targeting angle. A range of 0 to 4800 amps was assumed for NM2D2 (a B2 magnet).

The beam is rising in front of the NM2D1 magnets. The NM2D1 and NM2D2 magnets are used to bend the beam down. At 900 GeV/c, the two B2s in the NM2D1 string are not enough to bend the beam down to the minimum angle required (-4.0 mr); therefore, the minimum value of NM2D2 must be greater than zero. If the minimum current of NM2D2 were to be reduced to zero, then the range of the AVB system would increase by 20%.

18

The criteria to choose the fields and positions of NM2D1 and NM2D2 were:

a- Maximum energy of 900 GeV.
b- Minimum targeting angle -4.0 mr.
c- Maximum current for NM2D1 and NM2D2 is 4800 amps.
d- At a targeting angle of -4.0 mr NM2D1 runs at its maximum current (4800 amps). This was done to maximize the AVB's range.

With the above criteria the range in vertical targeting angle is:

800 GeV/c: from -4.0 mr to -5.8 mr
900 GeV/c: from -4.0 mr to -5.6 mr

The magnets will be positioned for a maximum momentum of 900 GeV/c to increase the range of the AVB system.

2.4   Optics

2.4.1   The goals

The three goals that guided the design of the primary beam optics were:

1- To achieve the requested beam size.
2- To form a beam waist at the target.
3- To minimize the dispersion at the target.

The requested beam size is $\sigma \leq 250\,\mu m$ for both the horizontal and vertical beam profiles. A waist at the target will provide: a) minimum beam size change through the target, and b) beam size stability. Since the beam coming out of the Tevatron is not monochromatic, to achieve maximum position and angle stability the dispersion at the target needs to be minimized. As the reader follows the logic behind the design it will become clear that some compromises have to be made. For

example, it is possible to have a waist at the target with almost no dispersion only if the beam size is substantially smaller than 250 μm. Or, it is possible to have a 250 μm beam and minimal dispersion only if there is no waist at the target.

2.4.2   The constraints

In trying to meet the above goals it was found that of all the constraints the main three are: a) the beam phase space, b) the beam as it comes from Switchyard, and c) the beam size at the NM2 quadrupoles.

Beam phase space conservation is the strongest constraint. On the other hand this is the least known quantity in any beam design. The values of the emittance obtained by C. D. Moore et. al. were used: $\varepsilon_H = 8\pi$ mm μrad horizontally, and $\varepsilon_V = 6\pi$ mm μrad vertically.[11]   The emittance here is defined as $\varepsilon = \sigma_x \sigma_\theta \pi$ mm μrad.

There is a small amount of flexibility in changing the beam delivered by Switchyard. As can be seen in Figure 2.4.1, Q90 affects all three areas (Proton, Meson and Neutrino), Q100/Q101 affect both Meson and Neutrino, and Q106 affects the two Neutrino beams: E815 and KTeV. The last four quadrupoles, Q420, Q424, NM2Q1 and NM2Q2, only affect the KTeV beam. Of these four quadrupoles, two are in Switchyard enclosure G2 (Q420 and Q424) and two in enclosure NM2 (NM2Q1 and NM2Q2). The polarities and currents of these last four quads can be chosen as needed. Figure 2.4.2 shows the measured and predicted beam profiles for the neutrino area given by C.D. Moore et al.[5]. Figure 2.4.3 shows the R_{16} matrix element for the NM/KTeV line in units of mm/0.01% (R_{16} is known as the dispersion. If $R_{16}=1$, then a beam momentum change of $\Delta p / p = 0.01\%$ will produce a beam motion of 1mm).

---

[11] "Tevatron Extraction Model," by C. D. Moore, R. Coleman, G. Goderre, M. Yang.

KTeV Primary Beamline Optics from Switchyard Extraction to the NM2 Target

Horizontal				Vertical

Location	Bend/Focus	Element	Bend/Focus
51.19'		Extraction Lambertsons	10.498 mrad
136.48'	-23.218 mrad	Skew Dipoles	-7.367 mrad
215.30'	- 0.370 mrad	H90	
226.99'	f = 213.28'	Q90	f = -213.28'
292.33'		PSep	-0.117 mrad
413.21'	1.567 mrad	VH94	-3.050 mrad
502.04'		PLam	
661.18'	f = -164.36'	Q100	f = 164.36'
711.91'		VT102	-0.188 mrad
724.37'	f = 235.16'	Q101	f = -235.16'
783.42'		MSep	-0.134 mrad
854.54'		VT103	0.196 mrad
1043.53'		MLam	
1225.11'	0.274 mrad		
1258.21'		V100	9.799 mrad
1333.72'		Q106 (off)	
1368.96'		MuSep	-0.0838 mrad
1752.31'	-2.468 mrad	MuLam	
2273.42'		VT420	0.068 mrad
2281.28'	f = 324.08'	Q420	f = -324.08'
2348.34'		MuBends	-12.269 mrad
2370.39'	-31.718 mrad		
2453.97'	f = -240.69'	Q424	f = 240.69'
2464.93'	0.1415 mrad	H424	
3286.55'		NM1U	3.433 mrad
3734.39'	5.374 mrad	NM2EU	3.153 mrad
3775.89'	f = -61.89'	NM2Q1	f = 61.89'
3823.39'	f = 43.01'	NM2Q2	f = -43.01'
3866.39'		NM2D1	-7.419 mrad
3897.89'		NM2D2	-0.788 mrad
3924.89'		NM2TGT	

FIGURE 2.4.1.

Beam elements from A0 (Tevatron extraction point) to the KTeV target. The last element in Switchyard is the H424 trim.
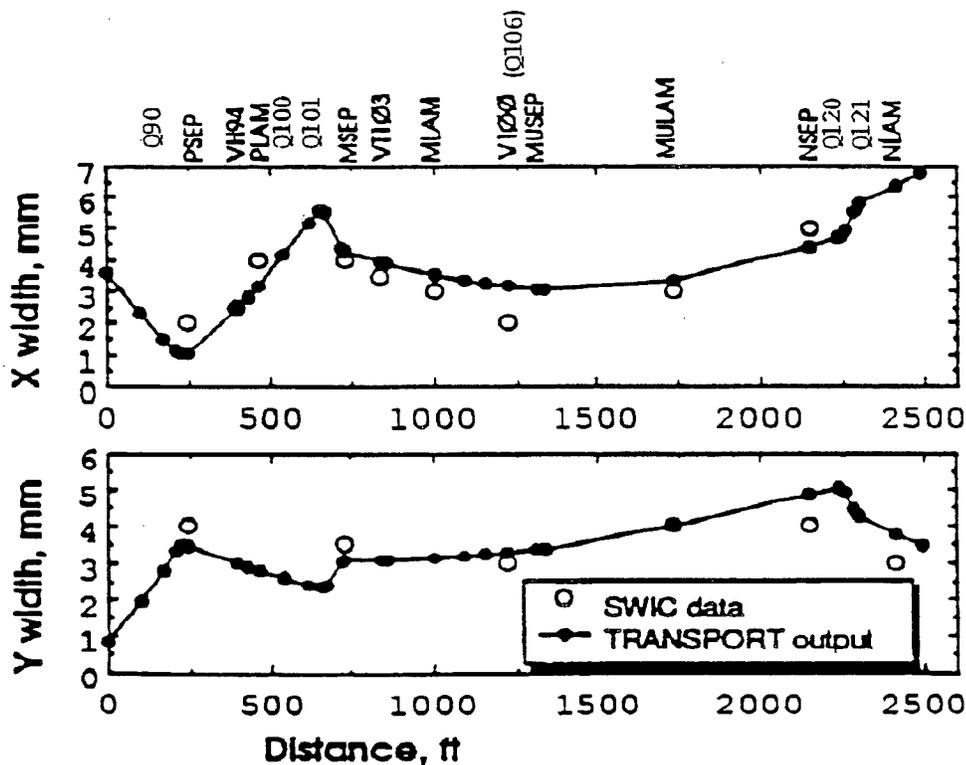
Figure 2.4.2.

Measured and predicted beam profiles for the neutrino area as given by C.D. Moore et al (1).

For a waist at the target, the beam size at the last set of quadrupoles is determined by the emittance. Using an emittance of 8π mm μrad and a beam size of 250 μm, the beam size 100 feet upstream of the target will have to be about $\sigma = 1$ mm (that is (8/0.25) micro radians times 100 feet).

2.4.3 The options

The value of R_{16} in G2 can be controlled using the Q100 and Q101 quadrupoles[12]. If the dispersion is non zero at the Q420-Q424 G2 quadrupoles (see

---

[12] The change in the currents is of the order of 5%. Studies show that this change has minimal effect in Meson and Neutrino.

Figure 2.4.3), then these two quadrupoles can be used to focus the dispersion into NM2. If the dispersion is very close to zero in NM2, then NM2Q1 and NM2Q2 will have little effect on it, and therefore it will remain very close to zero. To focus the dispersion, Q420 and Q424 would have to run at a higher current, producing an intermediate focus between G2 and NM2 (see Figure 2.4.4). This produces a large beam at NM2Q1 and, consequently, a very small beam size at the target waist. There can be target heating problems if the beam size at the target is too small.

If the dispersion is not minimized, then the G2 quads can be used to produce a smaller beam in NM2 and therefore a larger beam size at the target waist (see Figure 2.4.7). The beam sizes are very small everywhere but the dispersion has increased.

Figure 2.4.8 shows a case in which the dispersion at the target is close to zero. A disadvantage of this solution is a bigger beam at NM2Q1, and therefore a much smaller beam at the horizontal waist. A bigger beam has the potential to produce unwanted muons by scraping in the magnets. If the beam is too small, target heating problems are a risk. Again, the vertical beam size was chosen to satisfy the requirement $\sigma_x \sigma_y \approx 0.025 mm^2$.

To select the quadrupole's polarity, the options described above must be kept in mind. The G2 quads should be effective to focus the dispersion and to keep the beam size at the target waist at a reasonable level. To satisfy this, Q420 has to be defocusing and Q424 to be focusing. This will increase the dispersion going from Q420 to Q424 but at the same time it will make the quadrupoles more effective. For the quadrupoles in NM2, the farthest upstream quadrupole has to be focusing to keep the beam from getting too small and unstable at the target waist. Then NM2Q1 will be focusing and NM2Q2 defocusing.

About the dispersion

The term "minimize the dispersion" should be quantified. The momentum spread in the Tevatron during collider run is $\Delta p / p \approx 0.38 x 10^{-4}$ at 95%[13]. Taking into account the increase of momentum spread with increasing intensity, a

---

[13] C. Hojvat, Stan Pruss and G. Jackson, private communication.

momentum spread of $\Delta p / p = 0.5 x 10^{-4}$ is used. Then for a beam motion of less than 100 microns and 25 micro radians, the dispersion should be less than two meters and 0.5 radians. In units of $mm / 0.01\%$ and $\mu r / 0.01\%$ this translates to $R_{16} \leq 0.1$ and $R_{26} \leq 20$.

Matching with the Tevatron lattice

The Tevatron lattice for fixed target has a dispersion at A0 of 2.5 meters and -0.028 radians[14]. Thus the TRANSPORT input file was started at A0 with these values for the dispersion. Another consideration could be to make an achromatic transfer from the D0 extraction septa to the KTeV target. As this problem is not well enough understood, work should continue in this area.

Figures 2.4.4, 2.4.5 and 2.4.6 show cases with and without the Tevatron dispersion. As can be seen in this plot there is some control over the dispersion using Q100 and Q101. The changes in these quadrupoles are of the order of 5% and the effect that these changes have on the Meson area are minimal.

2.4.4   The design

Our choice for the optics is given in Figure 2.4.4. In this case the smallest distance, measured in beam widths, between the center of the beam and the face of a magnet is about 7 sigma. The beam forms a horizontal waist at the target. The vertical beam size was chosen such that $\sigma_x \sigma_y \approx 0.025 mm^2$. This last number is set by target heating[15]. Referring to Figure 2.4.4., the dispersion calculations are $R_{16} \Delta p/p \approx 50 \mu m$ and $R_{26} \Delta p/p \approx 3 \mu rad$. As mentioned above, the momentum spread in the Tevatron is about $\Delta p / p \approx 0.5 x 10^{-4}$ at 95%.

---

[14]   Extracted from a SYNCH output provided by Al Russell.
[15]   During start up, the Run Conditions will only allow low intensity. Among other things this will protect the target. If beam studies show that the beam can be too small, we will narrow the windows in the NM2Q1 and NM2Q2 current interlocks to protect the target.

KTeV Primary Horizontal Beam Position Dispersion (R16) to NM1
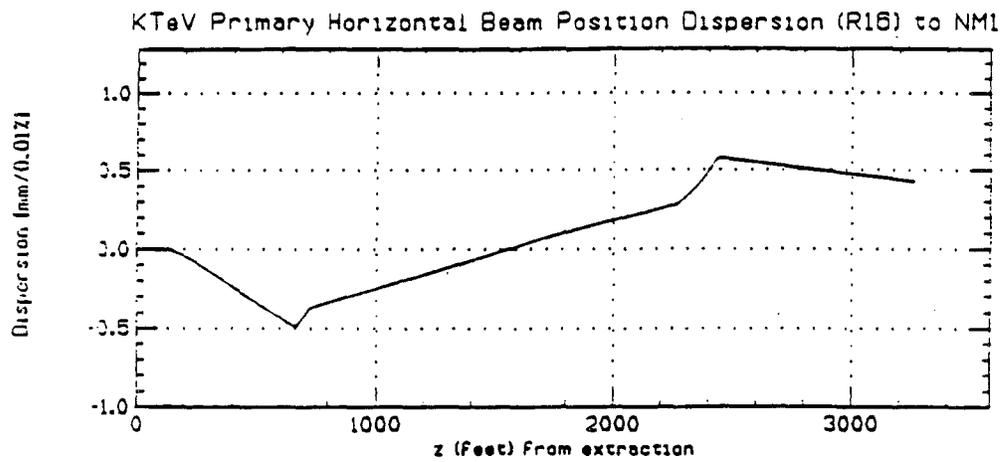
Figure 2.4.3.

Dispersion (R_{16} matrix element) from A0 to NM1. The units are mm/0.01%.
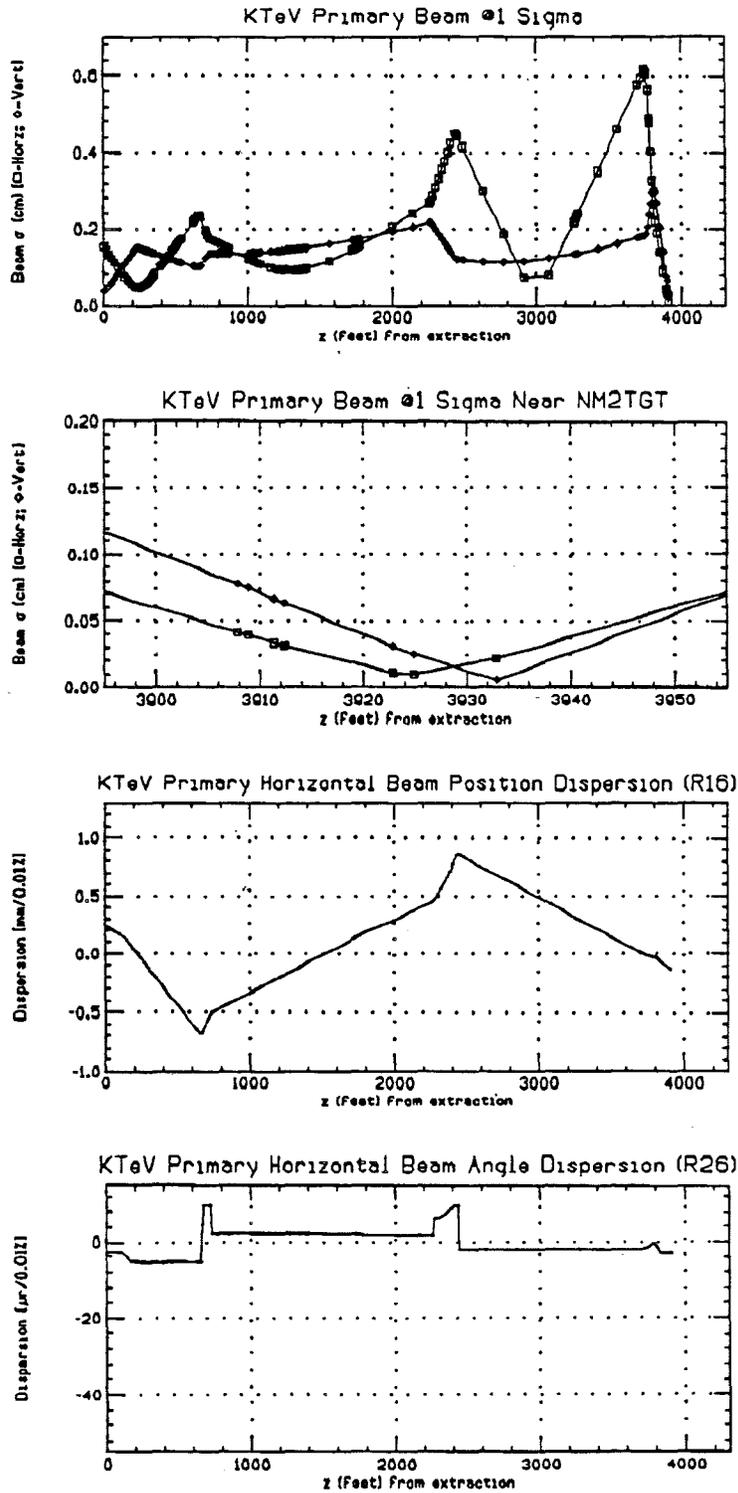
Figure 2.4.4.

a) Beam profile (sigma) from A0 to the target, b) beam profile in the target region (target at z=3925'), c) R_{16} and d) R_{26}. The requirements at the target were a waist in x and .25mm in y, and the minimization of the dispersion. Q100 and Q101 were changed by 7.8% and 6.1% respectively; these changes have very little effect in the vertical plane.

KTeV Primary Horizontal Beam Position Dispersion (R16)

KTeV Primary Horizontal Beam Angle Dispersion (R26)
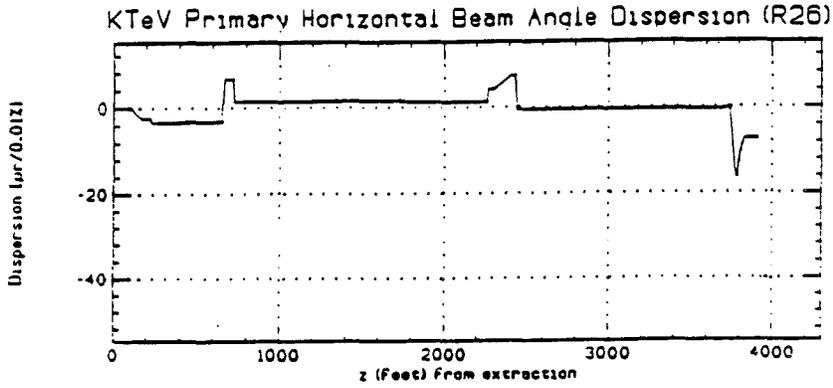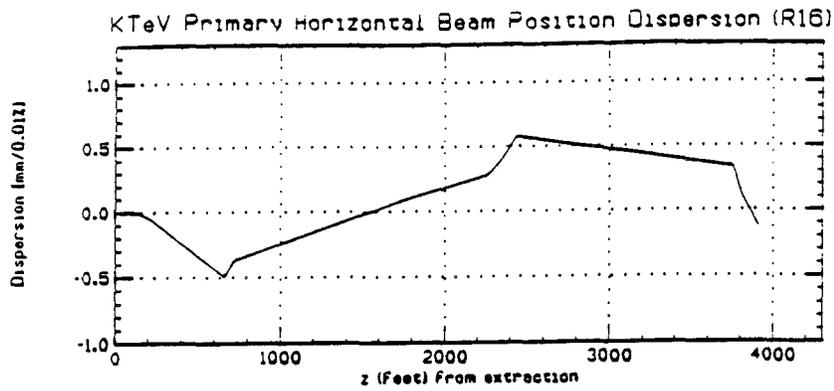
Fig. 2.4.5: a) R_{16} and b) R_{26} for zero Tevatron dispersion and no changes in Q100 and Q101. All the other magnet currents are the same as in Fig. 2.4.4.

KTeV Primary Horizontal Beam Position Dispersion (R16)

KTeV Primary Horizontal Beam Angle Dispersion (R26)
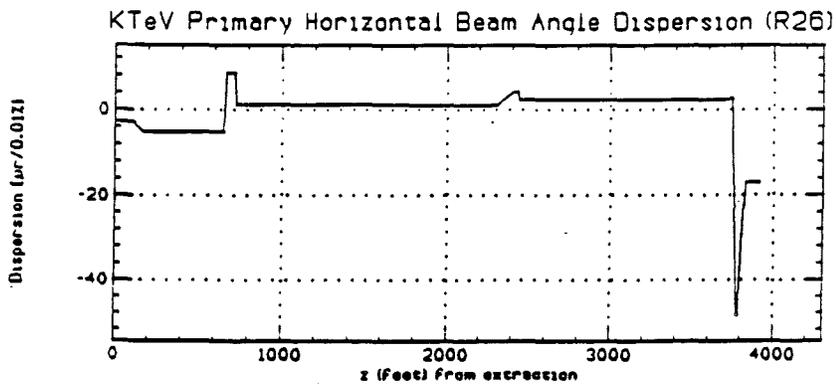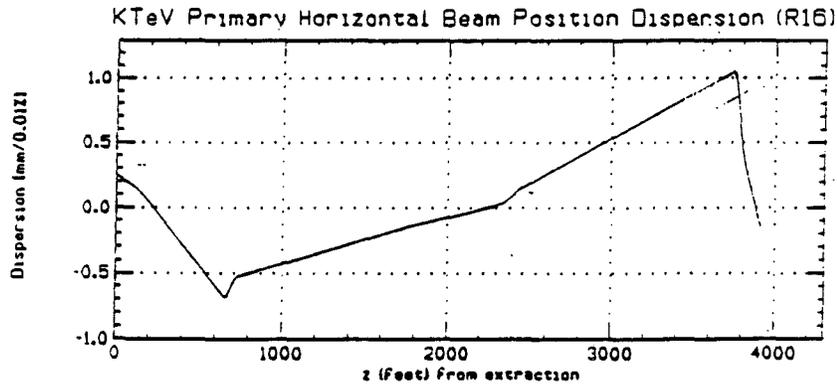
Fig. 2.4.6: a) R_{16} and b) R_{26} for Tevatron dispersion matching and no changes in Q100 and Q101. All the other magnet currents are the same as in Fig. 2.4.4.
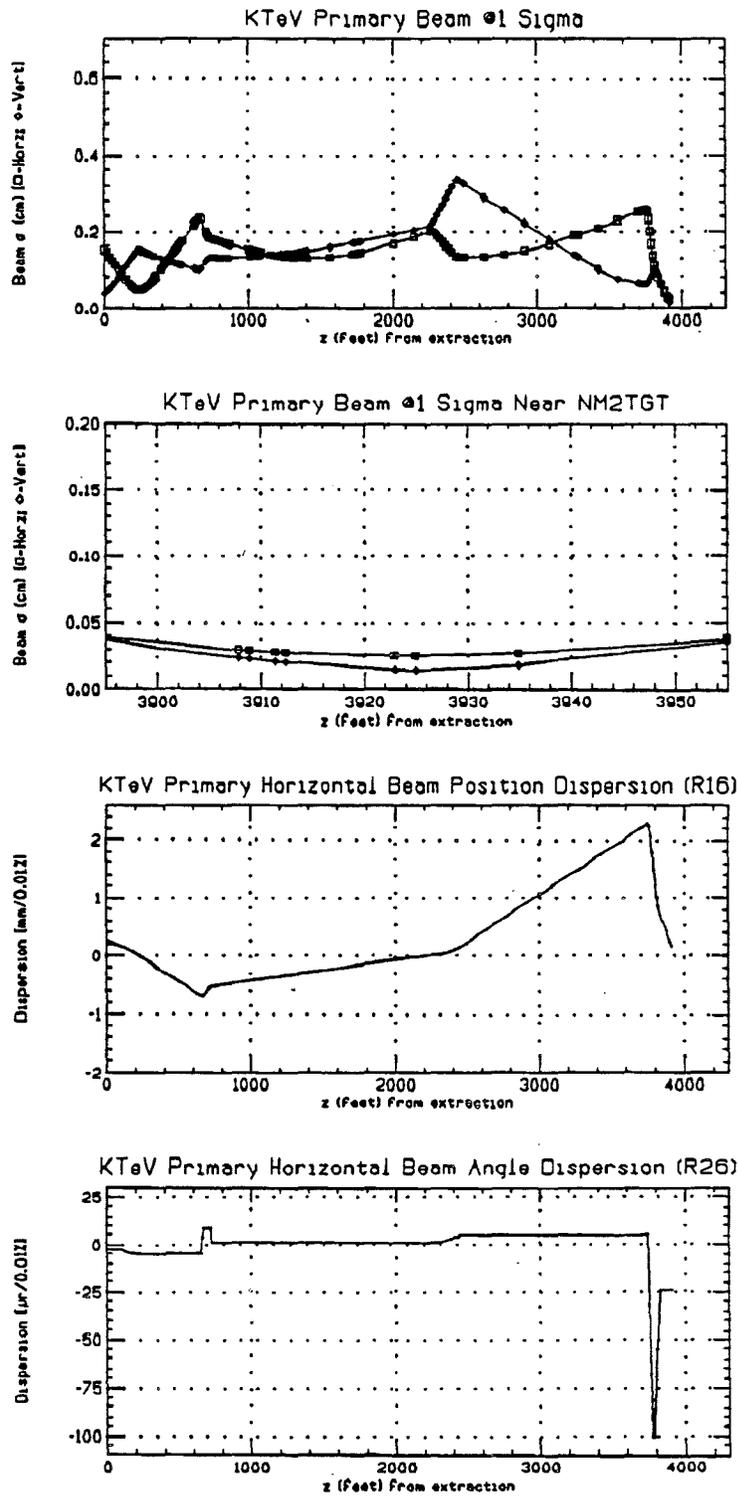
Figure 2.4.7.

a) Beam profile (sigma) from A0 to the target, b) beam profile in the target region (target at z=3925'), c) R_{16} and d) R_{26}. The requirements at the target were a beam waist and maximization of the beam size at the waist. No changes were made to Q100 and Q101.
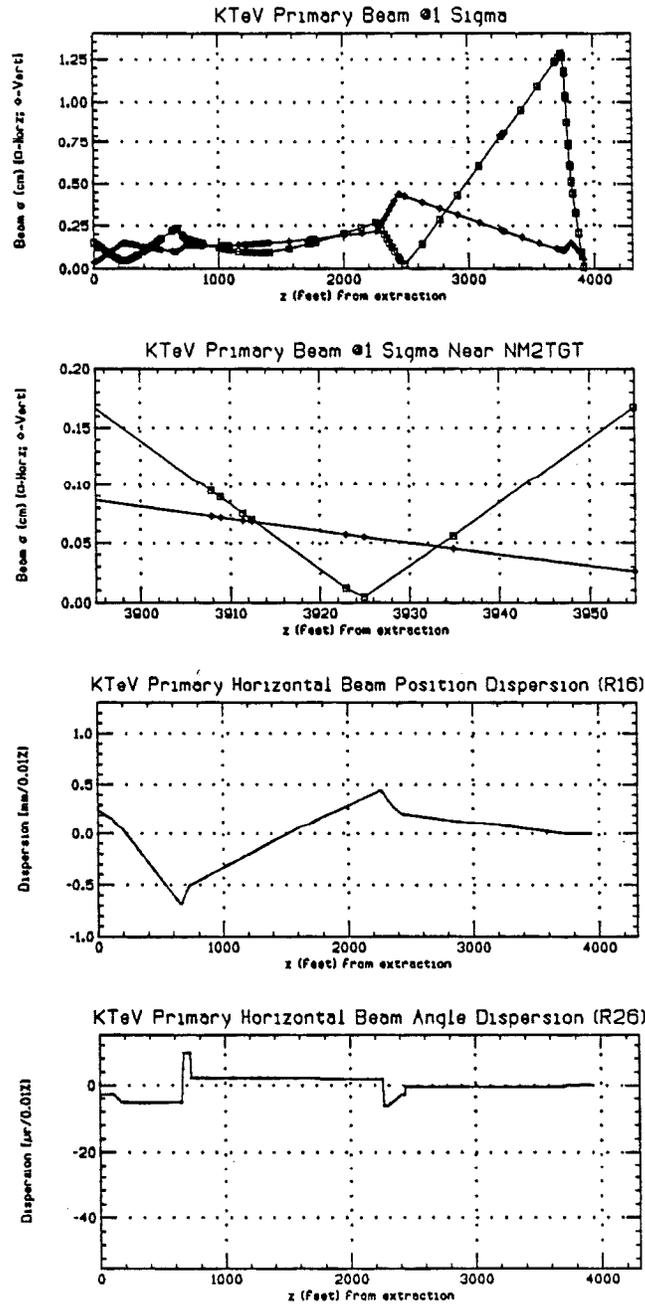
Figure 2.4.8.

a) Beam profile (sigma) from A0 to the target, b) beam profile in the target region (target at z=3925')
and c) R_{16} and d) R_{26}. The quadrupoles in these plots have the same polarities as those in Fig. 2.4.7.
But the requirements at the target were a waist in x and 0.55mm in y, and the minimization of the
dispersion. Q100 and Q101 were changed by 7.8% and 6.1% respectively; these changes have very little
effect in the vertical plane.

Table 2.4.9.

Quadrupole Gradients

Quadrupole	Figure 2.4.3	Figure 2.4.4	Figure 2.4.7	Figure 2.4.8
Q100	2.9744	3.2056	2.9744	3.2056
Q101	-3.0808	-3.2688	-3.0808	-3.2688
Q420	-2.2397	-2.2397	2.0901	2.0251
Q424	3.0525	3.0525	-2.0953	-2.0726
NM2Q1	3.9032	3.9032	3.7133	3.3060
NM2Q2	-4.0036	-4.0036	-4.0761	-2.8599

Table of quadrupole gradients (in KG/inch) for the figures in this section.
Figures 2.4.5 and 2.4.6 have the same quadrupole gradients as Figure 2.4.3.
The beam energy is 800 GeV.

Table 2.4.10

Quadrupole Currents

Quadrupole	Figure 2.4.3	Figure 2.4.4	Figure 2.4.7	Figure 2.4.8
Q100	60.0	61.4	60.0	61.4
Q101	-59.0	-62.6	-59.0	-62.6
Q420	-42.9	-42.9	40.0	38.8
Q424	58.5	58.5	-40.1	-39.7
NM2Q1	750.1	750.1	713.6	635.3
NM2Q2	-769.4	-769.4	-783.3	-549.6

Table of quadrupole currents (in Amps) for the figures in this section.
Figures 2.4.5 and 2.4.6 have the same quadrupole currents as Figure 2.4.3.
The beam energy is 800 GeV.

2.5 Stability

2.5.1 The Sources of Instabilities

There are four sources of instabilities:

1- The beam moves as it is extracted from the accelerator.
2- The current of the magnets between extraction and the KTeV target changes with time. This can be due to:
    a- Power supplies instabilities
    b- Small adjustments due to changes in beam splits or beam extraction.
3- Changes in beam splits.
4- The position monitoring devices move with time.

The beam instabilities can be classified in two groups: 1) slow instabilities, or beam motion over a period of a few or more spills, and 2) beam roll, or beam motion during the spill.

The plan to cancel the slow instabilities is to use EPICURE (Research Division's beam control system) to monitor the beam position at different SWICs and to make small corrections in the magnet's currents to keep the beam stable. EPICURE can be used to make these corrections on a spill by spill basis. What is needed for this strategy to work is: a) reasonably stable power supplies (thus avoiding making changes in every spill), b) enough sensitivity in the magnets to make small corrections, c) stable beam instrumentation, and d) reliable read-back of the instrumentation. The first three issues will be examined in the following subsections.

Beam roll can be produced by changes in beam momentum, position or slope during extraction. It can also be produced by poor magnet regulation after beam extraction, but the known regulation of the magnets between extraction and the KTeV target is compatible with the required beam stability (see the following section). The effects of beam motion at extraction due to small changes in

momentum was covered in the previous section under the dispersion studies. If the beam position and/or slope at extraction were to change during the spill, the plan to cancel its effects on the KTeV target is to use in a closed loop two Switchyard magnets (MuLam and H424) to keep the beam stable at two positions (the downstream end of G2 and the upstream end of NM2). The reasons for this are: a) ACNET (Switchyard's beam control system) can make several corrections during the spill, b) during the period of one spill all the instrumentation is very stable, and c) only a quarter of a millimeter beam stability at the downstream end of G2 and the upstream end of NM2 is needed in order to have 50 microns stability at the KTeV target. The details will be examined in the Beam Roll subsection.

2.5.2   Power supplies stability

Table 2.5.1 shows the change in beam position and angle at the target when the dipoles' field is changed by 100 ppm (10^{-4}). The main bends between A0 and the target are shown in the table. The contributions of the dipoles and quadrupoles not shown in the table are very small. The units are microns and micro radians.

Table 2.5.1.

Magnet	Δx (μm)	$\Delta \dot{x}$ (μrad)	Δy (μm)	$\Delta \dot{y}$ (μrad)
Ex. Lamb.	0	0	-10	2
SKDP	21	-6	5	1
VH94	-2	-1	2	2
V100	0	0	55	-25
MULAM	-5	1	0	0
MUBEND	148	15	-108	43
NM1U	0	0	11	-3
NM2EU	-41	-1	6	0
NM2D1	0	0	-13	-1
NM2D2	0	0	-1	0

There are four magnets that have large contributions: SKDP, MUBEND and NM2EU and V100. Both SKDP and MUBEND are superconducting magnets and

with a HOLEC transductor can regulate to 20 - 50 ppm[16]. NM2EU is a regular magnet. Studies performed on beam motion during the last fixed target run with NE9E show that regular power supplies regulate to better than 150 ppm over a period of days (see Figure 2.7.1). Studies performed on NEFE with a hall probe show that between the beginning and the end of the spill those magnets were stable to better than 100 ppm. As in NM2EU, the magnets of the NE9E and NEFE strings are B2s. The fact that the regulation of NM2EU is close to the requested 100 microns position stability means that close attention must be paid to the power supply that will run that magnet. If needed, NM2EU can be run without ramping[17]. The V100 string does not have a HOLEC transductor, so its contribution may approach the 100 microns level.

2.5.3 Canceling slow instabilities

Slow instabilities are those that occur over a few or more spills. Examples of these are the small adjustments made to magnets due to changes in beam splits or beam extraction. To correct these instabilities, the beam position will be measured every spill and, if necessary, corrections will be made by computer to magnet currents between spills. To do this, the relation between a current change in a magnet and the beam position change in a SWIC has to be known. Throughout this section, the word "SWIC" will refer to beam position monitors in general, although the beam position monitors can be a BPM or any other beam position measuring device.

KTeV requires careful control of the primary beam from the upstream end of enclosure NM1 to the target, located in NM2. Currently, KTeV is able to control and monitor all devices from enclosures NM1 to the target via the EPICURE control system. However, in order to use Epicure to control the position of the beam at the upstream end of NM1, Epicure control has be extended to the switchyard magnets VT420 and H424.

---

[16] A. Visser, M. Coburn, private communication.
[17] Leon Beverly, private communication.

Figure 2.5.1 illustrates a conceptual layout of the magnets and SWIC's from VT420 to the target. As can be seen in the figure, there are four SWICs to measure beam position: NM1WC, NM2WC1, NM2WC2 and NM2WC3. Each one will be used to measure vertical and horizontal beam positions. There are nine dipoles to make beam corrections: VT420, H424, NM1U, NM1H, NM2EU, NM2V, NM2D1, NM2D2 and NM2H. Note that the MuBends (a large cryogenic string) are not included. The relation between the changes in the dipole's field and the changes in beam position at the SWICs is linear. The following matrix gives such a relation in units of microns per gauss. A beam energy of 1 TeV is assumed.

V420

MuBend

H424

NM1WC

NM1U

NM1H

NM2WC1

NM2EU

NM2V

NM2D1

NM2D2

NM2H

NM2WC2
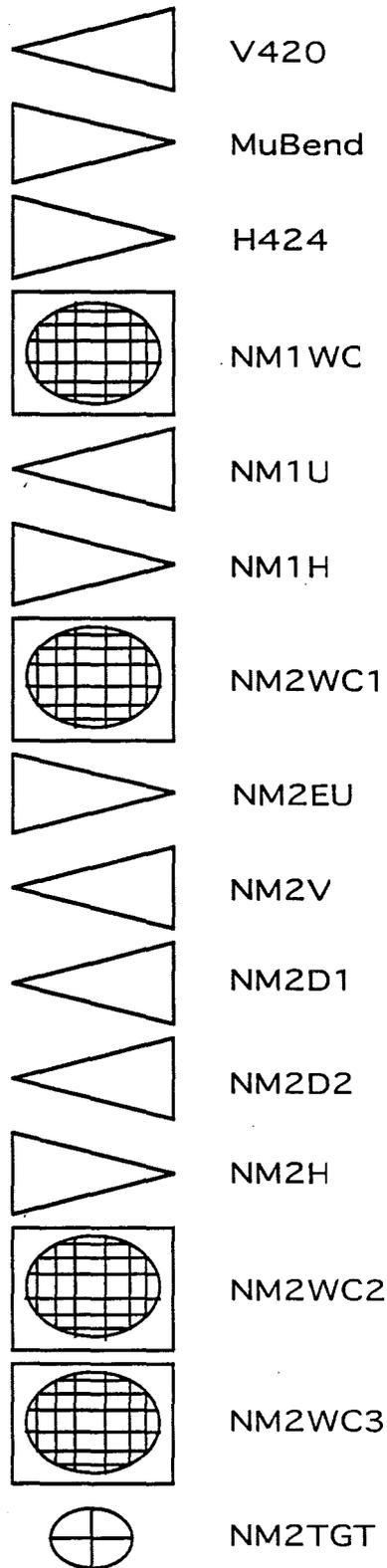
NM2WC3

NM2TGT

Figure 2.5.1.
SWIC's and Magnets used in Calculating Tuning Matrices
(Schematic - not to scale)

$$
\begin{pmatrix}
H424Vs \\
NM1WCV \\
NM2WC1V \\
NM2WC2V \\
NM2WC3V \\
NM2TGTV \\
H424Hs \\
NM1WCH \\
NM2WC1H \\
NM2WC2H \\
NM2WC3H \\
NM2TGTH
\end{pmatrix}
=
\begin{pmatrix}
0 & -0.39 & 0 & 0 & 0 & 0 & 0 & 0 & 0 & 0 \\
-0.15 & -12.9 & 0 & 0 & 0 & 0 & 0 & 0 & 0 & 0 \\
-0.23 & -19.0 & 23.7 & 0 & 0 & 0 & 0 & 0 & 0 & 0 \\
-0.08 & -6.94 & 11.6 & -0.437 & -5.12 & -0.81 & 0 & 0 & 0 & 3.89 \\
-0.04 & -3.41 & 6.80 & -0.422 & -6.29 & -1.39 & 0 & 0 & 0 & 3.53 \\
-0.03 & -2.74 & 5.89 & -0.419 & -6.52 & -1.50 & 0 & 0 & 0 & 3.47 \\
78.5 & 0 & 0 & 0 & 0 & 0 & 0 & 0 & 0 & 0 \\
-17.5 & 0 & 0 & 0 & 0 & 0 & -22.6 & 0 & 0 & 0 \\
-71.9 & 0 & 0 & 0 & 0 & 0 & -34.7 & -2.88 & 0 & 0 \\
-8.68 & 0 & 0 & 0 & 0 & 0 & 2.96 & -0.79 & -0.016 & -21.9 \\
-6.00 & 0 & 0 & 0 & 0 & 0 & 4.86 & -0.71 & -0.089 & -23.9 \\
-5.49 & 0 & 0 & 0 & 0 & 0 & 5.21 & -0.70 & -0.103 & -24.3
\end{pmatrix}
\begin{pmatrix}
MuLam \\
VT420 \\
NM1U \\
NM2V \\
NM2D1 \\
NM2D2 \\
H424 \\
NM1H \\
NM2H \\
NM2EU
\end{pmatrix}
$$

For beam control, the beam position is measured and changes are made to the magnet currents. Therefore, the previous matrix has to be inverted. Only square matrices can be inverted. The beam position at H424 is controlled by Switchyard, therefore it will not be included in the calculations. NM2TGT will not be included either because there is no instrumentation there. If the beam position at H424 is not going to be controlled then MuLam is not needed. As a control device either NM2D1 or NM2D2 can be used to make vertical corrections at the target. After eliminating rows one, six, seven and twelve, and columns one and five, the matrix can be inverted. The result is:

$$
\begin{pmatrix}
VT420 \\
NM1U \\
NM2V \\
NM2D2 \\
H424 \\
NM1H \\
NM2H \\
NM2EU
\end{pmatrix}
=
\begin{pmatrix}
-0.0775 & 0 & 0 & 0 & 0 & 0 & 0 & 0 \\
-0.0621 & 0.0422 & 0 & 0 & 0 & 0 & 0 & 0 \\
-0.471 & 1.67 & -5.19 & 3.00 & -0.240 & 0.123 & -0.538 & 0.0954 \\
0.0291 & -0.301 & 1.57 & -1.63 & 0.0087 & -0.00442 & 0.0196 & -0.00347 \\
0 & 0 & 0 & 0 & -0.0443 & 0 & 0 & 0 \\
0 & 0 & 0 & 0 & 0.534 & -0.347 & 0 & 0 \\
0 & 0 & 0 & 0 & 0.0320 & -0.678 & 15.2 & -13.9 \\
0 & 0 & 0 & 0 & -0.0251 & 0.0129 & -0.0565 & 0.0100
\end{pmatrix}
\begin{pmatrix}
NM1WCV \\
NM2WC1V \\
NM2WC2V \\
NM2WC3V \\
NM1WCH \\
NM2WC1H \\
NM2WC2H \\
NM2WC3H
\end{pmatrix}
$$

In the range we work, the relation between current and field is linear. Because the relation between field and position is also linear (for small changes), a matrix that will relate the changes in magnet currents and beam positions can be obtained.

40

The question of accuracy of control is now addressed. That is, given the minimum current change what is the smallest beam position change that can be made? Table 2.5.2 summarizes the relevant information to do the calculation. Magnet currents and fields were calculated for 1 TeV.

Table 2.5.2

Magnet	Type	Field [kG]	Curr. [Amp]	Bend [mr]	d[G]/ d[Amp]	Max. Curr. [Amps]	Minimum Change [Amps]	[Gauss]
V420	3.5-2-35	2.57	65	-0.0684	396.0	200	0.00610	2.42
H424	EPB	1.55	148	0.141	10.5	1700	0.0763	0.801
NM1U	EPB	18.80	2075	3.430	3.8	1700	0.0763	0.290
NM1H	4-4-30	0.00	0	0.000	25.0	200	0.00610	0.153
NM2EU	B2	17.05	4414	6.23	3.42	5000	0.153	0.522
NM2V	4-4-30	0.00	0	0.000	25.0	200	0.00610	0.153
NM2D1	B2	20.30	5293	7.42	2.14	5000	0.153	0.327
NM2D2	B2	4.31	1399	0.778	3.90	5000	0.153	0.595
NM2H	4-4-30	0.00	0	0.000	25.0	200	0.00610	0.153

Because some magnets are run near saturation, the relation between current and field varies between magnets (c.f. H424 and NM1U). The minimum change in the current was calculated assuming the 15 bit precision of an 1151 power supply reference card[18]. The change in field due to a change in current was calculated at the β fields specified in the Field column. Note that currents for some magnets are calculated to be above the maximum power supply current -- this is because all work is done at 1000 GeV, whereas the actual beam will be 800 GeV or 900 GeV.

From this information, the minimum change at NM2WC3 can also be predicted. Table 2.5.3 summarizes this information (note that units for motion are micrometers). Blanks indicate no coupling:

---

[18] Although the 1151 has a 16 bit register, the current firmware only supports 15 bit precision. See "RD Controls Hardware Release Note 26.0".

Table 2.5.3

Minimum change at NM2WC3

Magnet	V420	NM1U	NM2V	NM2D1	NM2D2	H424	NM1H	NM2H	NM2EU
NM2WC3V [μm]	8.2	2.0	0.064	2.1	0.83				1.8
NM2WC3H [μm]						3.9	0.12	0.014	12.0

The above table shows that adequate control of the beam is possible. The EPICURE software to read beam positions every spill and make magnet corrections between the spills was developed and tested in the Neutrino primary beams during the last Fixed Target run. For the next Fixed Target run, this software will be extended to run in all beam lines, including KTeV.

SWIC Stability

The stability requirements for each of the SWICs determine which SWICs to use for beam control. If there are no magnets between the SWICs or between the SWICs and the target, then the SWIC's stability is the only relevant issue. If there are magnets in between, then their stability also becomes an issue. Three cases will now be explored, one without and two with magnets in between the instrumentation or the target.

Case 1: There are no magnets between NM2WC2 and the target. For purposes of the calculation, NM2WC2 is 12.5 feet from the target and NM2WC3 is 2 feet. Thus, in units of microns and micro radians:

$$\begin{pmatrix} x_T \\ \dot{x}_T \end{pmatrix} = \begin{pmatrix} -0.190 & 1.19 \\ -0.312 & 0.312 \end{pmatrix} \begin{pmatrix} x_{NM2WC2} \\ x_{NM2WC3} \end{pmatrix}$$

Assuming that NM2WC2 and NM2WC3 move independently, the error contributions must be added in quadrature. For example:

$$\Delta x_T = \sqrt{(-0.190 \bullet \Delta x_{NM2WC3})^2 + (1.19 \bullet \Delta x_{NM2WC3})^2}$$

Thus a $40\,\mu m$ stability in NM2WC2 and NM2WC3 will provide a $50\,\mu m$ stability in beam position and $18\,\mu rad$ stability in beam angle.

Case 2: Assuming that the magnets in NM2 are perfectly stable, then the SWICs, NM1WC and NM2WC1, can be used for beam control. This is a good assumption for all the magnets except NM2EU (see Section 2.5.2). The relation of the SWIC's motion and the beam motion at the target in units of microns and micro radians is given by:

$$\begin{pmatrix} x_T \\ \dot{x}_T \end{pmatrix} = \begin{pmatrix} -0.591 & 0.246 \\ -0.014 & -0.008 \end{pmatrix} \begin{pmatrix} x_{NM1WC} \\ x_{NM2WC1} \end{pmatrix}$$

Moving one SWIC at a time, it is noted that if $\Delta x_T \le 50\,\mu m$, then $\Delta x_{NM1WC} \le 85\,\mu m$ and $\Delta x_{NM2WC1} \le 200\,\mu m$. The angular stability is better than a micro radian.

Case 3: Assuming that the magnets in NM1 and NM2 are perfectly stable, then H424 (the last SWIC in G2) and NM2WC1 can be used for beam control. Horizontally there is only a trim in NM1, so NM1 should not contribute to the beam motion. The relation of the SWICs motion and the beam motion at the target in units of microns and micro radians is given by:

$$\begin{pmatrix} x_T \\ \dot{x}_T \end{pmatrix} = \begin{pmatrix} -0.202 & -0.144 \\ -0.005 & -0.017 \end{pmatrix} \begin{pmatrix} x_{H424} \\ x_{NM2WC1} \end{pmatrix}$$

Moving one SWIC at a time, it is noted that if $\Delta x_T \le 50\,\mu m$, then $\Delta x_{H424} \le 250\,\mu m$ and $\Delta x_{NM2WC1} \le 350\,\mu m$. The angular stability is better than a micro radian.

To calculate the last two matrices the following transfer matrix between NM2WC1 and the target was used:

$$\begin{pmatrix} x_T \\ \dot{x}_T \end{pmatrix} = \begin{pmatrix} -0.34549 & 74.4209 \\ -0.021688 & 1.77726 \end{pmatrix} \begin{pmatrix} x_{NM2WC1} \\ \dot{x}_{NM2WC1} \end{pmatrix}$$

This corresponds to the solution of Figure 2.4.4. The units are microns and micro radians. The distances between SWICs is: 413 ft. from NM1WC to NM2WC1, and 1209 ft. from H424 to NM2WC1.

Over short periods of time, Case 3 is the preferred one. Over long periods it is not certain whether NM2EU will not change by more than 100 ppm, nor is it certain that two enclosures separated by 1200' (G2 and NM2) will not have relative horizontal displacements of more than a quarter of a millimeter. Therefore, Case 1 is recommended for the slow instabilities and Case 3 for the beam roll.

2.5.5 Beam Roll

This is the plan to correct for beam roll. If the beam position at H424 and NM2WC1 is measured with a precision of 50 microns (achievable using BPMs) and Case 3 of the previous section is used, then a stability at the target of 15 microns in beam position and 1 micro radian in beam angle should be achievable.

To correct for beam roll, the beam position at H424 and NM2WC1 will be measured and the magnets H424 and MuLam will be used to keep the beam stable at the previous positions. This loop will be closed adapting software that already exists in ACNET. The ACNET beam control system is capable of making several corrections during the spill.

The transfer matrices from A0 (extraction) to the target give an idea of the beam stability required at extraction. The following transfer matrices correspond to Figure 2.4.4. The units are microns and microradians.

$$\begin{pmatrix} x_T \\ \dot{x}_T \end{pmatrix} = \begin{pmatrix} -0.0137 & 4.252 \\ -0.1876 & -14.72 \end{pmatrix} \begin{pmatrix} x_{A0} \\ \dot{x}_{A0} \end{pmatrix} \quad \begin{pmatrix} y_T \\ \dot{y}_T \end{pmatrix} = \begin{pmatrix} -0.1151 & -12.21 \\ 0.1183 & 3.860 \end{pmatrix} \begin{pmatrix} y_{A0} \\ \dot{y}_{A0} \end{pmatrix}$$

For example, the following equation shows that the beam stability at the target is more dependent on angular stability at extraction than on position stability at extraction:

$$D x_T = \sqrt{(-0.0137 \bullet D x_{A0})^2 + (4.252 \bullet D \dot{x}_{A0})^2}$$

Thus, a 1 micron movement at extraction results in an 0.0137 micron movement at the target, whereas a 1 microradian movement at extraction results in a 4.252 micron movement at the target.

2.5.6   Conclusions

Table 2.5.4 shows a summary of Cases 1 and 3 of the subsection on SWICs stability:

Table 2.5.4

Parameter	Case 1	Case 3
Beam position stability (assuming stable instrumentation)	25 μm	15 μm
Beam angle stability (assuming stable instrumentation)	10 μrad	1 μrad
Required instrumentation stability	40 μm	250 μm
Assumes magnet stability	No	Yes
Separation between instrumentation	10'	1200'
Needed instrumentation position resolution	20 μm	50 μm

Case 3 relies on BPMs to measure beam position. Short BPMs can achieve a resolution of 50 microns at beam intensities of 3×10^{12} protons per pulse. Case 1 relies on new instrumentation to measure the beam position. The expected resolution of the new instrumentation is 20 microns (see section 2.7).

Case 3 is clearly better if one assumes that both the instrumentation and the magnets are stable. In the time scale of a few pulses this is certainly true. This is why the plan is to correct beam roll in this way. Over longer periods of time, it may be easier to keep NM2WC2 and NM2WC3 stable to 40 microns relative to the KTeV detector than to keep H424 and NM2WC1 stable to a quarter of a millimeter relative to each other and to the KTeV detector. Case 1 does not assume any special magnet stability. This is an advantage because to achieve a beam position stability of 50 microns at the target, NM2EU needs to be stable to 125 parts per million (see subsection on Magnet Stability).

Case 3 will then be used for fast corrections and Case 1 for slow ones. It should be mentioned again that since Case 3 uses ACNET the capability for making fast corrections already exists.

2.6   Target Scans

Table 2.6.1 illustrates the beam scan capabilities at the target. "Position scan" is defined as moving the beam position at the target without changing the angle. "Angle scan" means changing the beam angle without changing the beam position. The numbers were calculated for a beam energy of 800 Gev.

Table 2.6.1

Type of Scan	Horizontal	Vertical
Position	7 mm	5 mm
Angle	200 μrad	1.8 $mrad$

These numbers are calculated using the relation between magnet fields and SWICs positions given in section 2.5. For example, for a horizontal position scan the matrix relation plus the constraint that the beam moves the same amount in NM2WC2 and NM2WC3 were used.

2.7 Instrumentation

NM1

Two short external beam BPMs and a vacuum SWIC in NM1 are needed. This instrumentation is used on a regular basis at the Lab.

NM2

Two short BPMs and a vacuum SWIC for the upstream end of NM2 are needed. Again this is instrumentation used on a regular basis at Fermi Lab. For the region near the target, very good position resolution and the ability to accurately measure beam profiles is also needed. The current plan is to develop a wire SEM with 100 micron wire spacing. The standard wire SEMs that have been used in the past at the Lab do not work with slow spill. The reason for this is that the signal is too small when spread over 20 seconds. To enhance the signal the wires can be coated with CsI. These CsI coated wire SEMs have been tried at CERN and proved to work. The plan to acquire the expertise at the Lab is the following: a) the EED department is building a 100 micron wire spacing SEM, b) the CsI coating of the wires is going to be done by Dave Anderson's PDG Group, and c) the wire SEM is going to be tested at BNL.

How well can the average beam position with a 100 micron wire spacing instrument be measured? If the channels of the Scanner are all equal and the beam spans several wires, the average can be measured at least an order of magnitude better than the wire spacing. Of course there are problems with the Scanner, halo, etc. Figure 2.7.1 is a practical case of a one millimeter SWIC used with a regular Scanner. Each point in the figure corresponds to the average of the SWIC profile in the middle of the spill. A change of 150 parts per million in the beam momentum or in the NE9E currents produced a one millimeter displacement in the beam position (y axis in the figure) at NECPWC[19]. So the beam position oscillation seen in the figure represents an instability of 150 ppm peak to peak. The data was taken at the end of the last Fixed Target run and there was no time to determine if the

---

[19] NE9E is a string of five B1 magnets.

oscillation was caused by changes in the momentum or the NE9E magnets. However, it can be seen that the beam average was measured to better than one fifth of a wire spacing. This claim can be made because the difference between two successive points is on the average better than one division. The assumption is that with the 100 microns wire spacing SEM, one can determine the average beam position to 20 microns.
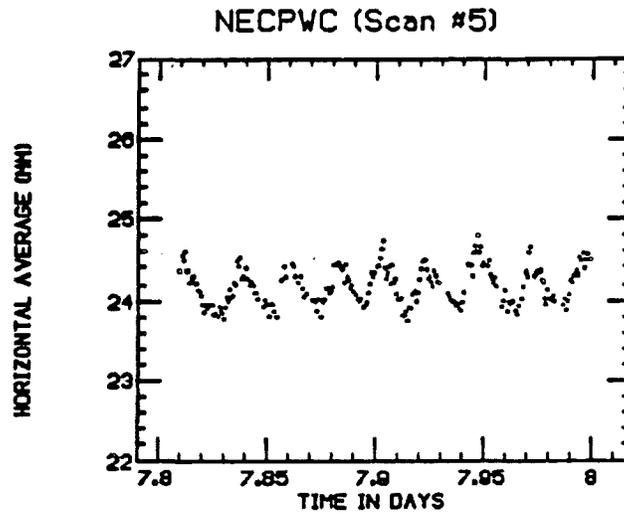
Figure 2.7.1

Average beam position at NECPWC as a function of time.
Each point corresponds to a SWIC reading in the middle of the spill.
The units are millimeters and days. The oscillation is due to a change
of 150 ppm in either the beam momentum or the NE9E current.

2.8. Muon Halo

This section will concern itself with muons transported to the target along with the primary beam. These muons will be assumed to have been produced from interactions at four different points: MuSep, MuBend, H424, and NM1. In all models a primary beam energy of 800 GeV and a 20s spill time is assumed. In this section, the detector is assumed to be a 4m by 4m area centered on the neutral beam, located 185m downstream of the target.

HALO Calculations and Impact

The program HALO was used to simulate beam interaction and muon production. Figure 2.8.1. shows the elements used in the model, with production points indicated by an asterisk. A primary beam intensity of 5×10^{12} ppp was assumed. HALO assumes muon production from four sources: pi+, pi-, K+, and K-decay. A separate run must be made for each production source. In all models, production is assumed to occur from one million protons interacting with one radiation length of iron. After each run, the muon distribution at the target was written to a file. This file was then used as the input spectrum to TRAMU, which transported the muons to the detector.[20]

---

[20] TRAMU is a subroutine in CASIMU which is responsible for muon transport. CASIMU will be detailed more fully in Section 4.4.2.

Target

NM1 Source

H424

H424 Source

MuBends

MuBend Source

MuLams

MuSep Source

MuSep
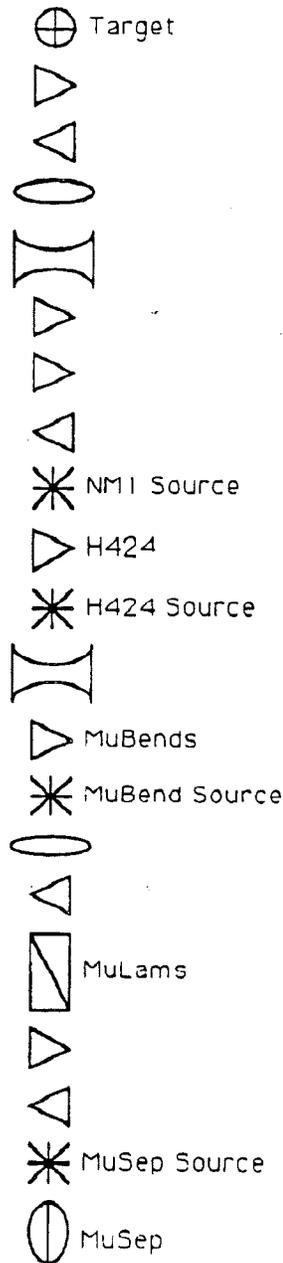
Figure 2.8.1.
Primary Beam Layout Used to Model Muon Halo
(Schematic - not to scale)

50

Table 2.8.2. shows the resulting muon rates at the target hall and the detector plane. Results are summarized in muons per interacting proton (p*) and kHz per interaction proton.

Table 2.8.2.

Location	Target Hall		Detector Plane	
	muon/p*	kHz/p*	muon/p*	kHz/p*
MuSep	2.18E-04	1.09E-08	0.00E00	0.00E00
MuBend	6.48E-05	3.24E-07	7.89E-07	3.95E-11
H424	4.29E-03	2.14E-07	2.67E-04	1.34E-08
NM1	6.42E-04	3.21E-08	2.80E-05	1.04E-09

H424 is the worst source for halo, due to the long (~800 foot) straight section between it and the next bend (located in NM1). This allows plenty of space for pions produced at H424 to decay.

Table 2.8.3. summarizes potential interactions and resulting rates at the detector.

Table 2.8.3.

Location	Source	Rate
H424	3mil Ti vacuum window	19kHz
NM1	Vacuum SWIC	16kHz
TOTAL:		35kHz

Table 2.8.4. summarizes rates at the detector due to 1% beam scraping at four locations.

Table 2.8.4.

Location	Rate	
MuSep	0	kHz
MuBend	2.0	kHz
H424	670	kHz
NM1	52	kHz

Operational Expectations, Control

Clearly, beam scraping must be avoided and as little instrumentation as possible must remain in the beam.

The SWIC in NM1 may be kept out of the beam, except for diagnostic use. As the window at H424 separates the cryogenic vacuum system from the conventional vacuum system, this source cannot be eliminated.

Adequate control must be provided in order to reduce beam scraping to less than 0.01% at H424 and 0.1% at NM1. This would result in background due to beam scraping at the 10kHz level.

2.9   Component's Identification

All the magnets exist. Four beam line BPMs and their associated electronics have to be acquired. The two target wire SEMs and the associated scanner have to be developed. The two vacuum SWICs and the intensity monitor SEM already exist.

2.10   RD/AD Beam Control Link

The plan is to use ACNET (the Accelerator Division Beam Control System) to correct for beam roll. To correct for instabilities that happen over a time scale of a few spills or more, the plan is to use EPICURE (Research Division Beam Control System). Therefore a communication channel between the two systems is needed. The ACNET system needs to be able to read the BPMs and the SWICs in NM2, and the EPICURE system needs to be able to read the current changes in the part of the KTeV beam line that is controlled by ACNET.

3. CRITICAL DEVICES/ INTERLOCKS

3.1 Primary Beam

3.1.1 Precluding downstream primary transport

A combination of careful alignment, configuration control processes, and active current interlocks will be used to prevent the primary beam at 800 GeV from exiting the KTeV Target Pile:

1- Interlock the AVB currents to $I_{NM2D1} + 0.5*I_{NM2D2} \geq 4630$ amps. This will ensure that the minimum targeting angle will be -4.0 mrad. These supplies should also be controlled such that they will always bend positively charged particles down.

2- Interlock the NM2EU current to ±68 amps from the nominal value.

3- NM1U and NM2EU will be used as collimators to limit positions excursions. Therefore they must be carefully aligned and their configuration maintained by using "RED TAGS" on lock outs on position-adjusting devices.

4- Interlock the quadrupole currents to: a) $0.217\, I_{NM2Q1} + I_{NM2Q2} = -567 \pm 86$ amps, and b) $I_{NM2Q1} \leq 1011$ amps.

The extreme position changes allowed with these interlocks are shown on Figure 3.1.1, which is taken directly from Appendix 3. The precise values of the current interlocks depend on the final configuration of the Primary Beam line, but the methodology presented in Appendix 3 is applicable in case this should change.

Primary beam must not be transported through the neutral beam channel into the KTeV experimental hall since it is designed only to accept secondary beam of much lower energy and intensity. In addition beam line elements downstream of the targeting station within NM2 are not set to transport 800 GeV particles. Because

of this, the introduction of primary beam into the neutral beam channel could result in higher than normal losses downstream of the targeting station. This could cause significant residual radiation dose rates, contamination, and increased air activation. Routine maintenance and unscheduled repairs would be more difficult. Therefore the goal in selecting the interlocks is to insure that the 800 GeV primary beam is confined to the well-shielded target station.

To prevent the beam from exiting the KTeV Target Pile, we specifically prevent an 800 GeV primary proton from entering the neutral beam aperture of NM2S2, the first major element downstream of the KTeV Target Pile. The calculations for these interlocks were done to prevent a primary proton having the maximum possible deviation from the beam centerline from leaving NM2BD (the NM2 Beam Dump). The maximum allowed deviation from the primary beam centerline places a primary proton on the edge of the aperture of the Beam Dump. The assumptions to insure careful alignment between NM1 and NM2 are that when the beam is vertically centered at NM1U and NM2EU, the quadrupoles do not significantly steer the beam and the incoming angle of the beam on the target is minimally -4.00 mrad. These assumptions are easily checked when the beam is first turned on. The NM2S1 magnet (the Target Sweeping Magnet) running at the nominal 5kG will not provide adequate protection to prevent beam from being horizontally steered into the neutral channel of the secondary beam, so all calculations were applied to achieve adequate protection through vertical steering. The resulting current limits on the NM2 magnets were based on limiting the possible angles that a primary beam can have going into the quadrupoles. The interlock on NM2S2 was calculated to prevent beam from being directed into NM3 in the accident case of the AVB system tripping off.

Please see Appendix 2 for a detailed discussion on the calculation of these interlocks.

KTeV Primary Beamline Apertures - NM1 through NM2
Elevation view

NM1U NM1H Berm (not to scale)

NM2EU NM2V NM2Q1 NM2Q2 AVB Dipoles NM2H NM2S1 NM2BD NM2S2 NM2S3

PRIMARY COLLIMATOR

Nominal Primary Beam Centerline

TARGET

Neutral Centerline

Allowed Uncertainty for ±0.5" Between Enclosure Survey

NM1U configuration controlled

Case 1

Case 2

410' long Beam Pipe

1"

10'

NM2EU interlocked to ±68 amps from nominal and configuration controlled

NM2 Quadrupoles interlocked to:
0.217*I_{NM2Q1} + I_{NM2Q2} = -567 ±86 amps
I_{NM2Q1} ≤ 1011 amps

AVB Dipoles interlocked to
I_{NM2D1} + 0.5*I_{NM2D2} ≤ 4630 amps

Figure 3.1.1: KTeV Primary Apertures. Shown here are the vertical apertures for the magnets from NM1 to the KTeV Target Hall, with the Nominal Primary Beam Centerline shown for the path of primary beam with the AVB system set to bend the beam to -4.00 mrads at the Target. The two extremes shown as thick solid lines are for beam entering NM2 at ±0.6629 mrads relative to the nominal beam trajectory, the beam paths from the lower aperture limit of either NM1U or NM2EU to the upper aperture limit of the other. The thick dashed lines are for beam entering at ±0.0947 mrad relative to the nominal beam trajectory, the beam path due to the allowed survey tolerance between enclosures, staying on the same side of the nominal beam along the edge of the NM1U and NM2EU apertures. The solid beam paths cross each other in the beam pipe region between NM1 and NM2. The magnets are set to produce the maximum allowed deviation from the nominal with these extremes at the downstream end of the Beam Dump.

Case 1 is for the NM2 quadrupoles set to R_{21}=-0.500 mrad/cm and R_{43}=-0.430 mrad/cm.

Case 2 is for the NM2 quadrupoles set to R_{21}=-0.500 mrad/cm and R_{43}=-0.687 mrad/cm.

For both cases, the AVB system is set to its minimum limit, and NM2EU & NM2V to their maximum upward bending limits. The range for allowable quadrupole current settings lie between these extremes. Note that the AVB and NM2S1 magnets are not configuration controlled in this scheme. [From Figure A3.1 from Appendix 3.]

3.1.2   Critical Devices /Coupling with Neutrino Area

Besides the special interlocks listed in Section 3.1.1 to preclude primary beam transport downstream of the target hall, the KTeV primary beam will utilize upstream Critical Devices, that when disabled will protect the KTeV beam enclosures and experimental area from any beam transport, and hence any significant prompt radiation.

The primary beam Critical Devices for KTeV are the same as used in previous runs for the NMUON beam line. These are MULAM and MUBD located in the AD Switchyard beam transport system. These elements will continue to have typical Research Division Critical Device interlocks fitted, as well as a Failure Mode Backup circuit, which reverts to disabling upstream Switchyard devices to ensure further redundancy in safety protection.

All enclosures associated with the KTev beamline will have standard Research Division enclosure interlocks which will monitor all access points. Each Interlock Section will have a Radiation Detector Chassis incorporated into the Summation Chassis to permit the use of interlocked detectors if the need arises.

Monitoring of target hall magnet temperatures and flow of RAW cooling water can also be sensed by the interlock system.

As for previous running of the NMUON beamline, shared tunnel geometry imposes a strong coupling between KTeV beam operation and interlock status of the Neutrino Area upstream enclosures. The Neutrino Primary run condition must be satisfied to operate KTeV beam.

3.2   Secondary Beam

3.2.1   Critical Devices

A required feature, due to the location of the KTeV experimental area in the upstream NMUON beam area, is that disabling of the primary beam to NM2 will be needed to ensure radiation protection for the NM3 secondary beam enclosure and the KTeV experimental hall.
This is due to the intense muon fluxes present in these enclosures from primary beam dumping in the NM2 target hall. Projected muon rates in the decay enclosure and experimental hall are shown in Figures 4.4.10 and 4.4.11. These rates could be reduced somewhat by requiring the primary target to move to an "out" position as part of disabling the secondary beam. However, even then they would still be well above the 2.5 mr/hr limit for access into the enclosures.[21]

Hence, the same critical devices MULAM and MUBD are projected for the KTeV secondary beam. A fast activated beam stop is planned to be installed in NM2 downstream of the beam dump system, which will selectively stop the neutral hadron beam from exiting NM2. The function of this device is very useful for aiding in selective radiation and particle rate measurements in the downstream enclosures. However, it is not adequate as a Critical Device element due to the beam dump muon fluxes.

3.2.2   Experimental Hall Interlocks

The decay enclosure and the experimental hall will also have standard Research Division enclosure interlocks and a Radiation Detector Chassis incorporated into the Summation Chassis in order to monitor and/or control prompt radiation rates.

Access interlock doors between the counting room area and the experimental hall will be positioned in the passage ways to the experimental hall, allowing

---

[21] W. S. Freeman, et al., "Radiation.Shielding Requirements for the KTeV Facility," January 13, 1993.

unlimited access in the counting room areas outside of these doors. The results of calculations addressing radiation levels in these passages are presented in Section 6.

3.3 Access Issues

3.3.1 Access Requirements

The capability to separately and efficiently access each Fixed Target experimental hall with minimal impact to other experiments has been very important for the operational efficiency of the external areas Fixed Target program. The detector system redundancies built of necessity into the large collider detectors, due to their limited access options, are extremely expensive and not a realistic option for the Fixed target detectors.

Timely access into the experimental hall is especially important for the KTeV experiments due to the precision measurements involved. This has been reaffirmed in the Oct.'93 Director's Review of KTeV, and was recommended by that Review Committee as an Action Item to be accomplished for KTeV.

3.3.2 Options Considered

There are three currently accepted methods of controlling Fixed Target experimental hall radiation levels during access conditions. Each has been evaluated for possible KTeV application.

The first method is to utilize enough shielding between the targeting enclosure and the experimental hall to sufficiently range out the bulk of muons produced in the target pile. This method, suitable for long secondary beam lines, allows access into the experimental hall with the least disruption in overall program stability. By use of standard Research Division Access Device Controllers the secondary beam created from normal targeting is blocked with the use of redundant beam stops located downstream of the target pile. This approach can be used when a prompt dose rate less than 2.5 mr/hr can be maintained during the

access with continued primary beam targeting. As indicated in Section 3.2, beam dump muon fluxes preclude this method for KTeV with it's short secondary beam length.

A second method is to utilize a separate RAW cooled dump system at a location upstream of the targeting enclosure. Size of the dump and it's cost is driven by the intensity and duration projected for dumping the beam. Two factors which must be considered are groundwater activation and radiation rates, both prompt and residual. This was the method available in previous running in the Meson Area, where the pre-Tev II target piles remained available for use during either current targeting enclosure or experimental hall accesses.

For KTeV , the installation of an upstream RAW cooled beam dump could possibly be located in the downstream end of the AD/Switchyard Enclosure G2, if this were the method chosen. Other location options between G2 and NM1 would require new civil construction.

The third access method is to take away the KTeV primary beam using the upstream electrostatic septa splitting station, and redistribute it as feasible to other beamlines. Historically, this is the least preferable method due to the considerable disruption to other beam users. If this were the method chosen for KTeV, practical application difficulties should make as a priority task an effort to automate and improve the efficiency with which the various Switchyard primary beam intensities . can be controlled. Significant prototyping efforts including beam tests have previously taken place toward this end, as there would be significant improvement in operational efficiency for all fixed target users. The location of the SY electrostatic septa splitting station for KTeV, downstream of other area septa splits, also makes this a more challenging task to accomplish quickly for this beam without beam splitting control upgrades. This is due to beam tails from other splits effectively expanding the size of the beam to KTeV.

Resolution of a practical and reasonable access method to the KTeV experimental hall remains a major unresolved issue, needing approval and effort from both the lab Research and Accelerator Divisions.

4.   BEAM DUMP/MUON SWEEPING

The Beam Dump System is made up of the Primary Beam Dump and its associated shielding, the Muon Sweeping System and the Radioactive Water (RAW) Cooling System.

4.1   BEAM DUMP SYSTEM - OVERVIEW

4.1.1   System Function and Location

The Beam Dump System:

· stops the primary beam
· sweeps charged particles out of the neutral secondary channel
· sweeps muons away from the detector and personnel
· keeps muons below grade level, eliminating the issue of muons at
  the site boundary
· provides shielding to control residual radiation levels and
· provides ground water protection.

The components of the Beam Dump System are:

· Target Sweeping Magnet - NM2S1
· Primary Beam Dump - NM2BD
· E8/Hyperon Magnet - NM2S2
· Mu-Sweep II - NM2S3
· Target Pile Shielding
· Radioactive Water Cooling System - RAW water system

With the exception of steel to provide muon "ranging" buried between the NM2 and NM3 enclosures, the Beam Dump System is entirely in NM2.

The NM2 enclosure is made up of 3 principle sections; an upstream section which houses the components of the Primary Beam, a larger, "hall-like" section

which houses the components of the Beam Dump System, and a downstream section which houses components of the Secondary Beam. The hall is referred to as the KTeV Target Hall. See Section 2 for a description of the Primary Beam and Section 5 for a description of the Secondary Beam. Plan and elevation views of the KTeV Target Hall and its associated components are found in Figures 4.1.1 and 4.1.2, respectively.

Not all beamline components in the KTeV Target Hall are addressed in this section. The target, the lead and beryllium absorbers, and the primary collimator are described in the section on the Secondary Beam.

4.1.2   Component Function & Location

Target Sweeping Magnet - NM2S1

The Target Sweeping Magnet is the first element following the target, and like the target, is located inside the steel shielding of the Target Pile. The label NM2S1 indicates that it is the first sweeping magnet in the NM2 enclosure. This magnet provides early horizontal sweeping and early absorption of charged secondaries.

NM2S1 also fulfills a limited radiation safety role as a fixed-hole or "shadow" collimator. The magnet steel geometrically shadows the aperture of the beam dump, eliminating any primary beam "line-of-sight" through the dump aperture. This is independent of beam displacement at the target.

Because NM2S1 sweeps horizontally, the desired vertical placement of the primary beam spot on the beam dump depends only on the vertical angle of the beam at the target. Therefore no current interlock is required for NM2S1.

Primary Beam Dump

The Primary Beam Dump is also in the Target Pile and is downstream of the Target Sweeping Magnet (see Figure 4.1.1). The beam dump stops the primary beam. Under normal operating conditions the primary beam interacts in the front face of the dump below the aperture . However under certain conditions it is possible for the beam to dump inside the aperture. This issue is addressed in Section 3.
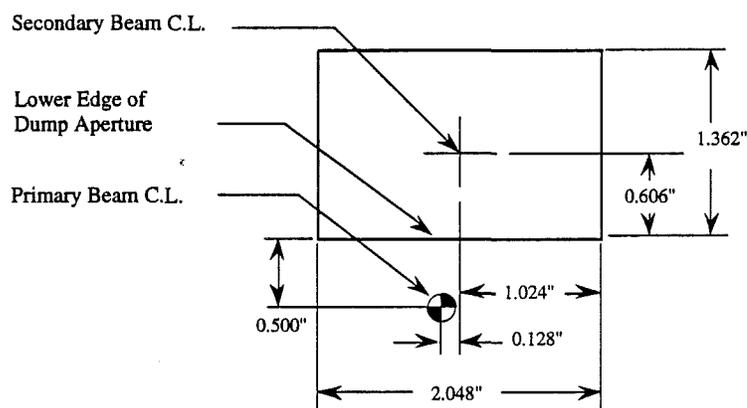

Figure 4.1.3
Primary Beam Position at Upstream Face of Primary Beam Dump
(Minimum incoming beam angle of -4 mradians is assumed for calculation.)
(Units are inches.)

E8/Hyperon Magnet - NM2S2

This magnet has been used elsewhere at Fermilab and is often referred to as the E8 Magnet or the Hyperon Magnet. Its correct designation for KTeV is NM2S2, indicating that it is the second sweeping magnet in the NM2 enclosure. NM2S2 is located immediately downstream of the Target Pile after the Primary Beam Dump.

NM2S2 separates prompt and decay muons from the target and dump into two muon "plumes" horizontally separated by sign. These plumes are directed to

either side of the neutral centerline resulting in a lower muon rate at the detector. The complete Muon Sweeping System is described in Section 4.4.

In addition, because of the large cross-section of NM2S2, few muons see a magnetic field component that sweeps them above grade level. As a result, the muon plumes remain below grade and muon rates above grade and at the site boundary are well below limits (see Section 4.4.1).

NM2S2 is also part of the radiation safety system providing backup sweeping and bulk shielding should the primary beam be lost within the aperture of the beam dump.

Mu-Sweep II - NM2S3

Mu-Sweep II is the third and most downstream magnet in the Beam Dump System. During design the "II" identified it as the second conceptual design iteration of the magnet. The current, correct designation, NM2S3, identifies it as the third sweeping magnet in NM2. All three sweeping magnets in NM2 have the same sign magnetic field, sweeping positives to the west.

NM2S3 has two principle functions. First, it contributes to the horizontal separation of the muon plumes away from the detector. See Section 4.4 for expected muon rates. Secondly, it provides cleanup sweeping in the neutral channel due to its location downstream of the lead and beryllium absorbers and the primary collimator.

Target Pile Shielding

The Target, the Target Sweeping Magnet, and the Beam Dump must have sufficient radiation shielding to allow beam-off access into NM2 for routine maintenance, repairs or measurements after primary beam has been delivered to the area. Also sufficient shielding must be present to provide radiation protection for groundwater during beam-on operation.

The required radiation protection is provided by approximately 900 tons of steel shielding which surrounds the elements of the target pile. The radial thickness of the steel is set by satisfying the groundwater requirements (see Section 6.8.2). The resulting steel thickness more then satisfies the 100 mr/hr at 1' residual activity limit at any accessible part of the Target Pile (see Section 6.9).

Cooling

A closed loop, water system is used to provide cooling for the Target Sweeping Magnet, its collimator inserts and the dump. This closed loop system is referred to as the RAW (Radioactive Water) cooling system.

The standard Research Division, LCW (Low Conductivity Water) system is used to provide cooling for components in the Target Hall that will not be activated with primary beam. The target (see Section 5) does not require water cooling.

4.1.3 Apertures

The apertures through the Target Sweeping Magnet, the Primary Beam Dump and the Hyperon Magnet were sized, where possible, to be 0.250 inches greater then the exclusion line limits proposed in the memo "Design Considerations for the KTeV Target Pile", January 24, 1993. This exclusion line (shown in the following figure) is designed so there is no direct line of sight through the collimator to material upstream of the primary collimator. This insures scattering from the apertures upstream of the primary collimator do not enter the apparatus. The dimensions of the exclusion area decrease vertically and increase horizontally with increasing distance downstream of the target.

The following figures show the aperture size, the exclusion lines (which define the "exclusion area"), and the size of the neutral beam envelope for the Beam Dump System elements that are upstream of the primary collimator. The apertures of these elements were sized in each plane according to the largest dimension of the exclusion area in each element.
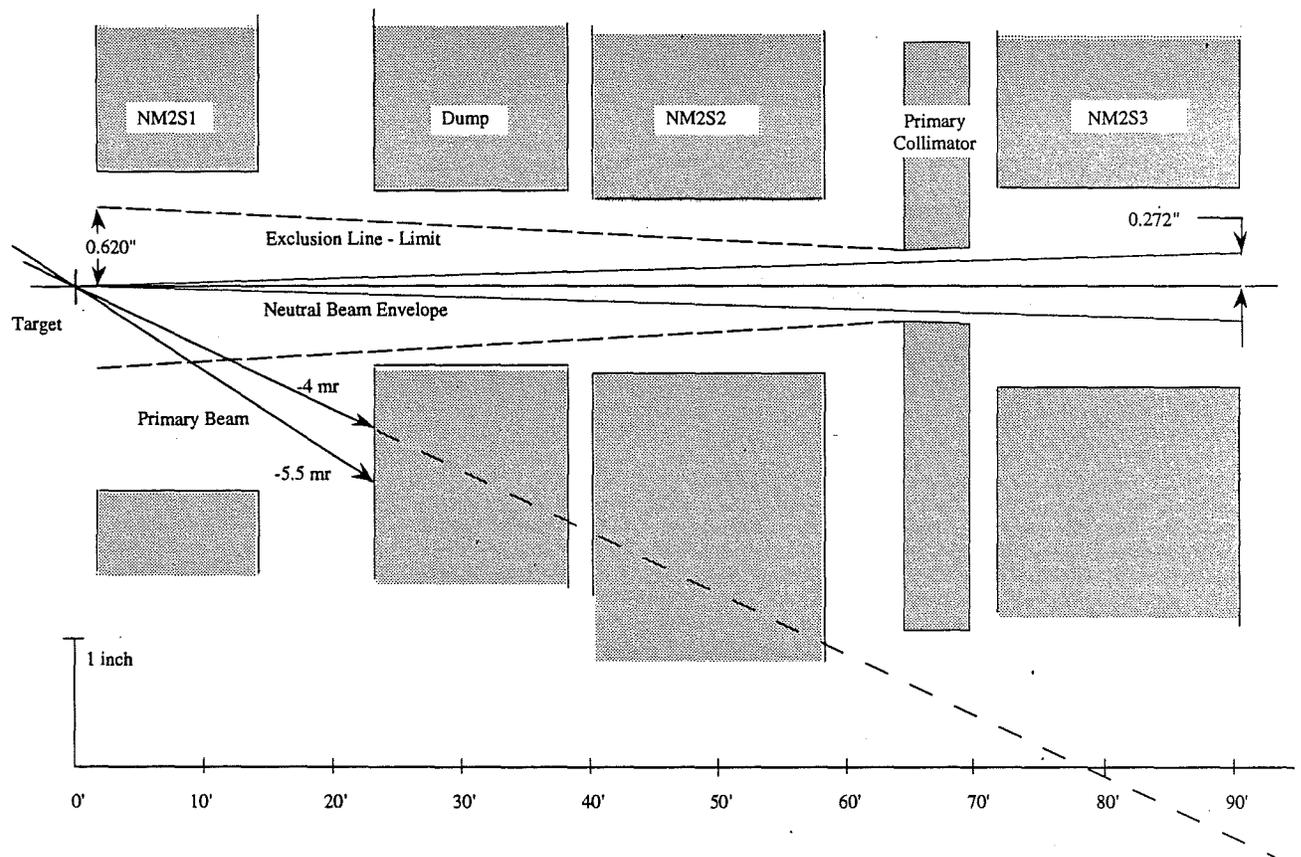
Figure 4.1.4

Apertures w/ Exclusion Lines through the KTeV Target Hall Elevation View

Reference: Neutral Beam
Elevation = 733.924'

Exclusion Region

Lower Edge of
Magnet Aperture

0.281"

0.900"

2.500"

Alignment Tolerances
Vertical: +/- 0.025"
Horizontal: +/- 0.025"

0.925"

0.255"

1.850"
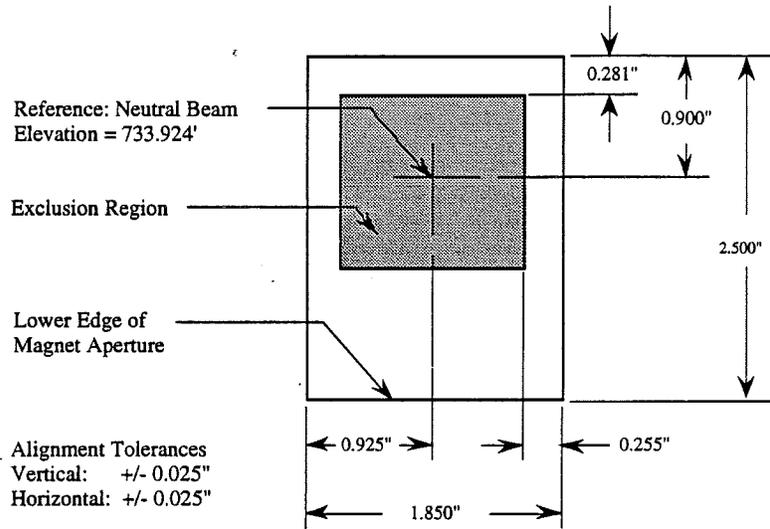
Figure 4.1.5

NM2S1 Aperture, Exclusion Area and Installation Tolerance
(Units are inches)

Reference: Neutral Beam
Elevation = 733.924'

Envelope of Accepted
Secondary beam

Exclusion Region

Lower Edge of
Dump Aperture

0.756"

1.362"

0.606"

Alignment Tolerances
Vertical: +/- 0.025"
Horizontal: +/- 0.025"

0.774"

1.024"

0.100"

2.048"
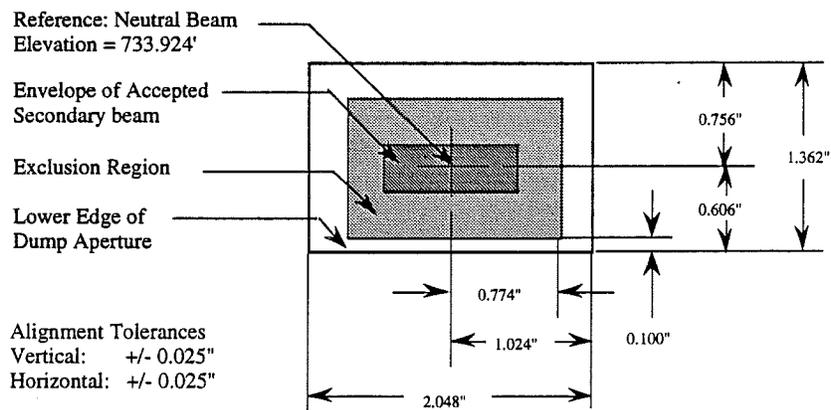
Figure 4.1.6

Primary Beam Dump Aperture, Exclusion Area and Installation Tolerance
(Units are inches)

Reference: Neutral Beam
Elevation = 733.924'

Envelope of Accepted
Secondary beam

Exclusion Region

Lower Edge of
Magnet Aperture

0.415"

0.665"

1.330"

Alignment Tolerances
Vertical: +/- 0.025"
Horizontal: +/- 0.025"

0.863"

1.113"

2.226"
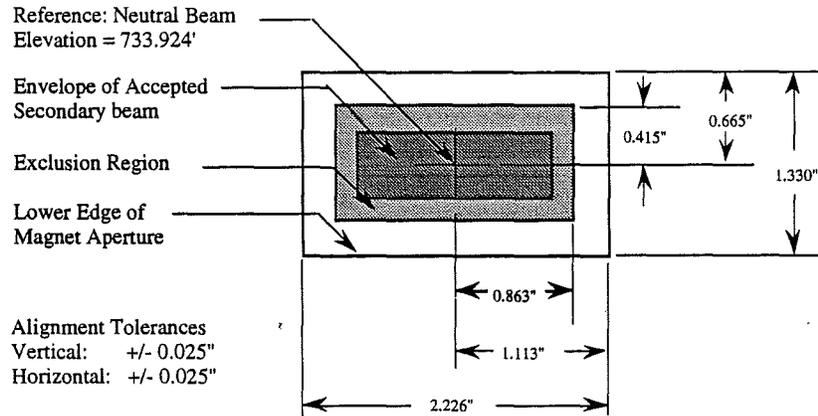
Figure 4.1.7

Hyperon Magnet Aperture, Exclusion Area and Installation Tolerance
(Units are inches)

4.2   DESIGN AND INSTALLATION

A list of common design requirements incorporated into the Beam Dump System follows:

- Provide vertical adjustment to account for settling.
- Provide access to all elements to permit alignment measurements.
- Design to use the Target Hall crane.
- No secondary beamline collimation will occur inside the target pile or elements that cannot be remotely adjusted.
- Where possible, apertures will be 0.25 inches larger than the exclusion line limits defined.
- Design should allow straightforward replacement with available spares.

4.2.1 Target Sweeping Magnet - NM2S1

NM2S1 is a modified version of the standard, Research Division, Target Dump Magnet, also referred to as an Eartly Dump Magnet. To accommodate the possible range of primary beam angles, positions and sizes, the "nominal" vertical aperture of the magnet is increased from 1.125 inches to 2.500 inches. This reduces the maximum magnetic field of the magnet from 20 kG to 9 kG. The expected operating field of NM2S1 is 5 kG.

To provide early absorption of pions, high density spacers made of brass or copper are inserted in the horizontal plane of the magnet aperture. These spacers define the horizontal aperture width of 1.850 inches and are pinned into place against the pole tips. The spacers are cooled with water from the RAW system. Figure 4.2.1 shows an engineering drawing of the modified magnet.

NM2S1 and its support structure will be pre-assembled and pre-aligned in the shop. This assembly will then be installed on the centerline of the neutral beam in the open Target Pile. Self-centering pins in the magnet support allow the alignment to be preserved should there be any need to exchange the magnet in the future.

Standard alignment fixtures are permanently attached to the east side of the magnet and are fiducialized to the aperture centerline both horizontally and vertically. These fixtures and the adjustable jacks that support the magnet are accessible through "ports" in the east side of the shield pile. The jacks will allow ±1 inch height adjustments to the magnet after installation.

Because the magnet position will be stable in the horizontal direction and the magnet aperture has been oversized 0.5" (±0.25") in the horizontal (and vertical) plane (with respect to the exclusion lines), no remote, external "post-installation" horizontal adjustment has been provided. Any further horizontal adjustment after installation will require opening the target pile.

4.2.2 Primary Beam Dump - NM2BD

The primary beam dump is a water cooled copper block, 15 feet long x 8 inches wide x 10 inches high, clad in two bands of steel, each 3 inches thick. The "inner" steel band runs the entire 15 foot length of the copper dump and the "outer" band is 7.5 feet long centered lengthwise on the dump. The resulting "stagger" in the steel bands is mirrored by an equivalent "stagger" in the steel shielding of the target pile dump cavity. This eliminates any "straight through" line-of-sight to the upstream end of the dump. Centering the outer band keeps the loading symmetric when handling the dump. Figure 4.1.1 shows how this package fits in the Target Pile steel shielding.

Figure 4.2.2 shows the dump design in more detail. There are 4 independent water loops through the copper. These water loops use a common manifold connected to the RAW water supply. The water manifold will be on the downstream end of the dump where it will be accessible for service.

Alignment fixturing is permanently attached to the east side and the downstream face of the dump. The alignment fixtures are fiducialized to the centerline of the aperture. A port is available through the Target Pile to access the upstream alignment fixture. The downstream fixtures are visible at the downstream face of the Target Pile.

Like the target sweeping magnet, the dump is supported on jack stands that are accessible through ports in the east side of the Target Pile. These stands allow a ±1 inch vertical adjustment in the height of the dump to correct for any settling in the Target Pile that may occur.

The dump is installed and aligned in the same way as the Target Sweeping Magnet. That is, the dump and its support structure will be pre-assembled and pre-aligned in the shop and installed as a single assembly.

Because the beam dump position will be stable in the horizontal direction and the dump aperture has been oversized 0.5" (±0.25") in the horizontal plane (with respect to the exclusion lines), no remote, external "post-installation"

horizontal adjustment has been provided. Any further horizontal adjustment after installation will require opening the target pile.

4.2.3 E8/ Hyperon Magnet - NM2S2

The Channel

Studies using POISSON[22] and CASIMU[23] (see Section 4.4.2) led to the pole tip and channel design shown below. Steel is used to extend the NM2S2 pole tips and copper spacers define the aperture in the horizontal bend plane. The copper provides mechanical support and is becomes part of an extended beam dump should the primary beam be dumped inside the Primary Beam Dump aperture as described in Section 3.1.1.
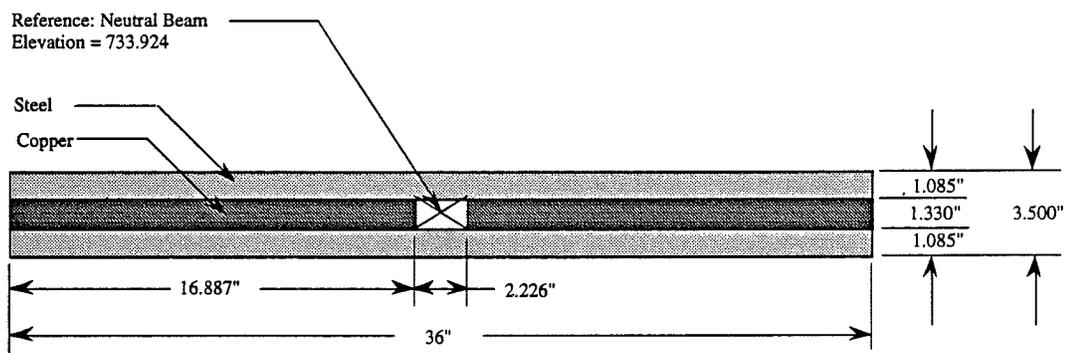
Figure 4.2.3
Hyperon Magnet Channel

---

[22]POISSON is a generic name for a set of codes that solve the generalized Poisson Equation for magnets; see Los Alamos Accelerator Code Group, Reference Manual for the POISSON/SUPERFISH Group of Codes, LA-UR-87-126 (January, 1987)

[23]CASIMU is a modified versino of the hadronic cascade program CASIM; see A. Van Ginneken, Fermilab Report FN-272 (1975)

Because beam could be dumped at the end of the Primary Beam Dump (Section 3.1.1), water cooling is provided for the Hyperon Magnet Channel (which is immediately downstream of the dump). (These water cooling paths are not shown in Figure 4.2.3). Cooling water is supplied by the RAW water system. The magnet coils are cooled with LCW. At full current, the field across the pole tips is expected to be 23 kG.

Support Structure

The support stand for NM2S2 is designed to allow position adjustments horizontally and vertically as small as 1 mil. Vertical adjustments are made by temporarily lifting the I-beam (and magnet) on jacks, installing or removing shim stock of the right thickness between the vertical columns and the supporting I-beam, then replacing the I-beam on the shimmed column.

The support columns sit on brass plates that allow horizontal adjustments to be made by jacking against fixed stops. See Figure 4.2.4 for a conceptual engineering drawing of NM2S2 and its support structure.

The Hyperon Magnet steel and coils are available for NM2S2. The steel requires some clean-up from long outdoor exposure as well as preparatory work to accept the support structure.

The magnet and its supports will be pre-assembled in the Meson Assembly Building, partially dismantled for shipping, then re-assembled in the NM2 Hall (after completion of the Target Pile).

4.2.4   Mu-sweep II - NM2S3

NM2S3 is a new magnet, not yet constructed. See Figure 4.2.5 for a conceptual engineering design. The coils are designed. Most of the required steel is available on-site including Maryland Cyclotron Steel left over from the spectrometer magnet construction. The magnet will be assembled in the KTeV

Target Hall on a support structure that will permit both vertical and horizontal adjustment.

This is a "C-Type" magnet with the return yoke displaced to the west, outside of the westward going muon plume. The magnet poles give an additional kick to the muon plumes, further separating them horizontally away from the detector. The magnet is 19 feet long with a magnetic field of 19.3 kG. The coils will be water cooled with LCW.

To accommodate the installation of Mu-Sweep II, the cable tray and LCW on the west wall of the downstream end of the Target Hall will need to be either modified or raised. The cable tray will need to be temporarily removed during the magnet installation.

4.2.5   Target Pile Shielding

The Target Pile houses in beam order, the Target and Target Drive, the Target Sweeping Magnet and the Primary Beam Dump.

The steel shielding of the target pile, starts 8.2 feet downstream of the beginning of the KTeV Target Hall and extends 41.3 feet to the end of the Primary Beam Dump.   See Figure 4.1.1.

Requirements for groundwater radiation protection set the outer dimensions of the steel shield. These dimensions require approximately 44 inches of steel below the beam centerline and 60 inches radially to the sides and top.   See Figure 4.2.6. The program CASIM[24] was used to establish the amount of steel necessary for groundwater protection.   This analysis is described in Section 4.3.2.

The target is recessed 3.0 feet downstream of the beginning of the Target Pile in an re-entrant cavity.   Cabling for the target mover, instrumentation cabling (e.g., SWIC and klixons) and the RAW water cooling loop for the target magnet inserts

---

[24]A. Van Ginnekin, CASIM, Program to Simulate Transport of Hadronic Cascades in Bulk Matter, Fermilab Report FN-272 (1975)

are routed through the upstream, re-entrant cavity of the Target Pile. Klixon cabling for the dump is routed through the downstream face of the target pile.

The bus that provides power and RAW cooling for NM2S1 are brought through vertical ports in the top of the steel shielding that are located at the west, downstream end of the magnet. Access "ports" are also provided horizontally through the steel for alignment and jack adjustment. These ports are normally plugged and are opened only when alignment measurements or vertical adjustments to the target magnet or the dump need to be made. The alignment and adjustment ports are made of 2" diameter tubing that fits through rectangular flame cut holes in the steel plates. The gaps between the tubing and the steel plates are filled with steel stock.

The new target pile has been designed using steel pieces from the existing MC6 and NM2 target piles. The residual activity and contamination levels within these piles will determine the success of this plan. Handling, grinding, and flame cutting limitations on radioactive steel will determine whether and how any given piece from MC or NM is used in the new pile. An attempt to identify alternative sources of steel is underway.

As currently configured, the NM2 target pile does not match KTeV's requirements and will be entirely removed. And although pieces of the current pile are intended to be re-used for KteV, there is insufficient space in the NM2 enclosure to allow simultaneous staging and construction.

Staging areas will be developed in the Meson Area and as close to NM2 as the KTeV Experimental Hall construction will allow, to handle the the removal of the MC6 and NM2 target piles. Radiation and dimensional measurements of each piece will be made to determine the disposition of each piece as it is removed from its existing target pile. Cutting will be done either in the staging areas or the Target Service Building depending on the radiation class of the steel. Unused steel will be sent to the railhead.

A steel stacking plan, referencing MC6 and NM2 Target Pile design drawings has been developed. Figure 4.2.7 shows two views of the new KTeV Target Pile steel

plate stacking plan. Additional drawings, not included here, show each of the steel layers in detail. Each steel plate has a number painted on it which identifies its original source and its location in the original pile. Five digit numbers identify the steel as coming from MC, two digit numbers identify the steel as coming from the old NM2 Target Pile.

Both the KTeV Target Hall and the MC6 target piles have existing 20 ton crane coverage. This, along with "drop hatch" access limitations in NM2 determine the maximum size of any piece to be handled in NM2.

Because space is not available in the upstream section of NM2 to store spare magnets, a wedge shaped piece of the target pile may be removed to allow the passage of a 20 foot B2 magnet (See Figure 4.1.1). This wedge shaped piece is normally in place and can be removed by the crane if necessary. See Figure 4.1.1.

4.2.6 Cooling

Radioactive Water Cooling System (RAW)

The RAW cooling system will provide cooling for the NM2S1, its inserts and the Beam Dump. It will be located downstream of NM2S3 and the absorbers, against the west wall (see Figure 4.1.1). This area is under crane coverage and personnel access will be by ladder over NM2S3.

These elements represent a total thermal load of approximately 55 kW, which is slightly below the 60 kW capability of the existing system in NM2. ICW (Industrial cooling water) can be supplied to add another 20 to 30 kW of cooling to the RAW system if necessary. RAW piping along the west wall of the Target Hall is available to be used with minimal modifications.

Low Conductivity Water (LCW)

In the KTeV Target Hall, LCW is required by NM2S2 and NM2S3. While these elements and the components of the primary beam can be supplied at the limit of the existing LCW system, the addition of the secondary beam LCW

requirements exceeds the 300 gpm flow rate of the current 4" header. The header size will be increased to 6" enabling the 570 gpm flow rate required by KTeV however the existing piping within NM2 will not require any significant modification. See Table 7.2 for flow requirements.

4.3 INSTALLATION

The NM2 components will be installed in the following order:

- Primary beam magnets and beam pipe in the NM2 upstream extension
- Secondary beam elements and beam pipe in the NM2 downstream extension
- The Target Pile Steel and
    - The Target Sweeping Magnet
    - The Primary Beam Dump
- The Hyperon Magnet
- Mu-Sweep II
- RAW cooling system
- Target, SWICs, Absorbers and Primary Collimator.

Since NM2S2 effectively blocks the access way to large pieces, pre-staging of the NM2S3 steel in NM2 after the target pile installation but before the NM2S2 installation will be required. Space is available in the downstream NM2 section for pre-staging NM2S3.

Handling and staging plans are being developed to account for post-installation staging that might be required during repairs or access to the target pile. Sufficient space is available in the NM2 enclosure to accommodate this. Figure 4.2.8 shows an open Target Pile and indicates which steel plates (dashed lines) must be removed to replace the Target Sweeping Magnet. The fixture which helps to preserve alignment by guiding the magnet onto its already aligned stand can also be seen.

Figure numbers mentioned in this section follow next.
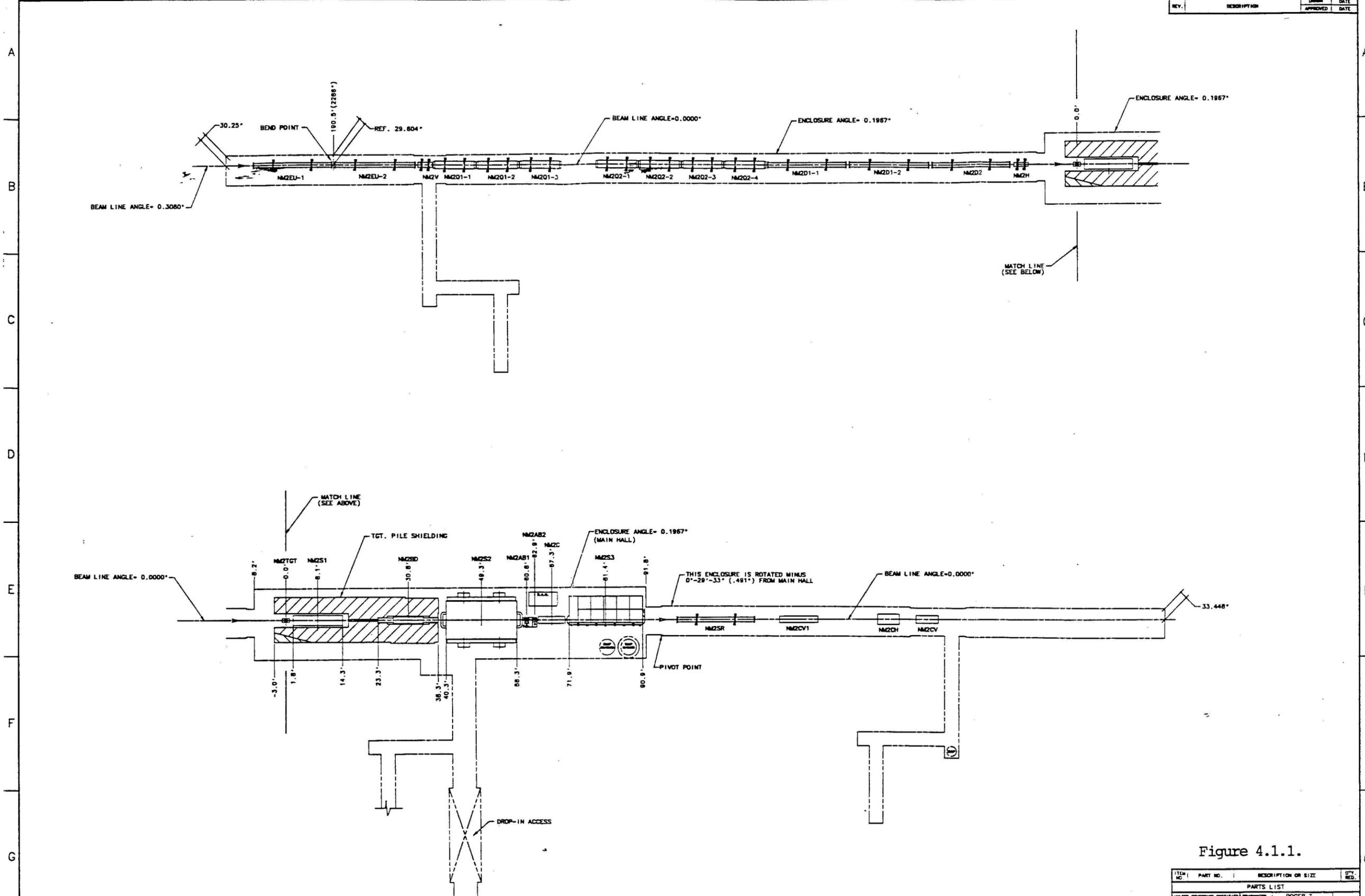
PLAN VIEW OF THE NM2 ENCLOSURE.

The KTeV Target Hall starts at -8.2' and extends to 91.8'.

The KTeV target is at 0.0'.

Figure 4.1.1.

ELEV. VIEW
SCALE: 1/4"=1'-0"
ALIGN. TOL.- ±0.025"

An elevation view of the KTeV Target Hall.

Figure 4.1.2.

Figure 4.2.1.

SECTION B-B

BEAM DIRECTION

SECTION A-A
FULL SCALE

TARGET SWEEPING MAGNET

NOTES::
1. TO REASSEMBLE COIL PLUMBING AFTER MAGNET IS REASSEMBLED LONGER
   LENGTHS OF TUBING ARE NEEDED (BENT TO SUIT).NEW TAPPED HOLES
   FOR MANIFOLD CLAMPS ARE ALSO NEEDED.
2. USE THERMON HEAT TRANSFER CEMENT (STANDARD GRADE THERMON).
3. COPPER TUBING TO BE CONTINUOUS(NO JOINTS).
   ALLOW ENOUGH TUBING LENGTH TO MAKE CONNECTIONS.
4. POLE PIECE TO BRASS INSERT (ITEM 2) TO BE TIGHT.
   COIL TO BRASS INSERT (ITEM 2) TO BE SNUG.
   THIS IS TO BE ACHIEVED BY SHIMMING.

ITEM NO.	PART NO.	DESCRIPTION OR SIZE	QTY. REQ.
20	9204.000 MD-202252	GUIDE	1
19	9204.000 MD-202241	FLAT FOOT ASS'Y	1
18	9204.000 MD-202240	LOCATING FOOT ASS'Y	2
17		1/2" FLAT WASHER	20
16		HEX HD. SCREW 1/2-13 UNC-2A X 1 1/4"LG.	20
15	9204.000 MD-202253	GUIDE	4
14	MD-267255	BRASS INSERT L.H.	1
13	MB-267254	MANIFOLD CLAMP	2
12		COPPER TUBING TYPE K 3/8 X .035 WALL	AS REQD
11		SOCKET HD. SCREW 1/4-20 UNC-2B X 3 3/4" LG.	4
10	MC-267253	LOWER WATER MANIFOLD	1
9	MC-267252	UPPER WATER MANIFOLD	1
8		ROLL PIN (SST) 3/8 DIA. X 3 1/2" LG.	4
7		FLAT HD. SCREW 1/4-20 UNC-2A X 3/4" LG.	32
6		FERRY HD. CAP SCREW 3/4-10 UNC-2A X 7 1/2" LG.	8
5	MD-267251	SPACER PLATE	2
4	MD-267250	BRASS SHIM	AS REQD
3	MD-267249	G-10 SHIM	4
2	MD-267248	BRASS INSERT	1
1	9204.000-ME 201095	H FRAME MAGNET	1

PARTS LIST

		DRAWN	RON C.	9/93
		CHECKED	G SMITH	9/27/93

KTEV TARGET BOX
LISTED

FERMI NATIONAL ACCELERATOR LABORATORY
UNITED STATES DEPARTMENT OF ENERGY

RD/MECHANICAL SUPPORT DEPARTMENT
KTEV TARGET BOX
REWORKED H FRAME MAGNET

SCALE 1/8=1"   3832.231-ME-267247   SHEET NO. 1 OF 1

Figure 4.2.2.
Primary Beam Dump

Figure 4.2.4.

NM2S2 (old E8/Hyperon magnet) and support structure.

TYPICAL INTERNAL WELD JOINT
SCALE: FULL

DETAIL VIEW C
SCALE 1:2

DETAIL VIEW B
SCALE 2:1

TYPICAL WATERLINE CONNECTION
SCALE: FULL

SECTION VIEW A-A
SCALE 1:8

DETAIL VIEW D
SCALE 1:4

WEIGHT OF STEEL = 310,192 Lbs.
WEIGHT OF 2 COILS = 11,490 Lbs.
Total weight=321,682 lbs.

Figure 4.2.5.
Mu-Sweep II

13		NEOPRENE RUBBER PADDING	
12		LINEBASE OR WOOD FILLER	
11		COIL OUTER SUPPORT BRACKET	5
10	MB-267138	ALUMINUM WATER INLET/OUTLET	16
9		COIL INNER SUPPORT ASSEMBLY	4
8		COIL OUTER SUPPORT ASSEMBLY	4
7		STEEL POLE: 11.15x16x228	2
6		1/2x18 STAINLESS TUBE .049 Wall	8
5	MC-2671411	ALUMINUM BUS BAR	6
4		EXTRUDED ALUMINUM VACUUM TUBE	1
3	MB-2670961	STAINLESS STEEL SPACER	2
2	MB-2670961	ALUMINUM CONDUCTOR	
1	ME-26713718	TURNS X 8 LAYERS COIL PACK	2
ITEM NO.	PART NO.	DESCRIPTION OR SIZE	QTY

PARTS LIST

FOR REFERENCE ONLY

FERMI NATIONAL ACCELERATOR LABORATORY
UNITED STATES DEPARTMENT OF ENERGY

RD/MECHANICAL SUPPORT DEPT.
KTeV MU SWEEP II MAGNET
GENERAL LAYOUT

TYP. SECTION THRU H-MAGNET

TYP. SECTION THRU DUMP

U.S. END VIEW

SIDE VIEW

Figure 4.2.7.

Front and side view of target pile.

Cross-section of target pile showing target sweeping magnet (H-magnet), fixtures and installation plan. The dump is installed in a similar way.

Figure 4.2.8.

CROSS SECTION AT Z = 146M (478.997')

SCALE: 1/4" = 1'-0"

(LOOKING UPSTREAM)

3' X 3' BOX

DOSE AND ERROR IN mREM/HOUR

FIGURE 4.4.10.

FERMI NATIONAL ACCELERATOR LABORATORY
UNITED STATES DEPARTMENT OF ENERGY

RD/MECHANICAL SUPPORT DEPT.
KTeV EXPERIMENTAL HALL - MUON DC
CROSS SECTION AT Z=146M (478.997

3832.200-ME-267106

Muon Dose per 1E18 Protons at Site Boundary
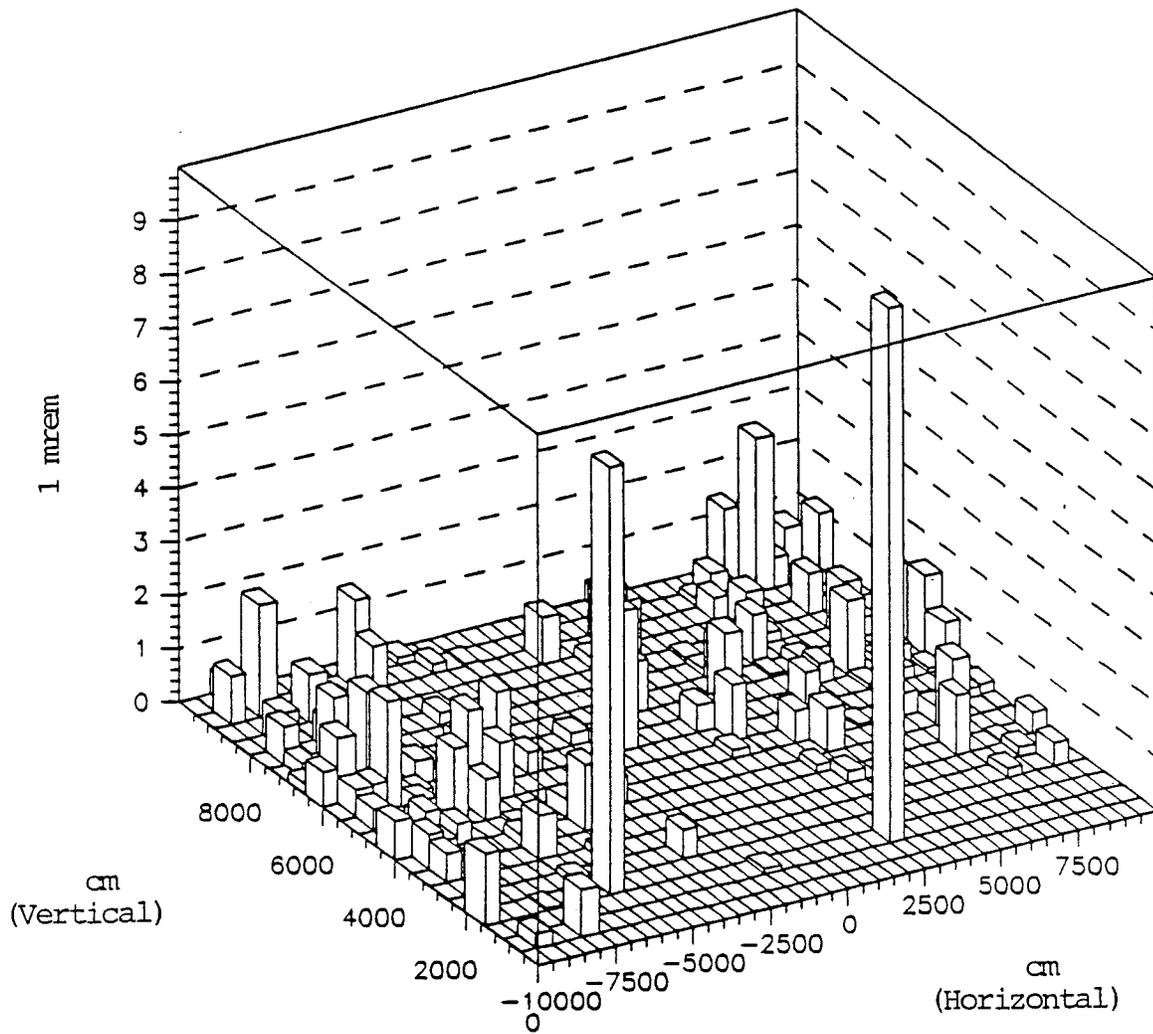
FIGURE 4.4.12.

June 2, 1994

5. SECONDARY BEAM

5.1 The Layout of Elements in the Secondary Beam as shown in Table 5.5.1.

Table 5.1.1

z (m) upstrm edge	z(m) dnstrm edge	x (cm) half-width	y (cm) half-width	B (kg)	Name
-0.15	+0.15				target
0.58	4.39	2.35	+2.29 to -4.06	5.0	NM2S1 (Eartly sweeper)
7.10	11.66	2.66	+1.92 to -1.54		primary passive dump
12.27	17.76	2.83	1.69	23.0	NM2S2 (hyperon sweeper)
18.21	19.39				Be and Pb filters
19.50		0.54	0.58		Upstream/defining
	21.50	0.60	0.66		two-hole fixed collimator
21.90	27.69	4.91	2.00	20.0	NM2S3 (µ sweeper2)
30.47	36.53	4.96	4.96	13.0	spin rotator dipole
39.00	41.00				slab collimator
42.76	45.81				beam stop
46.24	47.76				horiz. "jaw" variable collimator
49.24	50.76				vert. "jaw" variable collimator
85.00		2.12	2.12		Downstream/defining
	88.00	2.20	2.20		two-hole fixed collimator
90.27	92.10	11.56	4.45	≤18.0	final sweeper
123.4	125.2				regenerator
169.0	171.0			7.7	analysis magnet
184.0	184.2				trigger scintillator hodoscope
186.0	186.5				CsI

Half width in x and y planes refer to the inner aperature of the magnets.

5.2 Flux Calculations

The K_L fluxes are calculated using the Malensek parameterization[1] assuming K_L flux is the average of the charged kaons fluxes. The Malensek fit agrees reasonably well with the E731 momentum spectrum[2] as shown in Fig. 5.2.1. The K_L flux calculated is about 30% higher than observed in the E731 vacuum beam. We use the E731 K_L estimate of 1×10^7 K_L per 1×10^{12} incident protons to normalize the KTeV predictions.[3] This is reliable since the E731 target, targetting angle, absorbers, and solid angle is essentially identical to KTeV.

The neutrons are more difficult to predict. We have used information from previous E731 data on the rate of interactions in two detectors placed directly in the neutral beam (the regenerator, veto counters and back-anti photon veto) which give $n/K_L = 2 \pm 1$ for the E832 vacuum beam. This ratio is based on subtracting the rate due to the known K_L flux and correcting for detector efficiencies. Some of these efficiencies are momentum dependent due to energy thresholds in the detectors. We measure the K_L momentum spectrum in previous experiments and use a fit to neutron production measurements[4] to get the shapes of the momentum spectra. As a check, we have used the same neutron fit and the measured K_L to predict $n/K_L = 0.5$ while a similar independent estimate found $n/K_L = 1$.[5] The implications of this uncertainty are discussed more in section 5.11.

The photon fluxes were estimated using a fit of data from an FNAL photon beam[6]. The lambda flux was calculated using fits to data[7]. The neutral particle fluxes for 1×10^{12} incident 800 GeV protons on Be target with a 4.8 mrad targetting angle is shown in Fig. 5.2.2 before any filtering. Photons dominate the neutral particle spectrum. To reduce the photon component we insert lead filter to reduce

---

[1] A.J. Malensek, Fermilab FN-341.

[2] J.R. Patterson , Determination of Re (ε'/ε) by the Simultaneous Detection of the Four $K_{L,S} \rightarrow \pi\pi$ Decay Modes, Dec.1990, U. Chicago dissertation.

[3] L. K. Gibbons, A Precise Measurement of CP-Violation and other Kaon Decay Parameters, August 1993, University of Chicago dissertation.

[4] Edwards et al, Phys. Rev. D18, 76(1978) modified with a pt dependence from Engler et al, Nucl. Phys. B84, 70(1975).

[5] private communication, R. Bernstein.

[6] private communication, A.J. Malensek.

[7] Pondrom et al, Phy. Reports,122,67,(1985)

the photon flux to an acceptable level. We also add Be filters to improve the n/K_L ratio. In addition we target at 4.8 mrad to improve the n/K_L ratio (Fig. 5.2.3). The results below include these filters. Note these rates are for the "standard" beam of 0.25 μsteradians per beam. This is a conservatively small size motivated by the E832 beam specifications. A larger beam might be possible, particularly for E799II. As

Fig. 5.2.1 Comparison of E731 data and Malensek parametrization of KL momentum spectrum
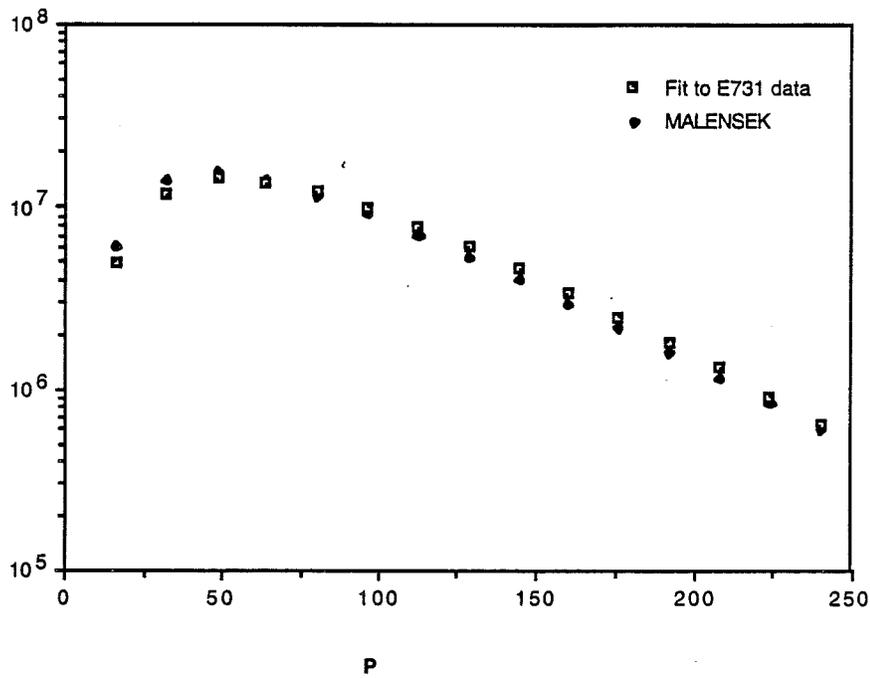
Figure 5.2.2 KTeV neutral particle fluxes at production before filters for 1 E12 incident 800 GeV protons (4.8 mr targetting angle)
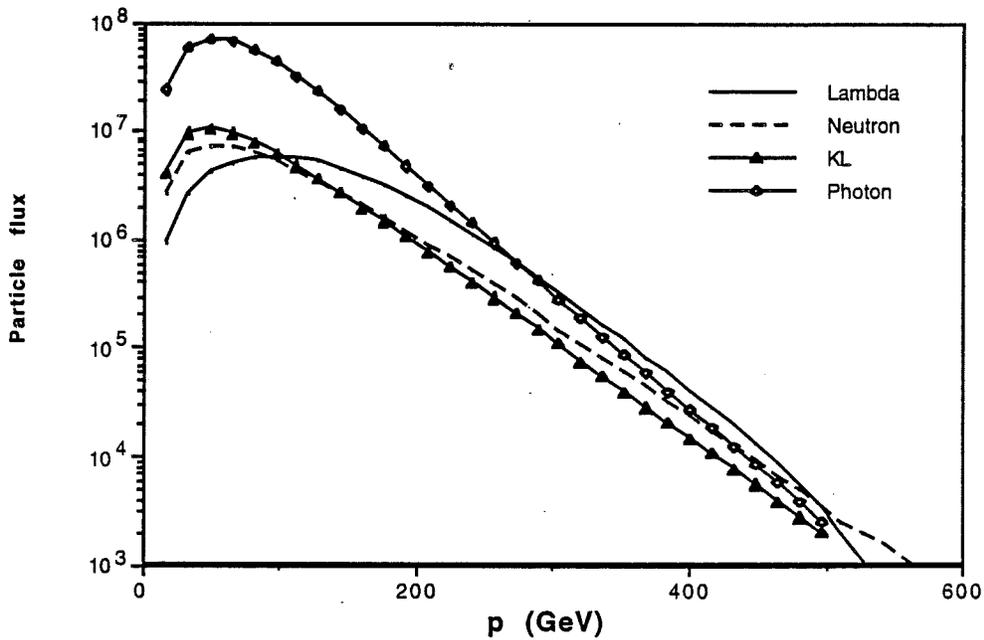
Figure 5.2.3   KL flux (no filters) per 1E12 incident 800 GeV protons and KL/neutron ratio vs. vertical targetting angle (Note: KTeV range = 4.0 to 5.5 mr, "nominal" = 4.8 mr)

Vertical Targetting Angle (mr)
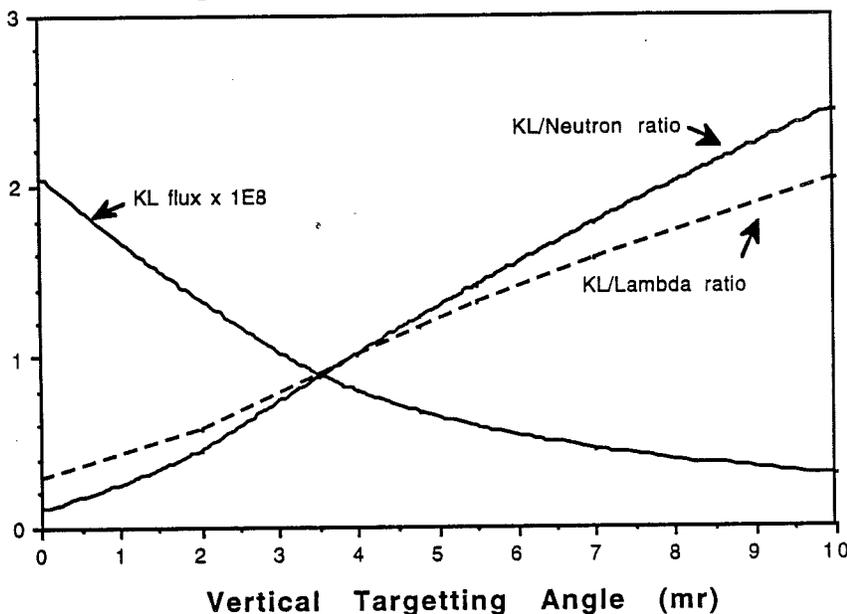
discussed further in section 5.8 we plan to build collimator inserts which would also allow us to run with either 1.5 or 2.0 x the standard solid angle of 0.25 μsteradians per beam subject to backgrounds and radiation damage of the CsI.

Table 5.1.2

Neutral Fluxes

	E832 vacuum	E832 regenerator	E799 both beams
incident protons	3.5×10^{12}	3.5×10^{12}	5×10^{12}
K_L	3.5×10^7	1.4×10^7	2.9×10^8
neutron	7.0×10^7	2.2×10^7	1.1×10^9
lambda	1.7×10^4	5.2×10^3	2.6×10^5
filters	3" Pb + 20" Be	3"Pb + 38" Be	3" Pb
K_L transmission	.19	.076	.55
n transmission	.10	.031	.54

Neutral fluxes at z = 90 m from the target including filters per spill (solid angle = 0.25 μster. per beam). The transmission includes the effect of absorption and scattering from the filters.

5.3 Justifications for Beam Stability Requirements

In order that the measurement to ε'/ε in E832 not be compromised by systematic effects, E832's ε'/ε analysis requires the sizes and positions of the two neutral beams be stable to 0.5 mm, that the areas be equal (to 1%), and that the kaon momentum spectra be equal (to 0.1%).[8] In the final analysis, after the results from the two beams are used optimally and after the Monte Carlo has been appropriately tuned to fit the data, these systematic problems should disappear. The goal is to keep the beam-related systematic problems well below the level of sensitivity of the experiment. The requirements are based primarily on the E731 analysis.[9] Additionally, there are analytic/numerical calculations- primarily relating to variations in the momentum spectrum. Finally there are various results based on a series of runs with a small Monte Carlo program to address specific issues such as beam geometry and 2π acceptances. The sensitivity of ε'/ε to neutral beam motion was estimated by comparison of different E731 data sets and the corresponding Monte Carlo correction sets. Because of the target and collimator alignment instabilities, the beam areas varied from about 2% to 10%. For each data set the Monte Carlo collimator positions are adjusted to match the beam shape for that data set. Therefore, by analyzing different data sets with non-corresponding Monte Carlo corrections for the ε'/ε analysis, we are able to estimate the change in ε'/ε induced by a changed in beam position at the regenerator.

The result is $\dfrac{d\varepsilon'/\varepsilon}{dX_{reg}} = 3\times10^{-4}/\text{cm}$ where X_{reg} is the neutral beam position at the regenerator in the plane of the two beams.[10]

A similar analysis was done with regard to the momentum equality of the two beams.

The result is

$$\frac{d\varepsilon'/\varepsilon}{d<p_{sec}>} < 3\times10^{-3}/\text{GeV}.$$

---

[8] private communication, B. Hsiung.
[9] Ibid, B. Hsiung.
[10] Ibid, B. Hsiung.

Using the variation of the momentum spectrum with production angle of 0.7 GeV/mrad, this corresponds to $\dfrac{d\varepsilon'/\varepsilon}{d\theta_x} < 2x10^{-3} / mrad$. One may also estimate[11] this dependence with a Monte Carlo with the KTeV geometry and using the Malensek momentum dependence. From these, one may estimate the sensitivity of ε'/ε to the production angle as it is effected through the momentum spectrum. The spectrometer acceptance averaged over z and p is Ω.

The result is

$$\frac{d\varepsilon'/\varepsilon}{d\theta_x} = \frac{d\varepsilon'/\varepsilon}{d\left(\Delta\Omega/\Omega\right)} \frac{d\left(\Delta\Omega/\Omega\right)}{d\left(\Delta<p_{sec}>/<p_{sec}>\right)} \frac{d<p_{sec}>/<p_{sec}>}{d\theta_x} =$$

$$(1/6) \qquad (0.34) \qquad (0.018/mrad) \quad = 1x10^{-3}/mrad.$$

which is not in disagreement with the E731 limit quoted above.

The E832 goal is to measure ε'/ε to at least 1 part in 10^4. In order to keep errors due to the beam small, our goal is 0.2 parts in 10^4. To keep the two beam fluxes equal to 1% the horizontal targetting angle must be stable to 0.28 mrad. To keep the mean momentum equal of the two beams equal to 0.1% the horizontal targetting angle must be stable to 28 μrad. To keep the beam momentum equal to 0.1% due to the vertical targetting angle is more stringent and is about 20 μrad. This is due to the 4.8 mrad vertical targetting angle compared to the 0.8 mrad horizontal angle. These results are obtained from the Monte Carlo using the Malensek momentum dependence. There are geometric tolerances also if the fluxes are to be equal (areas of two beams must be equal). These constraints are discussed in section 5.8.6.

The sensitivity of ε'/ε to the beam parameters has been propagated by standard error analysis. The term must be added in quadrature and be less than 0.2×10^{-4}.

$$\frac{d\varepsilon'/\varepsilon}{d<p_{sec}>} \frac{d<p_{sec}>}{d\theta_x} \Delta\theta_x + \frac{d\varepsilon'/\varepsilon}{dX_{reg}} \frac{dX_{reg}}{dx_{beam}} \Delta x_{beam} < 0.2x10^{-4}$$

The primary beam position on target is the x_{beam} term. For our 1mm x 1mm target, the position correlation term is negligible, so only the $\Delta\theta_x$ term contributes.

---

[11] D. Jensen, On the Sensitivity of ε'/ε to Primary Beam Parameters, Feb. 2, 1994, KTeV memo.

The result is $(1 \times 10^{-3}/\text{GeV})(0.7 \text{ GeV}/\text{mrad})(\Delta\theta_x) < 0.2 \times 10^{-4}$ or $\Delta\theta_x < 28$ μrad.

Ignoring angle changes the 2rd term above can be interpreted as target motion. The correlation term $\dfrac{dX_{reg}}{dx_{beam}}$ is 1.5 so the target stability due to this concern is 0.043 cm. However for good targetting efficiency on the 1 mm x 1mm target we require 0.020 cm positional stability of the primary beam and target.

5.4 Target Design

The KTeV target requirements are discussed in the Design Report[12]. The material of choice is BeO and the length is 30 cm or about 1 interaction length. Two different cross section size targets are planned, 1mm and 3mm. In addition, a small target is included to use with the collimator alignment scheme discussed in section 5.9. These targets will all be mounted in a remotely controlled target holder with a target-out position. A preliminary design of the target and target holder is shown in Fig. 5.4.1. The targets must be aligned with respect to the x of the neutral beam line precisely (200 microns). The heating issues associated with a 1 mm square target are summarized in Table 5.4.1. The heating calculations were done for 1 E13 incident 900 GeV protons per pulse with a 20 second spill length and a 60 second cycle time. Beryllium was evaluated as well as Beryllium Oxide for comparison.

---

[12] KTeV Design Report, January 22, 1992, FN-580.
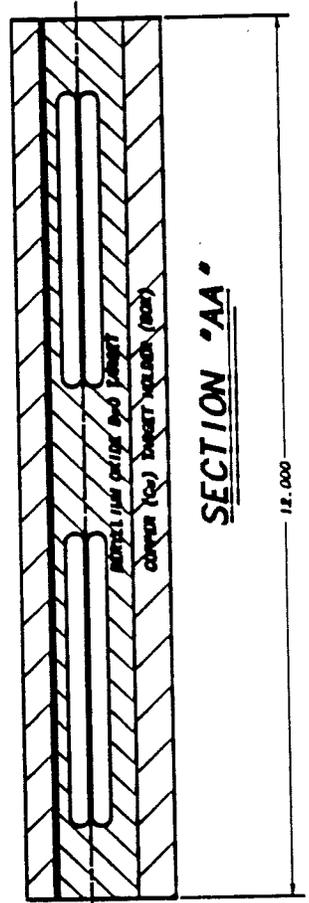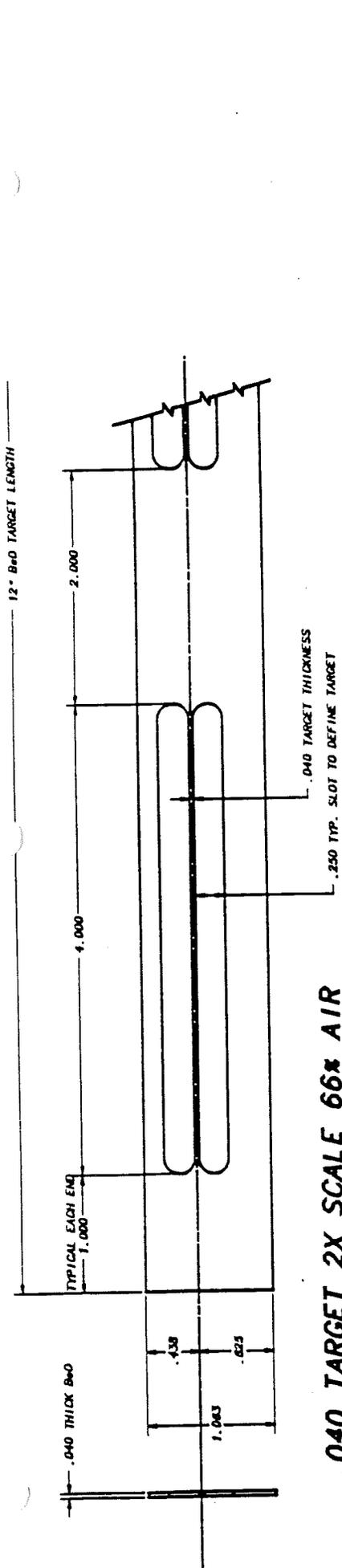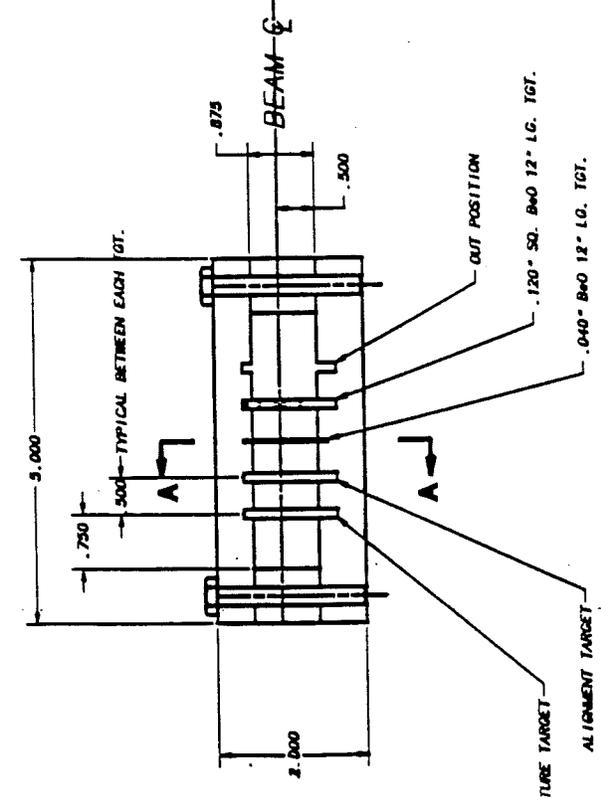
Figure 5.4.1   Conceptual Target Design - Full Scale

Table 5.4.1
Summary of Heating Calculations

Cooling Method	Beryllium		Beryllium Oxide	
	T(min)	T(max)	T(min)	T(max)
Forced Convection	310 K	360 K	310 K	420 K
Natural Convection	320 K	560 K	320 K	880 K
Radiation Only	700 K	1000 K	720 K	1350 K

1mm target diameter, beam sigma= 0.22 mm

Forced convection is helium gas flowing at 4 meters/sec. and maintaining a temperature no higher than 100 F (310 K). Natural convection is air at a temperature no higher than 100 F. An enclosed target cave will probably have higher temperatures because the air will be "stagnant". T(min) is the temperature just before the beam spill; T(max) is the temperature at the end of the spill. T(min) and T(max) are given after reaching steady state.

Beryllium:

> Emissivity = 0.25
> Density = 1.85 g/cc
> Specific Heat = 0.436 cal/g-C
> Melting Temperature = 1550 K

Beryllium Oxide:

> Emissivity = 0.25
> Density = 2.85 g/cc
> Specific Heat = 0.24 cal/g-C
> Melting Temperature = 2840 K

Assuming a slightly larger beam size and a larger target size gives the following:

Table 5.4.2

Cooling Method	Beryllium		Beryllium Oxide	
	T(min)	T(max)	T(min)	T(max)
Forced Convection	310 K	350 K	310 K	440 K
Natural Convection	420 K	510 K	560 K	820 K
Radiation Only	710 K	780 K	860 K	1080 K

3 mm target diameter, beam sigma= 0.35 mm

5.5 Primary Beam Dump Background Elimination

For reference the E731 dump is shown in Fig. 5.5.1; the radial separation was R = 4.86 cm for the neutral channel to the proton beam dump center. The spot size of the primary beam at the dump face was about 1 cm full-width for 99% containment. The dump face was located at z=8.98 m from the target center. The horizontal target angle of 4.8 mrad gives 4.32 cm separation at the dump. The target sweepers gave an additional 2.23 cm vertical separation at the dump face.

The background from the dump can be estimated from target-out data. From E731 the 2π target-out trigger rates for charged and neutral are 0.006 of target-in, the ET (total lead-glass energy above 28 GeV) target-out rate is 0.03 of the target-in rate.

The KTeV version with the dump face at z= 7.1 m and an 4.8 mrad vertical targetting angle is shown in Fig. 4.1.4. The radial separation and the spot size are similar to E731 [R=3.4 cm and spot size of 99% containment for < 0.6 (1.5) cm vertical (horizontal) full-width]. The radial separation of the projected proton beam at the face of the hyperon magnet is R = 8.1 cm. The length of the dump is much longer for KTeV and the downstream portion (hyperon magnet) is magnetized so we do not anticipate significant backgrounds from the dumping of the primary beam in the neutral channel.
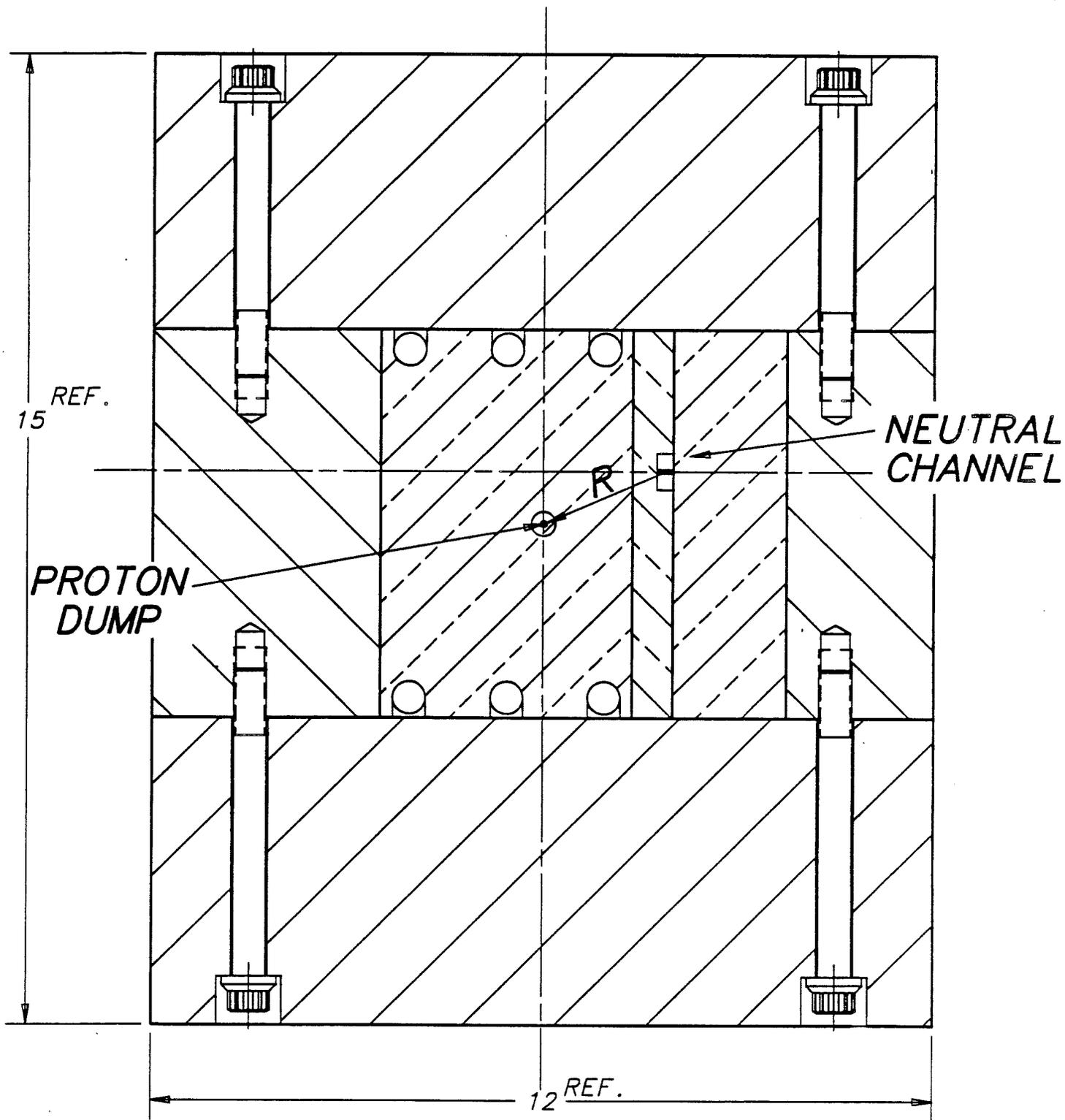
Fig. 5.5.1   E-731   Proton Dump   R=4.86cm

5.6 Elimination of Charged Particles from Neutral Channel

Fig 5.6.1 shows the relative amount of magnetic field vs distance from the target along the beam for MC and KTeV (not including the final dweeper at 90 m). Experience from sweeper studies in the MC beamline (E731) shows only small trigger rate effects in varying sweeper currents. For example reducing the most upstream MC sweeper by 2/3 increased the muon rate by 40% while two track trigger (with muon veto) and ET(>28 GeV in lead-glass) rates only increased by about 5%. Switching off the MC sweeper at z=30 m increased the two track trigger rate by 12%. Switching off the MC sweeper at z=57 m increased the two track trigger rate by 2%. For the KTeV beamline we will have additional magnetic sweeping relative to the MC beamline (1.7 times more field integral) due to the enhanced muon sweeping system. Even a 800 GeV charged particle leaving the target initially parallel to the neutral channel will strike the inner walls of the hyperon magnet almost 2 m from the downstream end of the 5.5 m long magnet.

5.7 Filter System- Photon Elimination and K_L/n Enhancement

In all of the past experiments using the MC beamline a lead filter was inserted to reduce the photon flux in the neutral beam. Fig. 5.7.1 shows data from E731 logbooks; the charged two track trigger rate with a "veto-on-hits" in the muon detector versus thickness of lead in the neutral beam. We have chosen 3" as the optimal thickness for the lead photon filter.

For E799I the only filter used was the lead discussed above. For E731 a "common" absorber of 20" of Be was placed in both neutral beams and a "movable-shadow" absorber of 18" of Be was placed in the same neutral beam as the regenerator. The various filter transmissions are given in Table 1. For example, the n/K_L in the E731 regenerator beam is reduced by 2.5 relative to using no Be filters (E799I), while the K_L flux is reduced by 5.1. The interaction length for high energy neutrons (K_L's) in Be is 40 (55) cm. The interation length for neutrons (K_L's) in lead is 16.8 (14.8) cm.[13] Fig. 5.7.2 shows the engineering design of absorber trays and movers.

---

[13] A. Gsponer et al, Phys. Rev. Lett. 42, 9 (1979) and T. J. Roberts et al., Nucl. Phys. B159, 56 (1979).

Fig. 5.6.1   E731 magnetic sweeping
Integral B*dl = 203 kg-m
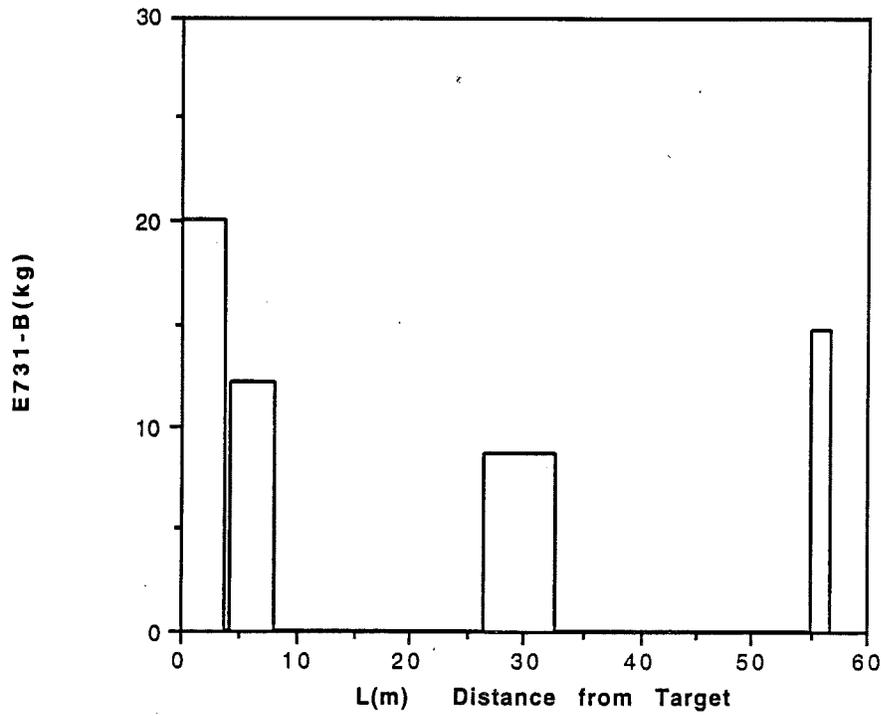
Fig. 5.6.2   KTeV magnetic sweeping
Integral B*dl = 340 kg-m
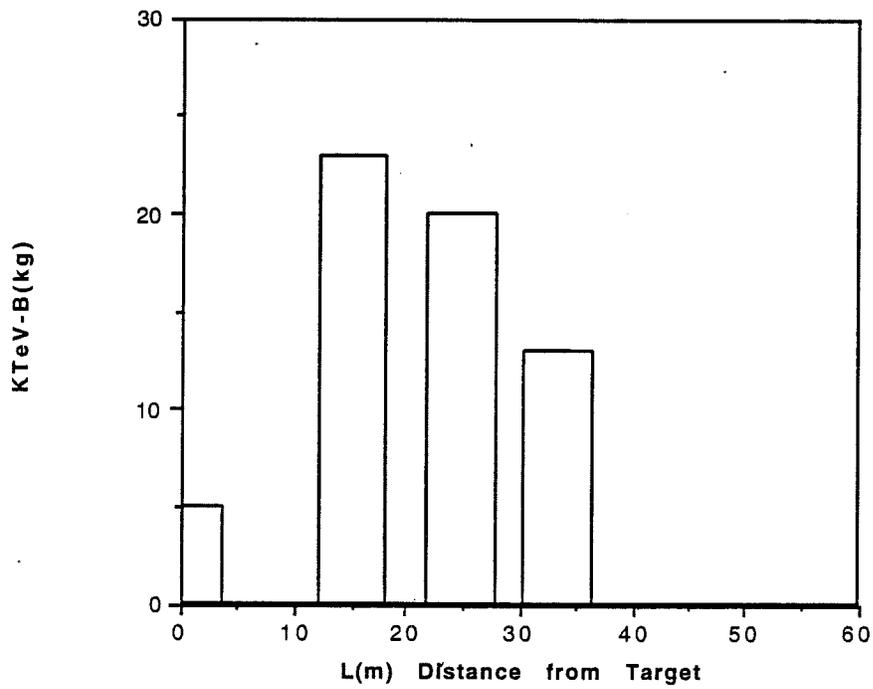
Fig. 5.7.1 E731 two-track trigger rate versus thickness of lead filter

Fig. 5.7.2 Absorber Trays and Movers

5.8 Collimator System

5.8.1 Design goals

It is crucial that the collimator system prevent beam halo from causing radiation damage to the CsI or introducing background triggers. Simulations indicate that the scattering of beam particles in filters combined with collimator misalignments was a source of beam halo (see section 5.11). The collimator scheme involves a primary collimator (z=19.5 to 21.5 m) and a defining collimator (z=85 to 88 m). The defining collimator provides the principle definition of the edges of the beam. To obtain sharp edges, it is located as far downstream as possible. Experience in the MC beamline shows that a collimator at z=85-88 m does not introduce a dominant background source for the experiment. GEANT studies are consistent with this observation. The primary collimator is located as close as possible to the target. There is a filter just upstream of the primary collimator. The function of the primary collimator is to limit the lateral size of the beam at the scattering source. The combination of the primary and defining collimators then defines the maximum deviation of a scattered neutral particle from the beam axis at the z position of the CsI calorimeter. The goal is to constrain all such scattered tracks to lie within the beam holes, missing the calorimeter. The holes in the CsI are 15.0 cm square separated by 30 cm (center to center) in the horizontal plane. The criteria we have adopted is that all scattered rays fall a minimum of 1 cm inside the holes.

The finite target size also has implications on the collimator design. The walls of the collimator are tapered to point to an apex downstream of the target (Fig. 5.8.1), so that no neutral track from the target can strike the inner walls of the collimator. In practice, the difference in taper is significant only for the primary
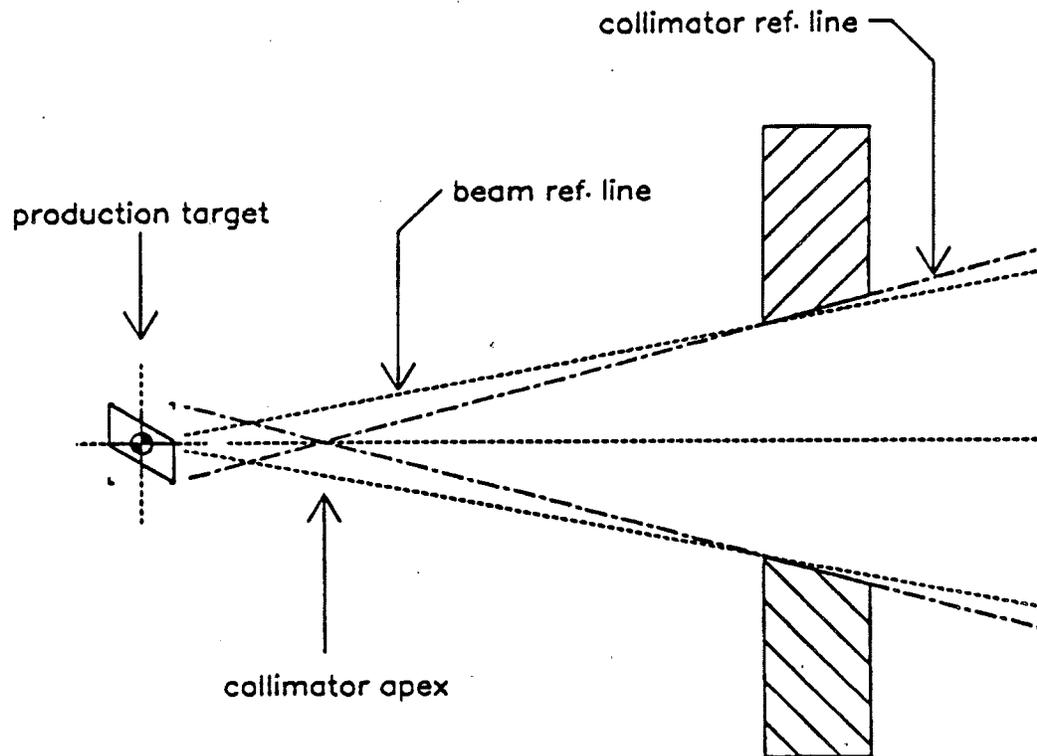
Figure 5.8.1 The walls of the collimator lie on lines that, projected forward, cross at a point called the *collimator apex*. If the target lies entirely upstream of the apex within the cone defined by these lines, then no neutral track emanating from the target can strike the inner walls of the collimator aperture.

collimator. These design considerations are discussed in more detail KTeV Design Report[14]. The results are listed below. Additional collimator inserts allow for

---

[14] KTeV Design Report, January 22, 1992.

beams with larger solid angle 1.5 and 2.0x the "standard" beam of 0.25 μsteradians per beam. The following are used to specify the "standard" beam

'Target' size   1mm x 1 mm x 30 cm
Beam separation   ± 15 cm at CsI (z=186m) center to center
X angular divergence ± 0.250 mrad
Y angular divergence ± 0.250 mrad
Neutral Beam Solid Angle = 4 x (0.250 mrad)^2 = 0.250 μsteradians per beam

In addition to the primary and defining collimators there are two other types of collimation; a slab and a pair of variable jaw collimators. The purpose of the slab collimator is to prevent scattered tracks out of one beam from crossing over to the other beam in the plan view. Fig. 5.8.2 illustrates the principle which is discussed in more detail in the KTeV Design Report[15]. The variable jaw collimators will be used, if needed, to reduce the flux on the defining collimator. Finally, we will have a fast acting beam stop to close completely to block the neutral beam for special studies and radiation safety measurements. We have existing jaw collimators and a beam stop which can be reused with some refurbishments. The slab is a new device. The primary and defining collimator are discussed in more detail in section 5.8.4 and 5.8.5.

---

[15] Ibid, page 74.

Fig. 5.8.2 KTeV Beam Envelope and Collimator Locations

Vertical size (cm) vs z (m)

CsI hole

E832 beam size

Horizontal Size (cm) vs z (m)

Slab

Primary

Defining

Scattered particle blocked by slab
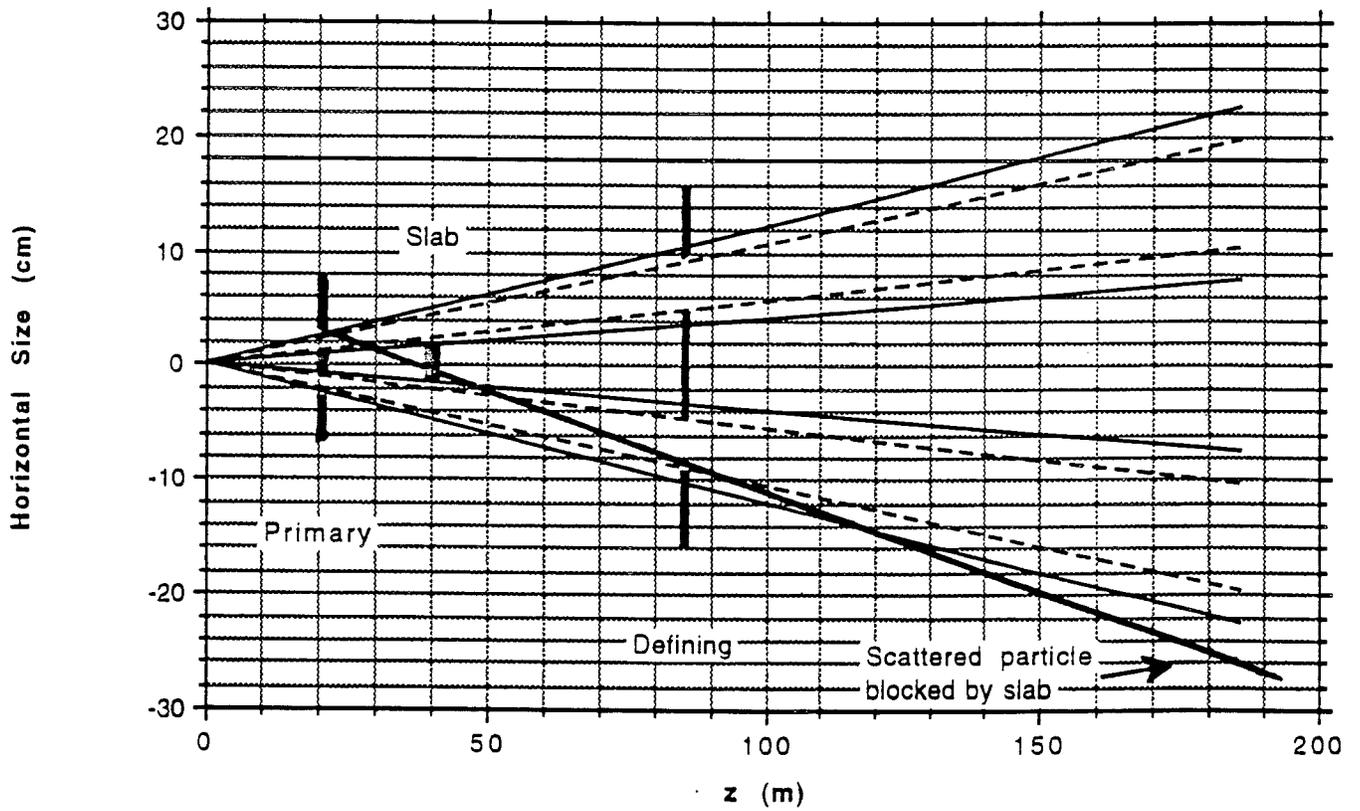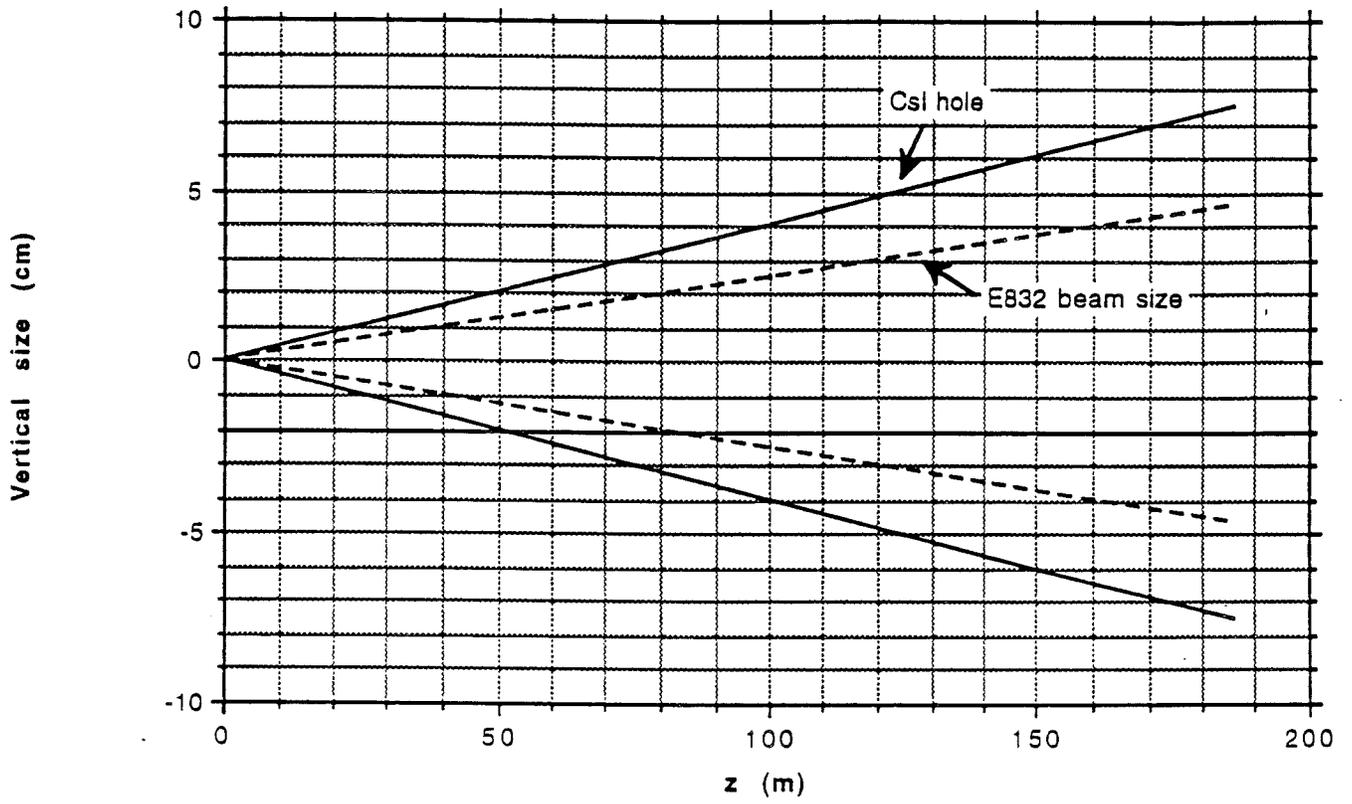
5.8.2 System layout and apertures for standard beam, aperature sizes are shown below in Table 5.8.2.

Table 5.8.2

Item	X(cm) full-width	Y(cm) full-width	Z(m) location
PC Collimator upstream hole	1.08	1.16	19.5
PC Collimator downstream hole	1.20	1.32	21.5
slab upstream width	2.03		39.0
slab downstream width	2.13		41.0
DC collimator upstream hole	4.24	4.24	85.0
DC collimator downstream hole	4.40	4.40	88.0
Beam size at CsI	9.30	9.30	186.0
Beam hole size at CsI	15.0	15.0	186.0

5.8.3 General considerations of collimator outer dimensions

The outer dimensions of the collimator must be large enough to contain the showers from neutral beam interactions. The neutral flux (n + K_L) passing through the CsI beam holes in the highest intensity running for E799II (both beams) is 0.8-2.1x10^9. The range quoted reflects the uncertainty in the n/K_L ratio. Under these conditions the primary collimator (z=20.5 m) will be struck with a neutral flux of 0.8-2.1x10^{10} and the defining collimator (z=86.5 m) will see 0.3-0.7x10^9. This is for an incident proton intensity of 5x10^{12}.

The collimators used in MC were formed of a pair of variable jaw collimators, one horizontally-defining and the other vertical. The total length of both was 10-12 ft. Each jaw was a rectangular piece of iron approximately 4"x8" transversely. Fig. 5.8.3 shows a CASIM calculation[16] for 30 GeV and 300 Gev protons on iron cylinders of different sizes. We have compared the CASIM shower containment predictions

---

[16] CASIM , A. Van Ginneken & M. Awschalom, High Energy Particle Interactions in Large Targets, (1975); A Van Ginneken, Fermilab Report FN-272 (1975).

with GEANT. The GEANT predictions for a 1 m long iron cylinder is in good agreement with CASIM. For a length of 3 m the plateau of the GEANT curve is about 15% lower than the CASIM results while the shapes are similar. GEANT was also used to calculate similar shower containment curves for incident neutrons and K_L which gave essentially identical results as protons in GEANT. Based on these predictions, we have chosen 2m for the length of the primary collimator and a more conservative 3 m length for the defining collimator because of its proximity to the detector.

5.8.4 Primary / upstream fixed two-hole collimator

There is an existing collimator which may match our needs. Figure 5.8.4 shows one of these collimators. The design has a movable inner block with apertures to collimate the beam and a fixed outer iron shell. A great deal of experience with this design exists. The motion control is very accurate and reproducible. The radial shielding is currently about 10.5" to which we would add iron to bring the radial shielding to our 12" requirement. The effective shielding length (length of the inner block and downstream portion of the outer shell) is 1.9 m as is. The inner block will have two sets of holes; one for the standard beams and one for the optional larger solid angle beams (displaced from each other vertically in the inner movable block 4"x6").

Unfortunately, this existing collimator steel is slightly radioactive preventing machining which is needed to add the tungsten alignment masks (see section 5.9). Since this collimator is a "clean-up" collimator and not the defining collimator, we will eliminate the alignment masks on this collimator to minimize the modifications needed.
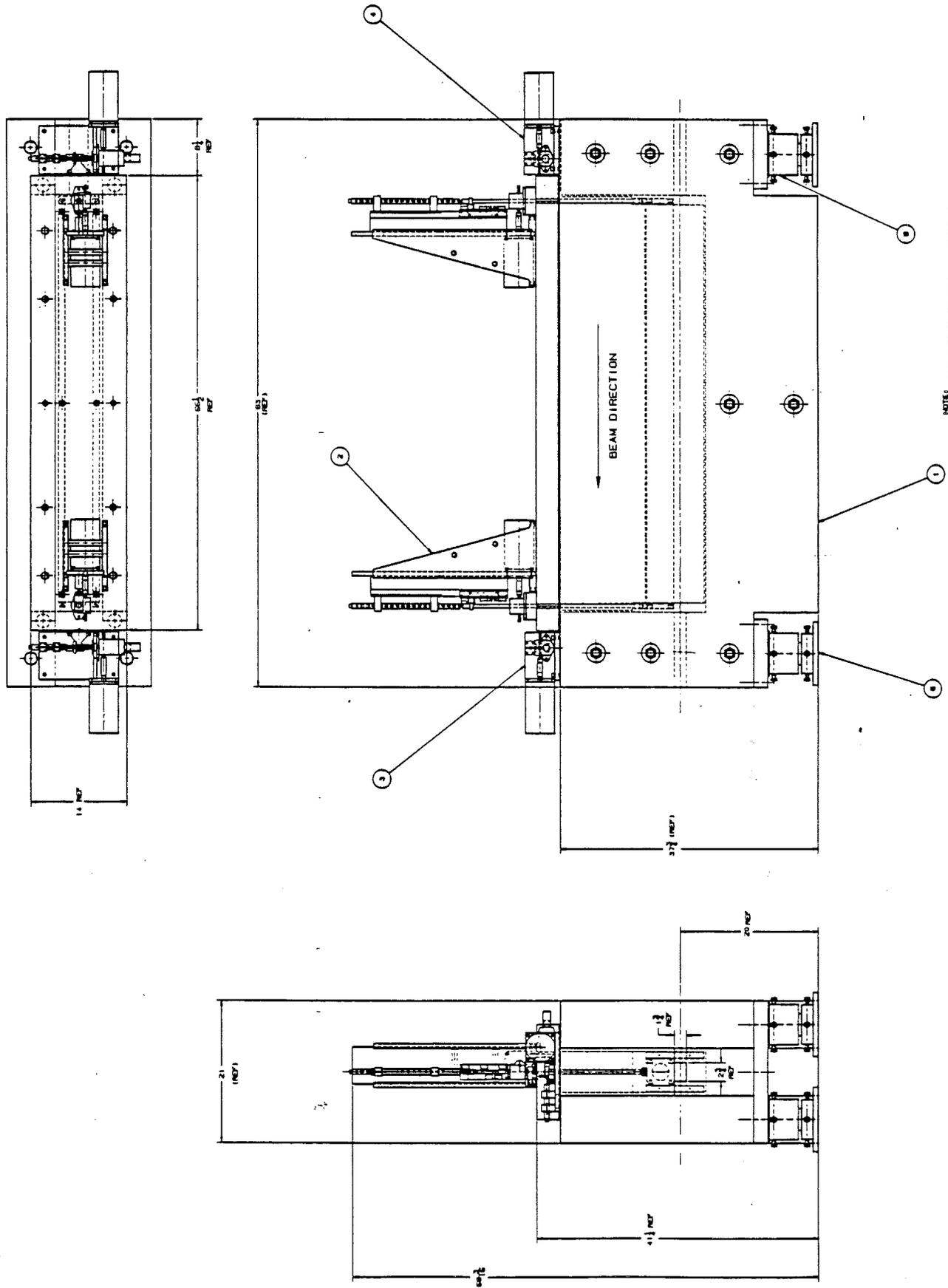
Fig. 5.8.4   Existing Collimator to be
Modified for Primary Collimator

Fig. 5.8.3   Fraction of incident energy deposited *vs.* radius for 30 GeV/c and
300 GeV/c.   (From Van Ginneken and Awschalom)
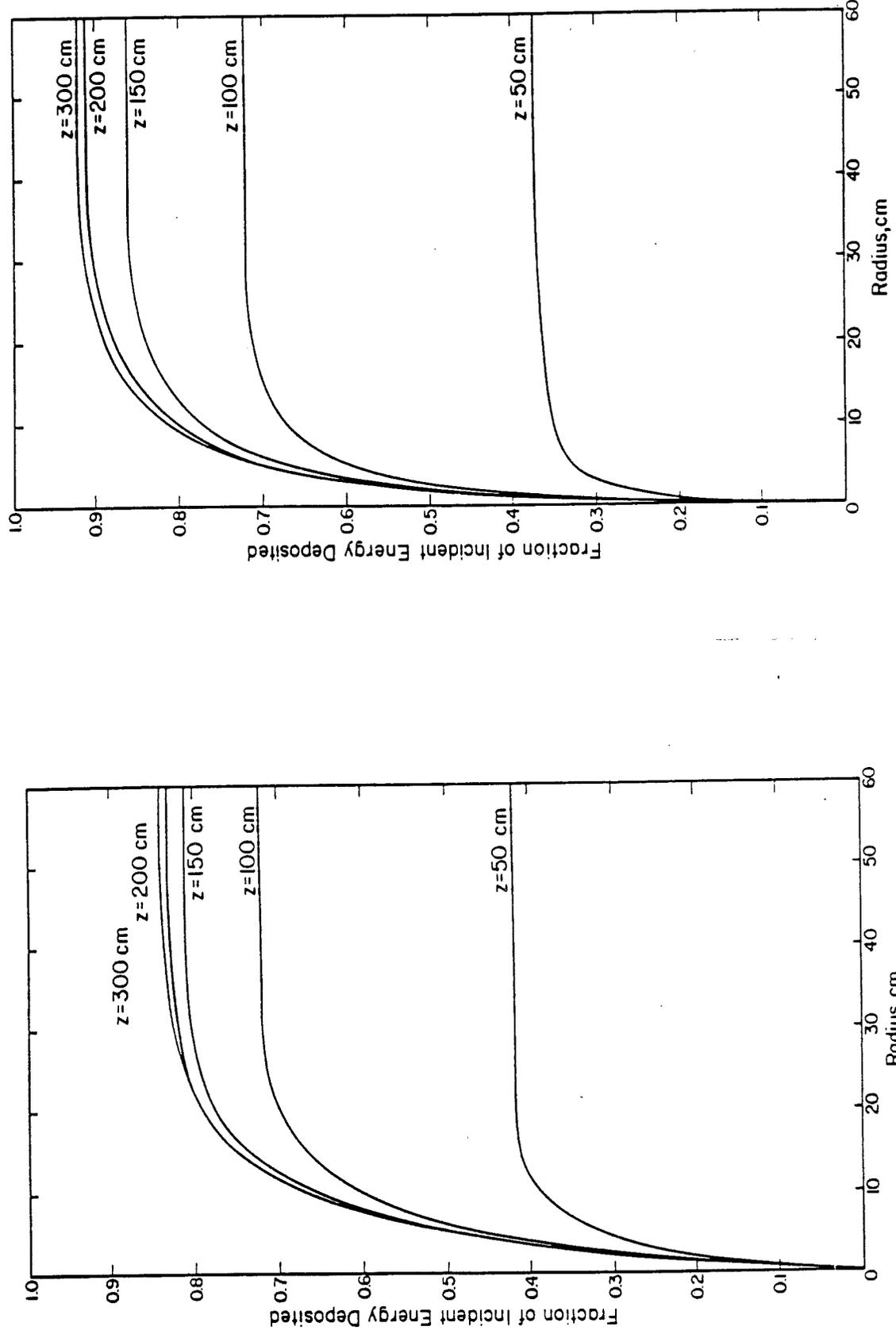
Fig. VIII.76.   300 GeV/c protons incident on a solid iron cylinder.   Fraction of the incident
kinetic energy deposited as ionization, plotted as a function of radius for various cylinder
lengths.   The beam of 0.3 cm × 0.3 cm cross section is centered on the cylinder axis.

- 141 -

Fig. VIII.74.   30 GeV/c protons incident on a solid iron cylinder   Fraction of the incident kinetic
energy deposited as ionization, plotted as a function of radius for various cylinder lengths.
The beam of 0.3 cm × 0.3 cm cross section is centered on the cylinder axis

- 139 -

5.8.5 Defining / downstream fixed two-hole collimator

The defining collimator (Figure 5.8.5) differs from the primary collimator in that it is located close to the detector and is also required to be a vacuum device. Because of this vacuum requirement existing collimators such as being used for the primary are unsuitable. The general design features as discussed earlier are a fixed hole collimator with a neutral channel insert which can be manually changed to another hole size if needed. Such a change of inserts is expected to take approximately 8 hours.

Making a collimator insert with a 1" tungsten liner around the neutral channel reduces the spray off the collimator by about 50% according to GEANT. The majority of this spray off the defining collimator is low energy photons. These studies also indicate that using the jaw collimator to reduce the flux on the defining collimator reduces the collimator spray as effectively as the W liner assuming 5-10 mils alignment and motion control accuracy on the jaw collimators. Given the cost tungsten we have chosen iron inserts rather than tungsten and will rely on the jaws to reduce backgrounds from the defining collimators if necessary.

We have chosen 3 m for the length of the defining collimator because of its proximity to the detector. Again we have used CASIM calculations (fig. 5.8.3) as well as our own GEANT studies to select this length.

Following this defining collimator is a magnetic sweeper which also provides additional hadronic shielding. We could, if necessary, also place approximately 1 m more of shielding between the defining collimator and the sweeper. The location of this collimator is the same as our most downstream collimator in MC. Previous studies of the effect of varying the MC sweeper just downstream of this collimator indicated very small charged particle contributions to the trigger (<5-10%). In fact we may choose in KTeV to run with this sweeper off as in the past. However the sweeper may be helpful in slightly reducing collimator spray; but it reduces the acceptance for lambda triggers in E799II by a factor of two. Fig. 5.8.4 shows a preliminary design for the defining collimator.
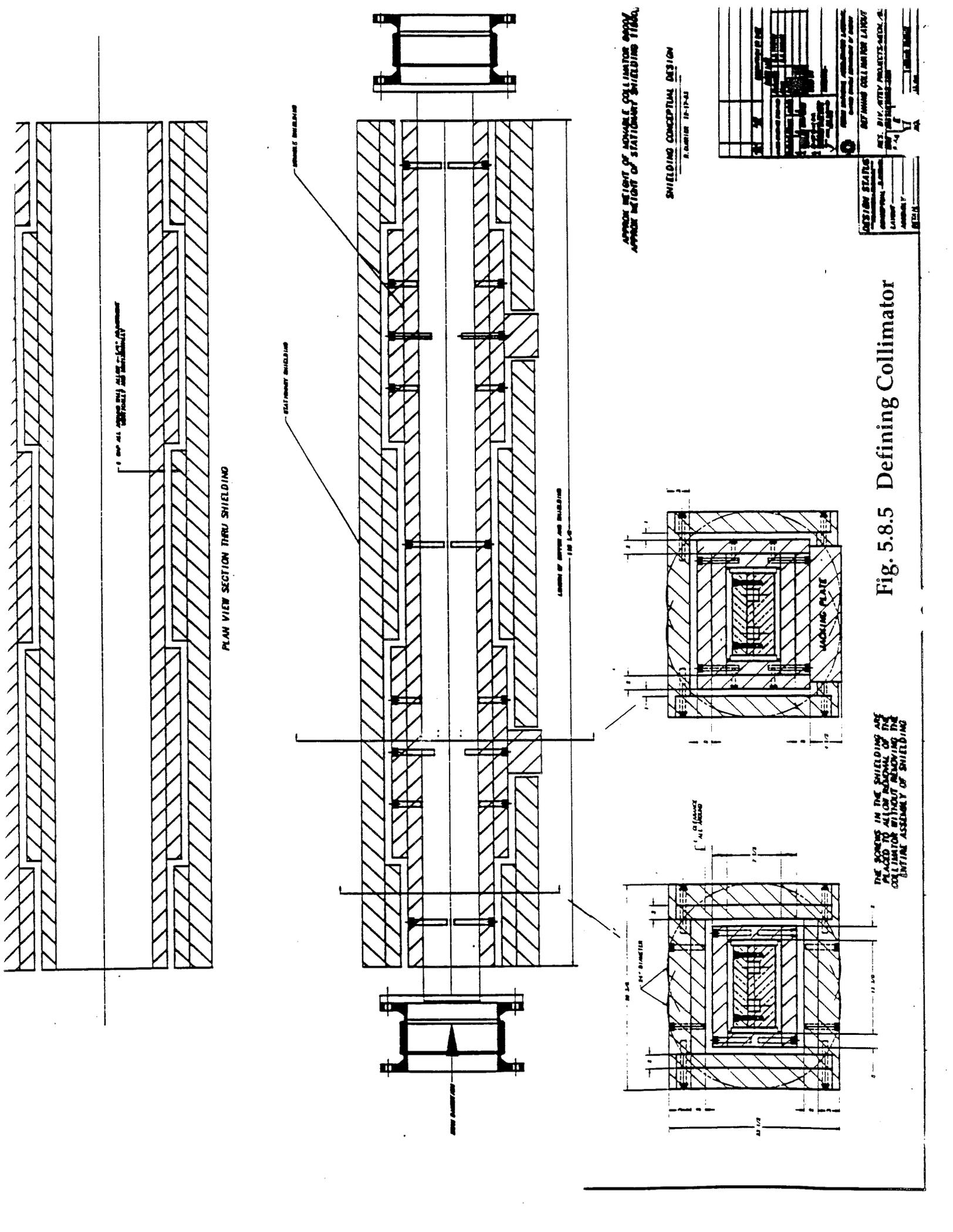
Fig. 5.8.5 Defining Collimator

5.8.6 Alignment and mechanical tolerances

The criteria for setting the defining collimator tolerances are:

a) The beam size and position at the CsI affected by no more than 0.5 mm from the sizes and alignment of the various collimator apertures.

b) The areas of the two beams must be equal to within 1%.

These criteria impose a horizontal and vertical tolerance of +/- 200 microns.

The criteria for setting the primary collimator tolerances come from :

The size of the beam at the CsI, including scattered rays must be less than 6.5 cm to provide a minimum of 1 cm clearance between the beam and the CsI edges(see Fig. 5.8.6). In order not to have the primary collimator define the beam, we have a clearance of ±500 (1000) microns in the horizontal (vertical). The mechanical and positioning error is approximately ±150 microns. Therefore, an alignment tolerance of ±200 microns is sufficient allowing some margin for positional instability. The alignment of the slab collimator is less critical; using the same criteria as for the primary collimator, a tolerance of ±1.3 mm is obtained.

5.9   Beam Instrumentation/Monitoring

Monitoring the alignment of the neutral beam elements to the required tolerances is critical to the KTeV program. The alignment section of this report discusses the procedures planned by the FNAL alignment department. We also plan to monitor the alignment using the beam itself. A system to do this is outlined in the Design Report.[17]   The defining collimator has tungsten masks(0.50" of tungsten) on both the upstream and downstream ends which flip in and out of the beam with a pattern of holes or slits which can be detected by a beam alignment monitor just downstream of the CsI beam holes. This scheme requires the insertion of masks, removal of the filters, and possibly a reduction in primary beam intensity to make a photon beam.   Even a crudely segmented detector can

---

[17] KTeV Design Report, January 22, 1992 and private communication , M. Crisler.
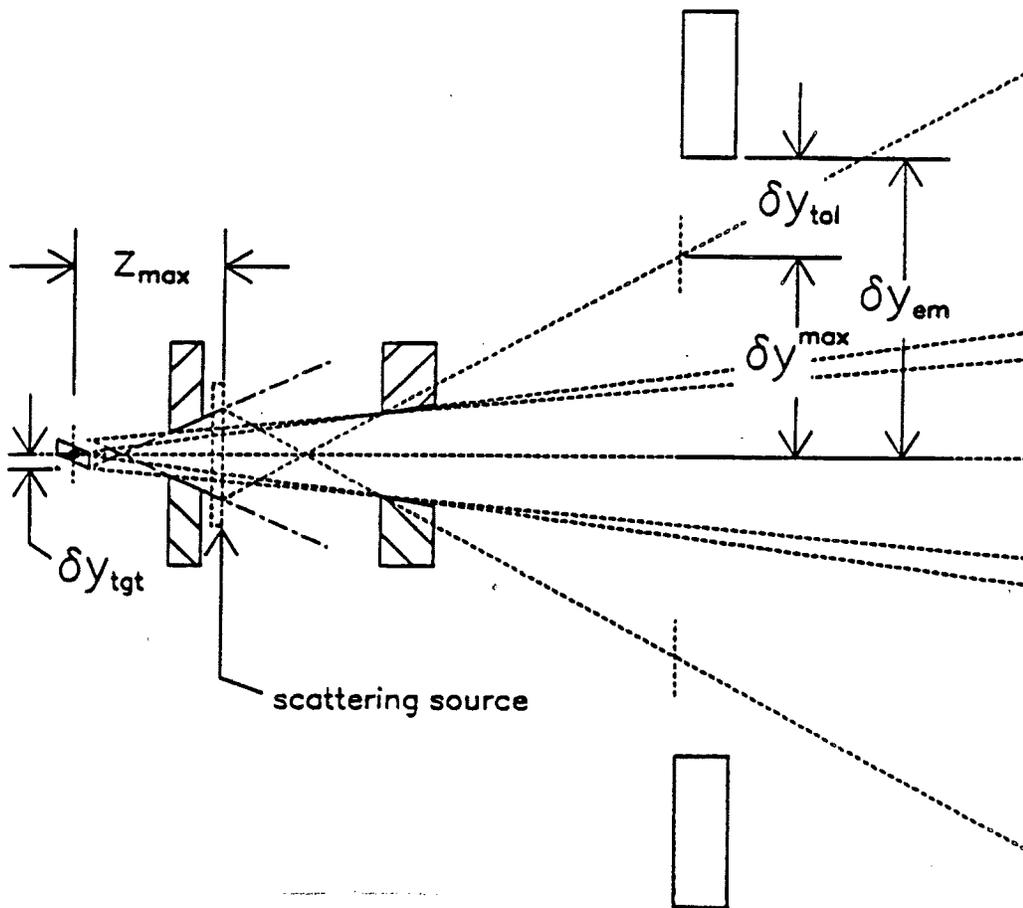
Figure 5.8.6 Elevation view of the collimator system showing the downstream most filter location and illustrating the clearance between the calorimeter and the scattered rays.

be used to monitor the alignment quite accurately (±50 microns). For example, Fig. 5.9.1 shows a mask pattern which could be detected by 5 scintillator counters. In addition we would require a single veto trigger plane scintillator upstream of a tungsten convertor (0.10") followed by additional planes(2 or 3) of scintillator which could be used to select events with pulse height consistent with an e^+e^- pair. This profile detector will be followed by the back-anti which could provide a threshold cut on the converted pair. The mask patterns, backgrounds, scattering as well as the required detector are being optimized using GEANT. Preliminary results indicate background levels are small (Fig. 5.9.2). Backgrounds from hadrons are approximately 10^{-3} of the hadron flux. We are also planning to build a profile monitor which could have sufficient segmentation to take a snapshot without the above requirements. To obtain the segmentation we will build a horizontal and a

pair of vertical scanning scintillators (2 mm wide) to sweep across both beam holes which will be placed downstream of the tungsten convertor. Both the alignment monitor and the profile monitor should be placed in a single unit which can be accurately placed and have an out position for normal data taking.

5.10 The Lambda Polarized Beam and Spin Rotations vs Sweepers

One of the considerations that enters especially into the magnets needed in the neutral beam is that of lambda production and polarization. In the following discussion, we ignore the finite targeting angle in the horizontal and assume that there is targeting at 4.8 mrad in the vertical direction. The polarization is rotated if the lambda travels through a field perpendicular to the polarization direction of the lambda. The polarization is unaffected by a field along the direction of the polarization. In the KTeV configuration, the production is vertical, so the polarization will be along the x axis of the spectrometer.

The first 3 magnets in the beamline have vertical fields and thus cause a rotation of the polarization. The angle is 11.2 degrees/(Telsa-meter). The rotation by the target sweeping magnet, E8/Hyperon, and Mu-Sweep II is 21, 142, and 117 degrees respectively, for a total of 280 degrees. The plan is to reduce this by lowering the current slightly in the sweepers to give 270 degrees so that the initial polarization along the x axis is rotated to lie along the z axis. Then the next magnet in the beamline (spin rotator magnet-modified 20' long B2 with 4" x 4" aperture) will rotate the polarization into the ±y axis depending on the spin rotator magnet polarity. The field required is 8.04 Telsa-m while the spin rotator can provide up to about 9.0 Telsa-m.
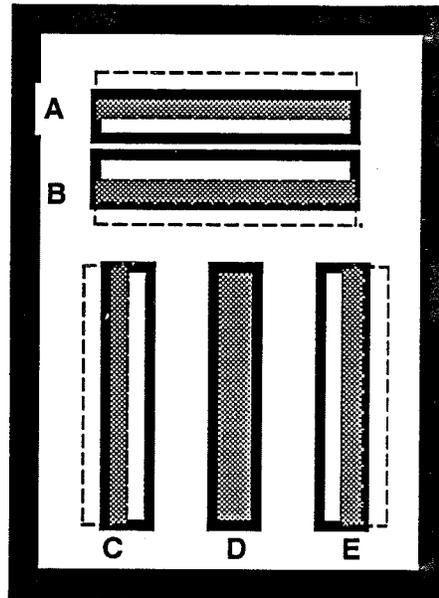
Fig.5.9.1 Signal pattern from perfectly aligned pair of masks (shown in shaded area). Dotted line represents one mask while heavy line represents the other mask. The detected signal D represents perfectly aligned holes in both masks while the others represent holes of the same area aligned pefectly but offset by 0.5* area. For example, a vertical translation down of the dotted mask would produce a larger signal A compared to B indicating the misalignment.
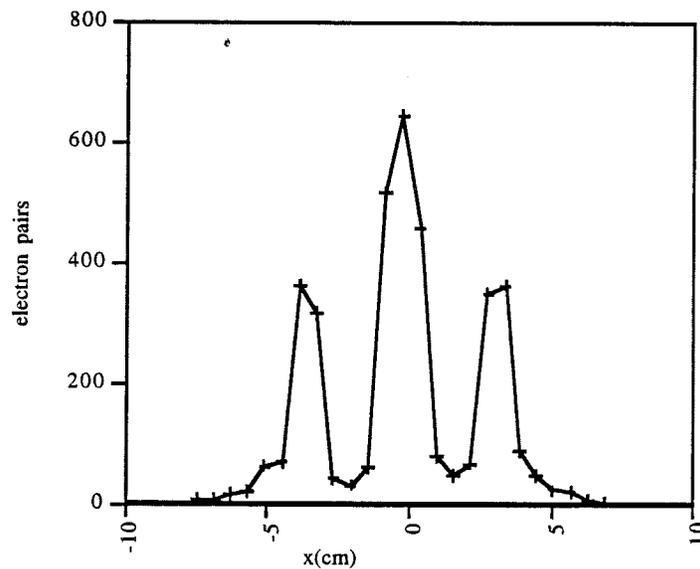
Fig.5.9.2 Pattern of detected electron pairs in alignment/profile monitor from 20,000 incident photons simulated using GEANT. Selection criteria is two charged tracks originating in convertor with total electromagnetic energy > 2.5 GeV.

5.11 Secondary Beam Simulations of Radiation Damage/Backgrounds

Two beams were simulated. In normalizing to particle fluxes through the calorimeter beam holes, for E731/E832 the regenerator beam was ignored compared with the more intense vacuum beam. For E799I/II intensity is taken to mean two beams. A week is taken to be 1×10^4 pulses. GEANT version 3.16 with the FLUKA hadronic shower generator comprised the software platform. The simulations of E799I/II were rerun with the GHEISHA generator to compare predictions. Differences in calorimeter radiation damage between the two generators are about 10%.

5.11.1 Comparison of Data and Simulations with E731 and E799-I

a.) E731

The E731 collimator positions are shown in Fig. 5.11.1. Even on this crude scale some misalignments can be seen: most fundamental is that the two-hole collimator did not precisely aim at the calorimeter beam holes. It is apparent after tracing a few rays that the upper collimator hole passes slightly more of the entering beam (the simulation gives about 10%). Fig. 5.11.2 shows the actual data for the E731 beams [18].

[18] J.R. Patterson , Determination of Re (ε'/ε) by the Simultaneous Detection of the Four $K_{L,S} \to \pi\pi$ Decay Modes, Dec.1990, U. Chicago dissertation.

(a) Elevation View.
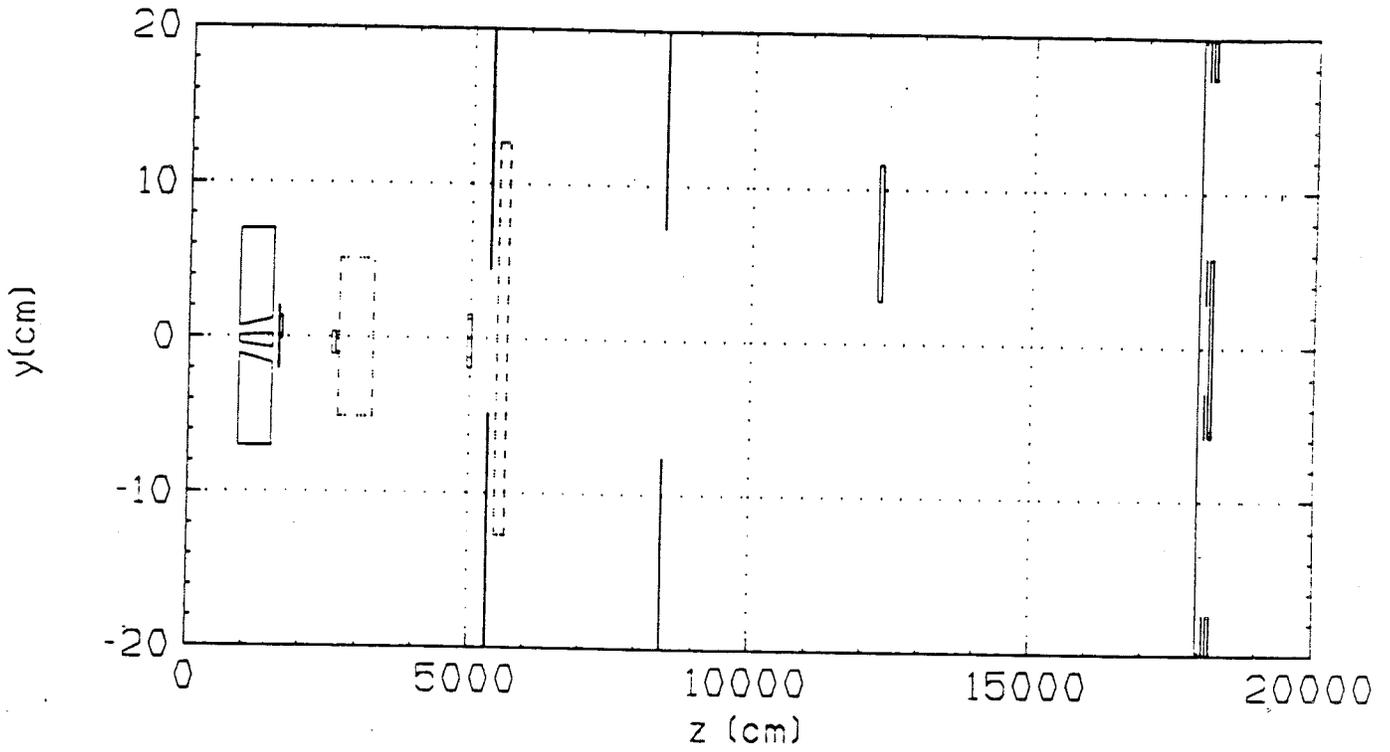
(b) Plan View
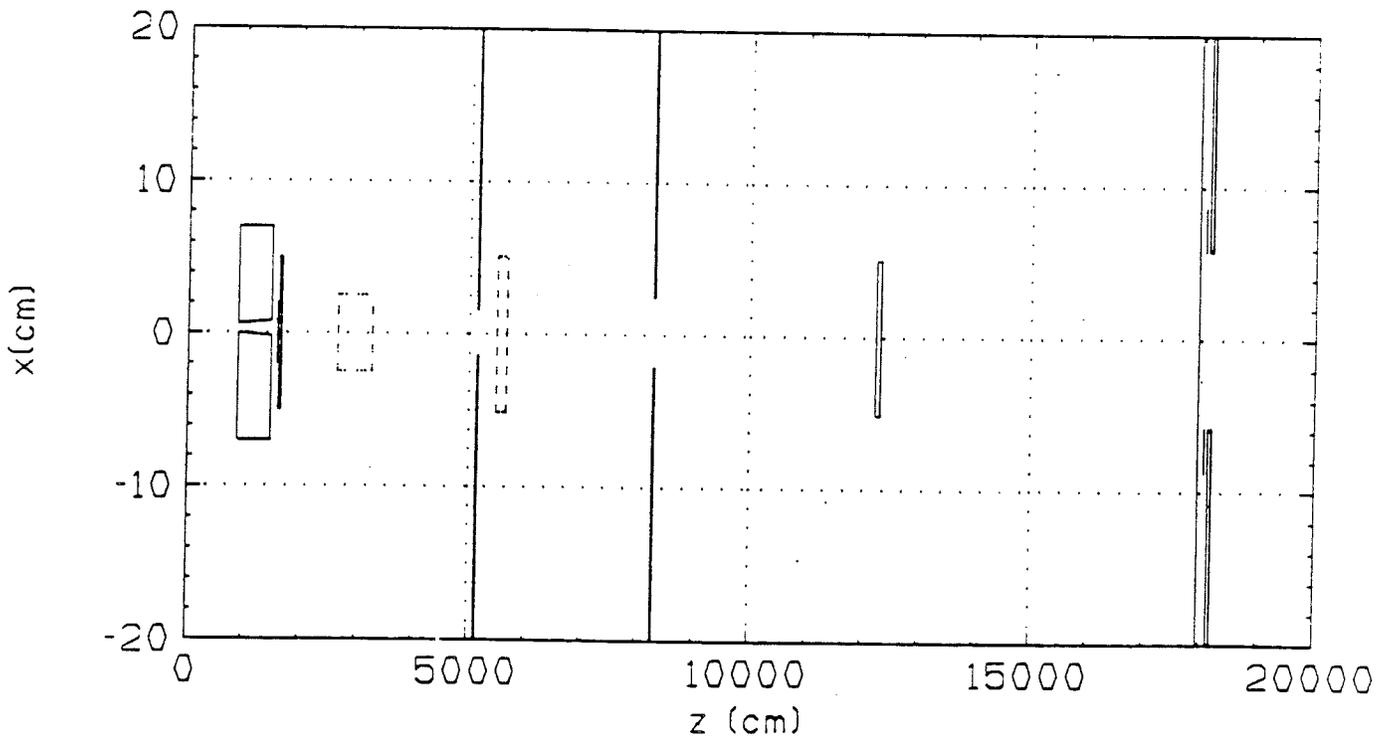
Fig. 5.11.1   Collimators, Be/Pb filters, B,C banks, Regenerator
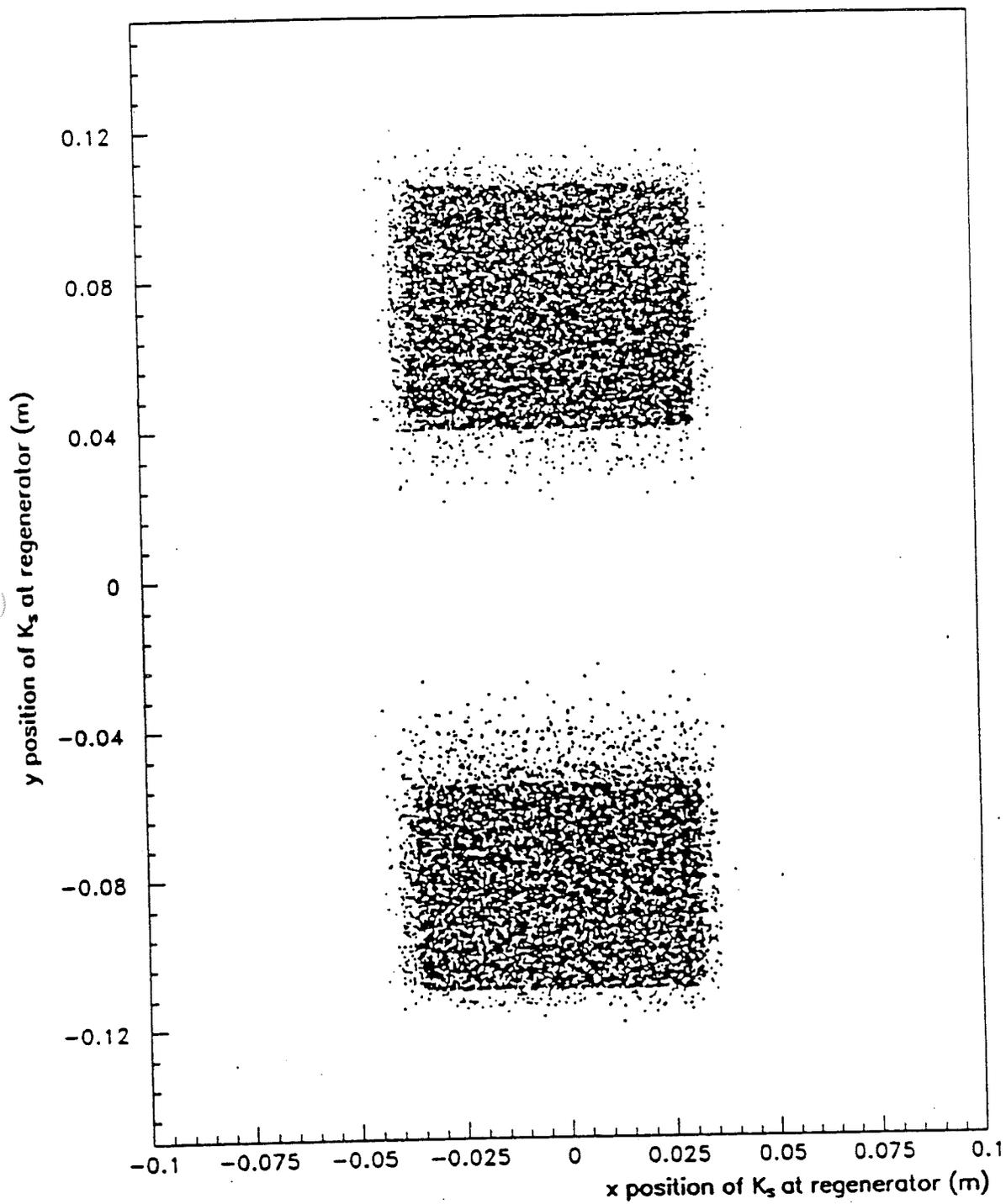
Fig. 5.11.2   The transverse position of the reconstructed kaon at the plane of the regenerator.

Beam elements in the simulation (see Figure 5.11.1) were:

1.) Two-hole collimator
2.) 50 cm Be filter
3.) 7.5 cm Pb filter
4.) 45 cm Be shadow absorber in the regenerator beam
5.) Fe slab at 23 meters
6.) Sweeping magnet at 30 meters
7.) Fe slab at 50 meters
8.) Vertical aperture jaws at 51 meters
9.) Horizontal aperture jaws at 53 meters
10.) Sweeping magnet at 57 meters
11.) Vertical aperture jaws at 83 meters
12.) Horizontal aperture jaws at 84 meters
13.) Sweeper magnet yoke at 119 m (no field)
14.) Regenerator
15.) Trigger counters (TC)
16.) Collar anti (CA)
17.) lead glass and beamholes

Material of all the elements was simulated in GEANT, except for some of the sweeping magnets iron (items 6 and 10) which were simulated by discarding any charged tracks that passed through them. In addition, particles that originated upstream of the last jaw pair (item 12) were not followed unless their energy exceeded 1 GeV. Downstream of 84 meters all tracks with E > 20 MeV were followed. The simulations also included a vacuum window, helium , and the drift chamber materials. Runs were made with this material replaced by vacuum and also air . In addition, runs were made with and without the TC.

The upstream aperture of the 2-hole collimator was randomly filled with track-starting points and the target was randomly filled with the corresponding particle origins. The direction so defined was assigned to a momentum selected from the Malensek distributions. Encounters with the walls of the 2-hole collimator were simulated, and a few cases were found in which hadronic elastic scatters in the collimator eventually led to calorimeter activity. After having done several

simulations where it was apparent that inelastic scatters in the Be, Pb, and 2-hole collimator consumed a large fraction of CPU time but did not lead to activity in the lead glass, events were dropped in the remaining simulations if the beam particle interacted inelastically in any of these elements.

Figure 5.11.3 shows some results of a neutron and a K_L run with all parameters nominal, set to what was measured for the experiment. The run statistics generally give 10^4 or more beam particles through the lead glass holes. Figure 5.11.3 shows an attrition of 30-50 between starting particles (Figure 5.11.3a, c) and those that get past the calorimeter (Figure 5.11.3b, d); momentum of the survivors is not much different from the starters except for the decay loss of low energy K_L due to their small Lorentz factor. Figures 5.11.3 e and f show energy absorbed in the lead glass as a function of x, y position of the individual ionization deposits. The cell contents are weighted by the absorbed energy and therefore give the simulated radiation damage. Figures 5.11.3 g and h show the central region enlarged. Damage due to neutrons is more centered than for the K_L's.

The points labeled "normal" in Figure 5.11.4 give our best estimate of the total radiation absorbed in the lead glass. Interactions in the regenerator are the main source for the neutron beam. When the regenerator and shadow absorber materials are both changed to vacuum, the radiation decreases by about 50% at the center and from a factor of two beyond 20 centimeters to an order of magnitude at the edges. The regenerator is comparatively less significant for the K_L beam. All decays were turned off for the run labeled "no decays" in Figure 5.11.4a. The difference between these points and the "normal" points marks a level which cannot be reduced. Since the points fall by a factor of 5 everywhere, decays must account for ~80% of the damage due to the K_L beam. Both the regenerator and the TC's were simulated for the "no decays" run.

The TC material (2 cm of scintillator plus wrapping plus air is a source of damage mainly inside a 40 centimeter radius. For neutrons the TC's were the source of 1/3 - 1/2 the damage. For K_L, they did not contribute significantly compared to the other sources.

EXP731. TRIG, CA. Pb, Be Filters

(a)[101] GENERATED. n-3.21·10⁵.

(b)[105] Beam thru PbG holes. n-6283

NEUTRONS

(e)[432] n-3.023·10⁴

(g)[432] n-1.142·10⁴

(c)[101] GENERATED. n-3.5·10⁵

(d)[105] Beam thru PbG holes. n-1.03·10⁴

KLONGS

(f)[432] n-7.783·10⁴

(h)[432] n-2.957·10⁴
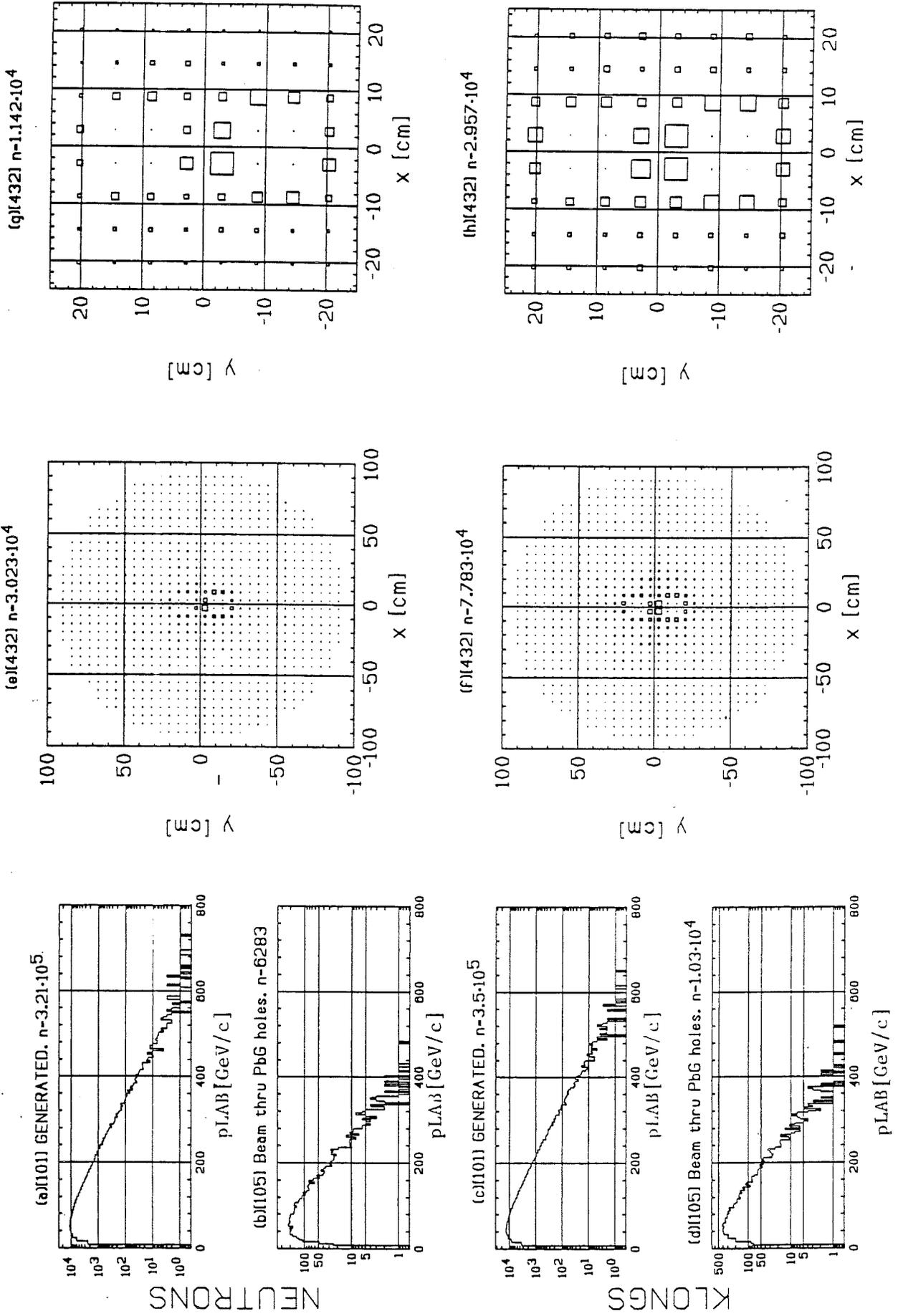
Fig. 5.11.3 Energy deposited in Leadglass.
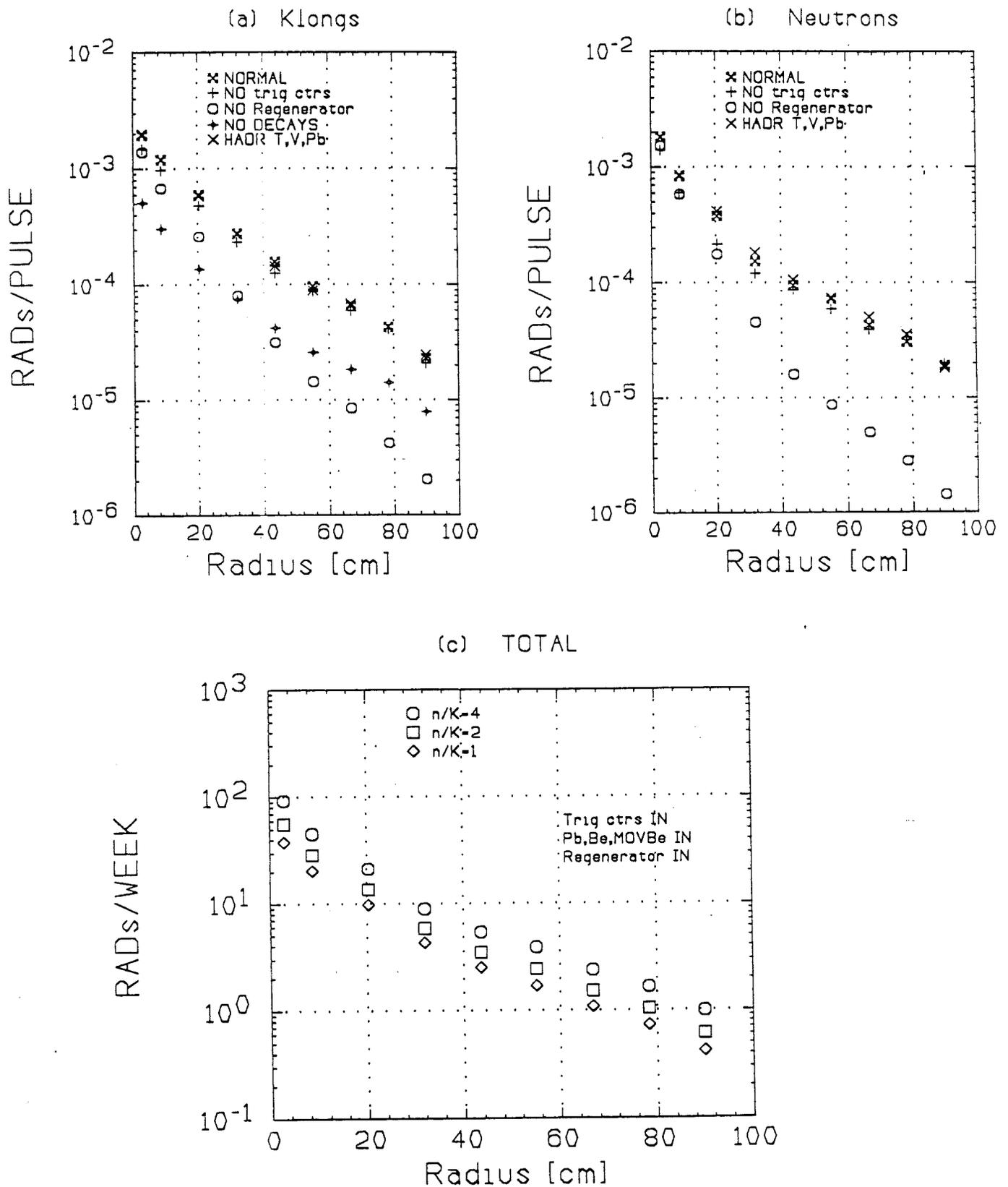
Fig. 5.11.4　EXP731.　Radiation vs radius

Under the assumption that a week of running contains 10^4 pulses at the Tevatron, the points can be converted to rads/week. Figure 5.11.5 has the Monte Carlo results for several assumptions on the n/K_L ratio. The pair of curves for each condition represents the statistical difference in two different runs. Figure 5.11.6 has the prediction superimposed on the data, and the agreement is reasonable using the $n/K_L = 2$ (for the E731 vacuum beam); the value that best matches other data from E731 as discussed in section 5.2.

b.) E799-I

Collimator positions are much closer to perfect alignment than for E731. The simulation runs were done essentially the same as for E731 except (1) regenerator and shadow absorber were absent; (2) there was no Be filter; and (3) TRD material, 2%X_0 of polypropylene, was added. The other TRD components were ignored. The kaon flux increased from 10^7 to 8.5×10^7. Figure 5.11.7 show energy absorbed in the lead glass due to K_L, n. The simulation was repeated without the TC's and TRD's; these detectors contribute about 1/3 of the K_L-induced background and $\approx 3/4$ of the neutron-induced background. Figures 5.11.8-9 show the results again with several assumptions on the neutron flux. This comparison matches best if $n/K_L = 4$ for E799 or $n/K_L = 2.8$ (E731 vacuum beam).

Figure 5.11.10 shows the origin of particles that enter the lead glass for the K_L runs. It is organized into four quarters, split vertically by weighting: (top six plots) equal weights for all hits, or (bottom six) hits weighted by energy of the particles that enter the lead glass. The horizontal split depends on whether the B and C banks and the TRD's are in or out. Figure 5.11.10a shows the vertex z for each particle that enters the upstream face of the lead glass. There are spikes near z $\approx$900 centimeters where tracking starts at the entrance to the 2-hole collimator, at z $\approx$1600 (the Pb filter), in a region at z $\approx$5000 where the last slab and upstream jaws are located, at z $\approx$8000 at the downstream jaws, and near z $\approx$18000 at the TRD and B, C counter banks. The final spike lies in the bin 18050 < z < 18100 which contains the collar anti counter. Beneath each major plot, the upstream (9 < z < 16 meters) and downstream (176 < z < 185 meters) regions are expanded.

146
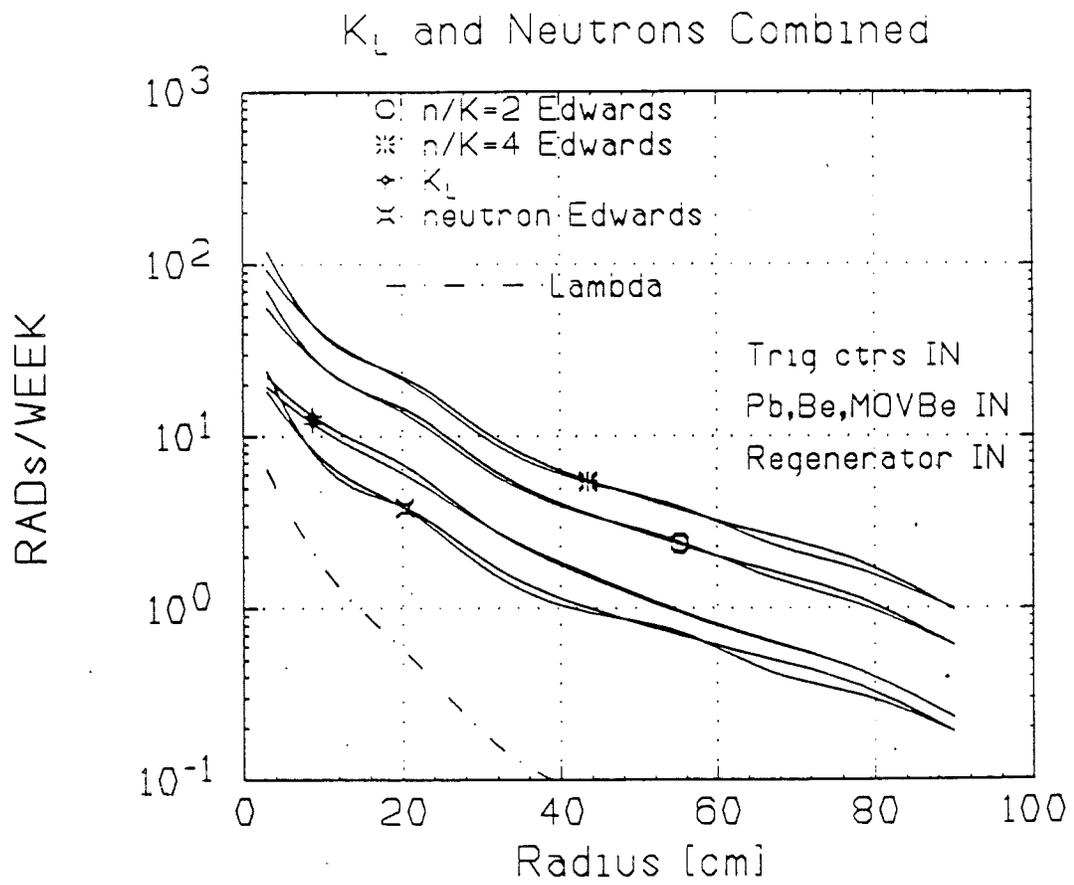
Fig. 5.11.5   Radiation vs radius. EXP731.

E731 accidental data
K_L and Neutrons Combined

Legend:
○ n/K=2 Edwards
※ n/K=4 Edwards
+ K_L
⋈ neutron Edwards

— — — Lambda

Trig ctrs IN
Pb,Be,MOVBe IN
Regenerator IN

Y-axis: RADs/WEEK
X-axis: Radius [cm]
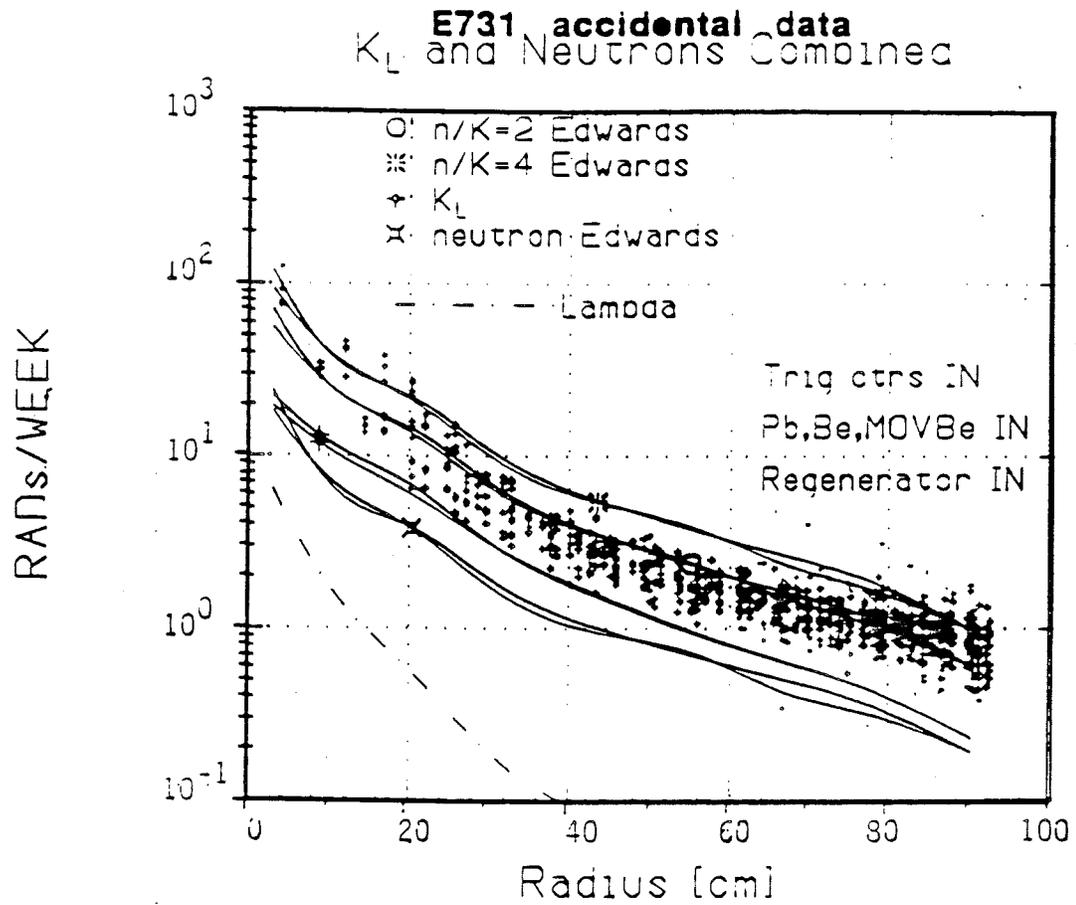
Fig. 5.11.6   Radiation vs radius. EXP731.
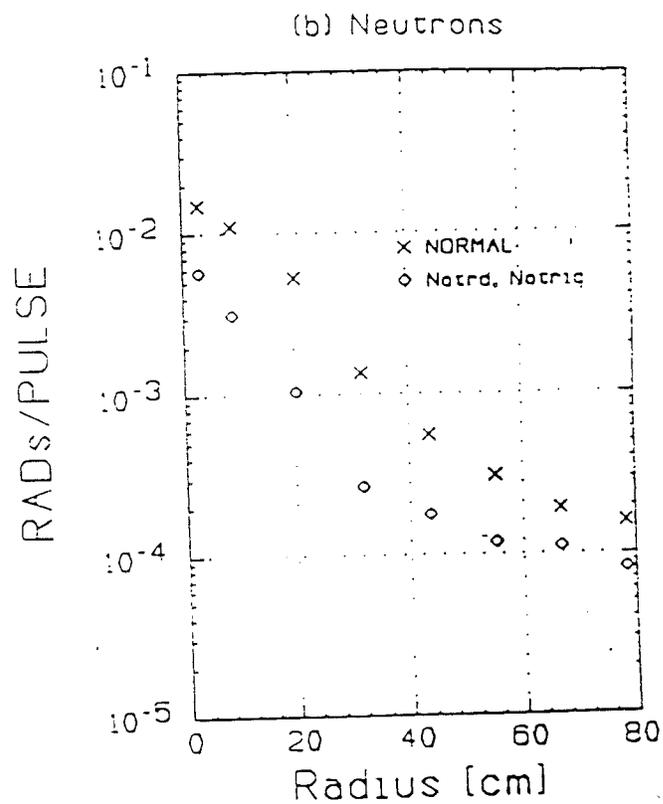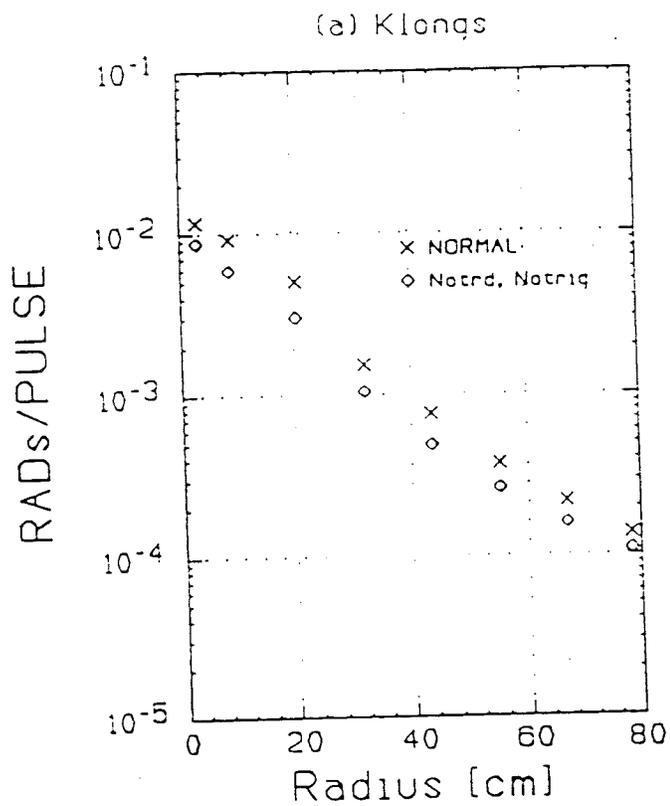
Fig. 5.11.7 EXP799-I. Radiation vs radius.
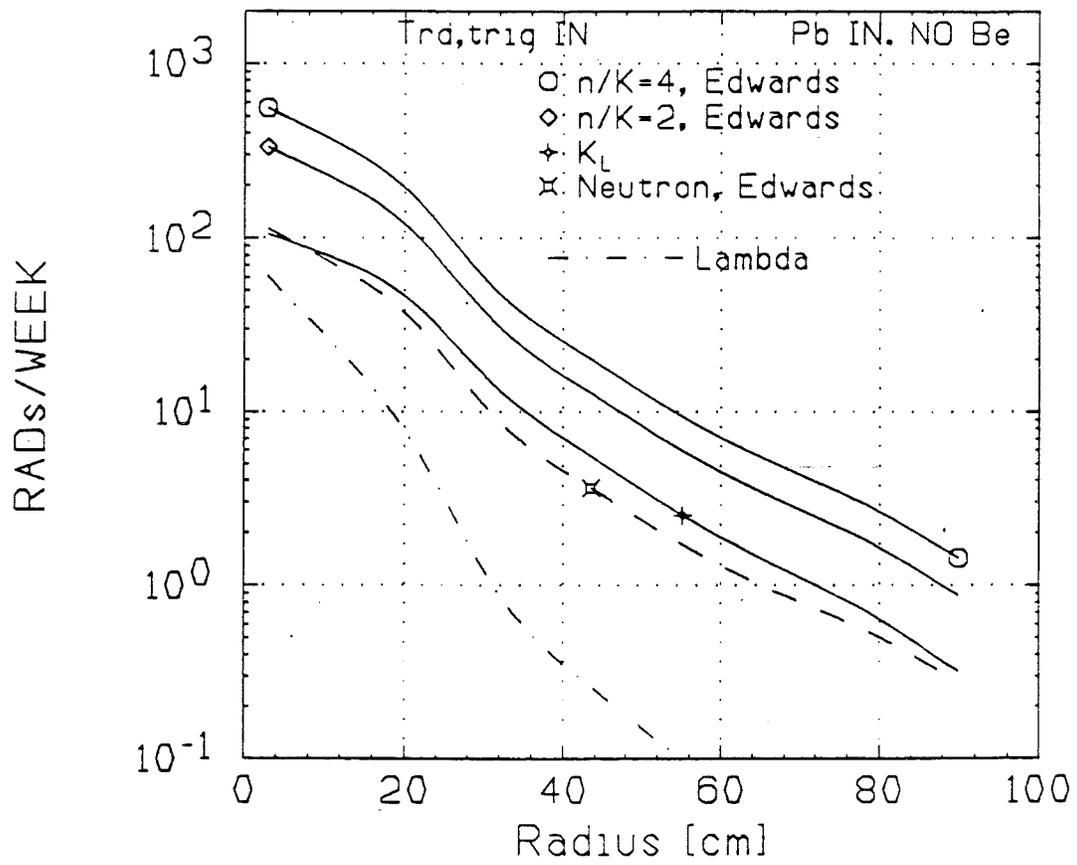
Fig. 5.11.8 Radiation vs radius. EXP 799-I.
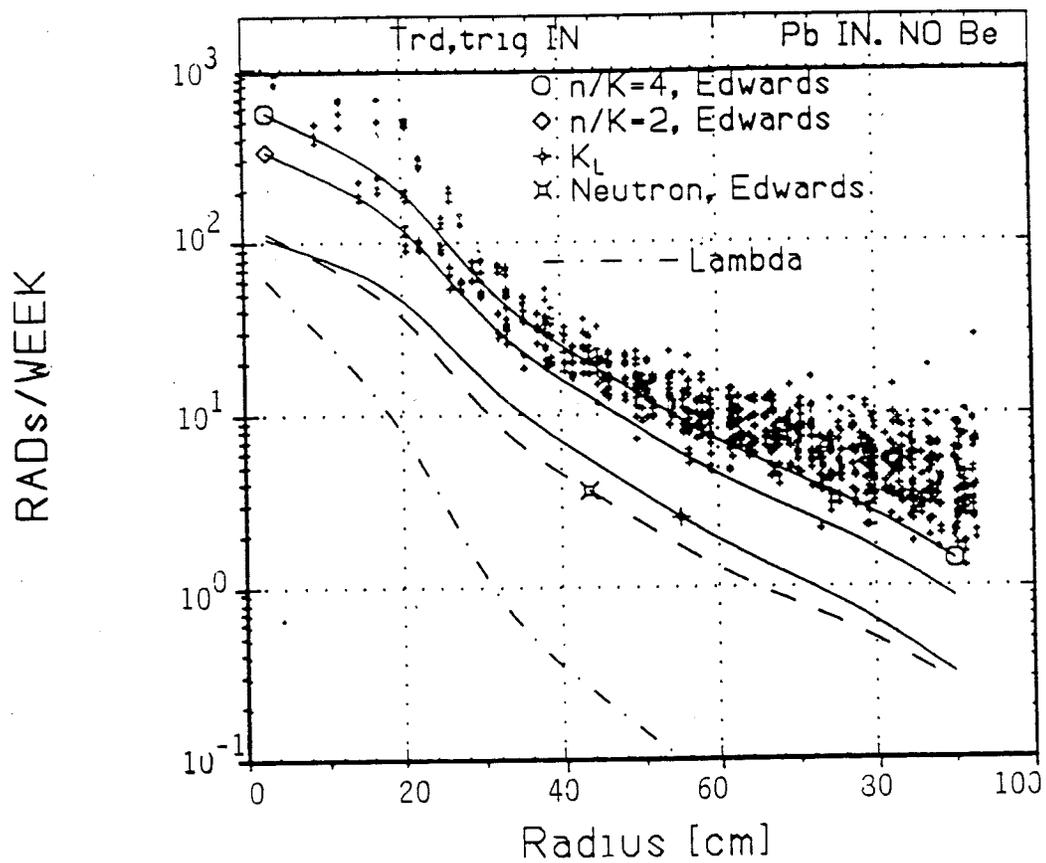
Fig. 5.11.9   Radiation vs radius. EXP799-I.
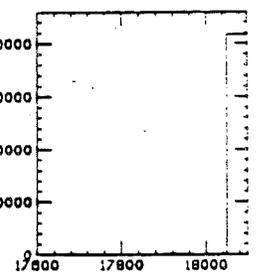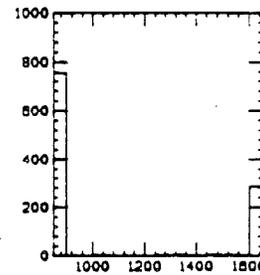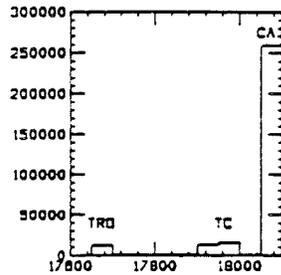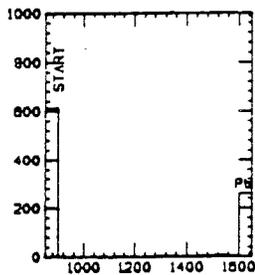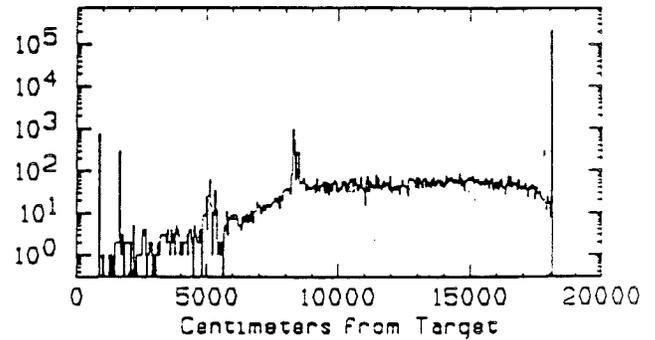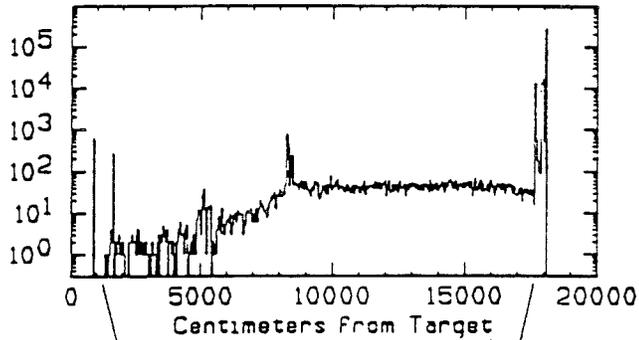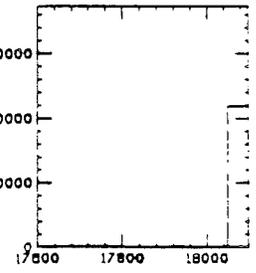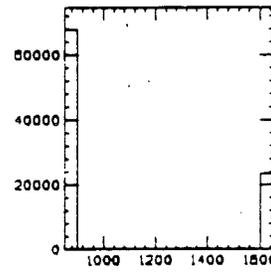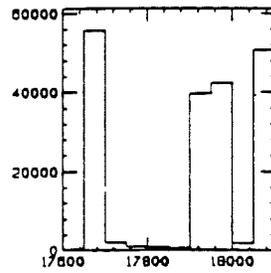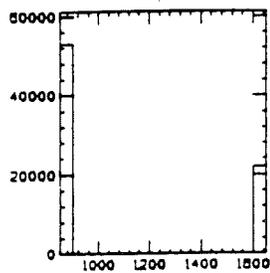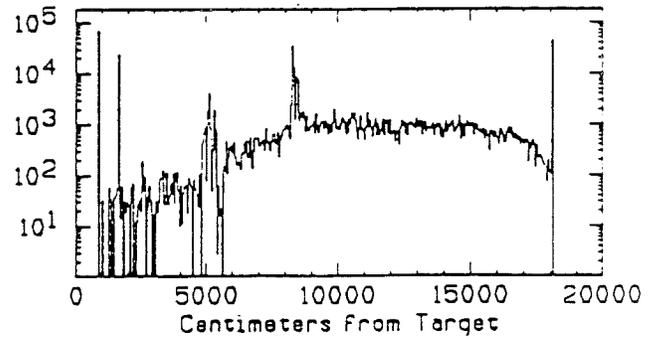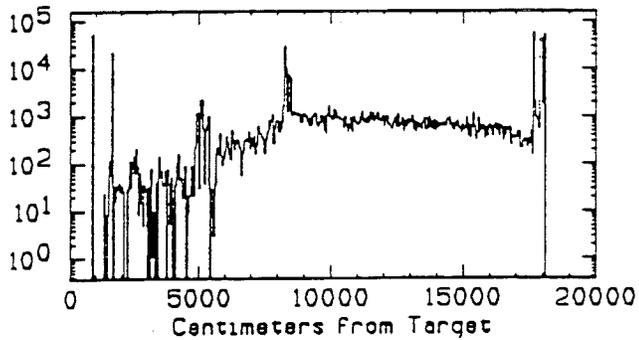
Fig. 5.11.10 Z-origin of particles entering PbG. E799-I

The number of hits that can be traced back to the 2-hole collimator entrance and the Pb filter is relatively small(~900), due to TC(~40,000) and due to TRD(~10,000). On the other hand, the energy-weighted plots, Figures 5.11.10c (with B, C, TRD) and 5.11.10d (without B, C, TRD) show that these are on a par for radiation damage with the material right in front of the lead glass. The detailed z-cut plots allow the particular collimator or filter element to be isolated. The area under the broad-z distribution (decays) between the spikes is ≈40% of the total area, comparable to that under the spikes.

Figure 5.11.11 shows the same set of plots for a neutron beam. The main difference is the near absence of decays. The GEANT prediction is about half of the pipe block energy or damage is correlated with interactions in either the TRD or TC. A recent study of E799I accidental data[19] finds 44% of the pipe block energy is correlated with TRD and TC interactions in good agreement with the Monte Carlo. This same study also measured the rate on the hottest drift chamber wire in the most upstream chamber in E799I after subtracting out the muons from our upstream target and beam dump gives 26 kHz for the hottest wire. While our GEANT model of the secondary beam charged particle flux indicates about 17 kHz for E799I from K_L decays only.

c.) Findings

Given the overall good fits to E731 and E799-I for the simulation model, we believe that the main sources of damage are identified. In E731, background from both K_L and neutron interactions in the regenerator dominates everywhere except within the blocks between the beams. Even there it contributes approximately 20% of the damage. These statements are based on Figures 5.11.4. The TC's explain about half the damage from neutrons near the center, but much less for r > 40 cm. A high energy neutron interaction in scintillator can make up to 50 secondary particles, mostly pions, that do not deposit a lot of energy in the thin TC's, but which are largely absorbed in the calorimeter that follows within ≈2 meters. For K_L, the counters were not a major contributor because K_L decays are a more prolific source. Much of our confidence in this simulation is due to the fact that it not only gets about the right magnitude of the damage for both E731 and E799 but also reproduces

---

[19] private communication, R. Tschirhart.

153

NEUTRON BEAM

nthru=$8.356 \cdot 10^4$ EQUAL WEIGHTS nthru=$7.456 \cdot 10^4$

(a) TRD,B,C (b) NO TRD,B,C
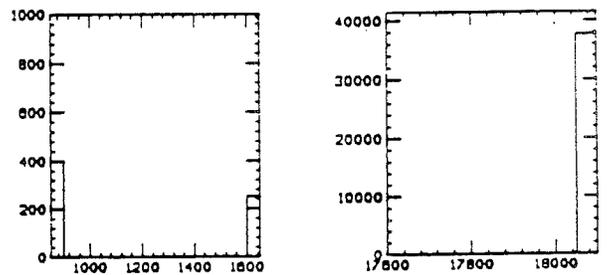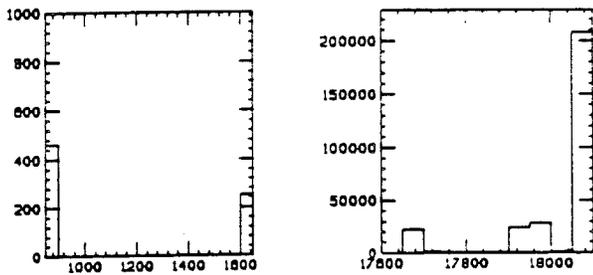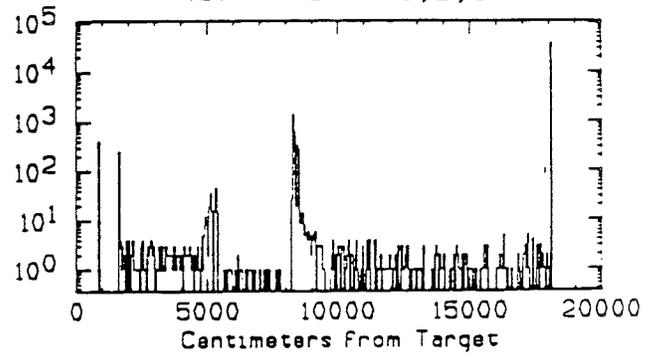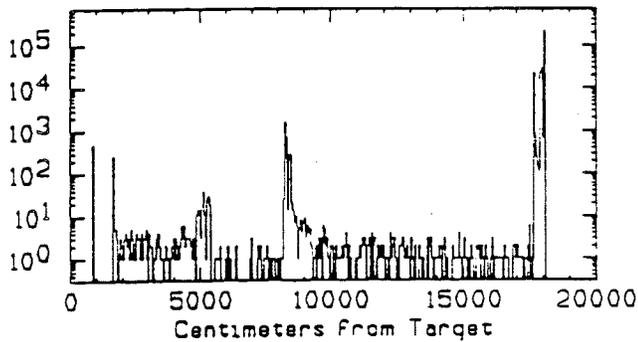
WEIGHTED by ENERGY

(a') TRD,B,C $\Sigma = 5.647 \cdot 10^5$ (b') NO TRD,B,C $\Sigma = 2.227 \cdot 10^5$
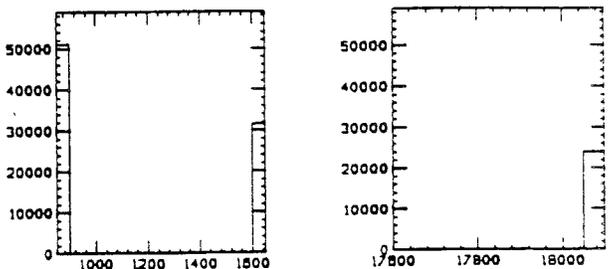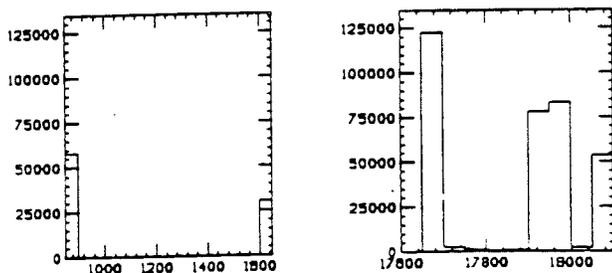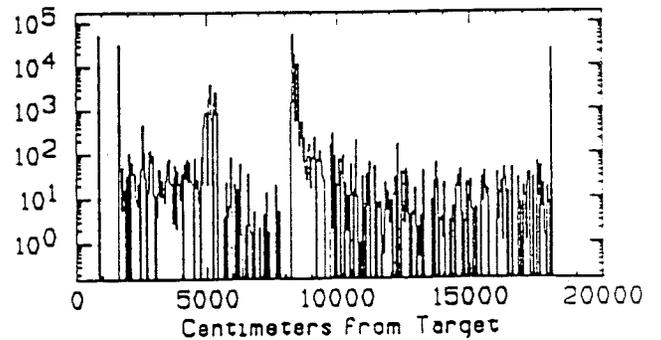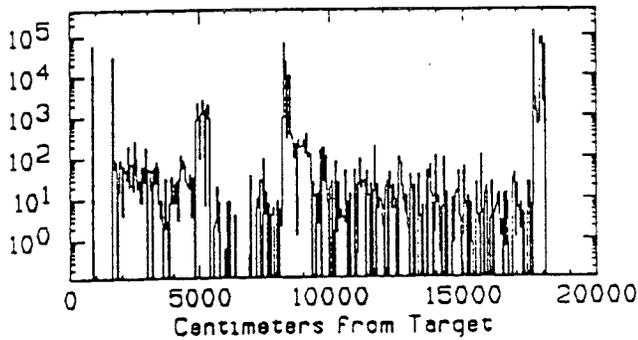
Fig. 5.11.11 Z-origin of particles entering PbG. E799-I

the observation that the lead glass radiation damage falls off with increasing radius much more steeply when the regenerator is absent.

5.11.2 Projections for KTeV - E799II and E832

In KTeV, the neutral beam will be more effectively collimated than in the earlier experiments. Figure 5.11.12 shows the plan and elevation views.

a.) E799-II

The K_L flux will be 2.9×10^8 for the sum of two beams. The elements in the E799-II simulation are:

1.) Pb filter
2.) Cu primary 2-hole collimator (PC)
3.) Fe vertical slab separating the beams horizontally
4.) Fe x-defining vertical jaws
5.) Fe y-defining horizontal jaws
6.) Sweeping magnet from 23-29 m, 25 kg, 40cm(x), 4cm(y)
7.) Cu downstream 2-hole collimator (DC)
8.) DC Insert
9.) Sweeping magnet
10.) Trigger counters (TC)
11.) CsI calorimeter

Material in the vacuum window, helium, and drift chambers was included. Figure 5.11.13 shows the origins of CsI hits. Four cases are shown: n and K_L with and without TC beamholes. Each run gave approximately 3×10^4 beam particles through the CsI holes. The individual numbers (nthru) are printed on the plots. Compared with the expected flux of 2.9×10^8 this tiny sampling (6×10^5) is a potential weakness of the Monte Carlo. It is possible that tails of distributions unsampled in this simulation could change the picture.

(a) Plan View

(b) Elevation View
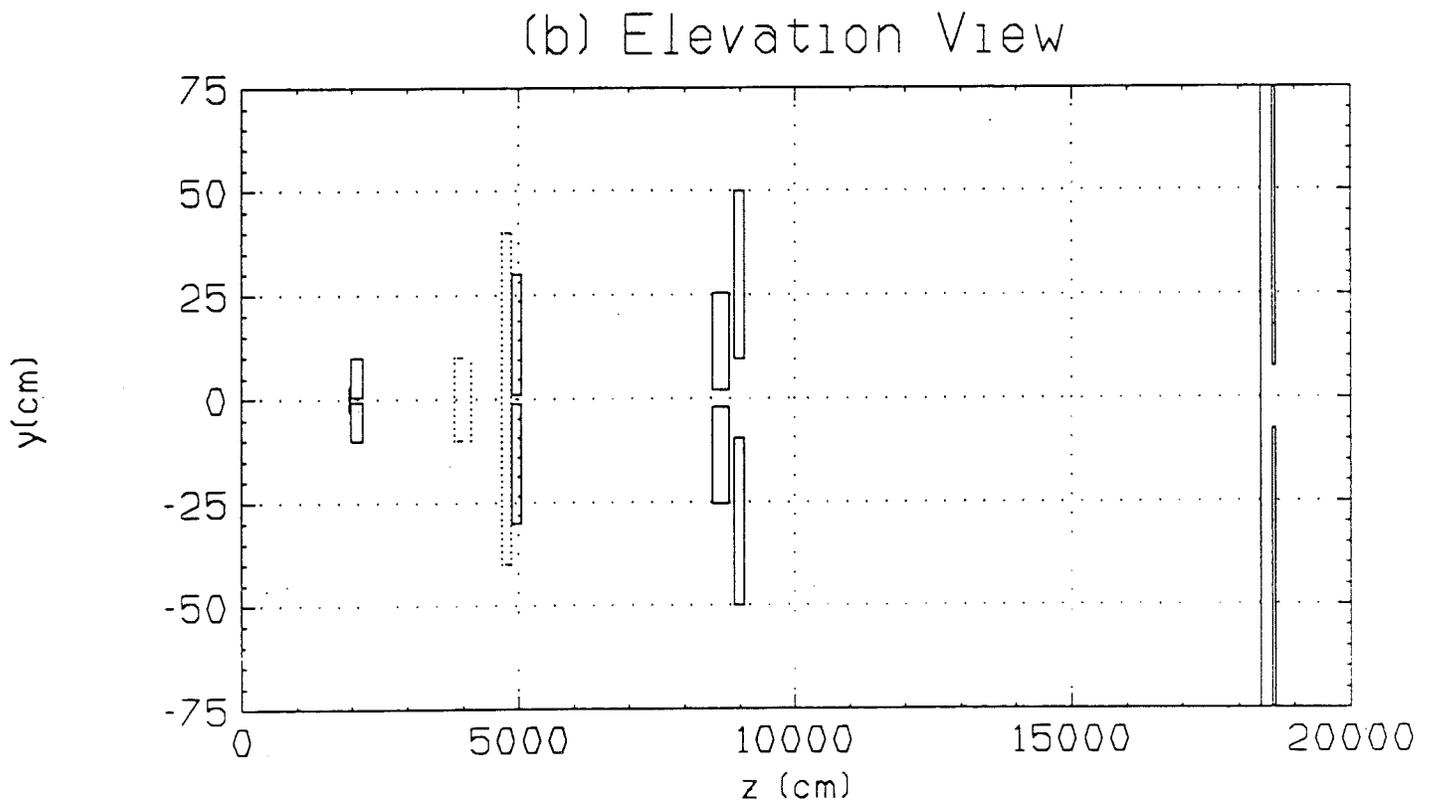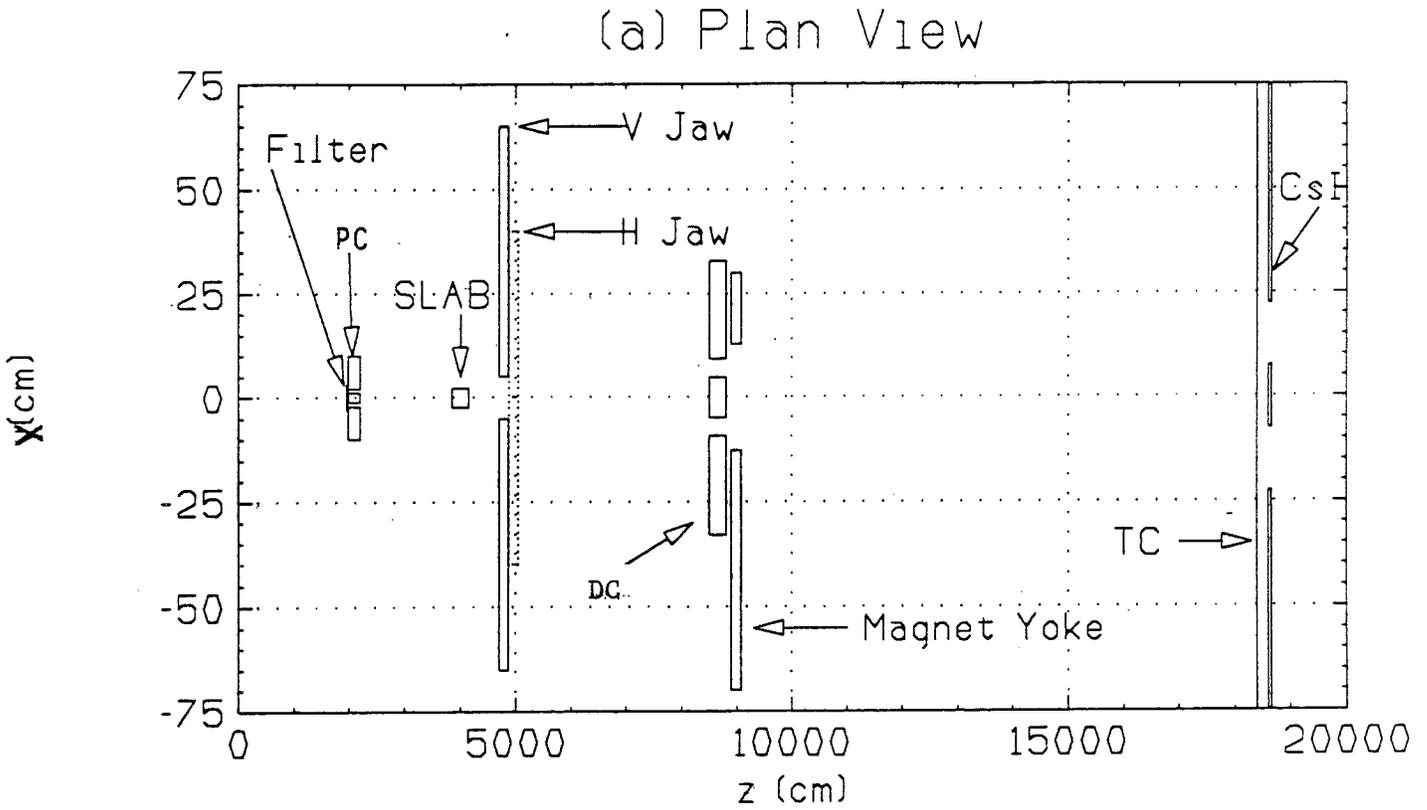
Fig. 5.11.12   KTeV Beam

Solid Trigger Counters

Trigger Counters with Beam Holes

a) [121] K_L, nthru=3.5·10^4
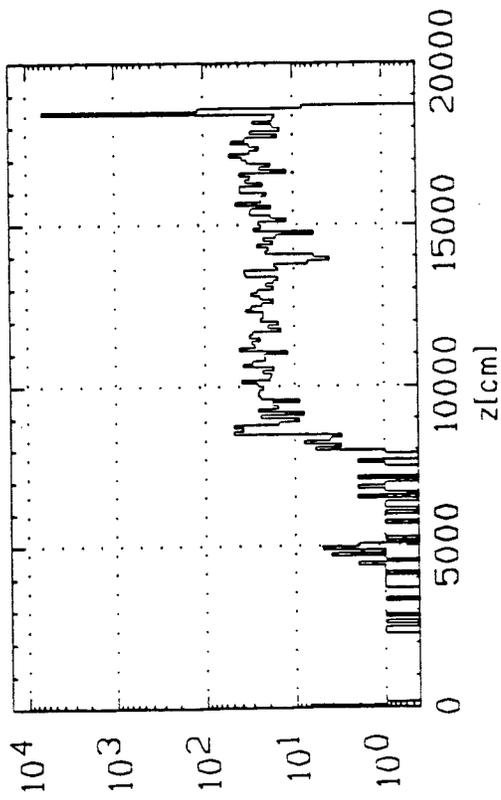
b) [121]neutron nthru=2.784·10^4
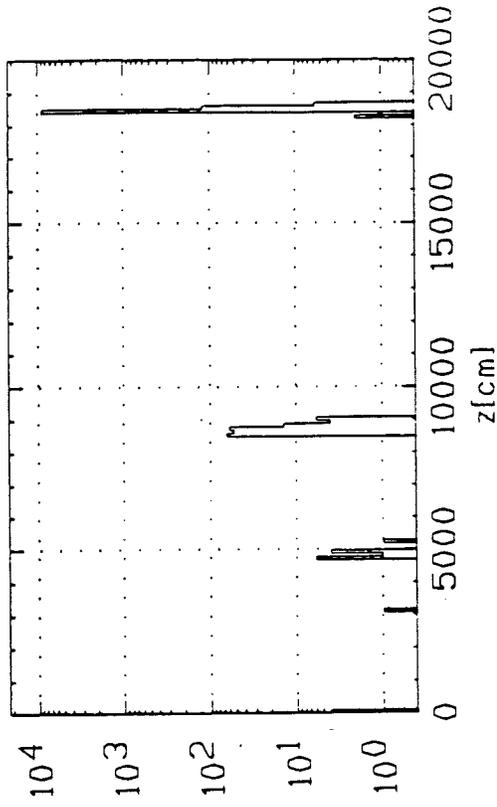
c) [121] K_L, nthru=3.34·10^4
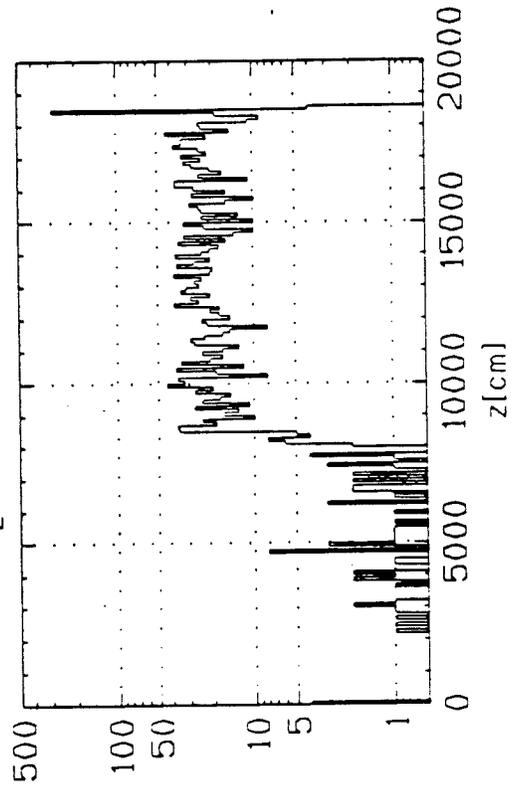
d) [121]neutron nthru=2.605·10^4

z[cm]
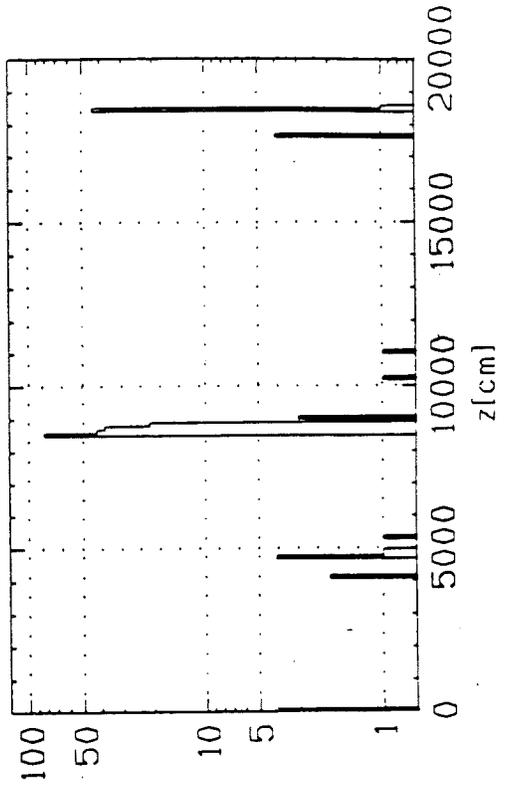
Fig. 5.11.13   E799-II Sources of CsI Hits

The z-coordinate of the vertex of any particle entering the CsI is enough to identify where the background comes from. K_L's decay over the whole path from 80 to 200 meters so the distribution is continuous from the downstream collimator to the CsI with a spike at the TC plane. The runs with TC beamholes show smaller spikes at the TC where some of the kaon daughters interact. (The main beams of course pass through.) A few cases where neutrons lead to CsI hits nearly all originate in the DC at z ≈88 meters. Figure 5.11.13a(b) shows $K_L(n)$ if the TC's are solid across the beam, and Figure 5.11.13c(d) if the TC's have beamholes. CsI hits go up a factor of ≈25 (7000/300, from the Figure 5.11.13a,c spike at z ≈186 meters) due to particles starting at the trigger plane.

To cite numbers for radiation damage as a function of position, the calorimeter is divided into square cells of width 15 cm. The numeration is shown in table below. The energy deposits in the CsI are plotted in Figure 5.11.14a (b)for K_L(neutrons). The damage from the kaons is not increased much above that from decays by the TC material. However, damage from neutrons in the pulse goes from negligible to near equality with the K_L including the TC material. Also shown are the effects of rotating the slab collimator by 2 mrad creating a horizontal tilt and of rotating the DC 2 mrad to create a vertical tilt. Even though this 2 mrad rotation is more than an order of magnitude larger than expected alignment tolerances, the radiation damage doesn't significantly increase.

Table of numbering of CsI Cells

```
5 5 5 5 5 5 5 5 5 5 5 5 5
5 4 4 4 4 4 4 4 4 4 4 4 5
5 4 3 3 3 3 3 3 3 3 3 4 5
5 4 3 2 2 2 2 2 2 2 3 4 5
5 4 3 2 1 1 1 1 1 2 3 4 5
5 4 3 2 1   0   1 2 3 4 5
5 4 3 2 1 1 1 1 1 2 3 4 5
5 4 3 2 2 2 2 2 2 2 3 4 5
5 4 3 3 3 3 3 3 3 3 3 4 5
5 4 4 4 4 4 4 4 4 4 4 4 5
5 5 5 5 5 5 5 5 5 5 5 5 5
```

How serious this TC material is depends on the n/K ratio. Figure 5.11.14c predicts 500 rads/week for a worst case. This damage would be less by a factor of two if the neutral beam can pass through holes in the TC. Repeating this analysis for the double solid angle option (.50 μster.), gives radiation damage which increases only slightly more than for the kaon flux. This work will be documented in a future KTeV memo.

The predicted beam profiles at the CsI for the case with TC beamholes are shown in Figure 5.11.15.

Figure 5.11.14. E799-II Radiation damage vs CsI group

Fig. 5.11.15 a) The flux of all particles hitting a plane just of the CsI
predicted for E799II.

b) The flux weighted by particle energy.

c) The flux of K_L's.
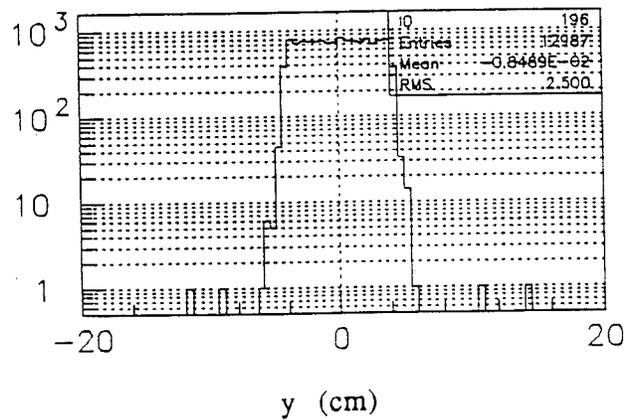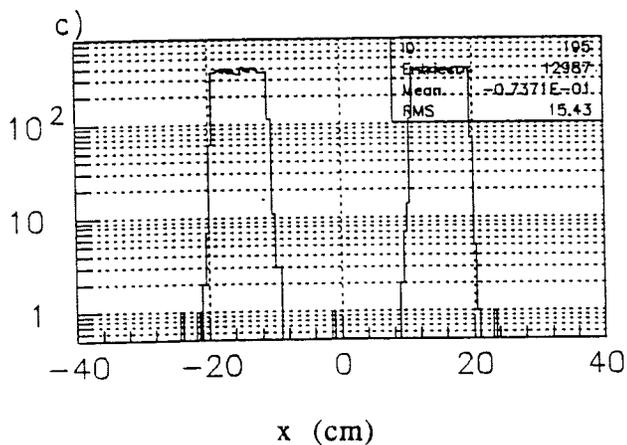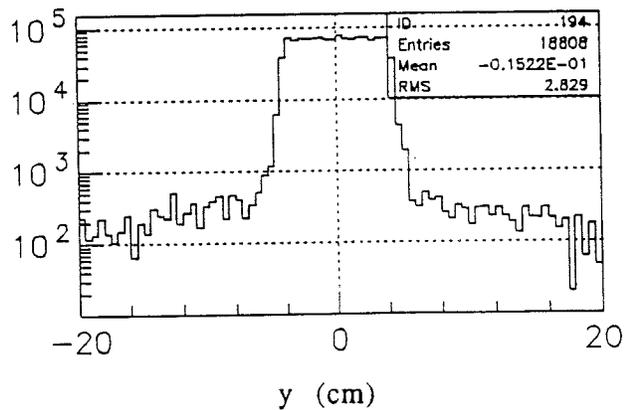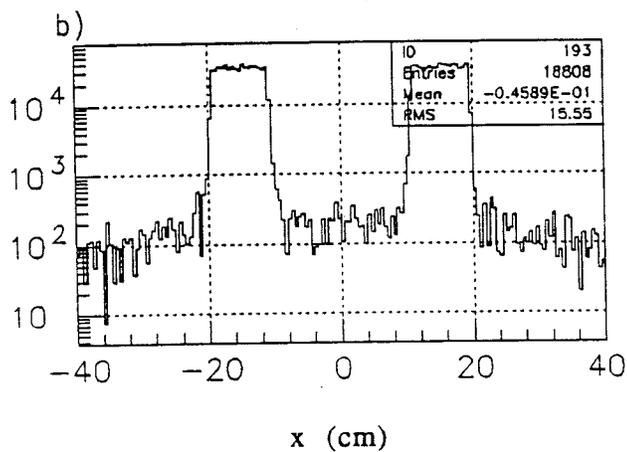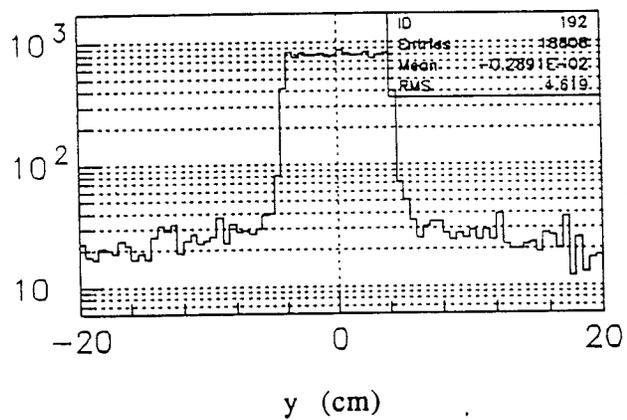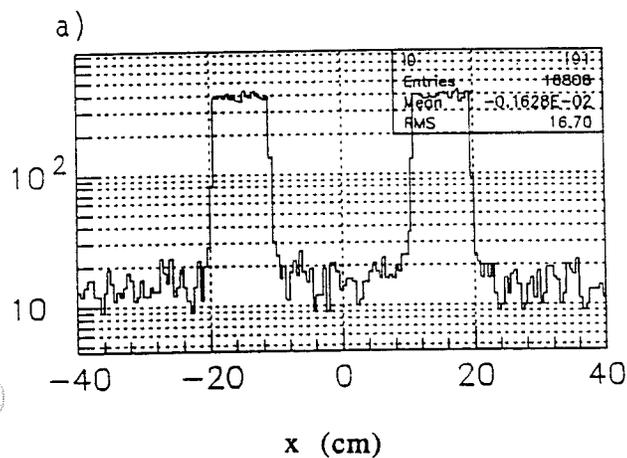
b.) E832

In addition to the beam elements listed above, E832 adds:

13.) Be shadow absorber
14.) Regenerator

The K_L flux for E832 will be about 3.5×10^7 for the vacuum beam. The CsI background picture is different from that of E799II. The regenerator dominates; Figure 5.11.16 shows the z-origin of particles that enter the front face of the CsI; the regenerator at 120 meters is prominent, especially in the neutron runs. Figure 5.11.17 summarizes the energy dumped in the CsI. The TC damage adds about 25% to that from the regenerator for both n and K_L. The beam profiles are shown in Figure 5.11.18 for the case with TC beamholes.

c.) Conclusion

The main features of radial dependence of measured radiation damage to the lead glass calorimeter in E731 and E799 are reproduced with a GEANT simulation. The level of damage is reproduced to a factor closer to two, and the shape is better than that. The contrast between E731 and E799 and the r-dependence is reproduced. A simulation to predict damage in CsI gives a level that almost surely will approach 200-300 rads/week at the center of the calorimeter in E799-II. The level may go as high as 500 rads/week depending on the neutron to kaon ratio of the beam. The damage will be reduced by about a factor of two by having holes in the trigger counters. In E832, regenerator-induced background is so high that the trigger counter material is almost of no incremental effect. Studies of the acceptance for $K_L \rightarrow \pi^+\pi^-$ with beam holes in the trigger counters[20] indicate a small loss in acceptance. Therefore, we plan to run both E832 and E799II with the same trigger hodoscope which has beam holes.

---

[20] Belz, J., et al., KTeV 0200, Modified KTeV Trigger Bank Layout, 5/5/94.

Solid Trigger Counters

[121] neutron nthru=$1.301 \cdot 10^4$

[121] K_L nthru=$1.968 \cdot 10^4$

Trigger Counters with Beam Holes

[121] neutron nthru=$1.453 \cdot 10^4$

[121] K_L nthru=$1.928 \cdot 10^4$
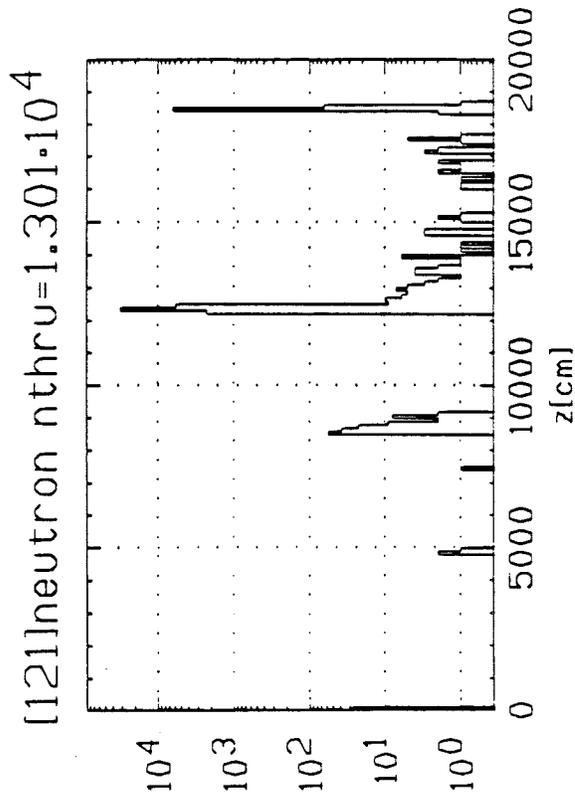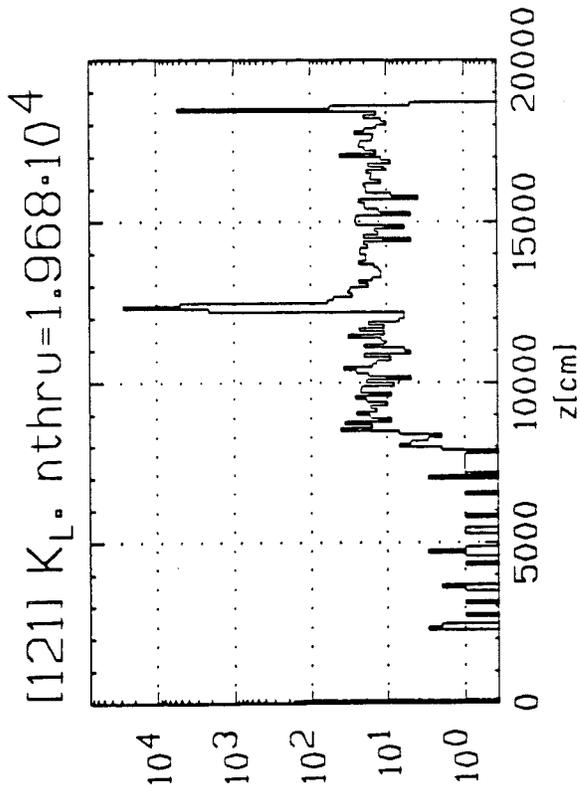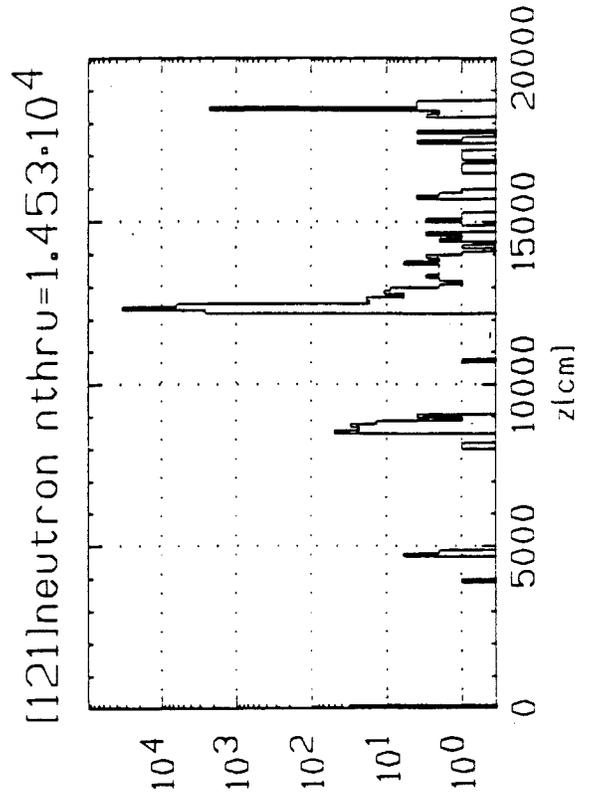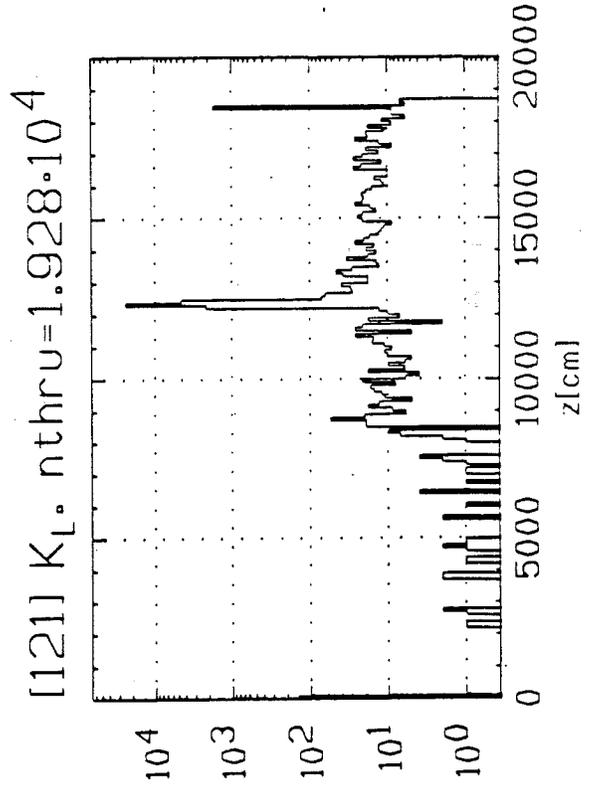
Fig. 5.11.16 E832 Sources of CsI Hits

Figure 5.11.17 E832 Radiation damage vs CsI group

Fig. 5.11.18   a)   The flux of all particles hitting a plane the CsI for E832
(showing both vacuum and regenerator beams).

b)   The flux weighted by particle energy.

c)   The flux of K$_L$'s.
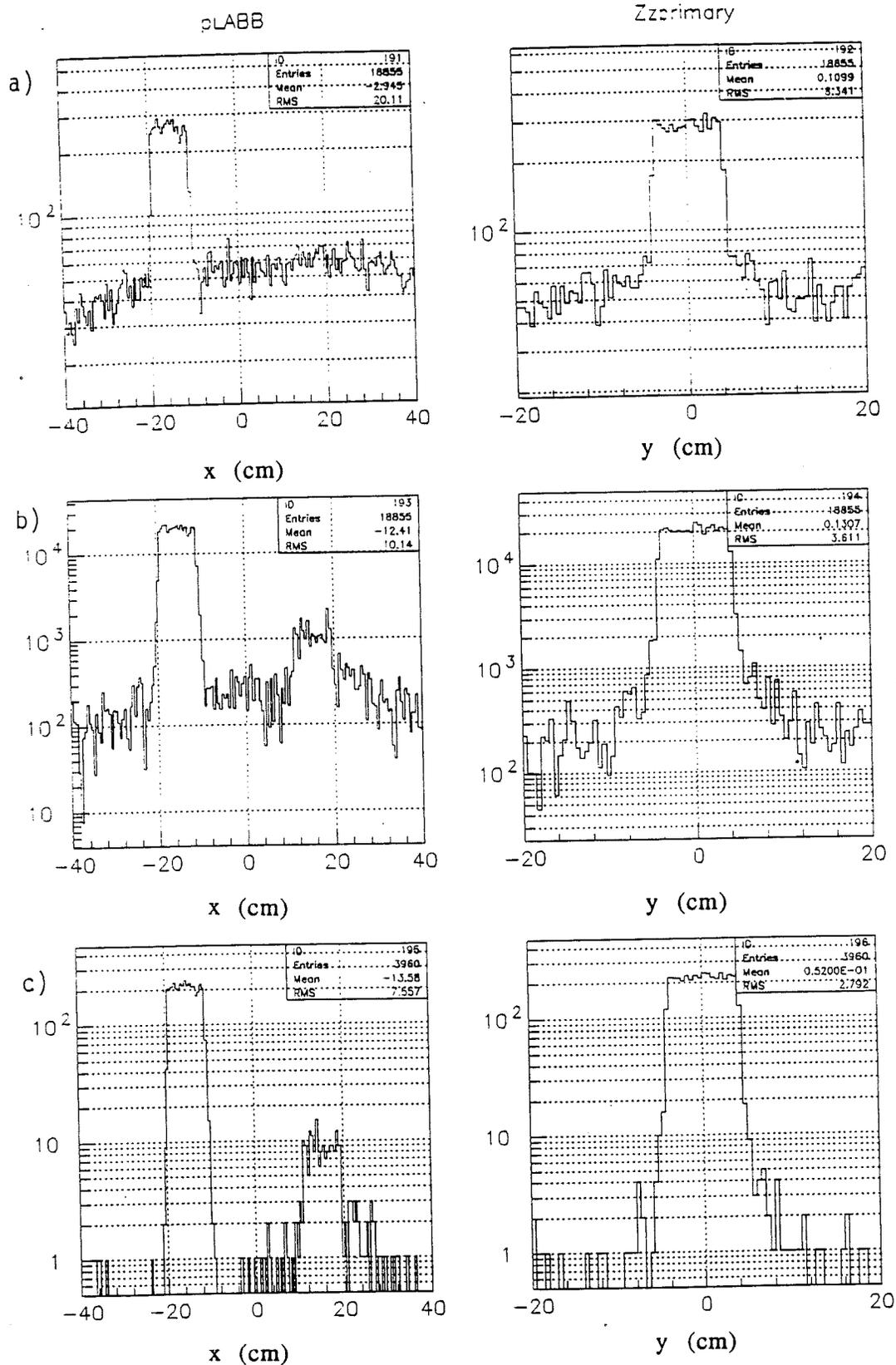
6.   RADIATION SAFETY

6.1   Method

Hadron shielding requirements for the KTEV and KAMI experimental program have been specified according to the requirements of the Fermilab Radiological Control Manual using the methodology of the 1991 Research Division Shielding assessment[1]. The "Cossairt Criteria", appropriately scaled to other energies, intensities, repetition rates, and distances were used to determine beam shielding requirements. The dose rate was assumed to vary

- linearly with the incident beam intensity and repetition rate
- with the beam energy to the 0.8 power
- such that each additional 2.6 feet of earth or concrete reduced the radiation dose by a factor of 10 transverse to the beam direction
- inversely with the square of the distance from the source to the start of the shield

The resulting expression used for the dose rate is

$$H = I^*(10^{-3} \text{ star/cm}^3 \text{ per proton})(10^{-2} \text{ mrem per star/cm}^3)(0.5/D)^2(E/1000)^{0.8}*10^{-(t/2.6)} \qquad \text{(Eq. 6.1)}$$

where

H	=	dose rate (mrem per spill)
I	=	beam intensity (particles per spill)
D	=	distance from beam line to shield (feet)
E	=	energy (GeV)
t	=	shield thickness (feet of earth)

---

[1] Research Division Shielding Assessment - Methodology- 1991

6.2   Beam Parameters

The assumed parameters of the primary and secondary beams are listed in Table 6.2.1. The effective secondary beam energy was derived from neutron momentum spectra calculated by Coleman using Malensek's standard parametrization of Atherton's data[2]. Differences in the average *energy* of the neutron and kaon spectra were ignored, but the *intensity* of neutrals in the secondary beam was assumed to be the sum of the calculated intensities for kaons and neutrons.

The secondary intensity was calculated based on an assumed primary proton energy of 900 GeV, a 45 cm long Be target, a targeting angle of 3.5 milli-radians (vertical) and 0.8 milli-radians (horizontal), a solid angle of 0.4 micro-steradians and two secondary beams. A 3 inch thick Pb photon filter was included in the secondary intensity calculations but Be absorbers were not included after the target since that was considered to be the worst case.

TABLE 6.2.1

	Energy [GeV]	Intensity [ppp]	Repetition Rate [hr^{-1}]
Primary Beam	900	3×10^{13} (5×10^{12})	60
Secondary beam (two beams)	80.5	1.4×10^{10} (2.3×10^{9})	60

KTeV primary and secondary beam parameters for worst-case accident. Intensities in parentheses indicate assumed intensities for normal running.

Note that the shielding requirements listed below for various areas are applicable only to KTeV operations. KAMI operations will require different amounts of shielding in some locations that are discussed later.

---

2 A. Malensek, Fermilab Report FN-341 (1981),
   Edwards et al., Phys Rev D18, 76 (1981).

6.3   Primary Beam Line Shielding

Primary beam line shielding has been specified assuming the worst-case accident scenario in which the full Tevatron intensity of 3×10^{13} protons per spill at 60 spills per hour at 900 GeV is lost in a beam line enclosure or in a buried beam pipe. The design goal was a worst-case accident dose rate of no more than 10 mrem per hour and no use of interlocked radiation detectors. Areas outside this shielding would then require only minimal occupancy and no radiation signs according to the current Radiological Control Manual criteria. To meet this goal at least 19.5 feet of earth-equivalent shielding is required over regions that contain a magnet inside a beam line enclosure, provided the magnet or other loss point is at least one meter from the enclosure wall (Cossairt criteria 2A). For regions containing a buried pipe, at least 21.5 feet of earth-equivalent shielding is required (Cossairt criteria 2C).

A review of shielding assessment drawings for the existing NM2 enclosure shows that 17 feet of shielding currently exist over most of that enclosure decreasing to 15.5 feet toward the north end. This is also sufficient for KTeV primary beam operations provided that four foot fences and high radiation area signs are present. Cossairt category 4A is the relevant one in this case, which has a minimum required thickness of 15.5 feet with a maximum allowed accident rate of 500 mrem per hour and no required use of interlocked detectors.

6.4   Secondary Beam Line Shielding

The amount of shielding required for the secondary beam line was calculated by scaling the Cossairt criteria to the secondary beam effective energy (80.5 GeV) and worst-case accident intensity (1.4×10^{10} neutrals per 3×10^{13} protons). The design goal was a worst-case accident dose rate of no more than 10 mrem per hour and no use of interlocked radiation detectors. Areas outside this shielding would then require only minimal occupancy and no radiation signs according to the current Radiological Control Manual criteria. To meet this design goal at least 8.5 feet of earth-equivalent shielding is required for secondary beam line enclosures that contain beam line magnets or other similar loss points located at least one meter

from the enclosure wall, and at least 10.5 feet is required for parts of the secondary beam line that consist only of buried pipe.

6.5   Experiment Hall Shielding

Beam-on hadron dose rates that have been estimated for the KTeV experiment hall design are discussed in this section.

6.5.1   Dose Rates and Shielding Requirements - Transverse Direction

A separate document[3] addresses general KTeV shielding requirements in detail. The design for the KTeV experiment hall most closely resembles the Type I design of the shielding document, a below-grade beam line with an unshielded hall over it and a counting room separated from that hall by a shielding wall sufficient in thickness to allow unlimited occupancy times. The design does not preclude the possible conversion at a later date to a hall more closely resembling the Type II design of the shielding document for KAMI operation. This provision would include the installation of shielding blocks over the entire experiment. One difference in the final design and the Type I hall is that the width of the experiment hall is somewhat smaller than the Type I hall, resulting in higher dose rates at grade level adjacent to the west wall of the hall.

Figure 6.5.1 shows dose rates for KTeV operation calculated at several locations in the experimental hall. The interior of the counting room is adequately shielded for the worst-case accident with dose rates well below 1 mrem per hour. The roof of the counting room adjacent to the east wall of the experiment hall can be divided into two regions, one that is shadowed by the six-foot-thick deck that forms the loading dock inside the experiment hall, and the other that is not. The shadowed region (about one third of the total length of the east wall) has dose rates well below 1 mrem per hour and would allow unlimited occupancy. However, the other two-thirds is not shielded and the calculated worst-case accident dose rates are

---

3 W. S. Freeman, et al., "Radiation Shielding Requirements for the KTeV Facility, (1/13/93).

Dose rate Legend
mrem/hr (mrem/spill)

Rates when no shielding
provided by loading dock

0.089 (0.0015)
159   *(2.6)*

398 (6.6)

138 (2.3)

Experiment Hall

Loading
Dock

Counting Room

0.0087 (--)
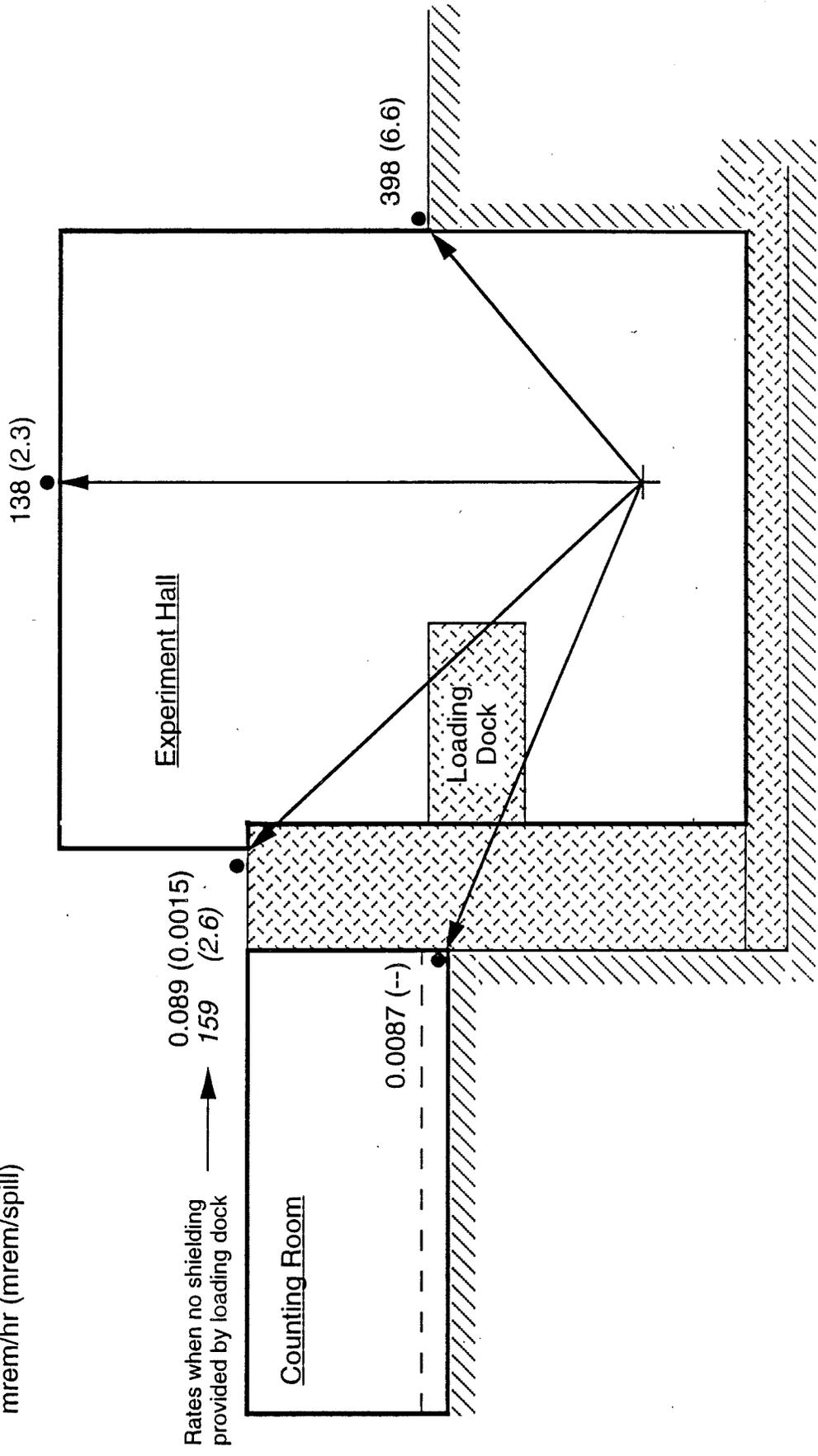
Figure 6.5.1.

Accident Dose Rates For Ktev Running

159 mrem per hour or 2.6 mrem per spill. If no interlocked detectors are used, the roof of the counting room would require posting as a "High Radiation Area" and fences with locked gates and access by authorized personnel only. If interlocked detectors are used then the calculated dose rate would require posting as a "Radiation Area" and chains or fencing. (Note: The cut-off for the posting requirement is 2.5 mrem per spill, and the calculated number of 2.6 mrem per spill is only slightly greater than this. So small changes in the assumed distance essentially make the whole roof of the counting room less than 2.5 mrem per spill and require only minimal occupancy with no posting requirement, provided dose rates due to normal operation are also acceptable.)

The roof of the experiment hall is slightly farther away from the beam line than the roof of the counting room and so the accident dose rates are slightly less - 138 mrem per hour or 2.3 mrem per spill. Without interlocked detectors, the roof would require posting as a "High Radiation Area" and fences with locked gates - access by authorized personnel only. With interlocked detectors, the area would require minimal occupancy and no posting provided dose rates due to normal operations were acceptable. The preferred alternative is to use interlocked detectors and not require posting of the rooftop areas.

The exterior of the building adjacent to the west wall is the place closest to the beam line and subject to the highest accident rates. The worst case accident rates are 398 mrem per hour or 6.6 mrem per spill. If interlocked detectors are not used, then the area adjacent to the west wall would require "High Radiation Area" signs, fences with locked gates, and access by authorized personnel only. If interlocked detectors are used, then the area would require posting as a "Radiation Area" with fencing and minimal occupancy.

The upstream region over the decay enclosure is designed to accomodate future KAMI running involving the transport and targeting of KAMI primary beam in the KTeV decay enclosure. This determines the amount of shielding ultimately required and drives the structural requirements of the decay enclosure. However for consistency, the minimum shielding requirements considering *only* KTeV running are included here (See Section 6.10.2 for KAMI operations). Neglecting the

possibility of future KAMI operations and assuming 12 feet from the beam line to the roof of the enclosure as shown in the design, six feet of earth-equivalent shielding is required to give a calculated accident dose rate of 9.6 mrem per hour, which would require only that the berm area be minimally occupied. The 11 feet minimum thickness indicated in the design would allow unlimited occupancy on that part of the berm during KTeV running since the accident dose rate would be about 0.1 mrem per hour.

6.5.2 Dose Rates and Shielding Requirements - Forward Direction

Dose rates at grade level in the forward direction, due both to normal running and accident conditions, were also assessed for the case where no additional shielding is in place over the beam line.

Rates from the Back-Anti (BA)

The dose rates adjacent to the north wall of the experiment hall were calculated with CASIM for normal and accident conditions by modeling the back-anti (BA) neutral beam dump and muon steel downstream using cylindrical approximations to the real geometry. Figure 6.5.2 shows the modeled geometry. An incident neutron beam was assumed. The star density in the downstream soil at a radius corresponding to grade level height (5 meters above the beam) was used to estimate the dose rate using the standard star density-to-dose conversion factor of 10^{-2} mrem/star-cm^{-3}. The results are that the worst-case accident intensity dose rate due to a loss on the BA is 2.6 $\pm$ 1.3 mrem per hour and the dose rate at normal operating intensity is 0.4 $\pm$ 0.2 mrem per hour.

Star density in this bin
converted to dose equivalent

Grade level

Soil

10

3

12

Muon Steel

Fe

Fe

2.5

1

2

3.75

BA

Fe

1.45

1.3
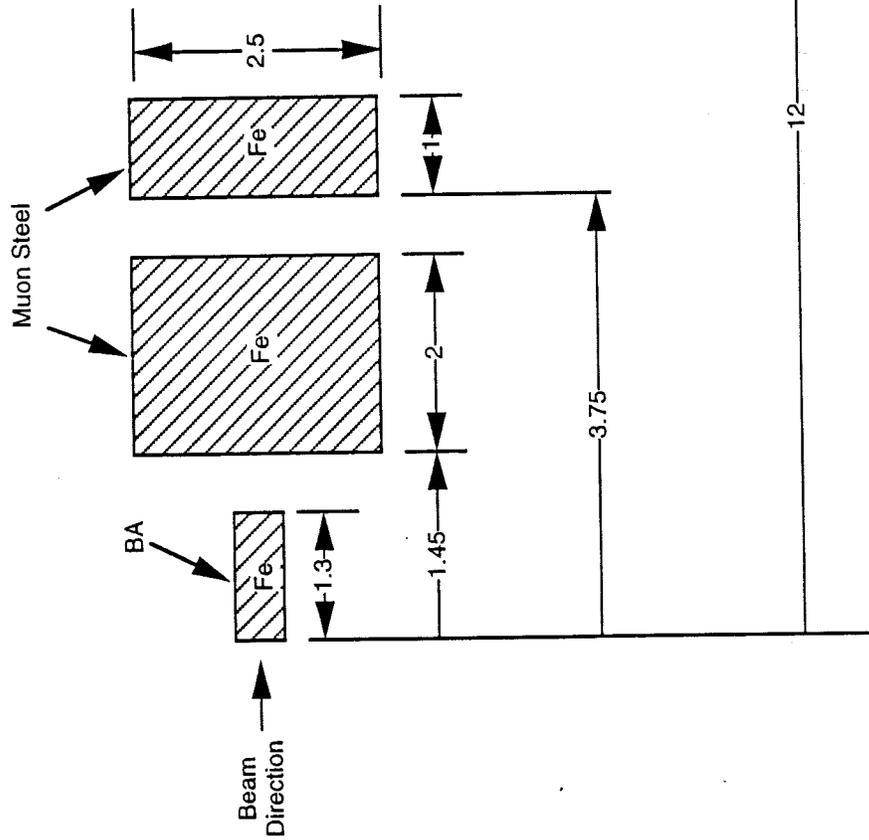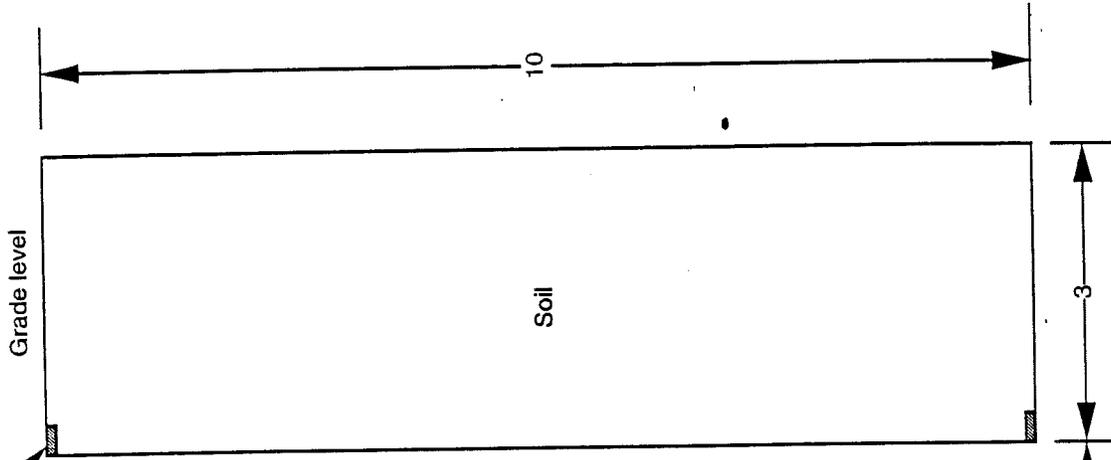
Beam
Direction

Figure 6.5.2.

CASIM Geometry (cylindrical symmetry)

Dose rate at grade level due to loss on the Back Anti
(all dimensions in meters)

Rates from Accidental Losses Upstream of the BA

The dose rates from accidental beam losses on an object placed in the beam line at three locations were also estimated from CASIM calculations. These rates were calculated to determine the need for any additional forward shielding. The assumed geometry is shown in Figure 6.5.3. Three loss point locations were considered:

i)   2.5 meters upstream of the BA, a distance just sufficient for a line-of-sight to exist directly from the loss point to grade level without passing through any of the muon steel downstream of the BA.

ii)   13.3 meters upstream of the BA, a location corresponding to the center of the most downstream helium bag.

iii)   30.8 meters upstream of the BA, a location at the downstream end of the vacuum decay pipe.

Star density in this bin converted to dose equivalent

Grade level

Soil

10

3

12

Muon Steel

Fe

2.5

1

Fe

2

Muon Steel

BA

Fe

1.3

1.45

3.75

various

Hypotetical loss point
(30 cmx2cm dia Fe cylinder)
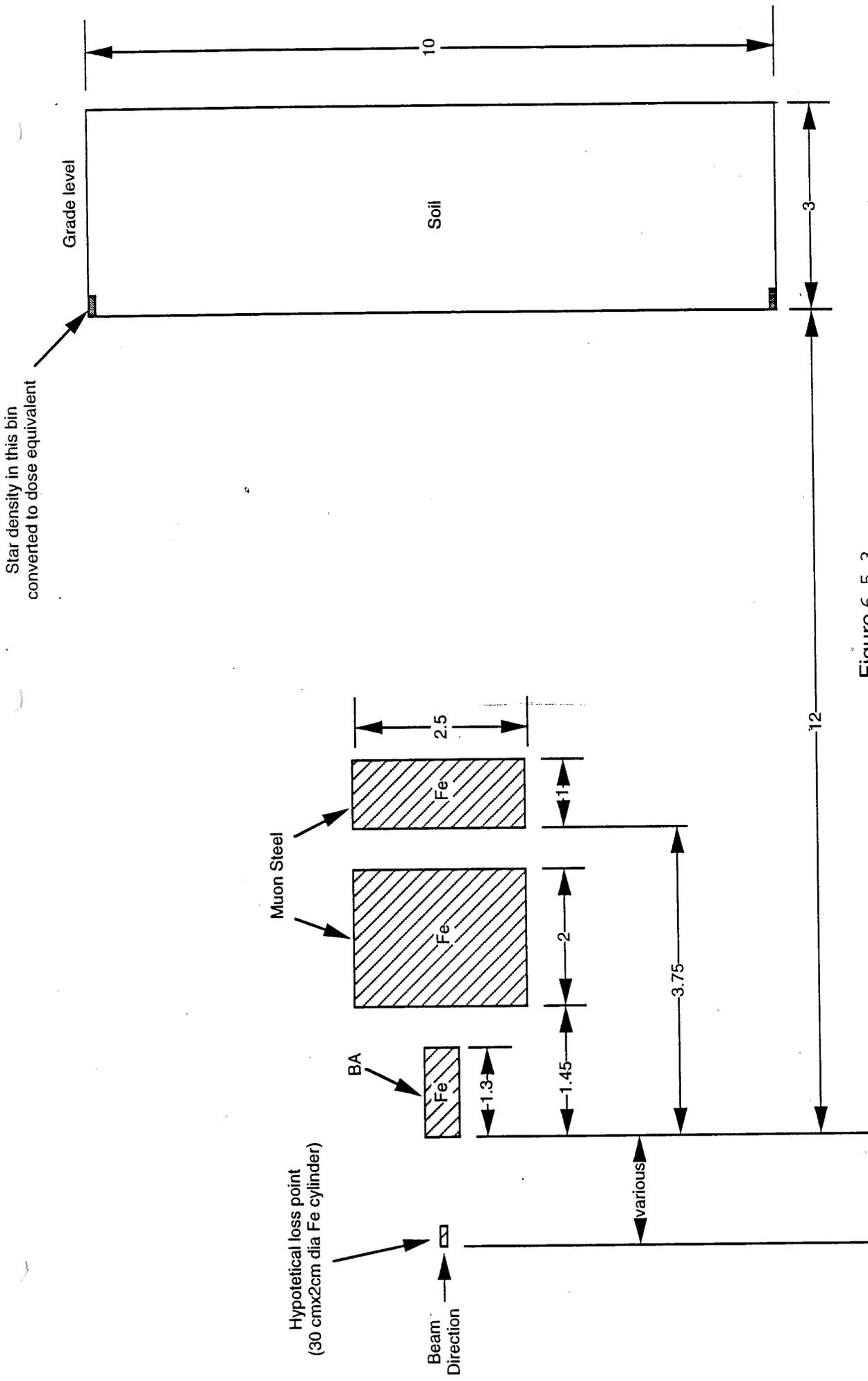
Beam
Direction

Figure 6.5.3.

CASIM Geometry (cylindrical symmetry)

Dose rate at grade level due to loss on a hypohetical iron
cylinder placed at various location along the beamline
(all dimensions in meters)

Separate CASIM calculations were done for a hypothetical 30 cm long by 2 cm diameter iron rod placed at each of the three loss points. The maximum star densities in the soil downstream of the hall at grade level were converted to dose equivalents and the results are shown in Table 6.5.1.

TABLE 6.5.1

Location	Dose Rate[1] (mrem/hour)	Dose Rate[1] (mrem/spill)	Shielding Req'd.- 10 mrem per trip (feet)	Shielding Req'd.- 2.5 mrem per trip (feet)
i	856 (1500)	14.3 (25)	1.5	3.8
ii	758 (1320)	12.6 (22)	3.6	8
iii	580 (1020)	9.7 (17)	3	8.5

1 - No forward shielding is included in these dose rate calculations

KTeV accident dose rates at grade level in the forward direction for beam losses of 1.4×10^{10} and 80.5 GeV and 60 spills per hour at three loss points in the experiment hall. Assumed loss is on a 30 cm long x 2 cm diameter iron rod. Numbers in parentheses indicate estimated worst case doses based on a 100 cm long rod, as discussed in the text.

The effect of changes to the dimensions of the loss point object were also studied at one location (location ii). The effect of an increase in the iron rod length from 30 cm to 100 cm was to increase the calculated dose rate from 12.6 mrem per spill to 22 mrem per spill. An increase in the radius of the 100 cm long rod from 1 cm to 15 cm resulted in a decrease from 22 mrem per spill to 9 mrem per spill. Therefore, the 100 cm long by 2 cm diameter rod was assumed to be the worst case and the calculated dose rates for the 30 cm long rod at locations (i) and (iii) were scaled upward by the factor 22/12.6 and used as worst-case dose estimates. These results are also shown in Table 6.5.1.

176

Hourly worst-case accident dose rates exceed 1000 mrem per hour, thus interlocked detectors are required. Without additional shielding in the forward direction, the area downstream of the hall would require fences with locked gates and posting as a high radiation area, with fences at the 2.5 mrem per trip boundary. This would interfere with the parking area and HVAC equipment. Thus additional shielding is required in the forward direction to reduce accident dose rates to acceptable values at grade level.

The amount of shielding necessary to attenuate the calculated accident dose rates to an acceptable level was determined from CASIM calculations by looking at the fall off of the star density in the downstream soil. Since this is in the forward direction, the usual factor of ten attenuation for every 2.6 feet of concrete does not apply. A typical attenuation curve in the forward direction obtained from CASIM is shown in Figure 6.5.4. This is taken from the calculation that assumed a loss point at the location of the last helium bag. The figure shows the star density at a fixed radius of 500 cm from the beam line (corresponding to grade level) as a function of the depth into the soil downstream of the hall. To reduce the calculated dose from 22 mrem per trip to 10 mrem per trip requires an attenuation factor of 2.2 which can be achieved with 110 cm (3.6 feet) of soil. To reduce the dose from 22 mrem per trip to 2.5 mrem per trip requires an attenuation factor of 8.8 which can be achieved with 245 cm (8 feet) of soil. A similar analysis was done by looking at the attenuation curves for the other two loss locations to determine the necessary shielding. The results are listed in the last two columns of Table 6.5.1. They show that 8.5 feet of soil (or concrete) in the forward direction, and interlocked detectors, would be sufficient to reduce the accident dose rate from losses at the three locations to 2.5 mrem per trip. The downstream area outside the hall would then require only minimal occupancy with no requirements for signs and ropes/fences. This amount of shielding will be provided by the installation of a six foot thick layer of shielding blocks over the two most downstream bays of the experiment hall.

Rates from the Regenerator

Losses on the active regenerator, located 68 meters upstream of the BA, must also be considered for both the accident case of 3×10^{13} and for normal running at

5×10^{12} protons on target. In the normal running situation, the regenerator only intercepts one of the two neutral beams at a time. Thus the dose rate will be reduced by a factor of twelve, not six, relative to the accident case.

Chart1

Star Density vs Distance from Loss Point for 490 cm<r<500 cm

Loss point location - Center of most downstream He bag
100 cm long x 2 cm diameter iron rod
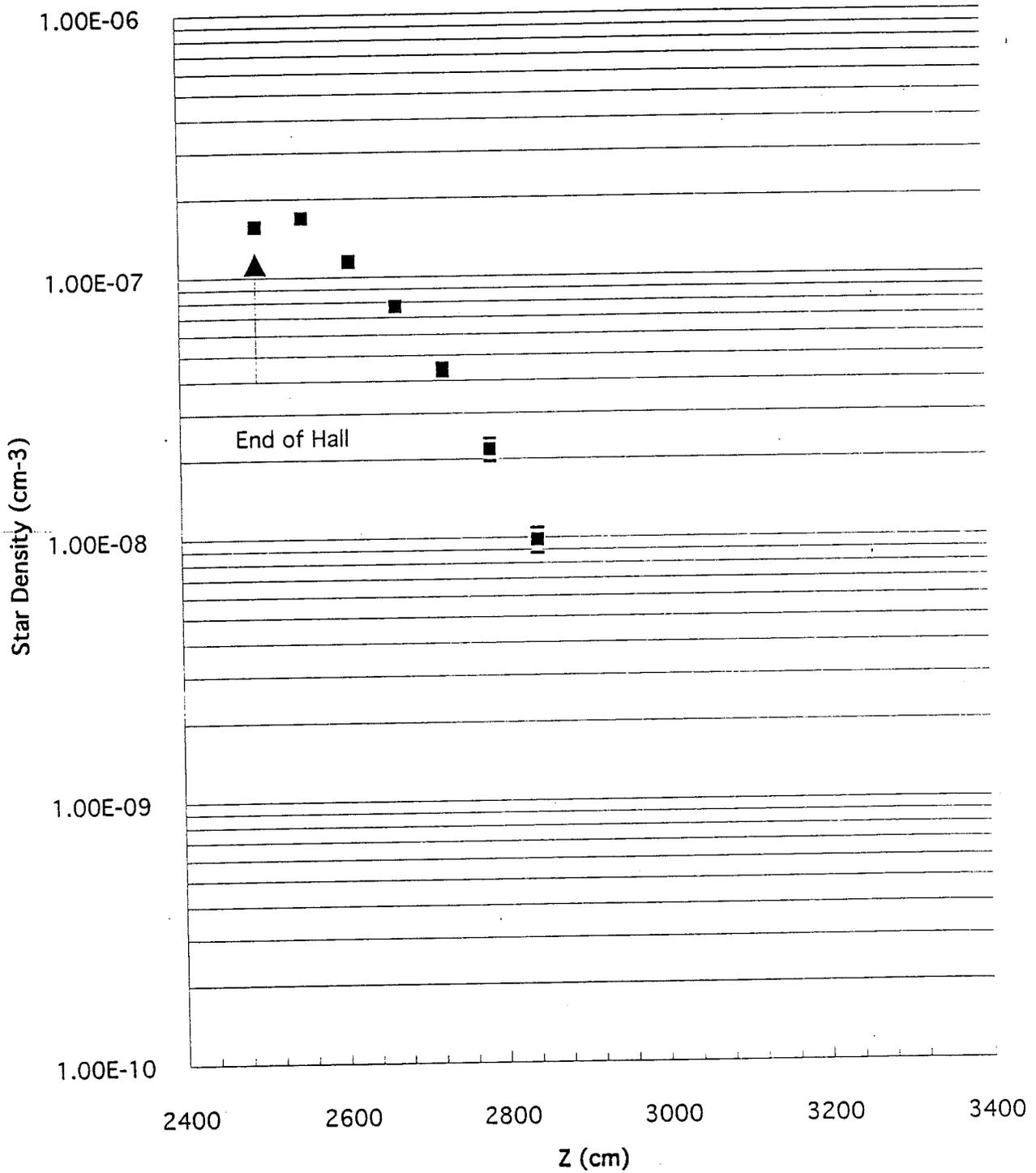
FIGURE 6.5.4.

In the absence of additional shielding, a line-of-sight will exist from the regenerator to a point four feet above grade level at the downstream end of the hall. This line passes over the spectrometer magnet steel and also over the concrete blocks that will be installed over the two downstream bays, so they do not provide any additional shielding in a region from four feet to eight feet above grade level at the north end of the hall.

The dose rates at the downstream end of the hall were calculated using CASIM. The modeled geometry is shown in Figure 6.5.5. It is a cylindrically symmetric geometry, centered on the beam line with the appropriate radial and longitudinal dimensions taken from the hall design. The regenerator loss point was modeled as a two interaction length (76 cm) carbon cylinder 3.8 cm in diameter. (The actual regenerator will be two interaction lengths of plastic scintillator 10 cm on a side). Two CASIM calculations were done. The first was for the case where no additional shielding is provided along the line-of-sight from the regenerator to the downstream end of the hall. The second was for the case where an additional concrete "regenerator forward shield" was inserted in a region along the line-of-sight to the downstream end. This shield was three meters in length.

To determine dose rates at the end of the hall, the star density was calculated in five hypothetical soil bins parallel to the beam direction at a radius from the beam line of 6.5 meters, corresponding to a distance of four feet above grade level. Each bin was 50 cm long and 10 cm in radial width. The star density results are shown in Figure 6.5.6 for both forward shielding cases. The addition of the regenerator forward shield reduced the maximum star density by about a factor of 27. The maximum values of star density were converted to dose rates using the standard conversion factor. The results are shown in Table 6.5.2.

Star Densities calculated in these bins

Soil

Concrete Shield Blocks.

μ1 μ2

BA

Regenerator Forward Shield
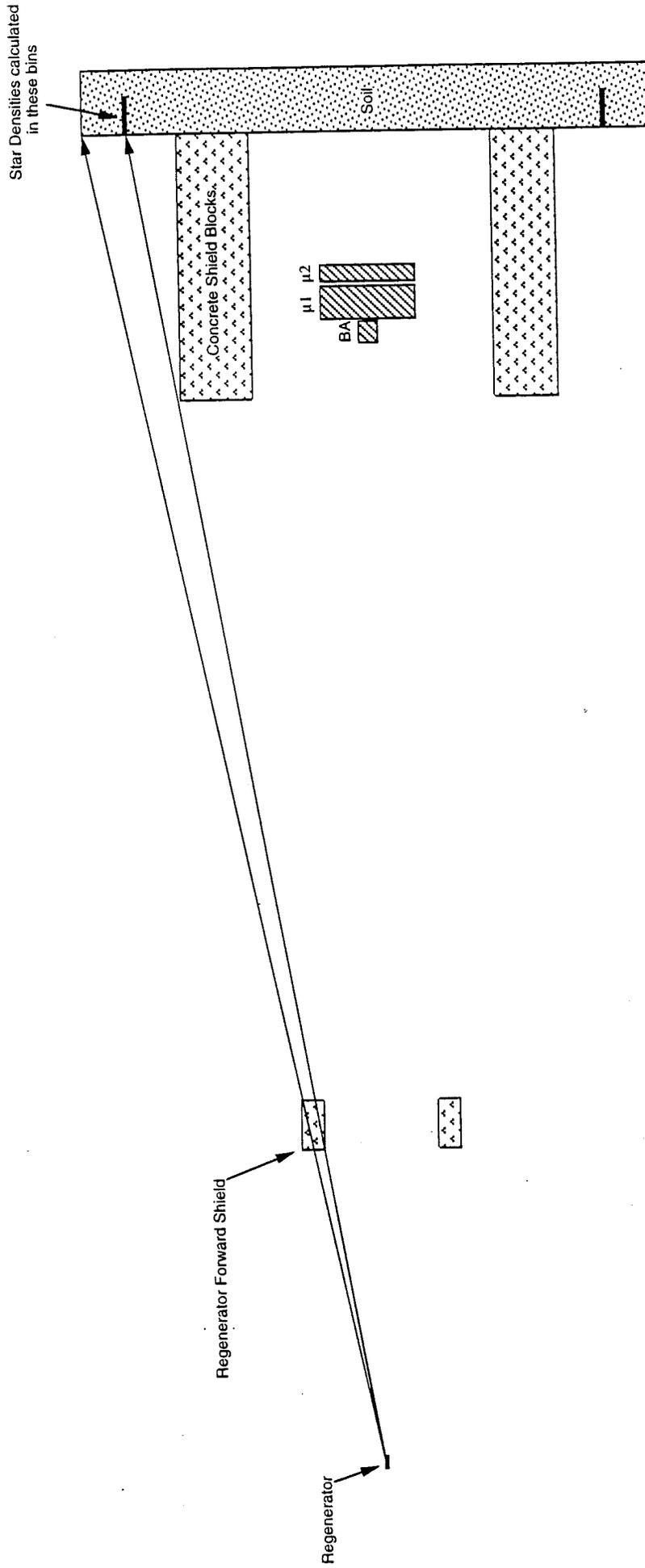
Regenerator

Figure 6.5.5.

Forward Shielding Geometry for CASIM Calculation of Regenerator Shielding

Star Density vs. Z for 650 cm < R < 660 cm

Loss on Regenerator - 6' shielding blocks added over dump region
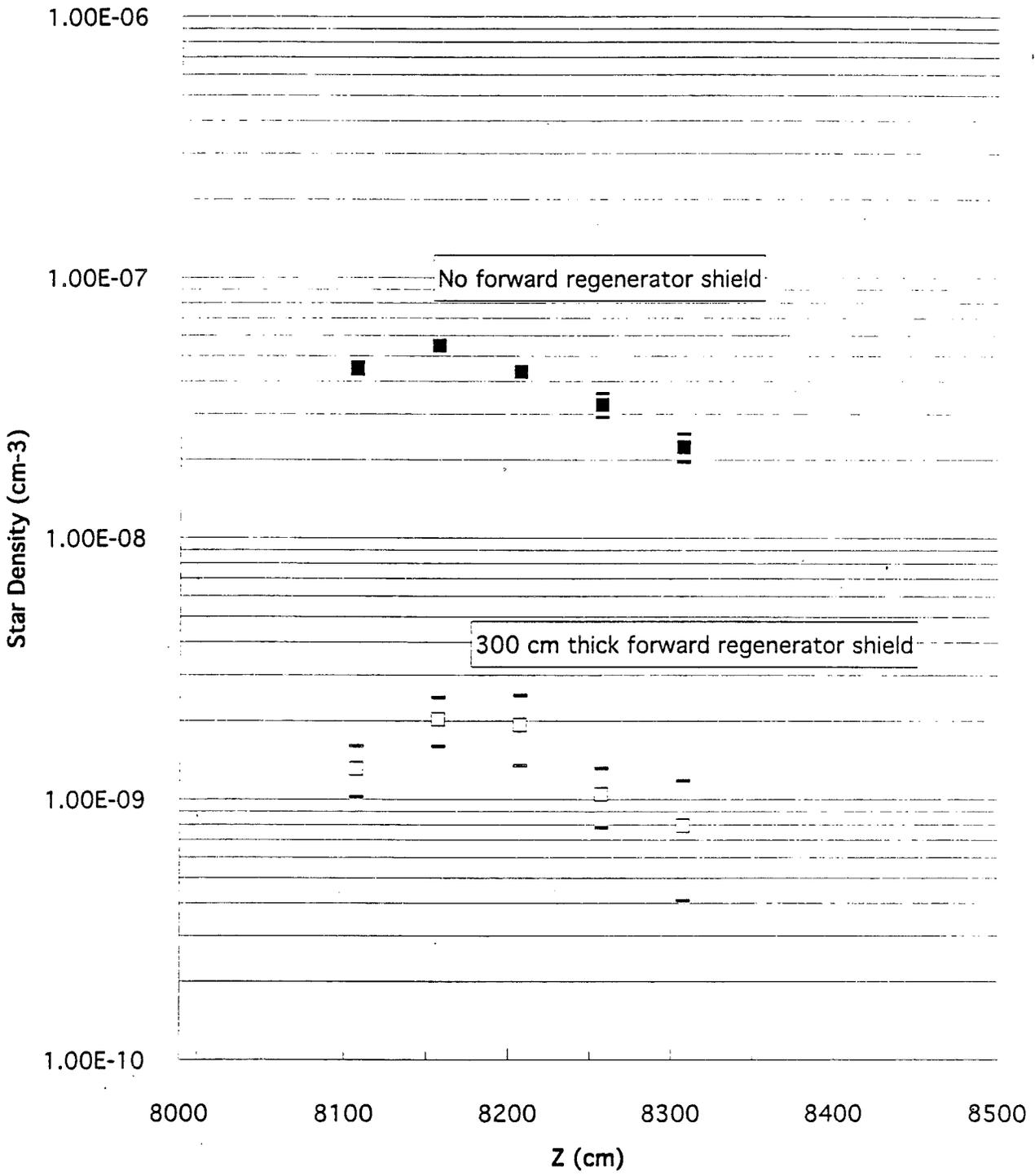
FIGURE 6.5.6.

TABLE 6.5.2

	Accident Case		Normal Running	
	(mrem/hr)	(mrem/spill)	(mrem/hr)	(mrem/spill)
No forward shield	460	8	38	0.6
3 m. thick forward shield	17	0.3	1.4	0.02

Rates at the downstream end of the experiment hall due to interactions in the regenerator. Accident case is 1.4×10^{10} per 3×10^{13}; Normal running is 1.2×10^9 per 5×10^{12}.

If the regenerator forward shielding is not present, then a normal running dose rate of about 38 mrem per hour could exist about four feet above grade level at the downstream end of the experiment hall due to interactions in the regenerator. This would require that the area downstream of the hall be fenced at the 2.5 mrem per hour boundary which would be at a considerable distance from the end wall and interfere with access to the parking area and HVAC equipment. With a 3 meter thick concrete shield, the dose rate from normal running is reduced to 1.4 mrem per hour, and the accident rate is reduced to 0.3 mrem per spill. The normal running rate would only require minimal occupancy downstream of the hall. The accident rate of 0.3 mrem per spill would only require minimal occupancy provided an interlocked detector is installed.

Forward Shielding Solution

The combined requirements for shielding in the forward direction can be satisfied by the following steps.

1) Provide at least ten feet of concrete-equivalent along the lines-of-sight from the regenerator to the points between four feet and eight feet above grade at the downstream end of the hall. The width of this regenerator forward shield should be wide enough to shield the entire north wall of the hall with the required ten feet of shielding.

2) Cover the two most downstream bays of the experiment hall with concrete shielding to provide at least the required 8.5 feet along all the lines of sight downstream of the north end of the decay pipe. A six foot layer of shield blocks over the downstream two bays should be sufficient.

3) "Red tag" the decay pipe for configuration control purposes.

4) Install an interlocked detector over the beam line at the downstream end of the hall near grade level to only require minimal occupancy for areas north of the hall.

6.6   Neutron Skyshine

Dose rates due to neutron skyshine have been roughly estimated using an empirical expression for the neutron fluence and simple assumptions about the source strength and effective energy of the skyshine neutrons.

The neutron fluence due to skyshine at a distance, r, from the source is given by

$$\Phi(r) = 2.8Q/(4\ \pi r^2)[1\text{-exp}(\text{-r}/56)]\text{exp}(\text{-r}/184.4) \qquad \text{(eq. 6.2)}$$

where Q is the source strength and r is in meters. This expression is thought to be valid for distances greater than 50 meters from the source[4].

To estimate the source strength, it is assumed that one skyshine neutron is emitted per incident particle per GeV of beam energy into 4π solid angle. This is then divided by 2 to get the number emitted into the upper hemisphere.

---

[4] A.J. Elwyn and J. D. Cossairt, Helth Physics, Vol. 51, No. 6 (1986).

The estimated dose rates due to skyshine assuming effective skyshine neutron energies of 1 MeV and 0.2 MeV are given in Table 6.6.1.

TABLE 6.6.1

Beam intensity (per spill)	Source strength,Q (n/spill)	Fluence, Φ @ 50m. (n/cm^2/spill)	Dose (mrem/spill)	Dose (mrem/hr)
1.4×10^{10}	5.6×10^{11}	2.2×10^3	0.073 (0.0036)	4.4 (0.22)

Parameters and dose estimates for skyshine dose rates due to worst case KTeV accidents. Numbers in parentheses are dose rates assuming effective neutron energy of 0.2 MeV

Note that there can be large differences in the estimated rates depending on the effective neutron energy and its corresponding fluence-to-dose conversion factor. These rates are applicable to an unshielded hall. If shielding is present over the loss point then the source strength, Q will have to be reduced by the appropriate amount. For example, with six feet of concrete shielding present over the BA the source strength could be expected to decrease by about a factor of 100, further reducing any dose rate due to skyshine.

6.7   Labyrinths and Penetrations

The attenuations of access labyrinths and penetrations for the KTeV experiment hall were calculated using the formalism of the RD shielding assessment and the associated FORTRAN program developed from that formalism. The results are summarized in Table 6.7.1. The personnel and equipment labyrinth designs, as well as HVAC ductwork, are acceptable for KTeV operation, with accident dose rates at the exits well below 1 mrem per hour, allowing unlimited occupancy at the exits for all but one case. The only exception is the large equipment hatch in NM3 which has a calculated dose rate below 10 mrem per hour and would only require minimal occupancy at the exit. There is an option to install concrete shield blocks similar to the NM2 equipment hatch if required. These shield blocks

will be required for KAMI operations with primary beam in the NM3 enclosure as discussed in Section 6.10.6.

The four large-diameter supply and return HVAC ducts at the downstream end of the experiment hall are sufficient in size for a person to enter. Administrative controls will have to be applied to prevent personnel entry (e.g. for maintenance and or repair) while beam is on.

The attenuations of two-legged and single-legged cable penetrations between the experiment hall and the counting room were also calculated and found to be acceptable. Existing cable penetrations associated with the NM beam line enclosures have not yet been re-evaluated for the higher 3×10^{13} worst case accident condition, but this is only a modest increase from the 2×10^{13} accident intensity of the previous run so it should not have a big impact. They currently are being evaluated as part of a general shielding reassessment for the entire neutrino area.

TABLE 6.7.1

Labyrinth Location	Number of Legs	Total Attenuation	Dose at Exit (mrem/hr)
NM3 upstream stairwell	4	1.8×10^{-8}	1.4×10^{-5}
NM3 equipment hatch	2	2.6×10^{-3}	2.1
Expt Hall - West side stairwell	2	2.5×10^{-5}	4.1×10^{-3}
Expt Hall - SE stairwell	3	3.9×10^{-6}	5.9×10^{-4}
Expt Hall - NE stairwell	3	6.0×10^{-6}	8.9×10^{-4}
Cable penetrations	2	1.1×10^{-7}	1.3×10^{-5}
Cable penetrations	1	1.5×10^{-3}	0.19
HVAC duct - West supply§	2	1.2×10^{-4}	2.7×10^{-3}
HVAC duct - West return	4	1.7×10^{-9}	2.9×10^{-7}
HVAC duct - East supply§	2	3.8×10^{-4}	8.3×10^{-3}
HVAC duct - East return§	2	6.5×10^{-5}	0.015
CsI Supply	4	2.0×10^{-18}	0.0
CsI Return	4	7.4×10^{-13}	0.0

§ - neglect attenuation of first leg of duct and treat as two-legged duct; but assume off-axis source with distance to mouth equal to length of first duct leg.

KTeV experiment hall labyrinth and penetration attenuations and doses at exits based on worst-case accident loss on-axis of 1.4×10^{10} particles per spill at 80.5 GeV and 60 spills per hour.

6.8 Ground Water Protection

The KTeV target station located in the NM2 enclosure has been modeled in CASIM and the levels of ground water activation have be calculated using the single resident well model (SRW).

6.8.1   Description of Modeled Geometry

The modeled target station design included the following components:

a)   beryllium target - 40 cm long x 1 cm diameter - similar interaction length to 30 cm long BeO

b)   target sweeping magnet (NM2S1) - 381 cm long x 60.8 cm high x 77.4 cm wide with a hole 5 cm high x 4 cm wide on the beam axis

c)   copper dump - 452.7 cm long x 20.4 cm wide x 25.4 cm high, with no holes

d)   E8/Hyperon magnet (NM2S2) - 548.6 cm long x 181.6 cm high x 291 cm wide, with a hole 0.5 cm high x 3 cm wide on axis

e)   steel shielding surrounding the target, sweeping magnet, and copper dump to reduce ground water activation and residual activity

minimum steel thicknesses used -
117.5 cm -   east and west sides of target and NM2S1
124.5 cm -   above target and NM2S1
83.9 cm -   below target and NM2S1
154.9 cm -   east and west of dump
151.1 cm -   above dump
106.7 cm -   below dump

Magnetic fields were not included in the calculations. For simplicity, the targeting angle was assumed to be zero degrees, and no holes were included in the copper dump. The magnets were modeled as simple rectangular blocks of iron with the dimensions given above. The beam height above the floor of the enclosure was 119.4 cm, which determined the maximum amount of shielding that could be added below the beam line. More room existed on the top and sides of the target station components. The southeast corner of the target station iron shielding was beveled to allow a wider passageway into the upstream end of the NM2 enclosure.

The NM2 enclosure was modeled as a concrete-walled enclosure surrounded by dirt out to a radius of 750 cm. The dimensions of the enclosure were taken from the existing construction drawings. The geometry of the modeled target station and enclosure is illustrated in figures 6.8.1 through 6.8.5.

6.8.2 Method and Results

Radioactivity concentrations in ground water must not exceed Environmental Protection Agency (EPA) limits. The EPA limits are derived from the requirement that the concentrations of radioactivity in community drinking water supplies must not result in doses of more than 4 mrem per year to individuals who use that supply as their sole source of drinking water. When only one isotope is present in the water then the 4 mrem per year requirement may be converted into a permissible concentration for that isotope. When more than one isotope is present then the appropriately weighted sum of concentrations must not result in more than 4 mrem per year. Using this criteria, the permissible individual concentrations are 0.4 pCi per ml for Na^{22} and 80 pCi per ml for tritium. However, there exists in addition an explicit regulatory limit of 20 pCi per ml for tritium. So the limits on ground water radioactivity for the case where both Na^{22} and tritium are present can be expressed as two conditions, both of which must be satisfied:

$$\frac{C(H^3)}{80} + \frac{C(Na^{22})}{0.4} \leq 1 \qquad \text{(condition 1)}$$

and

$$\frac{C(H^3)}{20} \leq 1 \qquad \text{(condition 2)}$$

The single resident well model (SRW) was used to calculate the ground water concentrations of tritium and Na^{22}, the principal isotopes of concern. This model assumes that all the radioactivity produced in unprotected soil outside an enclosure in one year is transported to the underlying aquifer and then diluted by 14,600 gallons of water (equal to 40 gallons per day times 365 days). In the SRW model credit is taken for radioactive decay en route to the aquifer using standard parameters for the rate of movement of tritium and Na^{22} through the soil.

Scale (meters)

	Be Target
▨	Copper
▧	Iron
◩	Concrete
☐	Soil

Beam →

A   B   C
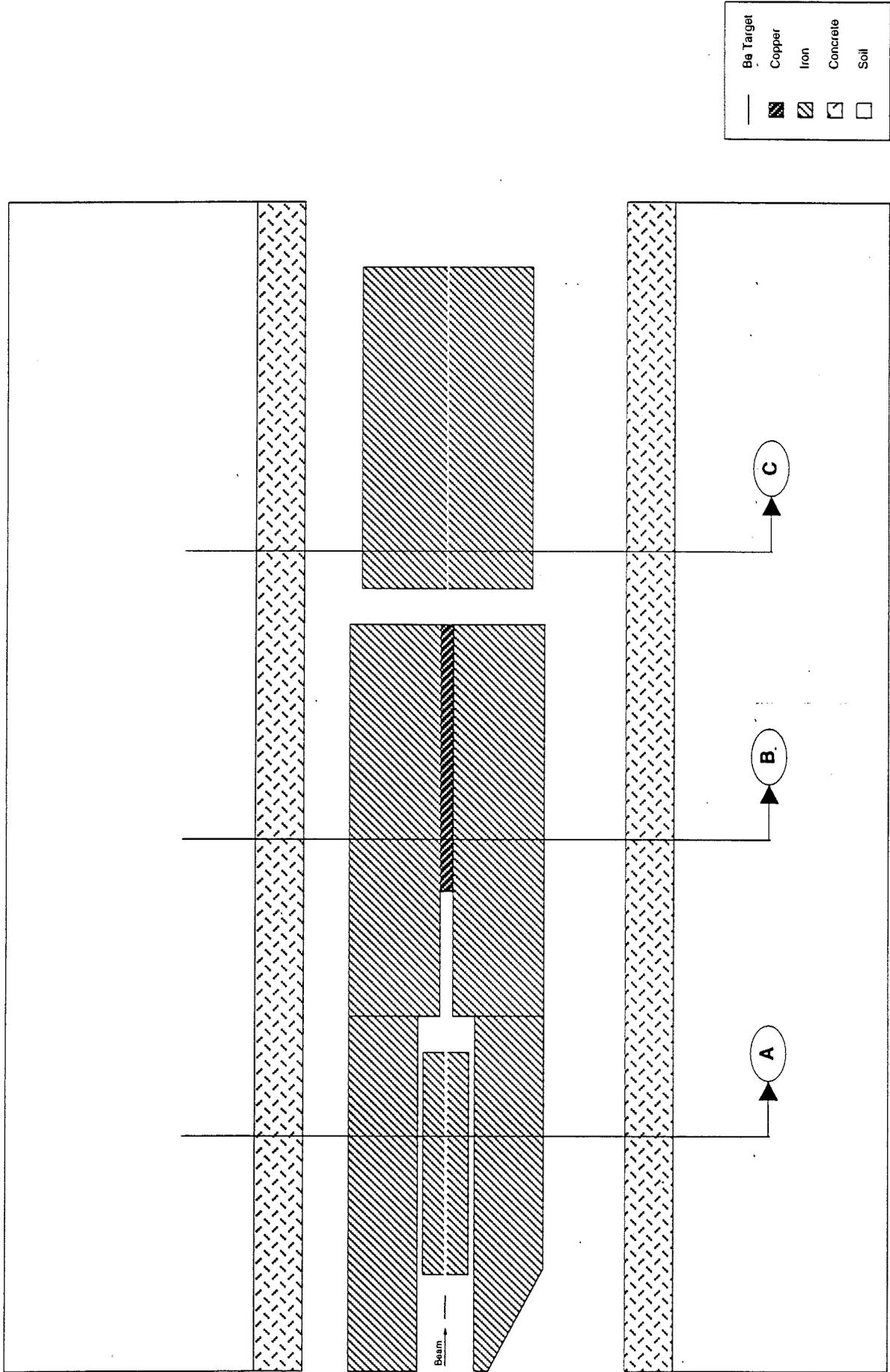
Figure 6.8.1.

Plan View of NM2 Target Station
CASIM Geometry
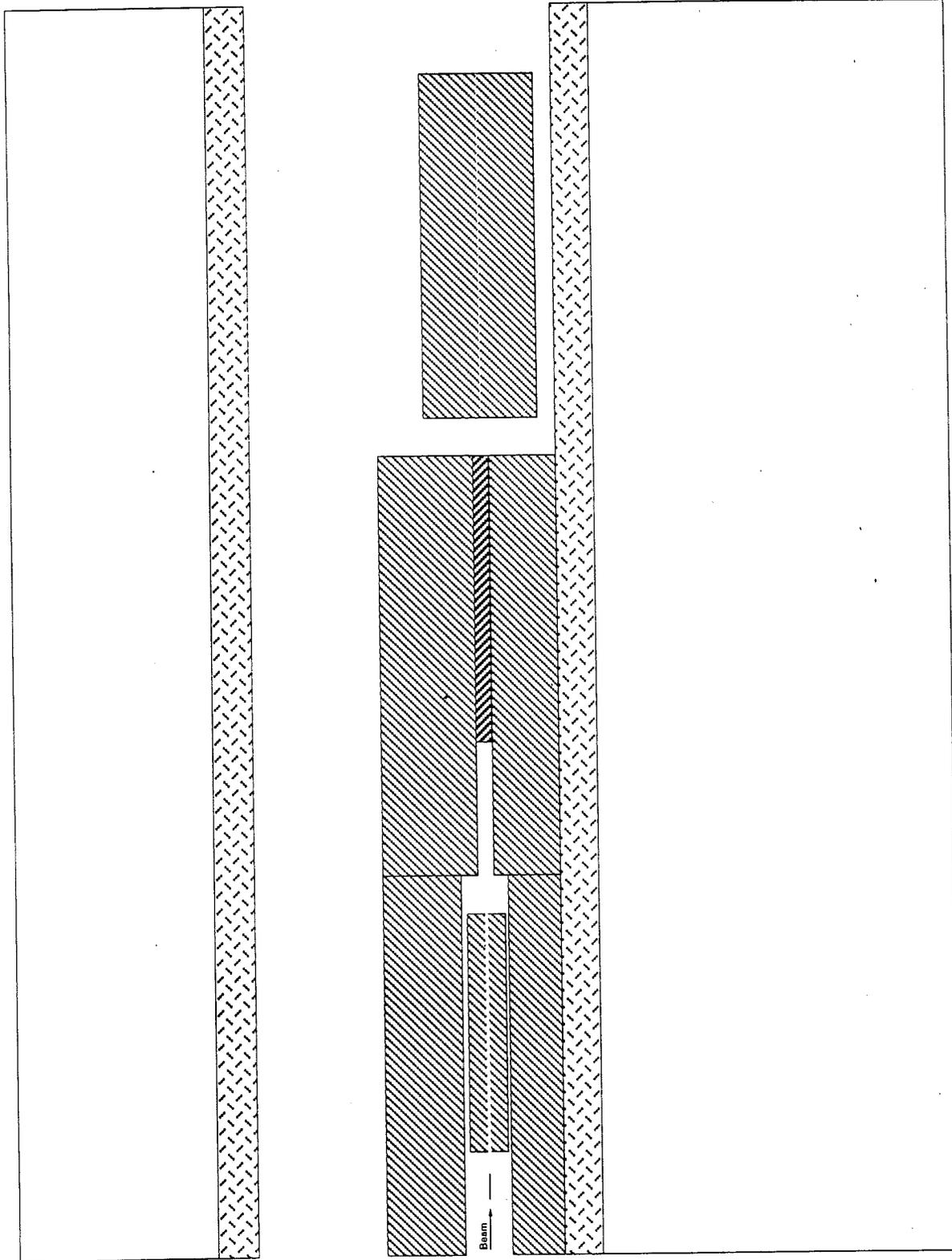
Figure 6.8.2.

Elevation View of NM2 Target Station
CASIM Geometry
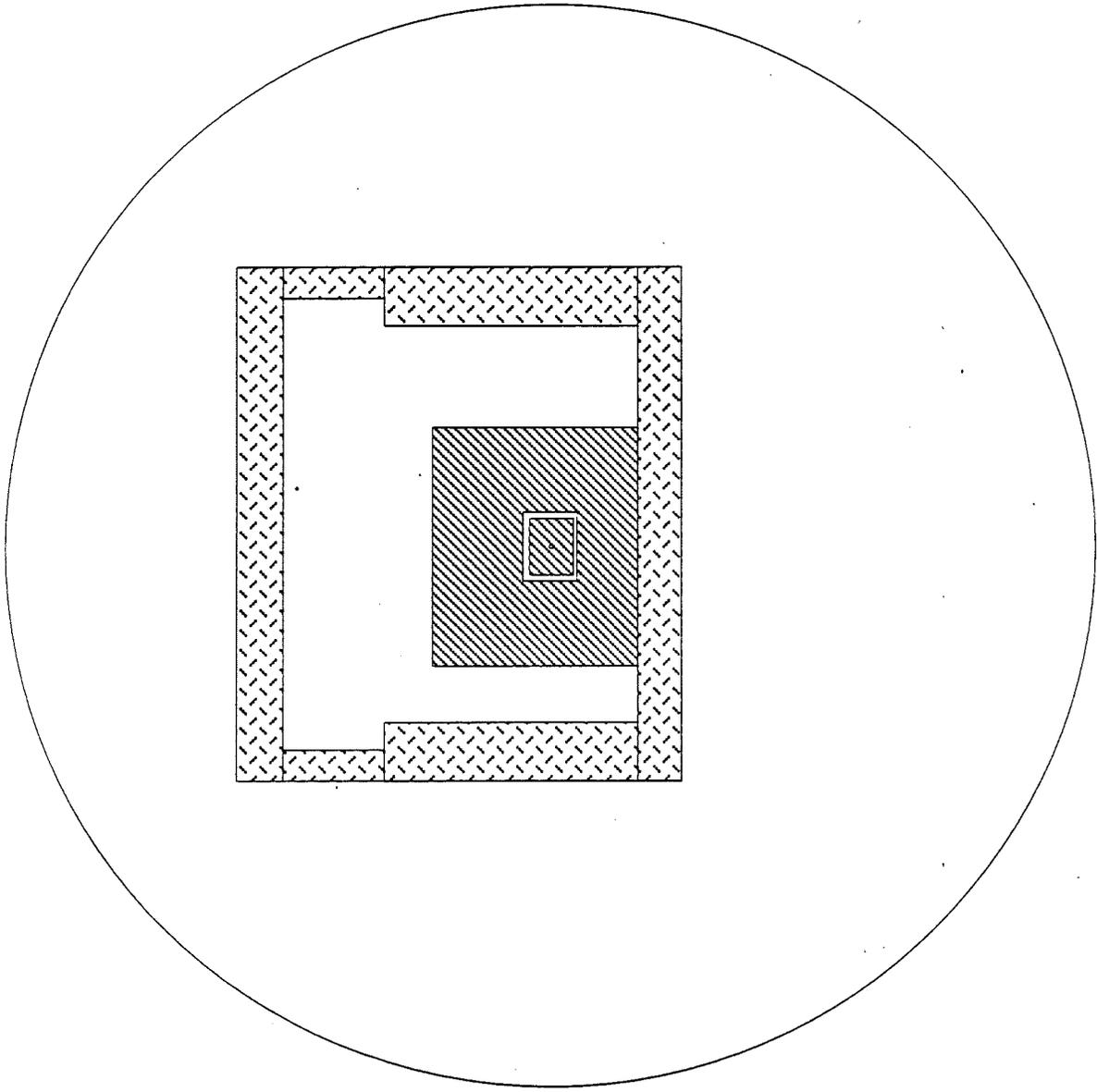
Section

A

Be Target
Copper
Iron
Concrete
Soil

Scale (meters)
0   1   2

Figure 6.8.3.

Cross Section thru Early Dipole
CASIM Geometry
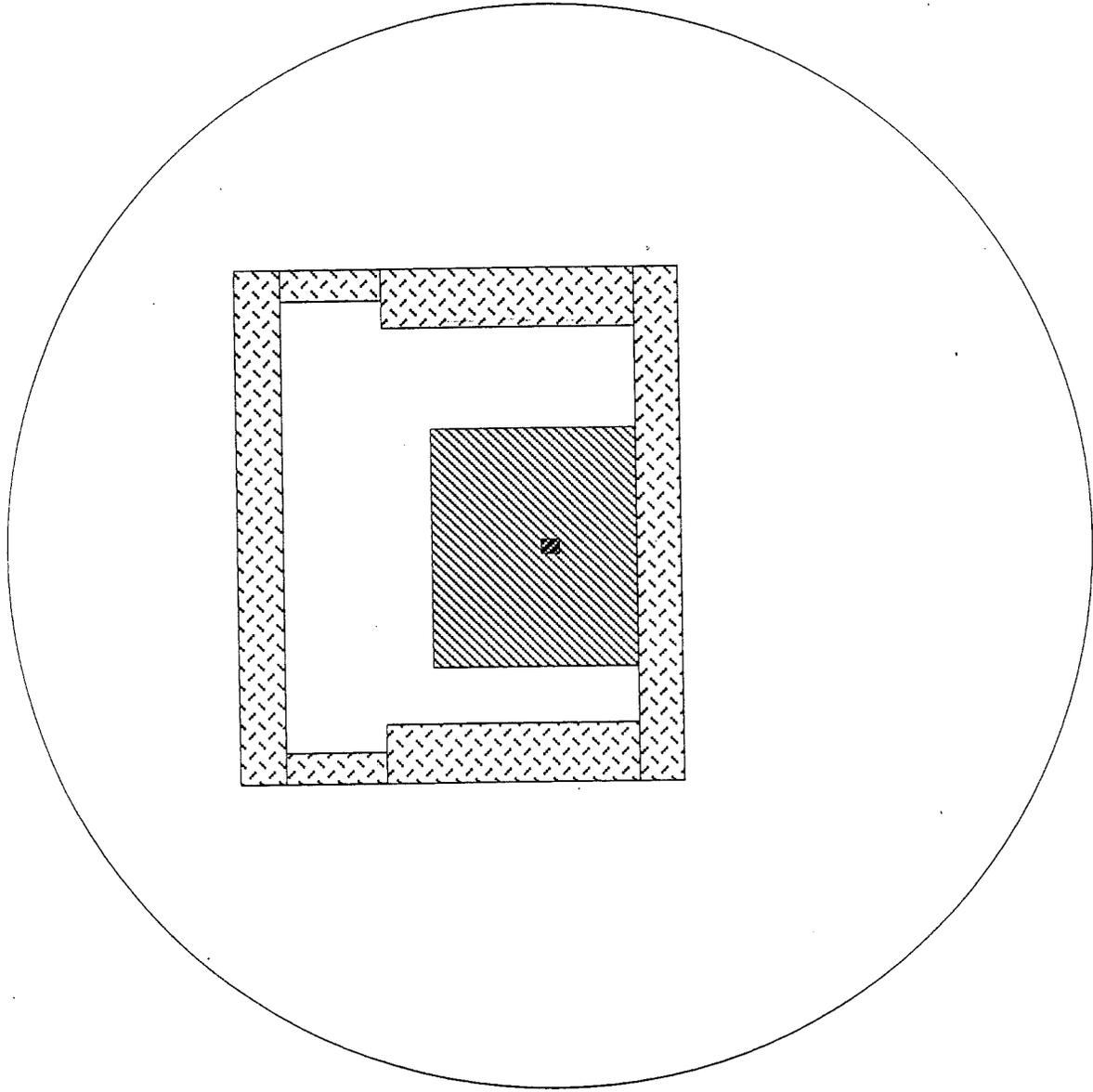
Section

B

	Be Target
▨	Copper
▧	Iron
▱	Concrete
☐	Soil

Scale (meters)

0　　1　　2

Figure 6.8.4.

Cross Section thru Beam Dump
CASIM Geometry
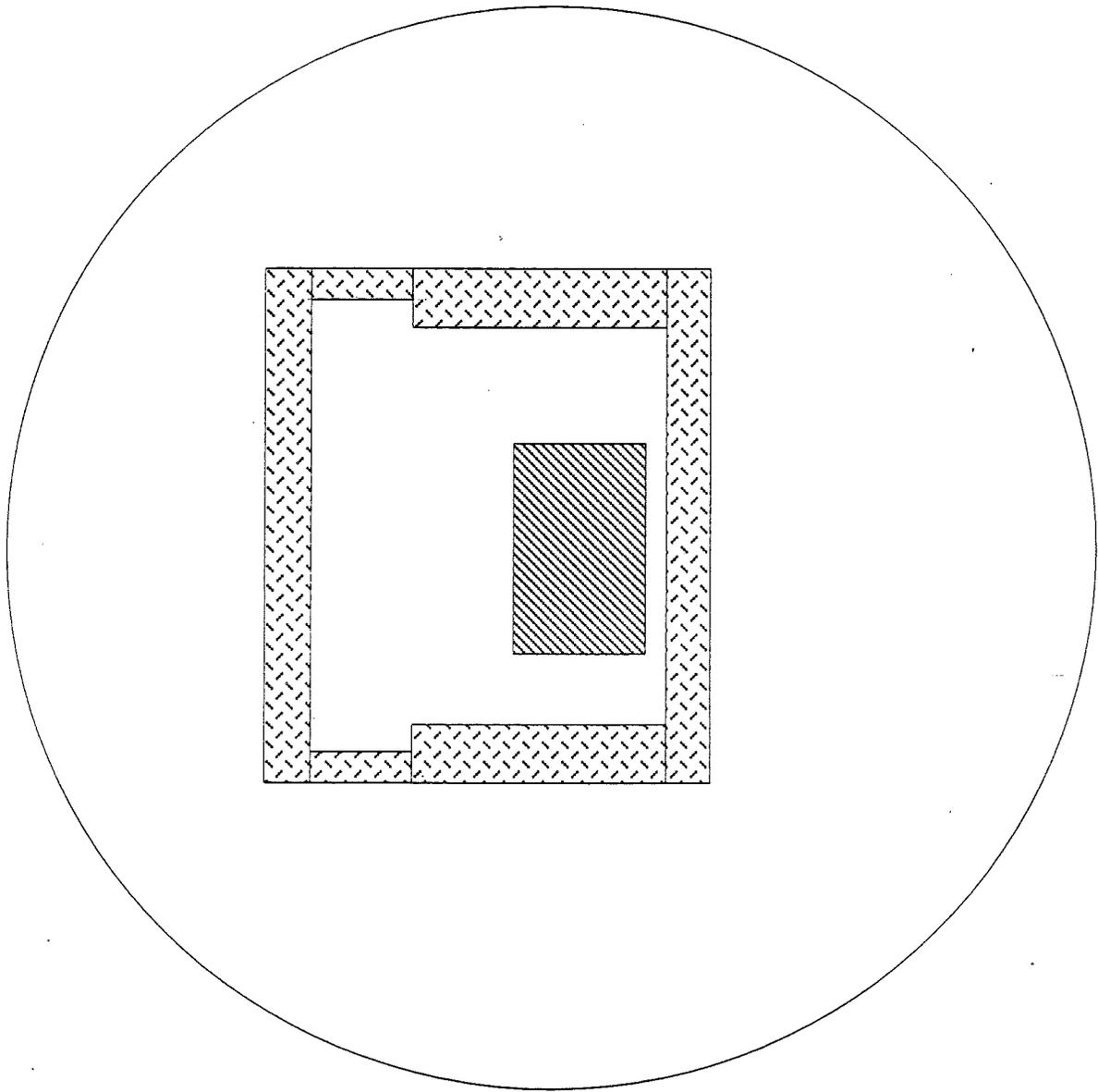
Be Target

Copper

Iron

Concrete

Soil

Scale (meters)

0   1   2

Figure 6.8.5.

Cross Section Thru Hyperon Magnet
CASIM Geometry

Because of the poor statistics and long execution time, ten CASIM runs for the same geometry were done with different starting seeds. The weighted average of the results from the ten runs was then used to calculate the tritium and Na^{22} activation levels produced in the ground water. See Figure 6.8.6 for the total stars produced for each CASIM run. The average of the ten runs was 1.62×10^{-2} stars per incident proton. The distance to the aquifer was assumed to be 37 feet. The results are shown in Table 6.8.1. Both the ground water radioactivity criteria listed above are satisfied with a safety margin. If the distance to the aquifer is assumed to be zero, (for example if a short circuit pathway to the aquifer existed that negated the possibility of radioactive decay en route) then the criteria are just satisfied.

TABLE 6.8.1

Stars per incident proton	1.62×10^{-2}	
Protons per year	2×10^{18}	
Distance to aquifer (feet)	37	

	H^3	Na^{22}
Mean lifetime (years)	17.7	3.74
Migration rate (feet per year)	7.5	3.2
Allowed concentrations (pCi per ml)	20	0.4
Leachable atoms per star	0.075	0.003
Calculated concentration (pCi per ml)	1.61	0.02
Ratio to allowed concentrations	0.08	0.05
Condition 1 value <1 ?	0.07 - OK	
Condition 2 value <1 ?	0.08 - OK	

Parameters and results for KTEV primary beam dump ground water activation calculation, assuming no short-circuit pathway to the aquifer.
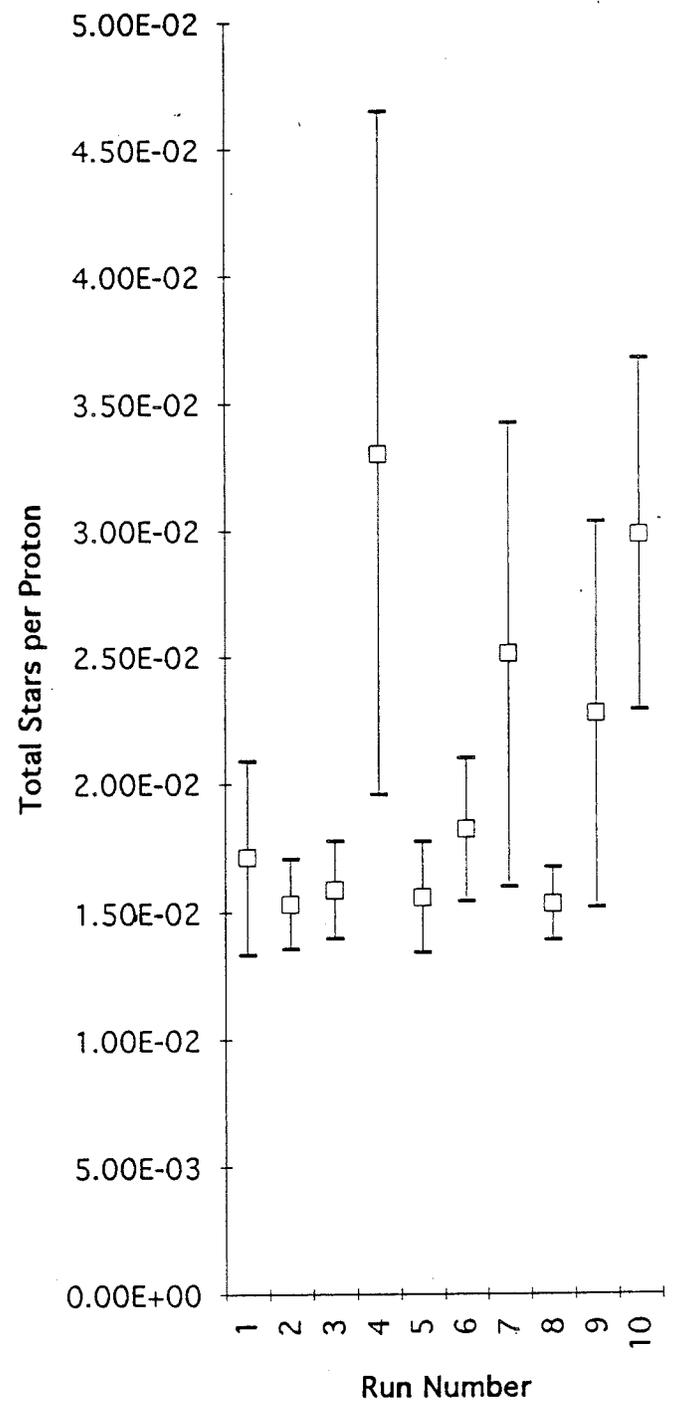
FIGURE 6.8.6.

6.9   Residual Activation of Target Station

Design criteria for dose rates at the external surface of the shielded target station due to residual activation are similar to those used for TeV II target station designs, along with additional constraints imposed by tunnel access issues into NM2. The TeV II criterium is that the worst case dose rate should not exceed 100 mrads per hour at the surface of the shield. This rate was decided upon based on the need for personnel to occasionally access enclosures containing primary target stations without receiving an excessive radiation dose. Of course residual rates for components within the target station shielding will be considerably higher and special precautions will have to be taken for any work involving disassembly of the target station itself.

For an infinite irradiation time followed by no decay time, the dose rate, D, at the surface of a solid iron shield is given by[5]:

$$D = \Omega/4\pi * \omega(\infty,0) * S * I$$

where $\omega(\infty,0)$ is the conversion factor, for infinite irradiation and zero cooling, that converts star density at the surface of the shield to dose rate. S is the star density calculated with CASIM, Ω is the solid angle subtended by the source at the measurement location, and I is the beam intensity in protons per second.

Solving for S with

D   = 100 mrads per hour
$\omega(\infty,0)$ = (9×10^{-3} mrads/hr) per (star/cm^3/sec)
Ω = 2π
I   = 5×10^{12} per 60 seconds

gives S=2.7×10^{-7} stars/cm^3.

---

[5] Fermilab Radiological Control Manual, Chapter 13.

Star densities less than this value give rates less than 100 mrads per hour for an infinite irradiation and zero cool-off time.

An additional issue in NM2 is that the normal access into the enclosure, including the upstream and downstream beam transport tunnels, requires close passage to the primary target station. For this reason, a more substantial target station shield is needed.

The CASIM calculations used for estimating ground water activation can also be used to estimate residual activation levels in the steel shielding. The results are that the dose rate at the bottom of the shield is estimated to be about 128 mrads per hour, the dose rates at the east and west sides are estimated to be about 3.3 mrads per hour and the dose rate on the top surface of the shield is estimated to be about 4.5 mrads per hour. These calculated rates do not consider cool-off time, but also do not consider thin spots in the shield, which are difficult to eliminate. The maximum dose rate is expected to be in the region of the target station that is about 1.6 meters downstream of the start of the copper part of the beam dump, near the maximum in the hadronic cascade in the dump and shielding. Since the bottom of the target station is not accessible to workers entering the enclosure, the dose rate greater than 100 mrads per hour on that surface is acceptable. Residual dose rates to the side and top of the target station should allow viable access without excessive personnel radiation exposure.

6.10 KAMI Operations

Beam parameters for KAMI operation[6], are given in Table 6.10.1.

TABLE 6.10.1

	Energy (GeV)	Intensity (ppp)	Repetition Rate (hr^{-1})
Primary Beam	120	3×10^{13} (3×10^{13})	1200
Secondary beam (single beam)	52.8	1.1×10^{10} (1.1×10^{10})	1200

KAMI primary and secondary beam parameters for worst-case accident. Intensities in parentheses indicate assumed intensities for normal running.

6.10.1 KAMI Primary Beam Shielding

Scaling the Cossairt criteria to KAMI beam energies and intensities results in the requirement of at least 21 feet of earth-equivalent shielding over a primary beam enclosure in order to have a worst case accident rate of less than 10 mrem per hour. This would result in the area being classified as minimal occupancy, but would not require fences or interlocked radiation detectors (Cossairt criteria 2A). Enclosures with as little as 17 feet of earth-equivalent shielding, posted with high radiation area signs, and protected by four foot fences with locked gates are also acceptable. (Cossairt criteria 4A, accident dose rate less than 500 mrem per hour). The shielding regions over NM2 that currently exist with 15.5 feet and are acceptable for KTeV operation would have to be increased to 17 feet everywhere for KAMI operations.

---

6 W. S. Freeman, et al., "Radiation Shielding Requirements for the KTeV Facility (1/13/93).

6.10.2 "Decay Enclosure" (NM3)

During KAMI operations, Main Injector primary beam will be targeted within the NM3 "decay enclosure". This operating mode drives the shielding and structural requirements for the enclosure. KTeV-only running would require substantially less shielding in this area, since only secondary beam will be present for KTeV (see section 6.5.1). The KAMI requirements for this area are the same as those in the previous section, 21 feet of earth equivalent shielding (Cossairt criteria 2A). Note that the actual distance from the beam line to the ceiling is 12 feet rather than the 3 feet assumed in the calculations of the Cossairt criteria, so the dose rate due to an accidental loss on a magnet in this enclosure will be further reduced from the 10 mrem per hour upper limit of category 2A.

6.10.3 KAMI Secondary Beam Shielding

Scaling to KAMI secondary beam energies and intensities, 11.5 feet of earth-equivalent shielding is required to have a worst-case accident of no more than 10 mrem per hour. This would require only minimal occupancy but not require fences or interlocked detectors. (Cossairt Criteria 2A). Enclosures with as little as 7.5 feet of earth-equivalent shielding would be permitted if posted with high radiation area signs and surrounded by 4 foot fences with locked gates (Cossairt criteria 4A).

6.10.4 KAMI Experiment Hall Shielding

Figure 6.13 shows the calculated worst-case accident dose rates at several locations around the experiment hall for the upstream regions of the hall where no shielding is added over the beam line. The counting room is adequately shielded, with dose rates well below the allowed 1 mrem per hour without interlocked detectors. On the roof of the counting room the worst-case accident dose rates are 1780 mrem per hour or 1.5 mrem per spill for the region not shadowed by the six-foot-thick loading dock deck. These rates will *require* the use of interlocked detectors to protect this region, since accident rates above 1000 mrem per hour are not permitted by the Radiological Control Manual. With interlocked detectors the accident dose per spill will require only that the area be minimally occupied, but no

other precautions would be necessary. The accident rates are 1 mrem per hour or 0.0008 mrem per spill for the region that is shadowed by the deck, which will be acceptable for a minimal occupancy area with no further precautions even without interlocked detectors, provided dose rates due to normal operations are acceptable.

The roof of the experiment hall has calculated accident dose rates of 1550 mrem per hour or 1.3 mrem per spill. This region also will *require* that interlock detectors be used because the dose rate exceeds 1000 mrem per hour. With interlocked detectors, the roof will be required to be minimal occupancy, with no further restrictions, provided dose rates due to normal operations were acceptable.

The area outside the west wall has calculated accident rates of 4470 mrem per hour or 3.7 mrem per spill. This will also *require* the use of interlocked detectors. Because the dose per spill is between 2.5 and 10 mrem the area will have to be posted as a "Radiation Area" with fencing used to define the boundary, and it will have to be minimally occupied.

Very small fractions of beam loss during normal operations could result in elevated levels of radiation on the roofs of the counting room and experiment hall. For example, a point loss of 1.6×10^{-5} of the normal secondary beam intensity could result in a rate of 0.025 mrem per hour on the roof of the experiment hall. According to the Radiological Control Manual areas with dose rates above 0.025
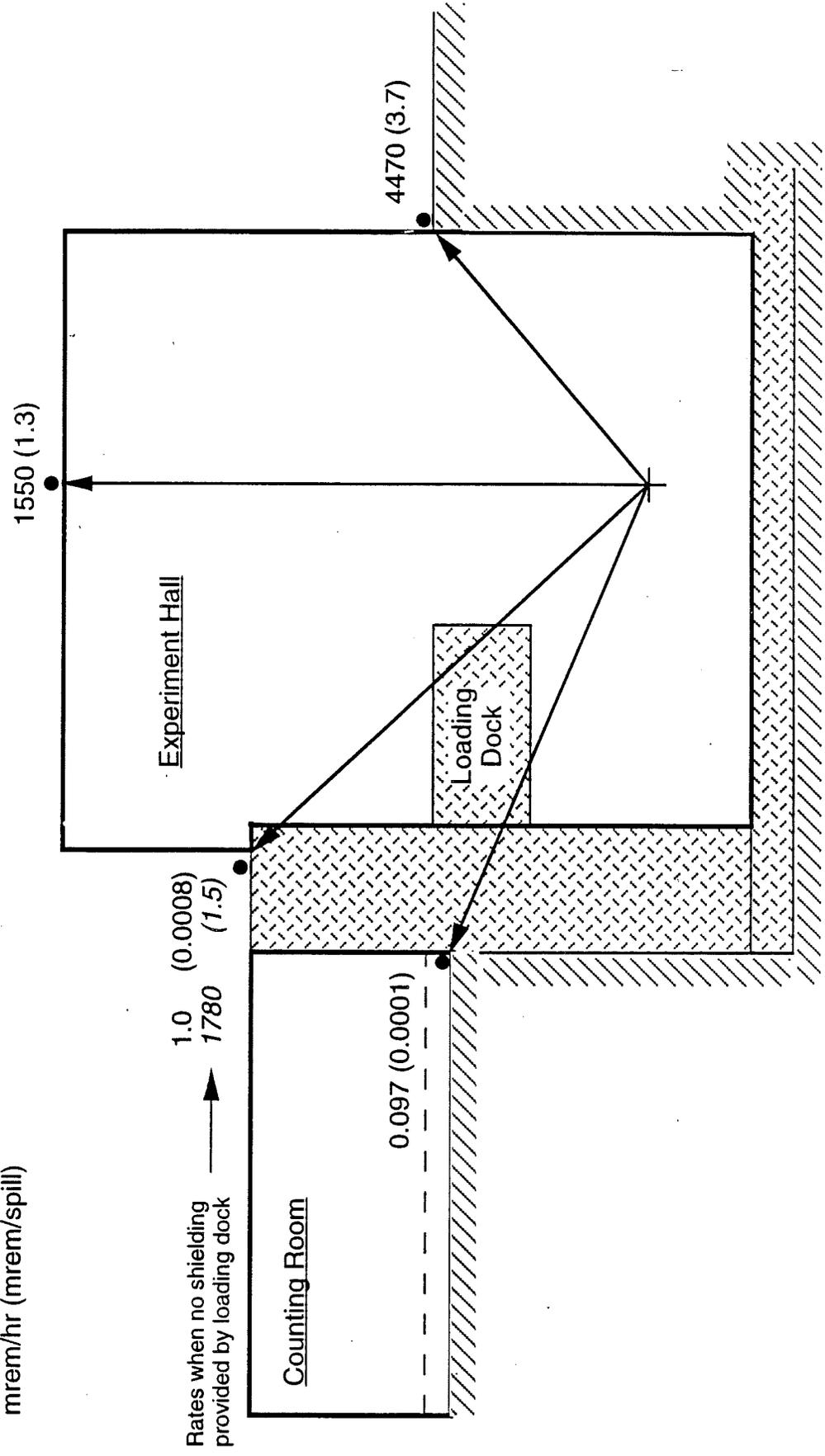
Figure 6.13.

Accident Dose Rates For Kami Running

Dose rate Legend
mrem/hr (mrem/spill)

Rates when no shielding
provided by loading dock

4470 (3.7)

1550 (1.3)

Experiment Hall

Loading Dock

1.0   (0.0008)
       (1.5)
1780

0.097 (0.0001)

Counting Room

mrem per hour from normal operations require posting as "Radiologically Controlled Areas", but there is no other restrictions provided the dose rates from normal operations in these minimally occupied areas do not exceed 2.5 mrem per hour and force them into the "Radiation Area" category.

Figure 6.14 shows the calculated worst-case accident dose rates at several locations around the downstream two bays of the hall where six feet of concrete shielding will be added over the experiment. The counting room is adequately shielded, with accident dose rates of 0.1 mrem per hour, well below the allowed 1 mrem per hour without interlocked detectors. On the roof of the counting room the worst-case accident dose rates are 1 mrem per hour or 0.0008 mrem per spill which are acceptable for a minimal occupancy area with no further precautions and do not require interlocked detectors.

The roof of the experiment hall has calculated accident dose rates of 10.2 mrem per hour or 0.0085 mrem per spill. This rate is on the boundary between requiring only minimal occupancy and requiring chains or fencing and posting as a "Radiation Area". In either case interlocked detectors will not be required to protect this area of the roof.

The area outside the west wall of the experiment hall has calculated accident rates of 1.6 mrem per hour or 0.0014 mrem per spill. This region will require only minimal occupancy and not require interlocked detectors.

6.10.5 Forward Shielding - KAMI

Since the dose per accident spill for KAMI secondary beam is slightly less than that for KTeV, the hadron shielding requirements in the forward direction should also be slightly less. This should be verified by CASIM calculations, which have not yet been done for KAMI secondary beam energy. These calculations should include a study of normal operating rates due to interactions in the neutral beam dump. The forward shielding issue for KAMI may also be affected by the amount of shielding installed downstream of the primary beam dump in the decay enclosure since this may contribute to the downstream dose as well.

Dose rate Legend
mrem/hr (mrem/spill)

1.64 (0.0014)

10.2 (0.0085)

Experiment Hall

Loading Dock

1.0 (0.0008)

0.097 (0.0001)

Counting Room
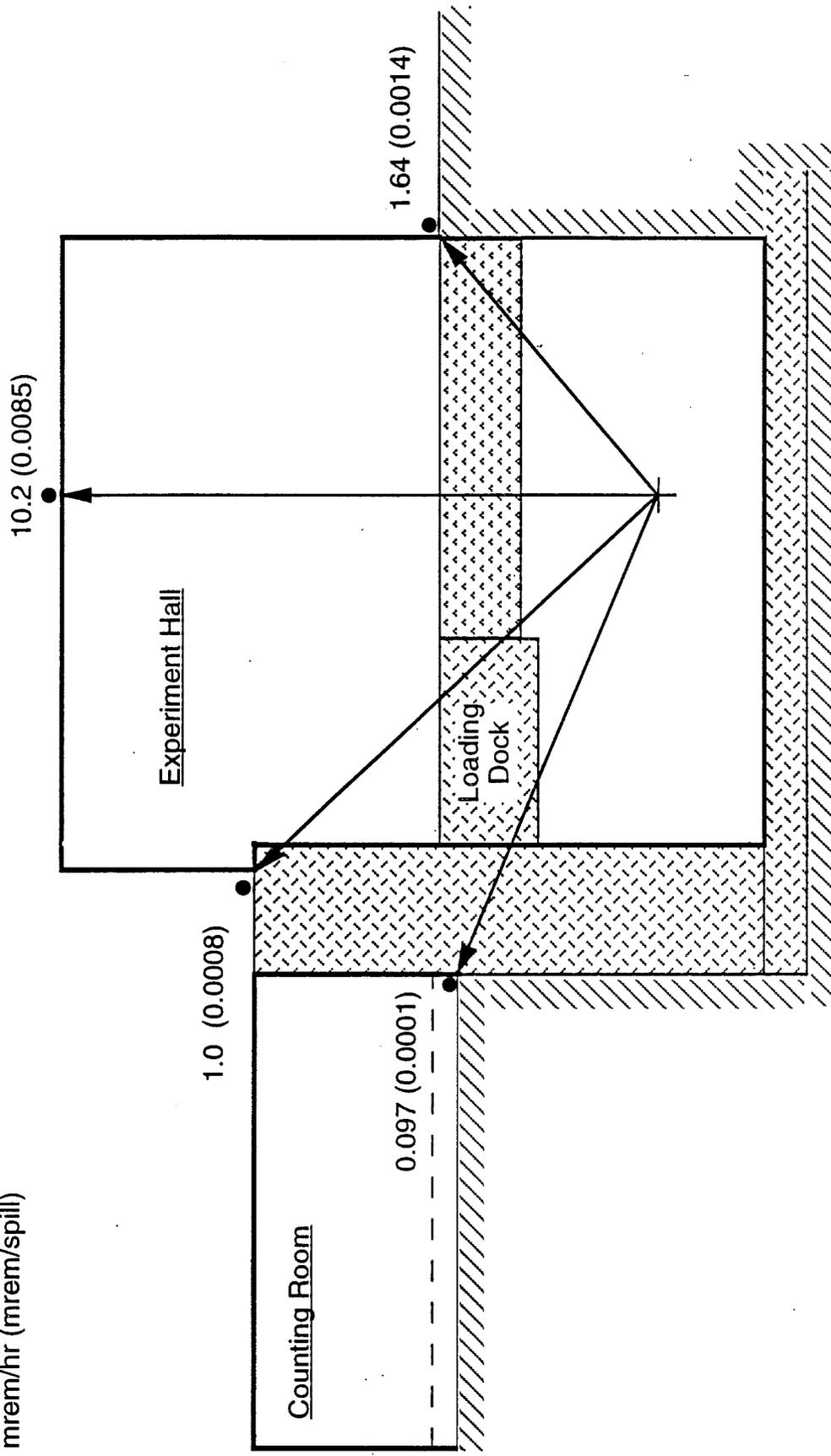
Figure 6.14.

Accident Dose Rates For Kami Running -
Shielding Blocks Installed

6.10.6 Labyrinths and Penetrations

The attenuations of access labyrinths and penetrations in the experiment hall were calculated using the formalism of the RD shielding assessment and the associated FORTRAN program developed from that formalism. The results are summarized in Table 6.10.2.

TABLE 6.10.2

Labyrinth Location	Number of Legs	Total Attenuation	Dose at Exit (mrem/hr)
NM3 upstream stairwell[1]	4	1.8×10^{-8}	0.8
NM3 equipment hatch[1]	2	2.6×10^{-3}	1.2×10^{5}
Expt Hall - West side stairwell	2	2.5×10^{-5}	0.05
Expt Hall - SE stairwell	3	3.9×10^{-6}	6.6×10^{-3}
Expt Hall - NE stairwell	3	6.0×10^{-6}	0.01
Cable penetrations	2	1.1×10^{-7}	1.5×10^{-4}
Cable penetrations	1	1.5×10^{-3}	2.1
HVAC duct - West supply[2]	2	1.2×10^{-4}	0.03
HVAC duct - West return	4	1.7×10^{-9}	3.3×10^{-6}
HVAC duct - East supply[2]	2	3.8×10^{-4}	0.09
HVAC duct - East return[2]	2	6.5×10^{-5}	0.17
CsI Supply	4	2.0×10^{-18}	0
CsI Return	4	7.4×10^{-13}	0

1 - primary beam source
2 - neglect attenuation of first leg of duct and treat as two-legged duct; but assume off-axis source with distance to mouth equal to length of first duct leg.

KAMI access labyrinth and penetration attenuations and doses at exits based on worst-case accident loss on-axis of 3×10^{13} protons per spill at 120 GeV for primary beam and 1.1×10^{10} particles per spill at 52.8 GeV and 1200 spills per hour for secondary beam.

Note that the large NM3 equipment hatch will require the installation of shielding blocks for KAMI running. To reduce the accident dose from 1.2×10^5 mrem per hour to 10 mrem per hour requires an additional attenuation factor of 8.3×10^5. This will be provided by a minimum of 11 feet of concrete shielding installed in the hatch. Also, the NM3 upstream personnel labyrinth will have its interlocked door at the top of the stairwell rather than at the bottom as is currently the case for the existing similar labyrinth in NM2. The midstream NM2 interlocked door will also have to be relocated to the top of the stairs to the NS7 Service Building for KAMI operations.

The attenuations and doses at the exits of two-legged and single-legged cable penetrations between the experiment hall and the counting room were also computed for KAMI secondary beam parameters. The results are also given in Table 6.10.2. The two-legged penetration has adequate attenuation for KAMI operations. If a one-legged 10 foot long straight-through penetration design was adopted, the attenuation would be insufficient for a continually occupied space like the counting room, unless interlocked detectors were employed, since the accident dose rate would be 2.1 mrem per hour.

The attenuation and doses at the exits of the four HVAC ducts at the downstream end of the experiment hall and the two CsI house HVAC ducts at the west side of the hall were calculated for KAMI beam parameters. The results are also given in Table 6.10.2. These ducts also provide acceptable attenuations for KAMI operations.

7. SITE & UTILITY REQUIREMENTS:

MODIFICATIONS TO EXISTING FACILITIES, POWER, COOLING REQUIREMENTS

The utility requirements for the magnets in the beamline are listed in Tables 7.1 and 7.2 located in this section.

Modifications to the existing facility to accomodate the listed magnets are minimal. All of the beamline magnets can be supplied water and power from the existing utilities. However, power supplies for the two magnets located in the new construction area will be located in NS7. As part of the new construction package, additional conduit is being installed between NM2 and the new construction to accomodate these power leads. Consequently, there is insufficient conduit capacity for bus work to bring magnet power from NS7 into NM2. Therefore, one additional set of penetrations are required between NS7 and NM2. Specifically, the penetrations are for 6 pair of watercooled bus from NS7 north to the access hatch, coring through the hatch and running the bus down the west wall of the hatch, then along the corridor ceiling into NM2 high bay where 3 pair will go upstream and 3 pair will go down stream. Of the 3 pair of Bus that go down stream, one pair stops in NM2, one pair goes to NM3 and the third pair goes to NM4.

Radiation safety personnel are looking at that routing to see if the gap the bus would create where it comes down the hatch is a problem. If not, we would not need any additional penetrations. If so, we will need to install penetrations for all 6 pair of bus plus a couple spares. These penetrations are 5" by 7" structural steel.

The existing LCW capacity in NS7 is sufficient to accomodate all of the power supplies located in that building for KTeV. Additionally, the LCW in NM2 is sufficient to serve all of the beamline magnets in NM2. LCW for the magnets in the experimental hall is going to be fed via new LCW supply and return piping from NS2 as part of the new construction. This same new supply and return completes the LCW loop which services NS7.

Alignment and survey techniques used to achieve the necessary precision will require some modifications to the existing NM2 facility for alignment site risers and monuments. These requirements are specified in Chapter 9.

Table 7.1
KTeV Magnet Power Requirements

Item	Description	Max. Current (DC amps)	Voltage	B Field (kilogauss or kG/in)	Maximum Power (kilowatts)	Power Supply
Pretarget						
NM1BPM1	Horizontal beam position monitor	NA	NA	NA	NA	NA
NM1BPM2	Vertical beam position monitor	NA	NA	NA	NA	NA
NM1WC1	Vacuum bayonet SWIC 1mm	NA	NA	NA	NA	NA
NM1U-1	Vertical bend EPB 5-1.5-120	1688	29.5	15.0	50	TR500
NM1U-2	Vertical bend EPB 5-1.5-120	1688	29.5	15.0	50	TR500
NM1H	Trim Horiz.. 4-4-30	180	50.0	4.0	9	PEI 20
NM2BPM1	Horizontal beam position monitor	NA	NA	NA	NA	NA
NM2BPM2	Vertical beam position monitor	NA	NA	NA	NA	NA
NM2WC1	Vacuum bayonet SWIC 1mm	NA	NA	NA	NA	NA
NM2SEM	Removeable intensity monitor	NA	NA	NA	NA	NA
NM2EU-1	Main Ring B2 4-2-240	4750	34.0	17.9	162	TR500
NM2EU-2	Main Ring B2 4-2-240	4750	34.0	17.9	162	TR500
NM2V	Trim Vert. 4-4-30	180	50.0	4.0	9	PEI 20
NM2Q1-1	Focus 4Q120	1175	42.8	5.5	50	TR240
NM2Q1-2	Focus 4Q120	1175	42.8	5.5	50	" " "
NM2Q1-3	Focus 4Q120	1175	42.8	5.5	50	" " "
NM2Q2-1	Defocus 4Q120	1175	42.8	5.5	50	TR240
NM2Q2-2	Defocus 4Q120	1175	42.8	5.5	50	" " "
NM2Q2-3	Defocus 4Q120	1175	42.8	5.5	50	" " "
NM2Q2-4	Defocus 4Q120	1175	42.8	5.5	50	" " "
NM2D1-1	AVB 1 - B2 4-2-240	4750	34.0	17.9	162	TR500
NM2D1-2	AVB 2 - B2 4-2-240	4750	34.0	17.9	162	" " "
NM2D2	AVB 3 - B2 4-2-240	4750	34.0	17.9	162	" " "
NM2H	Trim Horiz. 4-4-30	180	50.0	4.0	9	PEI 20
NM2WC2	Target SWIC	NA	NA	NA	NA	NA
NM2WC3	Target SWIC	NA	NA	NA	NA	NA
Target Pile/Sec. Beam						
NM2WALL	Upstream end of target hall					
NM2TGT	30 cm BeO target	NA	NA	NA	NA	NA
NM2S1	Eartly sweeper	1500*	29.0	20.0	44	PEI500
NM2BD	Dump	NA	NA	NA	NA	
NM2S2	E8 hyperon magnet - μsweep1†	1500*			500	TR500
NM2AB1	Common absorber	NA	NA	NA	NA	NA
NM2AB2	Moveable absorber	NA	NA	NA	NA	NA
NM2TCOL	Primary collimator	NA	NA	NA	NA	NA
NM2S3	Muon spoiler - μsweep2	1200*	116.0	18.9	139	TR240
NM2SR	Modified B2 4-4-240	4750	34.0	12.0	162	TR500
NM2CV1	Slab Collimator	NA	NA	NA	NA	NA
NM2BS	Beamstop	NA	NA	NA	NA	NA
NM2CH	2-jaw collimator	NA	NA	NA	NA	NA
NM2CV2	2-jaw collimator	NA	NA	NA	NA	NA
NM2BP	beam pipe(s)	NA	NA	NA	NA	NA
NM3CVH	Defining collimator	NA	NA	NA	NA	NA
NM3S	Argonne 10-4-72	3000	145.0	20.6	435	TR500
NM3BP1	18" beam pipe	NA	NA	NA	NA	NA
NM3BP2	30" beam pipe	NA	NA	NA	NA	NA
NM3BP3	48" beam pipe	NA	NA	NA	NA	NA
NM4AN	Spectrometer magnet#	2344*	342.0	550MeV/c	802	2-PEI500

# Nominal = 1919 A, 537 kW, 450 MeV/c	Total Max. DC Magnet Power	3371	
* DC only, † Rough est. Estimated Nominal Operating Power (with ramping)		1895	

Table 7.2
KTeV LCW Requirements

Item	Description	LCW Flow (gpm)	Temp. Rise (degrees F)	Pressure Drop (psi)	Maximum Load (kilowatts)	Power Supply
Pretarget						
NM1BPM1	Horizontal beam position monitor	NA	NA	NA	NA	NA
NM1BPM2	Vertical beam position monitor	NA	NA	NA	NA	NA
NM1WC1	Vacuum bayonet SWIC 1mm	NA	NA	NA	NA	NA
NM1U-1	Vertical bend EPB 5-1.5-120	4.7	80	100	50	TR500
NM1U-2	Vertical bend EPB 5-1.5-120	4.7	80	100	50	TR500
NM1H	Trim Horiz.. 4-4-30	6.4	50		9	PEI 20
NM2BPM1	Horizontal beam position monitor	NA	NA	NA	NA	NA
NM2BPM2	Vertical beam position monitor	NA	NA	NA	NA	NA
NM2WC1	Vacuum bayonet SWIC 1mm	NA	NA	NA	NA	NA
NM2SEM	Removeable intensity monitor	NA	NA	NA	NA	NA
NM2EU-1	Main Ring B2 4-2-240	16.4	65	200	162	TR500
NM2EU-2	Main Ring B2 4-2-240	16.4	65	200	162	TR500
NM2V	Trim Vert. 4-4-30	6.4	50		9	PEI 20
NM2Q1-1	Focus 4Q120	8.0	45	100	50	TR240
NM2Q1-2	Focus 4Q120	8.0	45	100	50	" " "
NM2Q1-3	Focus 4Q120	8.0	45	100	50	" " "
NM2Q2-1	Defocus 4Q120	8.0	45	100	50	TR240
NM2Q2-2	Defocus 4Q120	8.0	45	100	50	" " "
NM2Q2-3	Defocus 4Q120	8.0	45	100	50	" " "
NM2Q2-4	Defocus 4Q120	8.0	45	100	50	" " "
NM2D1-1	AVB 1 - B2 4-2-240	16.4	65	200	162	TR500
NM2D1-2	AVB 2 - B2 4-2-240	16.4	65	200	162	" " "
NM2D2	AVB 3 - B2 4-2-240	16.4	65	200	162	PEI 20
NM2H	Trim Horiz. 4-4-30	6.4	50	NA	NA	NA
NM2WC2	Target SWIC	NA	NA	NA	NA	NA
NM2WC3	Target SWIC	NA	NA	NA	NA	NA
Target Pile/Sec. Beam						
NM2WALL	Upstream end of target hall					
NM2TGT	30 cm BeO target	NA	NA	NA	NA	NA
NM2S1	Eartly sweeper - RAW water	9.0	33	90	44	PEI500
NM2BD	Dump - RAW water	60.0			22	
NM2S2	E8 hyperon magnet - μsweep1	50.0			500	TR500
NM2AB1	Common absorber	NA	NA	NA	NA	NA
NM2AB2	Moveable absorber	NA	NA	NA	NA	NA
NM2TCOL	Primary collimator	NA	NA	NA	NA	NA
NM2S3	Muon spoiler - μsweep2	19.0	49	150	139	TR240
NM2SR	Modified B2 4-4-240	16.4	65	200	162	TR500
NM2CV1	Slab Collimator	NA	NA	NA	NA	NA
NM2BS	Beamstop	NA	NA	NA	NA	NA
NM2CH	2-jaw collimator	NA	NA	NA	NA	NA
NM2CV2	2-jaw collimator	NA	NA	NA	NA	NA
NM2BP	beam pipe(s)	NA	NA	NA	NA	NA
NM3C	Defining collimator	NA	NA	NA	NA	NA
NM3S	Argonne 10-4-72	45.0	60	185	435	TR500
NM3BP1	18" beam pipe	NA	NA	NA	NA	NA
NM3BP2	30" beam pipe	NA	NA	NA	NA	NA
NM3BP3	48" beam pipe	NA	NA	NA	NA	NA
NM4AN	Spectrometer magnet#	172.0	39	200	802	2-PEI500
	Est. Total LCW Flow	**538**	**Max. DC Load**		**3393**	
# Nominal = 1919 A, 537 kW, 450 MeV/c	**Est. Nominal Operating Load (with ramping)**				**1917**	

8.   INSTALLATION

Constraints impacting the beamline component installation include the 20 ton capacity of the existing NM2 crane, the 10'-6 crane maximum hook height, the size of the NM2 equipment hatch, and clearence between the installed components and the NM2 building walls. All of the above constraints have been understood during the design efforts for each individual component.

Specific installation sequencing requirements are:

1.   Existing NM2 target pile must be completely removed because of insufficient staging space in the Target Hall.

2.   The steel for Mu-Sweep II [NM2S3] must be placed in the downstream end of NM2 prior to installing the Target Pile and E-8 magnet.

3.   It is preferred that the beamline elements upstream of the Target Pile be installed prior to the Target Pile installation.

4.   Target pile steel selection for steel used in the new NM2 target pile requires an area for staging the old NM2 target pile steel plus the additional steel required. Steel selection criteria include both geometrical considerations and minimal residual activity.

5.   The coils for the E-8 magnet must be placed in the downstream end of NM2 prior to stacking the target pile steel.

9.   Alignment and Stability

Section 9 represents a summary of the understanding to date of the alignment and stability issues associated with the KTeV beam and spectrometer. A plan for building an alignment network for the KTeV project is presented.

Progress has been made on understanding the details associated with alignment and monitoring of each component. This is a status report on that subject. A comprehensive plan will be produced by July '94 in preparation for the installation of KTeV.

The alignment of the beam and spectrometer elements plays an important role in KTeV. Precise alignment of the neutral beam brings some of the systematic errors in the physics measurements under control. The measurement of the spectrometer location provides a primary reference for the absolute energy calibration of the CsI detector.

A substantial improvement is required in the precision of the physics measurements in this next generation of kaon experiments. The geometry of the experiment must be more precisely determined. The error contributions related to positional uncertainties of hardware must not contribute to the overall errors.

The Fermilab Survey, Alignment, and Geodesy group (SAG) has made substantial progress in upgrading their capabilities. Simulations indicate, a standard level of 3 dimensional relative measurement accuracy for any component within the KTeV internal network of ±0.25 mm at the 95% confidence level can be provided. Errors in machining, fiducialization, or adjustment are not included.

Accuracies less than 0.25 mm requires special procedures and/or technology. Work is proceeding on understanding the crucial alignment parameters of each component. There have been continuing iterations trying to balance the needs and wants of the experiment and the capabilities of the SAG group.

Alignment tolerances for individual beamline and detector components are presented in Tables 9.1.1 and 9.1.2. Shown are the installation and measurement tolerances for installation purposes, not necessarily the alignment attainable with data from the experiment. Unless specified otherwise, it should be assumed that the device needs to be

stable within the measurement tolerance. All specifications and capabilities are at the 95% confidence level. It is important to note that the most stringent tolerances are only relative tolerances. The absolute (DUSAF) tolerances are of order 3 mm.

Overview

Alignment issues are driven by the physics requirements. The geometry of the CsI must be precisely known as well as its location with respect to the rest of the apparatus. The charged particle spectrometer (drift chambers and magnet) must be internally aligned since it is the basis for locating many other elements using the data. Its position relative to the CsI must be understood in order to cross-calibrate (in energy) the array. Chamber alignment is also important for proper operation of the trigger. (Ultimate understanding of the 'as is' positions of the chambers will be determined from the data.)

The definition of the secondary beams depends on the alignment of the beam-target-collimator system. The axis of the beam must coincide with the axis of the spectrometer. The beam axis (see below) will be the primary reference frame for the KTeV Beam/Spectrometer system.

It is also necessary that the primary beam impinge on the target. Though the exact value of the vertical targeting angle is not critical, it must be stable. The horizontal targeting angle must be set properly in order to keep the intensities and momentum spectra of the two beams equal.

As the goals of the experiment, and the alignment issues in particular, are centered first on the neutral beam, the discussion starts there. The primary beam will be discussed after the secondary beam followed by the spectrometer. The overall methods by which the KTeV geometry will be established and implemented are addressed in Sections 9.2 and 9.3.

Stability Issues

If the locations of elements are not stable within the specified accuracy, they must be monitored and corrected. This is a serious issue, for example, with the neutral beam elements. It is for these elements that the alignment is most critical and where monitoring the alignment is a particularly challenging problem.

As in past experiments, the motion of the target or collimators, hence the beam relative to the charged spectrometer can be determined using the drift chambers. However, it is difficult to tell which component actually moved. In order to keep the level of off-line corrections palatable and to safeguard against gross movements which could endanger the calorimeter, two independent stability monitoring schemes are being studied by the KTeV beams group. The first involves using the beam itself (See Section 5.9) and the second uses a completely beam independent approach dependent on gravity and/or lines of sight (See Section 9.3.2).

The primary beam must be stable on target (see Section 1.2.). The method planned is to use an active feedback automatic beam control system (See Section 2.5). This system is similar to that developed in other external beam lines except for beam roll correction which must be developed. It will eliminate most of the problems associated with magnet fluctuations. In order for this system to work within the tolerances specified, a beam monitor must be employed which is more precise than the standard SWICs. Prototypes are currently being developed. These beam monitors must also remain stable relative to the target for the system to be effective.

The spectrometer magnet and CsI must also be kept in alignment. The distance between the downstream face of the regenerator and z-calibrator to the upstream face of the CsI array must be well known at all times. Also, temperature variations must be monitored. It is also important to know how the floor may differentially sink/rise as this will determine the motion of the spectrometer elements.

Once the geometry has been established, it is necessary to understand issues of stability and resurvey. Significant shifts in the height of various elements may occur (See Section 9.3.2). The MCenter target pile continued to sink at the rate of a fraction of a millimeter per month even some years after installation (See Figure 9.1.1). However, soil borings indicate a better bearing capacity for KTeV by almost a factor of two and a settlement Monte Carlo[1] predicts only modest motion (See Section 9.3.2)

---

[1] STS Consultants, **Geotechnical Evaluation of Proposed KTeV Project**, Northbrook, IL, 1993

ME/MC Dump Elevation History
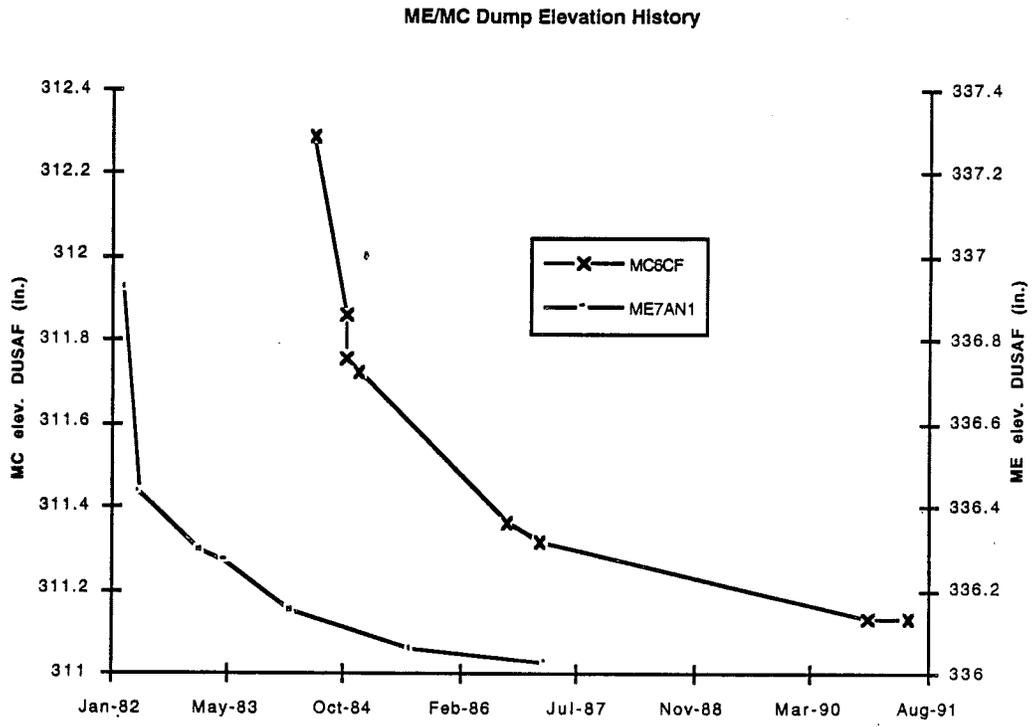
Figure 9.1.1 Elevation history of the MCenter target pile and the MEast SM12 magnet.

9.1   Alignment and Stability Requirements

This section addresses the alignment and stability requirements of each KTeV component or subsystem . They are divided into three major subsections: the neutral beam, primary beam, and detector. The primary and secondary beam element tolerances are summarized in Table 9.1.1 and detector element tolerances in Table 9.1.2

Table 9.1.1

KTeV Beamline Alignment Requirements Summary							
Item	Description	Installation Tolerance			Measurement Tolerance*		
		x=transverse	y=elevation	z= beam	x=transverse	y=elevation	z= beam
		x (mm)	y (mm)	z (mm)	x (mm)	y (mm)	z (mm)
Pretarget							
ALL	All regular beamline elements	0.5	0.5	5	0.5	0.5	5
Target SWIC(s)	Target beam position monitors	0.2	0.2	5	0.2	0.2	5
Target Pile/Sec. Beam							
NM2TGT	30 cm BeO target	0.2	0.2	5	0.2	0.2	5
NM2S1	Eartly sweeper	0.6	0.6	5	0.6	0.6	5
NM2BD	Dump	0.6	0.6	5	0.6	0.6	5
NM2S2	E8 hyperon magnet - µsweep1	0.6	0.6	5	0.6	0.6	5
NM2AB1	Common absorber	0.5	0.5	5	0.5	0.5	5
NM2AB2	Moveable absorber	0.5	0.5	5	0.5	0.5	5
NM2TCOL	Primary collimator	0.2	0.2	5	0.2	0.2	5
NM2S3	Muon spoiler - µsweep2	0.6	0.6	5	0.6	0.6	5
NM2SR	Modified B2 4-4-240	0.5	0.5	5	0.5	0.5	5
NM2CV1	Slab Collimator	0.5	0.5	5	0.5	0.5	5
NM2BS	Beamstop	0.5	0.5	5	0.5	0.5	5
NM2CH	2-jaw collimator	0.5	0.5	5	0.5	0.5	5
NM2CV2	2-jaw collimator	0.5	0.5	5	0.5	0.5	5
NM2BP	beam pipe(s)	10	10	NA	2	2	NA
NM3CVH	Defining collimator	0.2	0.2	5	0.2	0.2	5
NM3S	Argonne 10-4-72	0.5	0.5	5	0.5	0.5	5
NM3BP1	18" beam pipe	3	3	NA	3	3	NA
NM3BP2	30" beam pipe	3	3	NA	3	3	NA
NM3BP3	48" beam pipe	3	3	NA	3	3	NA

* Measurement tolerances are for installation purposes only.

Alignment tolerance requirements for KTeV beamline components.

9.1.1   The Neutral Beam System

The need for precise alignment of the neutral beam derives from the requirement for a clean and well defined neutral beam. Each beam must be well contained (no halo outside the defined beam area) in order that excessive physics backgrounds not be generated. The beam must also be well contained so as not to generate excessive energy deposition in the CsI.

The secondary beam starts with the target. It must be accurately located with respect to the primary and defining collimators. Other elements in the neutral beam (sweeping magnets, dump, and so on) must be clear of the neutral beam. Additional elements of the neutral beam (for example, the various absorbers and the slab collimator) must be aligned with respect to the neutral beam in order that their function not be compromised.

Alignment and stability requirements for the neutral beam are discussed in Section 5.8.6. These requirements are based on the criteria for beam stability in Section 1.2. There are a number of contributions to the error in the position of the collimators and target:

> a.   Mechanical Tolerances
> b.   Alignment Tolerances - this includes network, measurement, and fiducialization errors.
> c.   Uncertainties in primary beam location (see below)
> d.   Long term stability

Section 5 states the alignment allocation of the error budget for the primary and defining collimators is 0.2 mm transversely.

The primary target system will consist of several individual targets. At least three targets will be used:

> 1) 1 mm square 30 cm BeO
> 2) 3 mm 30 cm BeO
> 3) a short calibration/alignment target

An 'empty' target will also be available. They will be located on a remotely controlled mover which must be reproducible to less than the alignment tolerance. The target must be aligned and stable relative to the collimators and primary beam to 0.2 mm (See Section 5.3) and must be stable relative to the target beam position instrumentation to within 0.1 mm (See Section 2.5.4). It will be located inside a reentrant shielding cave allowing no direct line of sight between it and the collimators.

The common absorber will be selectable between varying lengths of Pb and Be. The motion must be very reliable so that the material covers all of both beams. The moveable absorber covers one beam only but alternates between spills. The motion must be very reproducible and reliable for about 10^6 cycles.

The primary collimator transverse alignment tolerance is 0.2 mm (see Section 5.6). It is important that there be rigid precision mechanical points attached to the collimator surface which can be measured from the aisle way. This requirement is the same for the defining collimator. Both collimators will be remotely adjustable in X and Y on each end.

The slab collimator will be constrained to travel in the vertical direction only with essentially two possible positions; in and out of the beam. The alignment portion of the slab collimator error budget is 0.5 mm in X and Y. The current plan is to drill 4 precision holes into each flange which will hold the fiducials.

The upstream vacuum decay region consists of vacuum pipes. These pipes must not present apertures to any parts of the detector. They are well oversized. The installation and measurement tolerances for these elements will be no more stringent than 3 mm in horizontal and vertical. The longitudinal tolerances are 5 cm for installation and 5 mm measured after installation.

The vacuum vessels after the regenerator tank will be discussed in Section 9.1.3.

Target Pile Elements

The tolerances on the target pile elements (excluding the target) are 0.6 mm. To avoid the problems of MCenter, there will be portholes into the pile for viewing the fiducials on the dump and sweeper magnet. This implies that these objects must remain rigid after they are fiducialized. In addition, there will be remote mechanical adjustment in the vertical plane. The portholes will be plugged when not being used. The apertures in

the horizontal plane on the Eartly sweeper and on the beam dump will be ±6.35 mm larger than necessary so that no horizontal adjustment will be needed after initial installation. The vertical apertures also have a clearance ±6.35 mm except for the bottom surface of the dump which is only 2.54 mm. Therefore, these items do not have to be stable to the measurement tolerances in Table 9.1.1.

Both NM2S2 and NM2S3 have transverse installation and measurement requirements of 0.6 mm. They will have the capability of horizontal and vertical adjustments. The current plan is to use shims, jacks, and rollers. The stability allowance is ±6.35 mm .

9.1.2   The Primary Beam

The primary beam is initially defined in Switchyard. The beam is transported to the KTeV primary target through the elements as detailed in Section 2. The beam is brought onto the production target with a downward vertical targeting angle and a zero horizontal targeting angle. The vertical targeting angle is variable using the AVB (Angle Varying Bend) system. Only small adjustments are possible in the horizontal using the trim system.

The tolerance to which the primary and secondary beams must be aligned in the horizontal plane is determined by the requirement that the intensity of the two neutral beams be equal to 1 % and that the momentum spectra be equal to 0.1% (See Section 5.3). The primary and secondary beams be aligned and stable to $\Delta\theta_x = \Delta\theta_y = 20$ µrad. This assumes a small (1 mm) target; and a beam size less than the target size. This is an issue particularly with respect to E832.

Primary Beam Element Tolerances

The primary beam elements are installed to the standard beam line tolerances of 0.5 mm in the horizontal and vertical. The only element(s) with special requirements is the targeting beam instrumentation (See Section 2.5.4). These will be used to control the beam position and angle on target and must be stable relative to the target within 0.1 mm. This requirement along with the target tolerances poses constraints on the engineering design in this area. It should also be noted that the Case 3 scenario (See Section 2.5.6) which mentions instrumentation stable to 250 µm at a distance of 1200' has not yet been addressed.

9.1.3 Detector Element Tolerances

Here we discuss installation and measurement tolerances for each of the detector elements starting from upstream. This section is summarized in Table 9.1.2. The detector is assumed to start with the Mask-Anti.

Table 9.1.2

KTeV Detector Alignment Requirements Summary							
Item	Description	Installation Tolerance			Measurement Tolerance*		
		x=transverse	y=elevation	z= beam	x=transverse	y=elevation	z= beam
		x (mm)	y (mm)	z (mm)	x (mm)	y (mm)	z (mm)
Experiment							
NM4MASK	Mask-anti	1	1	5	1	1	.0.5
NM4REG	Active regenerator	1	1	5	1	1	1
NM4TANKR/6	Vacuum decay tank	NA	NA	NA	NA	NA	NA
NM4RC6	Ring veto counter- vacuum	3	3	NA	0.5	0.5	1
NM4TANK6/7	Vacuum decay tank	NA	NA	NA	NA	NA	NA
NM4RC7	Ring veto counter- vacuum	3	3	NA	0.5	0.5	1
NM4TANK7/8	Vacuum decay tank	NA	NA	NA	NA	NA	NA
NM4RC8	Ring veto counter- vacuum	3	3	NA	0.5	0.5	1
NM4ZCAL	Z-calibrator (Pb glass in vacuum)	10	10	NA	1	1	1
NM4TANK8/9	Vacuum decay tank	NA	NA	NA	NA	NA	NA
NM4RC9	Ring veto counter- vacuum	3	3	NA	0.5	0.5	1
NM4TANK9/10	Vacuum decay tank	NA	NA	NA	NA	NA	NA
NM4RC10	Ring veto counter- vacuum	3	3	NA	0.5	0.5	1
NM4TANK10/W	Vacuum decay tank	NA	NA	NA	NA	NA	NA
NM4WIND	Sailcloth vacuum window	1	1	NA	0.5	0.5	0.5
NM4SHIELD	Thin Vac. window shield	NA	NA	NA	NA	NA	NA
NM4DC1	Drift chamber	0.25	0.25	0.5	0.25	0.25	0.25
NM4HE1	Helium Bag	NA	NA	NA	NA	NA	NA
NM4SA2	Spectrometer veto counter	3	3	5	0.5	0.5	1
NM4DC2	Drift chamber	0.25	0.25	0.5	0.25	0.25	0.25
NM4HE2	Helium Bag	NA	NA	NA	NA	NA	NA
NM4AN	Spectrometer magnet	0.5	0.5	1	0.25	0.25	0.25
NM4SA3	Spectrometer veto counter	3	3	5	0.5	0.5	1
NM4DC3	Drift chamber	0.25	0.25	0.5	0.25	0.25	0.25
NM4HE3	Helium Bag	NA	NA	NA	NA	NA	NA
NM4SA4	Spectrometer veto counter	3	3	5	0.5	0.5	1
NM4DC4	Drift chamber	0.25	0.25	0.5	0.25	0.25	0.25
NM4TRD1-8	Wire chambers	1	1	5	0.5	0.5	5
NM4HODO	Trigger hodoscopes (H & V)	1	1	5	1	1	3
NM4CIA	Spectrometer veto - CsI anti	1	1	2	0.5	0.5	1
NM4CA	Collar-anti#	0.1	0.1	NA	0.1	0.1	NA
NM4EMCAL	CsI Calorimeter	1	1	5	1	1	1
NM4MU0	Cosmic ray calibration telescope	NA	NA	NA	NA	NA	NA
NM4PB	Lead wall%	5	5	5	NA	NA	NA
NM4MU1	Muon counter/hadron veto	1	1	5	1	1	3
NM4FE	Muon filter%	NA	NA	10	NA	NA	NA
NM4BTRD	Beam TRD	1	1	5	1	1	5
NM4BA	Back-anti, beam veto	2	2	5	1	1	3
NM4BD1	Neutral hadron dump/muon filter	NA	NA	10	NA	NA	NA
NM4MU2	Muon veto	1	1	5	1	1	3
NM4BD2	Neutral hadron dump/muon filter	NA	NA	10	NA	NA	NA
NM4MU3	Muon veto	1	1	5	1	1	3

* Measurement tolerances are for installation purposes only.
\# Tolerances will be achieved through precision machining not using a survey crew (see text)
% Beam hole edges must be measured to 2 mm for the Pbwall & 1 mm for the muon filter

Alignment tolerance requirements for KTeV detector components.

Two spectrometer issues are central to alignment considerations. The first is that of aligning the charged particle spectrometer. The chambers must be well aligned with respect to one another and to the magnet. This assures proper operation of the trigger and cross-calibration of the CsI Calorimeter. Second, the locations in Z of the CsI, downstream face of the regenerator, the Z-Calibrator and the charged particle spectrometer play a fundamental role in setting the absolute energy calibration of the CsI calorimeter.

Mask Anti (E832 only)

The Mask Anti defines the start of the decay region for the K_L beam. In E731[2], the acceptance was largely governed by several limiting apertures. Those defined by the Active Mask and the Collar Anti were the most sensitive. A 650 μm error in the measurement of the size of the mask would bias ε'/ε by -0.5 x 10^{-4}. The size and location was ultimately understood with an uncertainty of 70 μm ($|\Delta Re(\varepsilon'/\varepsilon)| = 0.02$ x 10^{-4}) using Ke3's in the off-line analysis. This was driven by the systematic uncertainty in track projection from the drift chambers.

The KTeV drift chambers are the same ones used in E731 with improved electronics and wires. The resolution will be equal to or better than before. Therefore, the final, most precise understanding of both the size and the transverse position of the Mask Anti will be done using Ke3's found in the data. The installation tolerance is 1 mm in X and Y.

The tolerance for the Z installation is 5 mm but should be known to 0.5 mm with respect to the regenerator. The z distance between the Mask Anti and the regenerator can be measured prior to installation. The current engineering specification is that the distance cannot change by more than 0.5 mm. If that method proves impractical, a fiducial must be brought out of the vacuum so that it can be measured using one of the methods for z-calibration proposed in Section 9.3.2. This will be decided after additional engineering input is obtained from the FNAL Mechanical Support Dept.

The edges of the beam hole in each lead plate must vary by less than 100 μm.[3] The measurement of the plate to plate variation after assembly will tentatively be done by

---

[2] L.K. Gibbons et al, **A Precise Measurement of the CP-Violation Parameter Re(ε'/ε) and Other Kaon Decay Parameters**, 1993, pp. 305-309.

[3] J. Jennings, **Mask Anti Conceptual Design**, KTeV Collab. Meeting, 1994

UCLA using a special measurement jig which has not yet been designed. However, should this proposal prove impractical, the measurement must be made by a survey crew. Similar measurements using standard alignment techniques done on RC7 resulted in an error of $\sigma \cong 250$ μm. Therefore another method may need to be developed in order to meet this specification.

Regenerator (E832 only)

The regenerator is an important element in E832. It is housed entirely under vacuum. It is essential that it covers one of the two beams entirely without encroaching onto the other beam. The regenerator must also change beams every spill. The installation and measurement tolerances are 1 mm in both horizontal and vertical.

The downstream face of the regenerator determines the start of the decay region for the K_S beam. It is also a calibration point for the determination of the absolute energy scale. The position of the downstream face of the regenerator must be known to 1 mm with respect to the front face of the CsI array. The regenerator must move so that the front face remains in a plane parallel to the CsI array and which is also perpendicular to the beam line.

The tolerances in z measurement of the CsI, Regenerator, and Z-Calibrator are important, as an error here contributes directly to the error in ε'/ε. A z error of 1 mm will contribute minimally to the total final error. Note that the ±4 °F temperature tolerance for the experimental hall leads to worst case changes in the distance between the regenerator and CsI due to floor expansion of about 3.2 mm, which is larger than the 1 mm tolerance. There is a proposal to monitor this distance using an EDM (Electronic Distance Meter). See Section 9.3.2.

In order to measure the position of the regenerator, there will be viewing ports in the regenerator vessel. It will be possible to measure the position of the front face of the regenerator as a function of its position using conventional survey techniques. The plane of the front face of the regenerator will be referenced along a line that can then be referenced to the CsI array.

Other methods are being considered for monitoring the position of the regenerator with respect to fiducials outside the regenerator tank.

Vacuum Vetoes

The alignment requirements of the Vacuum Vetoes are discussed in the Vacuum/Veto design report[4]. The vetoes must be installed to an accuracy of ±3 mm in X and Y (and rotation). They should be measured after installation to 0.5 mm. The Ring Counters are not in general defining apertures for $K \rightarrow 2\pi$ decays in E832, though they may be for some of the E799-II modes. The absolute z location of the regenerator and its associated vessel will be chosen, and the location of the vetoes will be fixed by construction of the vacuum vessels. The z locations should then be measured to 1 mm.

The ring veto counters have each been provided with tooling balls. The internal geometry of the counters will be referenced to the external tooling balls and then alignment will be relative to those tooling balls. RC7 has been measured in detail. The inside edges are defined and understood to 0.25 mm.

Z-Calibrator

The design of the Z-Calibrator is in progress. It flips up into the beam for special runs. There will be viewing windows for alignment access. The purpose is to provide a z reference point to confirm the understanding of the z scale in the neutral mode analysis. The horizontal and vertical position is not critical (to 10 mm) as it is larger than the area it is required to cover. It must however be installed very accurately perpendicular to the beam - to 0.5 mrad. The z location of the Z-Calibrator must then be determined relative to the front face of the CsI (and of course the regenerator) to 1 mm. Monitoring this position is discussed in Section 9.3

Spectrometer Magnet

In discussing the spectrometer magnet, it must be noted that assumptions regarding survey accuracy and a number of other considerations have gone into the design specification for the magnet. Assumed in the design of the magnet was that it would be possible to determine the relationship between a track and the field to 1.0 mm. This is the total error budget allowed in the process of locating the field measuring equipment relative to the magnet, and then locating the chambers relative to those same fiducials. Also

---

[4] D. Jensen et al, **Vacuum Veto Design Report**, 1993

included in the error budget are errors associated with the magnet measuring facility[5]. The contribution to this error budget from the survey location of chambers relative to the magnet is 0.25 mm.

The installation of the magnet is to conventional tolerances. It is required that the pole pieces be in a horizontal plane. The location of the magnet must then be surveyed so that its position relative to the chambers is known to 0.25 mm transversely and 0.25 mm in longitudinal position.

The magnet will be extensively fiducialized. Seats for laser tracker corner reflectors will be epoxied to four places on each of the coils, as well as to the sides of the yoke of the magnet. The temperature of the yoke will also be monitored in order to develop predictors for motion that might be detected.

Drift Chambers

Due to their excellent resolution and efficiency, the drift chambers are the cornerstone by which most of the positional and stability information of the experiment is understood. Ultimately, the drift chamber locations must be known to a fraction of the resolution, which is approximately 80 microns. Figure 9.1.2 shows the level of motion experienced in E731[6]. Apparent motion of the target is amplified because of the long lever arm from the first chamber to the target. A 1 mm shift in the target position corresponds to only a 0.12 mm shift in the first chamber.

Special muon calibration runs are used to determine Δx, Δy, and $\Delta \theta$ relative to one another. This method had a reproducibility of about 5 μm for offsets and ~10 μrad in roll in E731[7]. Two-track events were used to determine the corkscrew rotations. Once the relative positions are determined, the chambers can be treated as a rigid body and the locations of other elements in the spectrometer relative to the drift chamber magnet system can be determined using track reconstruction.

---

[5] D. Jensen et al, **Spectrometer Magnet Design Report**, 1993

[6] L.K. Gibbons et al, **A Precise Measurement of the CP-Violation Parameter Re(ϵ'/ϵ) and Other Kaon Decay Parameters**, 1993, p. 84.

[7] Ibid. pp. 74-76.

The location of the target relative to the drift chamber system will be determined using $\Lambda \rightarrow p\pi$ events. The high momentum protons reduce the multiple scattering contributions to the error in finding the target location. This gave a single event sensitivity of 3 mm in E731[8], so 50k-100k Λ decays should give us ample statistics to be in the 10 μm range. This is better than can be done with a survey crew.

While the alignment group cannot measure transverse and roll as well as can be done with the beam, there are certain quantities to which the chambers are insensitive. Z positions need to be measured as well as possible. In MCenter, this measurement suffered from systematic problems. The z-measurement tolerance is currently 0.25 mm. However, it should be noted that the floor could expand/contract as much as 1 mm over the 20 m span of the drift chamber system with a building tolerance of ±4° F. This needs further study. Pitch and yaw cannot be measured directly, so it is important that the chambers be initially aligned to within 0.2 mrad of perpendicular[9]. Non-orthogonalities in the drift chamber wires can cause difficulty in measuring rotations. This must be measured during fiducialization with a tolerance of 0.15 mrad.

Even though the transverse positions of the chambers will be determined with the beam, they should be aligned and measured to a tolerance of 0.25 mm with respect to the beam and spectrometer magnet. This will keep the level of corrections to a minimum and satisfy the geometry requirements of the trigger.

Laser Tracker sphere mounts (4) will be mounted to each chamber. Before installation, the locations of the sense wires will be determined relative to the corner reflector locations. There will be some redundancy in order to be able to fully align the chambers and readily resurvey them.

Hodoscopes

The hodoscopes are to be installed conventionally. The installation accuracy is 1 mm. The counters should be set horizontally or vertically to that same 1 mm over their full lengths. The z location is not critical. The final z location should be measured to 3 mm.

---

8 L.K. Gibbons et al, **A Precise Measurement of the CP-Violation Parameter Re(ε'/ε) and Other Kaon Decay Parameters**, 1993, p. 81.

9 S. Somalwar, Private communication, 1993

The final understanding of the positions of the hodoscopes will be determined from the data. The edges of the holes in the trigger hodoscopes must be known to 0.25 mm, but will be measured using tracks[10]. The locations of the holes should be located to ±1 mm so that there is no chance of beam scraping on the inner edge of the holes.

Spectrometer and CsI Antis (SA's, CIA)

The same criteria applied to the RC counters apply to the SA's. The installation tolerances are the same. Measurement of the locations of these veto counters is important as it is difficult to study the counters with reconstructed tracks. Since three of the drift chambers are currently planned to be mounted on the SA stands, their overall stability needs to be the same as the drift chambers. Their z positions should be known to 1mm.

There is still some discussion within KTeV as to how well the CIA needs to be known. It is believed to not be a limiting aperture in E832. In E731[11], mismeasurement of the size and location of outer apertures such as this contributed little to the error of ε'/ε because it is located on the outer edge where the illumination is low. The tightest number being considered for E832 is 100 μm (aperture with respect to the CsI array), which can be studied using reconstructed tracks.

It is important that the CIA be installed and measured accurately. It should be installed to 1 mm transversely and measured to at least 0.5 mm.

Cesium Iodide Array

Several measurements must be made on the CsI array. However, measuring the array with a survey crew will be difficult since it is located in a hermetically sealed house in tight quarters. The current plan is to measure as much as possible using other means such as large micrometer calipers. As the position resolution of reconstructed clusters will be 1 mm, the crystal locations must be known to a small fraction of a millimeter. A precision measurement at this level would require a line of sight from experimental hall network monuments to the laser tracker then to at least three fiducials on the array using the same setup. Accomplishing this would consume precious space in the blockhouse and

---

[10] G. Thomson, Private Communication

[11] L.K. Gibbons et al, **A Precise Measurement of the CP-Violation Parameter Re(ε'/ε) and Other Kaon Decay Parameters**, 1993, pp. 305-309.

require additional resources and time during installation when other solutions exist. The current solutions hinge on four major assumptions:

1. Precise knowledge of the transverse locations of the crystals, Collar Anti, and CIA locations can be determined by the data.

2. Stacking can be done without the aid of a survey crew.

3. The supporting plates for the array will remain rigid, with deflections less than 125 μm.

4. The Collar-Anti will be positioned through precision machining of its reference surfaces and the cans onto which it is placed.

The precise transverse location of the array will be determined using Ke3's found in the data[12]. E731[13] had enough statistics to determine mean positions to 10 μm and rotation to a systematic uncertainty of 50 μrad. A minimum of one Ke3 per block per spill will be written to tape during regular E832 data taking[14]. Special runs will be made periodically if this illumination is insufficient.

The position of the individual crystals must be measured relative to each other and to the reference plates at stacking time. The current plan is that KTeV will measure these without a survey crew by using special large calipers. This method has not yet been field tested to confirm its feasibility, but needs to be very soon. The design of the blockhouse extension would need to be modified to accommodate a survey crew.

The requirements for the alignment group have been reduced to two sets of measurements with looser tolerances than before; but they are still very important. The first is setting the stand in place and measuring the perpendicularity of the horizontal and vertical reference plates. The blockhouse walls will not have been installed at this point, hence allowing access room. The second set of measurements is determining the three

---

[12] R. Ray, **Survey Issues for the CsI Array**, 1994

[13] L.K. Gibbons et al, **A Precise Measurement of the CP-Violation Parameter Re(e'/e) and Other Kaon Decay Parameters**, 1993, pp. 80-81.

[14] E. Cheu, Private Communication, 1994

dimensional position of the array with respect to the rest of the spectrometer during the final alignment. Since precise measurement will be done with the data, the tolerance for this process has been loosened to 1 mm. This is driven by keeping any beam halo from hitting the pipe blocks. At the 1 mm level, a survey crew can align the calorimeter using conventional optical techniques. The fiducials on the array reference plates will be accessed through 4" portholes adjacent to each tooling ball. The portholes will remain plugged except during the actual reading which will take minutes to perform. This is not long enough to degrade the atmosphere inside the blockhouse due to the positive pressure[15].

Since the absolute energy scale is set by the distance from the downstream face of the regenerator and from the Z-calibrator to the front face of the CsI, this will be a crucial measurement. The tolerance for this distance has been set to 1 mm. The pitch, yaw, and flatness of the CsI array itself should be less than this so as to not dominate this error. The initial z measurement will be made with a survey crew. Another means must be developed to monitor this parameter. The data is very insensitive to it. The current proposal is to use an EDM (Electronic Distance Meter) to measure the location of extensions from the support under the CsI array. This will make it possible to monitor the Z and the yaw. See Section 9.3 for more details. Roll and pitch will be monitored with electronic levels accurate to about 50 μrad.

Collar Anti

The Collar-Anti (CA) is located inside the CsI blockhouse. As with the Mask Anti, it is a limiting aperture for E832. In E731[16], a mismeasurement in size of the CA had a noticeable effect (in terms of the E832 error budget) on the observed ratio of K_L/K_S in the neutral mode (-0.021% for a 70 μm error). Its position was not as sensitive, but the experiment was able to determine its size and location with a systematic uncertainty of 15 μm.

For KTeV, the CA must be aligned to 100 μm[17] in horizontal and vertical with respect to the precision holes with which the beams pass through the CsI calorimeter.

---

[15] R. Ray, Private Communication, 1994

[16] L.K. Gibbons et al, **A Precise Measurement of the CP-Violation Parameter Re(e'/e) and Other Kaon Decay Parameters**, 1993, pp. 305-309.

[17] T. Yamanaka, Private Communication, 1994

Ultimately, the size and position will be verified with data, but it is necessary to have an independent measurement given its importance. Due to space constraints, it will be difficult to align this device using standard survey techniques. However, since the Collar Anti will be mounted directly to the supports where the beam passes through the CsI, one can "capture" it through precision machining and the use of shims if necessary. It's small size allows for direct measurements with a micrometer. Since the temperature inside the CsI house is strictly controlled and the CA is so small, there will be negligible size changes as a result of temperature effects ($<3 \, \mu m/C°$).

Particle ID (TRD's, muon system, BA)

The first section of the particle ID part of the detector consists of the Transition Radiation Detectors (TRD's). They must be installed to a survey tolerance of 1 mm and measured to 0.5 mm transversely[18]. They will be resurveyed relative to the drift chambers using tracks. They must be installed perpendicular to the beam within 1 mrad.

The muon system consists of shielding and scintillation counters. The shielding is 6" oversize so transverse position is not critical, but it should be perpendicular so there is a z tolerance of 1 cm for each corner. However, the beam hole edges in the first muon filter (Pb Wall) should be measured to 1 mm (2 mm)[19]. The counters should be installed and measured to 1 mm transversely.

The back anti must be installed to 2 mm[20]. Its position is not critical as it is not used as a part of the detector. It is rather a veto that is larger than the neutral beam (as it must contain the showers).

The beam TRD is not used for position information, and hence only needs to be positioned within 1 mm.

---

18 Y.B. Hsiung, Private Communication, 1994
19 Ibid.
20 Ibid.

9.2   METHODOLOGY

This section addresses the procedures necessary for the installation and positional maintenance of the KTeV components to the specified tolerances. The Fermilab Survey-Alignment-Geodesy Group (SAG) has considered three needed categories:

A.   External survey control network.

B.   High accuracy internal survey control network.

C.   Maintenance of the internal network and monitoring of relative component positioning.

When measurement errors are specified by the SAG group, the errors refer to the 95% confidence level errors. In the analyses below, these errors were calculated in three dimensions and then projected onto the horizontal and vertical planes. The 95% errors quoted correspond to 2.4 standard deviations in two dimensions.

There are two methods that may be considered for establishing the KTeV coordinate system. The first method consists of extrapolating the proton beam line on through the KTeV neutral beam line and thence to the spectrometer. This is a point-azimuth technique. Using this method, a simple extrapolation through the KTeV system at, for example, laser tracker resolution suggests that the errors in transverse location would be of order one millimeter. This is unacceptably large. A more careful preanalysis by the SAG group suggests that the errors by this technique would in fact be several millimeters.

The other method, discussed below, is based on a rectangular grid of monuments outside the KTeV halls tied to the KTeV system through sight risers. A preanalysis based on this method shows that it is several times more accurate. The detailed analysis by the SAG group suggests that this system is capable of sustaining a grid with accuracy of order 0.2 mm for the basic reference system. This level of accuracy can probably be improved to 0.1 mm or better for relative surveys in the KTeV neutral beam system. This would provide an adequate reference system for KTeV. The final alignment accuracy of various elements of the neutral beam and spectrometer has a rigorous lower bound set by the references themselves!

9.2.1 External survey control network

The External Survey Control Network will consist of eight or more survey monuments. To ensure a strong geometric figure, these monuments will be placed as near to the project site as construction will allow. This network will be tied to the current DUSAF site coordinate system using both conventional and Global Positioning System (GPS) techniques, yielding positional accuracies of ±3 mm relative to that site system. Initially, this network will be used by the construction contractor for a layout reference system and for quality control checks of the layout work by the SAG Group.

Internal to itself, this network will achieve relative positional accuracies of ±0.2 mm. This network will also be used to transfer the current DUSAF site coordinate system into the internal control network. This transfer will necessitate a high precision survey of the exterior network at the time the transfer is made.

9.2.2 High Accuracy Internal Control Network.

The High Accuracy Internal Network will make it possible to establish relative component positioning to ± 0.1 mm. It will also be the basis for a dynamic monitoring system for relative position checks on components. To achieve this, the internal network must be an independent survey, using the transferred points for constraint purposes. It will of course be necessary to reestablish the reference system from time to time because of the motion of the building and internal monuments (see Section 9.2.4).

Good control (reference) points are required for a strong network. These are points which represent constraints on azimuth and coordinates. Section 9.2.3 addresses the optimization of the number and location of these points.

The configuration of the network is limited by the shape and the geometry of the enclosures and the experimental hall. This dictates that the KTeV internal network be a longitudinal network. The preanalyses conducted on the two basic survey framework systems is based on two chains of braced quadrilaterals: seven in the NM2 enclosure and nine in the experimental hall. A braced quadrilateral has diagonal measurements to the corners. This primary underground control network will consist of 36 monuments, the positions of which must satisfy a number of criteria:

* the points must be easily accessible
* the density of the points has to be great enough to cover the objects to be surveyed
* the network structure must be flexible enough for any future needs

To improve the isotropy of the network and compensate the weaknesses caused by the poor ratio between the length and width of braced quadrilaterals, additional diagonal measurements spanning adjacent quadrilaterals will be made. Redundant observations will be performed to ensure quality and uniformity of accuracy.

The points of this primary control network will be fixed and used as the basis of a denser secondary network for component alignment. This densification network will be developed using primarily the Laser Tracking Interferometer. These points will be placed strategically to minimize the number of observations necessary for component positioning, also allowing for eventual smoothing routines, while providing monuments close to the beam line for optical tooling setups if practical.

The underground reference control system is represented by monuments permanently imbedded in the enclosure floor and monuments rigidly attached to wall brackets. The actual monuments are represented by high-precision socket type holders to support spherical reflectors whose centers define the monument coordinates in all three dimensions.

All the coordinates of the underground network will be computed utilizing three dimensional rigorous least square adjustments. Error propagation analysis indicates that this network should determine absolute tunnel monument positions to better than ±0.2 mm [±0.4 mm] and relative component positions to generally better than ±0.1 mm [±0.2 mm] for the case of six [four] sight risers.

A horizontal sight pipe is necessary for direct visibilty in between enclosures. This considerably increases the relative accuracy between critical components in NM2 and NM3,4 such as the collimators. The absence of this in MCenter caused severe problems with measurements between enclosures.

9.2.3 Network Preanalysis

In order to develop a plan for the number of monuments and sight risers, and to understand quantitatively the tradeoffs of various options, a network simulation and preanalysis was performed. In fact, two independent analyses were performed, using somewhat different methods, but leading to the same general results. In these analyses, various numbers of reference points were modeled. The reference points are well defined by sight risers tied to outside monuments and their relative error is assumed to be zero. The KTeV coordinate system is then built starting with and constrained by these reference points.

The minimal set of reference points is two. As many as 6 reference points were assumed. For each case the error ellipses in longitudinal and transverse directions were determined. The error ellipses correspond to the 95% confidence levels for the accuracy of that network. Results of these analyses are presented in Figures 9.2.1 and 9.2.2. The major axis corresponds with the horizontal plane and minor axis with the longitudinal. As can be seen in Figure 9.2.2, the longitudinal error is already well behaved in the case of two sight risers. However, the transverse error in Figure 9.2.1 is unacceptably large with only two sight risers. The errors with a larger number of constrained points (sight risers) are much more in line with the KTeV requirements. It is apparent that 4 sight risers is the minimum number necessary for KTeV, i.e. at least two more are needed over what is specified in the current civil construction package.

In the vertical plane, gravity provides additional constraints just as sight risers do in the horizontal. Using spirit levels alone, relative elevations between any two points in a controlled environment can be determined within 0.25 mm at the 95% confidence level.

9.2.4 Maintenance of the internal network and monitoring of relative component positioning.

Maintenance of the internal network and monitoring of relative component positioning will be required since all the survey and alignment tasks analyzed pertain to a static situation. The positional accuracies of the internal network and the component positioning are only valid during the time it takes to complete the survey (See Section 9.3.2 discussion on stability). The standard way to reposition critical components is with a

KTeV underground network with additional sight rise (Horiz.) axis at 95 % confidence level.
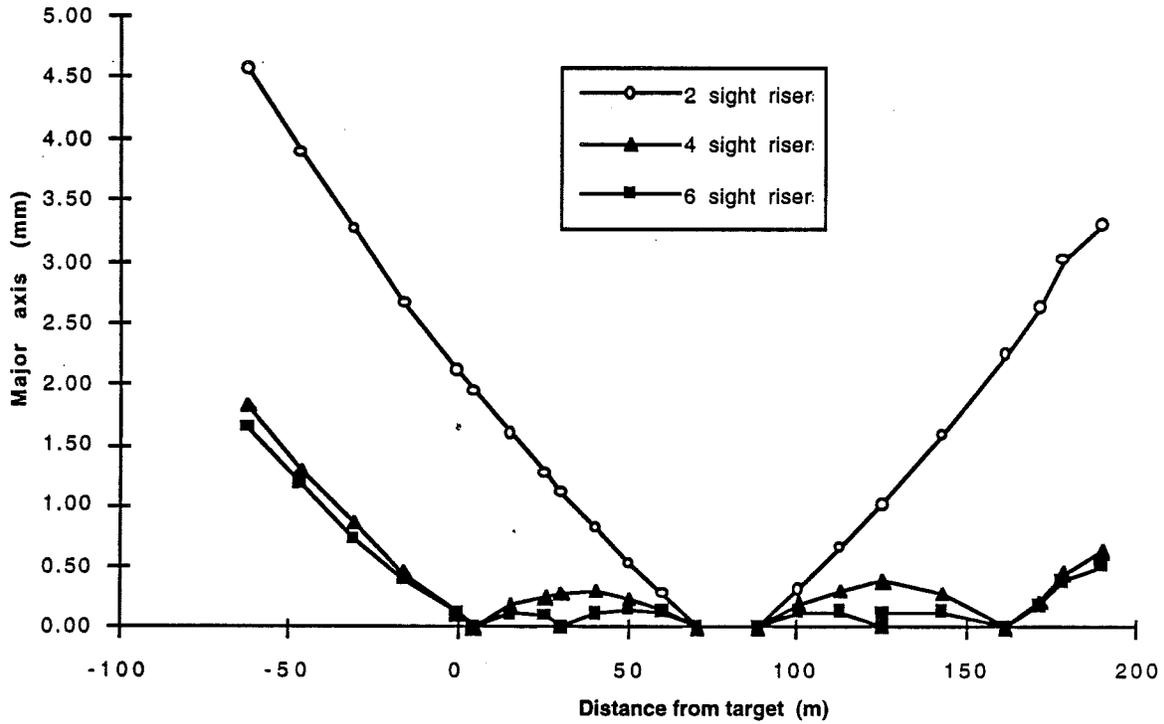
Figure 9.2.1 Results of pre-analysis showing the transverse error propagation at the 95% confidence level as a function of z for the current 2 sight riser configuration and for additional sight risers.

**KTeV underground network. Error ellipses: M
at 95 % confidence level.**
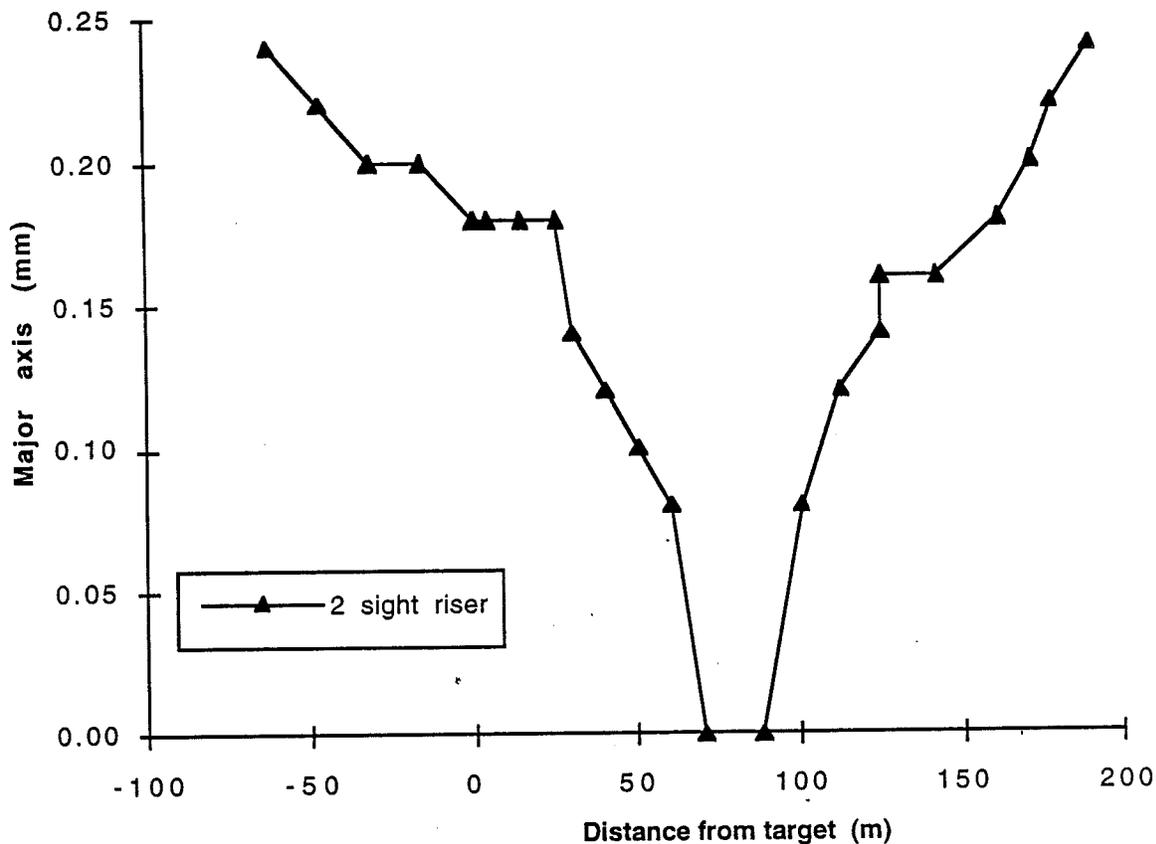
Figure 9.2.2 Results of pre-analysis showing longitudinal error propagation at the 95% confidence level as a function of z for the current 2 sight riser configuration.

survey crew. Depending on the circumstances, this may take from several hours to several days because the network will also need to be resurveyed. To monitor this movement, a dynamic monitoring system may be employed. The sophistication of this monitoring system depends on two factors:

1. The specified accuracies needed for relative positioning of critical elements.

2. The stability of the internal survey monuments established at or near the critical elements.

9.3   Implementation

Having established the alignment and survey methodology, an implementation procedure must be developed. There are four elements needed to implement the KTeV alignment plan:

1. Interface with the civil construction group to provide necessary specifications and assistance before and during facility construction.

2. Develop general and specific fiducialization and alignment procedures for beam and detector elements.

3. Give specifications for alignment hardware.

4. Provide for an on-line stability monitoring system which supplies information independently of beam and detector data.

9.3.1   KTeV civil construction issues

An array of monuments is installed in undisturbed soil in the area of the construction. These monuments will be used to monitor the civil construction. Many of them will be reused for the external network.

Figure 9.3.1 shows the design of the sight risers and underground monuments discussed in Sections 9.2 and 9.3.2 respectively. Figure 9.3.2 is a cross section drawing of the end of NM2 showing the location of the horizontal sight pipe used to bring survey control directly between enclosures.

After the KTeV civil construction is completed, the SAG group requires two weeks of sole occupancy of the experimental hall to establish the internal control network. The experimental hall needs to be free of obstructions at that time.
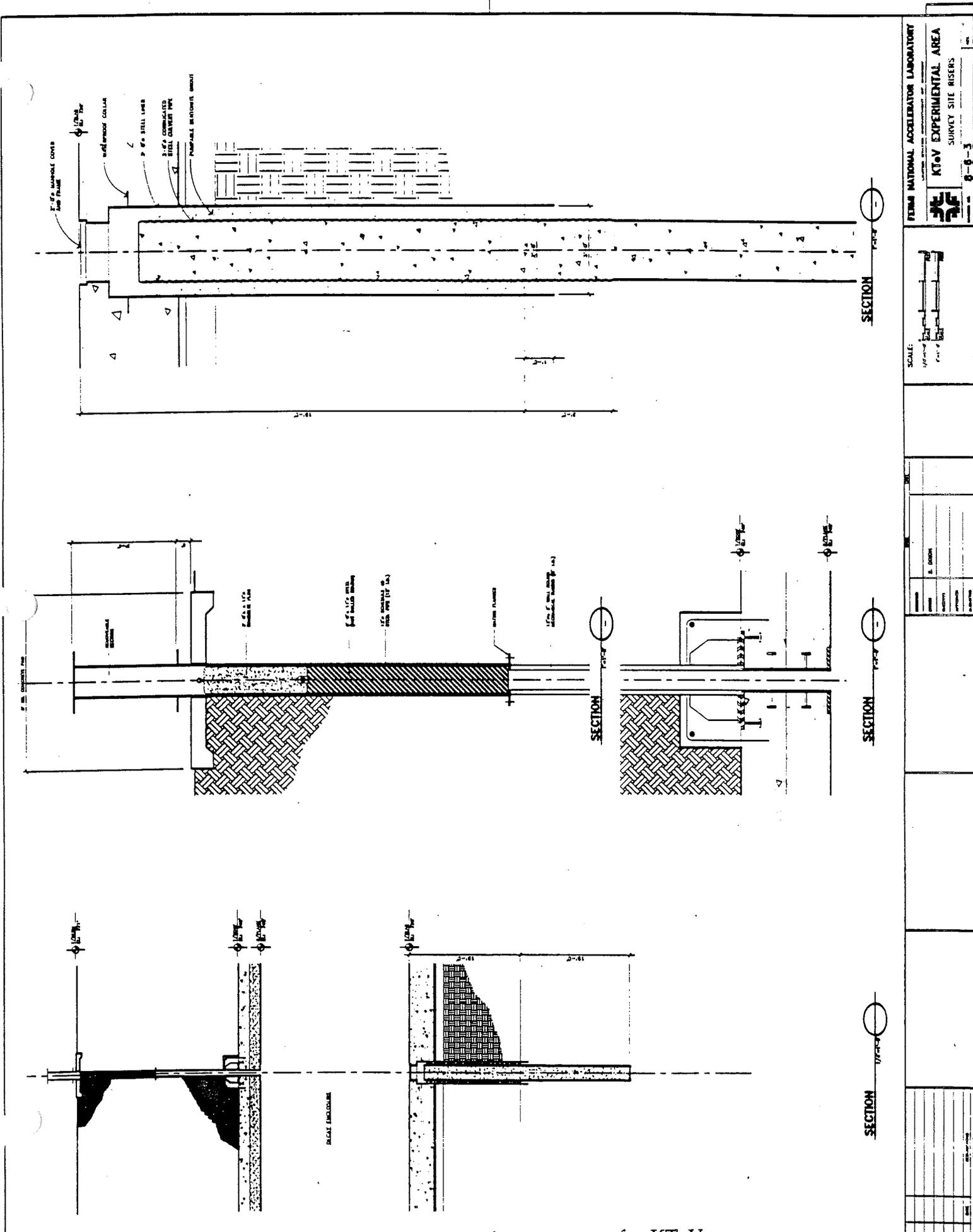
Figure 9.3.1 Design of sight risers and monuments for KTeV.

SECTION C

EXISTING NM2 ENC. NORTH END WALL - VIEW LOOKING SOUTH

SCALE: 1/2" = 1'-0"

Figure 9.3.2 Cross section drawing of the end of NM2 looking upstream showing the location of the horizontal sight pipe.

9.3.2   Stability

There are several factors which can upset the stability of internal floor monuments in an experimental hall in the 0.1 mm - 0.2 mm range. Among these are new construction, floor loading, temperature, weather, poor construction, etc. Measurements taken at other labs[21,22] provide evidence that these can be significant problems.

Data has been taken to study the stability of the existing NM2 enclosure. Over a period of 2 months, the dump area in NM2 is believed to have shifted vertically 0.5 mm in relationship to the rest of the enclosure. This number has an error bar of about ±50%. NM2 is an existing enclosure so it should not be suffering from the large settling effects often encountered in new construction. Since this is a short term study of only a couple months, it is not known whether this is a trend or an oscillation. However, it confirms that there is a need for stability monitoring of some kind.

Monitoring of relative horizontal motion in the NM2 hall has also been done using a set of optical instruments. This data is still being analyzed.

A soil contractor, STS, has attempted to predict the KTeV experimental hall settlement using a Monte Carlo called Settl/G[23]. Based on a series of soil borings, predictions have been made for initial (6 months) settling of the KTeV hall as well as long term (5 years). Figure 9.3.3 shows the location of the points which were calculated and Figure 9.3.4 shows the predicted settlement of those points at floor level and for two soil layers below floor level. The second soil layer ends at bedrock which is assumed stable. The numbers imply that settlement will be quite modest after initial installation and that soil layers closer to bedrock have less settlement. If these predictions are accurate, the rather large vertical motion detected in NM2 must not be due to settling. More data will be needed to make a complete assessment.

In order to try and provide better stability monitoring 2-4 permanent, isolated monuments are proposed. These monuments will provide a stable reference inside the new construction area. They would also aid by reducing the amount of time it takes to

---

21 Proceedings of the First International Workshop on Accelerator Alignment, pps, 4-24, SLAC, Stanford, 1990

22 Proceedings of the Third International Workshop on Accelerator Alignment, CERN, Geneva, 1993

23 STS Consultants, Geotechnical Evaluation of Proposed KTeV Project, Northbrook, IL, 1993
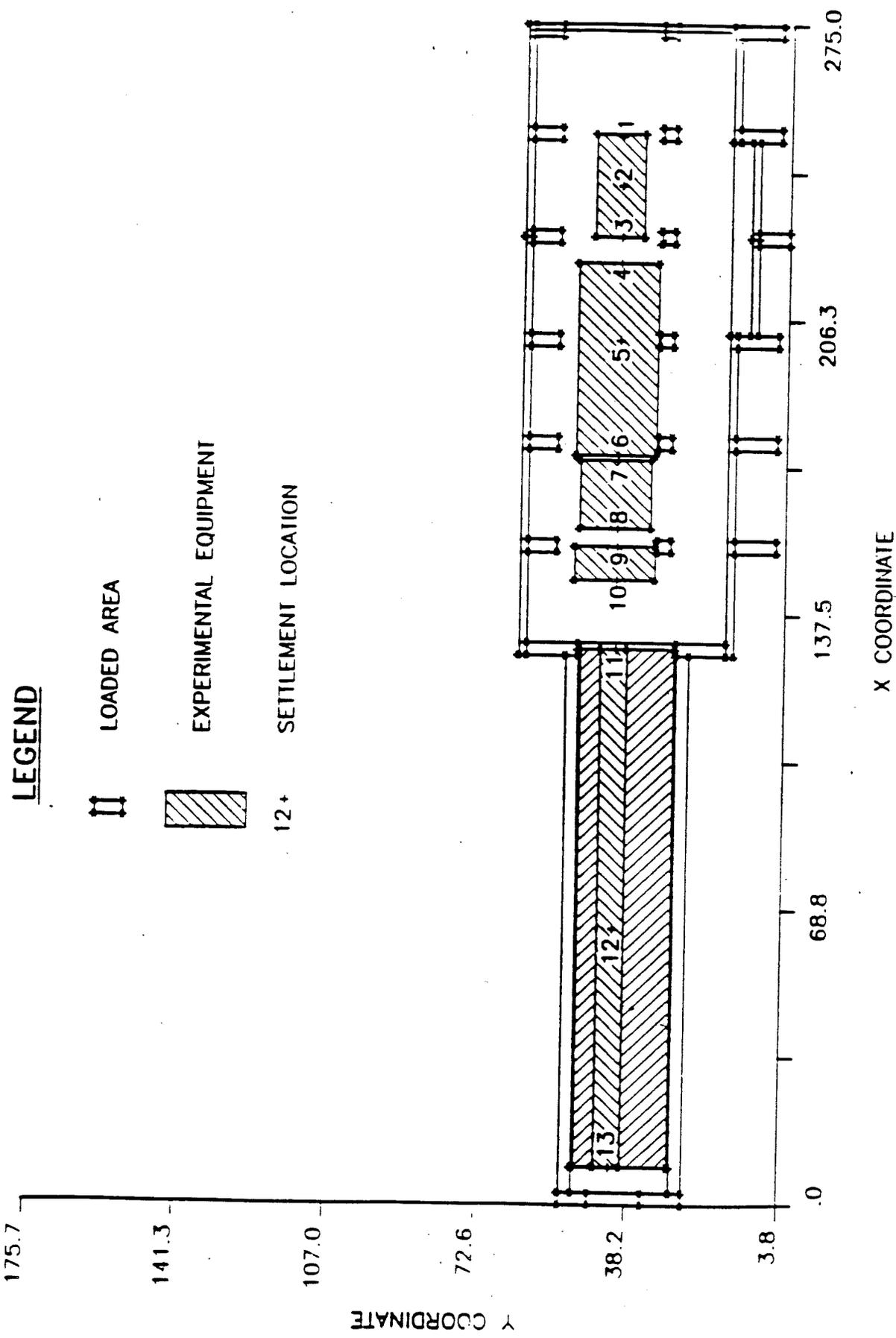
Figure 9.3.3 KTeV hall showing location of analysis points for STS Monte Carlo.

Table 1
KTEV - IMMEDIATE SETTLEMENT
(Initial 6 Month Period)

Settlement Location

Stratum Elevation (ft)	1	2	3	4	5	6	7	8	9	10	11	12	13
723.5-701.9	0.12	0.14	0.10	0.07	0.04	0.06	0.07	0.07	0.06	0.05	0.08	0.12	0.1
701.9-685.9	0.04	0.04	0.04	0.04	0.03	0.03	0.03	0.03	0.03	0.03	0.04	0.05	0.0
685.9-679.9	0.01	0.01	0.01	0.01	0.01	0.01	0.01	0.01	0.01	0.01	0.01	0.01	0.0
Total Settlement (inches)	0.17	0.19	0.15	0.12	0.08	0.10	0.11	0.11	0.10	0.09	0.13	0.18	0

Table 2
KTEV - LONG TERM SETTLEMENT*

Settlement Location

Stratum Elevation (ft)	1	2	3	4	5	6	7	8	9	10	11	12	13
723.5-701.9	0.02	0.03	0.02	0.01	0.01	0.01	0.01	0.01	0.01	0.01	0.02	0.02	0.
701.9-685.9	0.01	0.01	0.01	0.01	0.01	0.01	0.01	0.01	0.01	0.01	0.01	0.01	0
685.9-679.9	0.00	0.00	0.00	0.00	0.00	0.00	0.00	0.00	0.00	0.00	0.00	0.00	0
Total Settlement (inches)	0.03	0.04	0.03	0.02	0.02	0.02	0.02	0.02	0.02	0.02	0.03	0.03	0

*NOTE: If initial setup period is only 3 months. these long term settlement estimates should be doubled.

Figure 9.3.4 STS Monte Carlo prediction of short and long term settlement of the KTeV experimental hall floor and underlying layers of soil at 13 different points.

reestablish the internal network (See Section 9.2.4) inside the KTeV hall. The nearest existing stable monuments are located at TSB and PS3, which are too far away to be of use.

Figure 9.3.1 shows the design of the monuments. One such monument is initially included in the experimental hall construction package. These monuments are to be isolated from the slab and be deep enough to sharply reduce the effects of weather and building settlement. A deformable material such as bentonite will be used between the outside casing and the monument pillar to prevent motion due to lateral soil pressure. When considering the cost trade-offs of installing these monuments it is important to remember that the next generation of kaon experiments is expected to use the same facility and the alignment tolerances are predicted to be tighter than KTeV if ε'/ε is measured again.

Another source of possible instability is air gaps under concrete slabs. Good quality control must be maintained during construction to prevent this problem.

Monitoring

As previously discussed, motion due to floor instabilities could exceed tolerances specified for many components. This implies that any precision alignment could be obsolete soon after its completion. Since the most stringent alignment requirements are relative positions, an on-line monitoring system is being considered. Several systems are currently being employed at other labs. Many of them are turnkey commercial systems. These systems would provide information independent of beam data.

Target- collimator system

Substantive information has been obtained on two commercial systems so far. The first is Hydrostatic Leveling System[24] (HLS) system by Fogale-Nanotech of France. See Figure 9.3.5. This instrument would be used to monitor the elevations of the target collimator system and possibly some detector components. The HLS is a measuring instrument based on the principle of communicating vessels. The instruments would be connected along the KTeV beamline by a water filled tube which determines the reference plane and an air filled tube which guarantees pressure stability along the network. Each probe has a capacitive sensor which measures the water level. The system has a resolution

---

[24] **Proceedings of the Third International Workshop on Accelerator Alignment**, CERN, Geneva, 1993

of about 2 μm and a range of 2.5 mm. The non-linearity over the entire range is less than 1 μm.

CAPACITIVE SENSOR

COVER INTEGRATE WITH
CAPACITIVE SENSOR

4 SCREVS M4

CABLES FROM HEATER

HEATER SOURCE INTEGRATE
(0.1 TO 1 WATT) SUFFICIENT
FOR :1° TO 2°C

CABLE FROM CAPACITIVE SENSOR

Ra1.6

Ra1.6

VATERPROOF

MAXI LEVEL VATER

MINI LEVEL VATER

10°

Ø64

SHEETING FOR
ELECTRICAL
INSULATION

TEMPERATURE SENSOR

CABLE FROM
TEMPERATURE SENSOR

Ra1.6
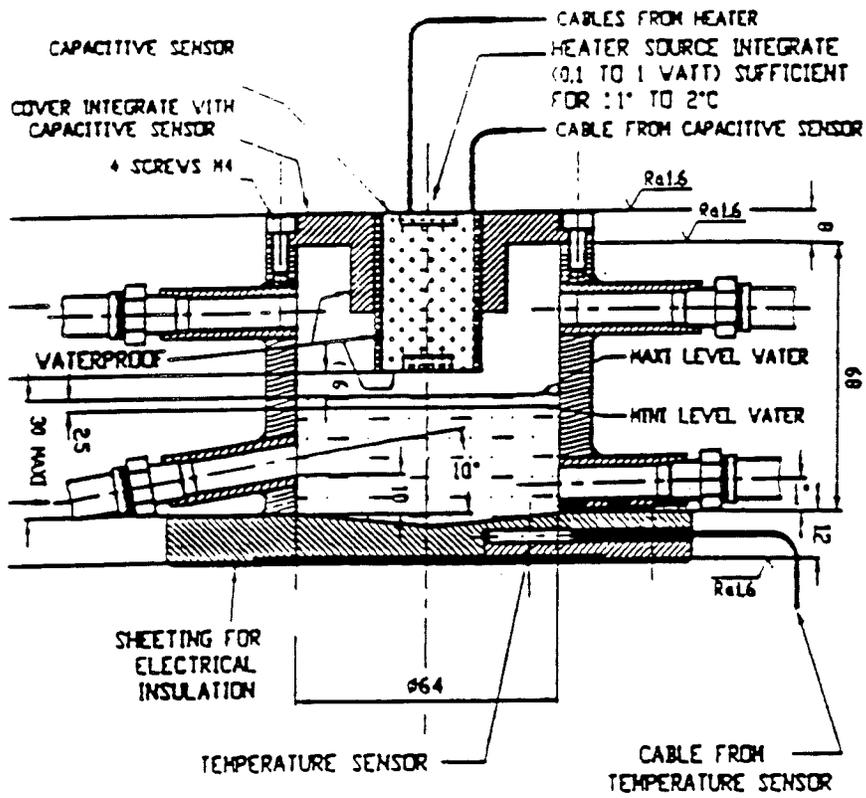
Figure 9.3.5 Cross-section of HLS vessel

The system has the advantages of being radiation hard (20 Mrad), more accuracy than required (could be used for next generation kaon experiment), is a commercially available turnkey system, and has been well tested by other labs. It is currently being used very successfully by ESRF and KEK. The ESRF (European Synchrotron Radiation Facility) system automatically realigns the entire ring with the machine on using servo-controlled jacks. The Argonne APS is currently procuring an HLS system so local access should be available soon. A disadvantage of this system is that it only measures vertical displacement.

It may also be necessary to measure horizontal displacement. There are some systems which are being employed at other labs, but more information needs to be obtained.

Z-calibration of the detector elements

One may estimate the floor expansion over the 60 m between the regenerator and the CsI assuming the floor changes temperature uniformly (this is unlikely). Such a calculation yields a projected motion of about 0.4 mm/°F or 3.2 mm over the specified 8°F temperature range in the experimental hall. Since the longitudinal distance between the regenerator, Z-calibrator, and CsI must be known to better than 1 mm, it is proposed that this distance be monitored.

There are inexpensive commercially available systems which meet this requirement. For example, the LEICA DI2002 EDM (Electronic Distance Meter) has an accuracy of ±0.6 mm and costs $11k. It has an RS232 interface which will allow computer readout and control. The SAG group has a LEICA/KERN ME5000 Mekometer which is accurate to 0.2 mm ±0.2 ppm which can be used for calibration. There are other systems available which also meet the specifications.

These systems require an unobstructed line of sight between the elements being measured. According to existing drawings, there are no components which come closer than 3" from the floor to the bottom of the support underneath the beam. According to the manufacturer, this is sufficient clearance to obtain an accurate reading. Field tests will be performed soon. Future detector support designs must not intrude into this 3" space. The regenerator and z-calibrator are in a vacuum tank and the CsI is in a hermetically sealed house. The current proposal involves bringing reference arms outside of the CsI house and

vacuum tanks and sighting underneath the spectrometer onto retro-reflectors attached to these arms.

9.3.3   General Alignment & Fiducialization Procedures

Following is a procedure to have a beam or detector element properly fiducialized and aligned. The contact persons are the KTeV alignment coordinators.

1. Each KTeV system manager will provide specific alignment tolerances and specifications.

2. The system manager must then submit engineering drawings which show fiducial points and alignment adjustments for review and comments. This will be an iterative process. For critical tolerance elements, alignment people should be involved from the beginning design phase.

3. Once a plan is in place, any hardware (such as sphere mounts or tooling balls) necessary for the fabrication process will be distributed by the alignment group.

4. The system manager should provide a tentative schedule indicating when the beamline element or detector will be ready to be fiducialized, installed, and aligned.

5. When arrival of the detector or beam element is imminent, The KTeV installation coordinator will then schedule a time and place for the above with the alignment group.

6. Results of each survey and alignment will be provided to the appropriate subsystem managers.

Component Fiducialization

Fiducialization of the components relates their effective beam centerlines to external mechanical points that are accessible to subsequent survey measurements. It is expected that every KTeV beam and detector component will need to be fiducialized. If some elements are being reused and have already been fiducialized once, it is assumed that they

248

will be refiducialized to conform to a system compatible with the laser tracking interferometer. The laser tracker will provide greater accuracy and also reduce the time necessary for component alignment.

Fiducialization plans for each component need to be completed during the engineering phase, prior to fabrication.

At present, we assume that each component will be fiducialized by Fermilab. This will assure that the fiducialization is compatible with the laser tracker platform and conforms with the overall alignment plan. If there is a proposal to independently fiducialize a beam or detector element, the methodology must be reviewed by the Fermilab SAG group.

Since the KTeV beamline and experiment consists of many different types of hardware, a specific fiducialization procedure is currently being developed for each element or class of elements. This will be included in the comprehensive alignment plan which will be presented as a stand alone document. The following are general criteria which must be considered during fiducialization

> During fiducialization, the critical parameters must be available in six degrees of freedom to the survey crew. For example, it may be necessary to remove drift chamber windows in order to see the wires or else provide an acceptable mark on the frame which is related to the wires in a very precise way.

> All components should be fiducialized so that at least three known mechanical points are visible from one setup which will be located near the alignment and personnel aisle ways provided in all KTeV enclosures. These points must either consist of a permanently fixed sphere mount which will hold a 1.5" retro-reflector for the laser tracker or a hole/guide which will accommodate a sphere mount in a reproducible way. Elements with critical tolerances should have their own permanent spherical mounts. See Section 9.3.4 for specifications and drawing of sphere mounts.

> The fiducial hardware should be attached to a rigid structure so that the offsets do not change measurably under stresses such as transport or

249

temperature change. The points should also be located as far apart from each other as possible.

Component Alignment

As discussed earlier, detailed alignment plans will be developed for each class of components. This will be included in the upcoming KTeV Alignment Plan document. Many considerations are already listed in Section 9.1.

9.3.4 Alignment Hardware Specifications

The geodetic measurements in the surface network are performed with state-of- the-art equipment already being used by the SAG group. These include: high-precision electronic distance measurement with the Kern Mekometer ME5000, angle measurement with Kern E2 theodolites, Wild N3 and Leica N3000 levels, and Trimble 4000SSE Geodetic Survey GPS dual frequency receivers.

Laser Tracking Interferometer

Until recently, the determination of precise three dimensional coordinates in industrial metrology has required two separate instruments or two setups. As instrumentation for the KTeV alignment, we propose to employ the Laser Tracking Interferometer system (the same as intended for the Main Injector). With this system all KTeV devices will be positioned using an interactive and iterative procedure from the layout of coordinates for the magnet support systems to the final smoothing of adjacent components. The automation of measurements and alignment procedures significantly improves their quality and speed compared to that of traditional methods. The SAG group now possesses this hardware. Preliminary tests indicate that the instrument performance is as expected.

The Laser Tracking Interferometer (See Figure 9.3.6) is a dynamic measuring system for three dimensional coordinate determination using a single beam laser interferometer, precise angular encoders, and a servo-tracking system. Simultaneous readings, 1000 times per second, of horizontal/vertical encoders and interferometer counts are calculated and the three dimensional position of the reflector target is displayed in real time. These coordinates are continuously compared with the theoretical coordinates and the resultant difference coordinate vector is displayed also in real time. For 30 microns interferometer accuracy and 1 arc second angular resolution, the Laser Tracker is estimated to provide
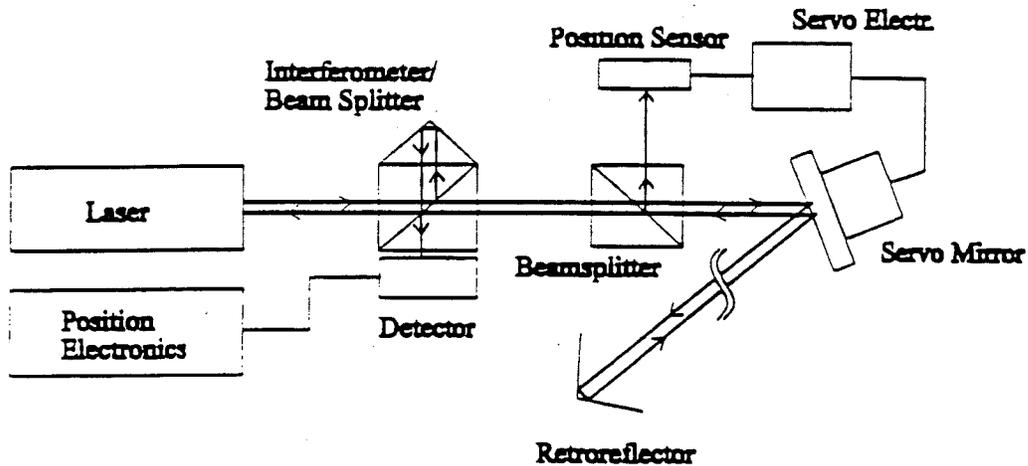
Schematic of servo-controlled tracking system

SYSTEM SPECIFICATIONS

CMS-3000 Tracker Head:

Width:	12.5"
Height:	23.0"
Depth:	7.5" min, 9.2" max
Weight:	80.0 lbs

Remote Power Unit (RPU) :

Width:	9.5"
Height:	12.0"
Depth:	17.0"
Weight:	25 lbs

Typical Tooling Stand:	Weight: 204 lbs
Assembly Floor Load:	Average = 37.5 bs/sq. ft
Repeatability:	At least 5 ppm o: measurement
Resolution:	Angular = 1 arc-second per angular unit
	Radial = from 0.5 to 5 microns per distance unit
Velocity:	From 1 to 6 meters/sec.
Acceleration:	> 2 g's
Distance Range:	0.17 meters (min.) to 30 meters (max.)
Elevation Range:	± 55 degrees
Azimuth Range:	>270 degrees

Figure 9.3.6 Schematic of Chesapeake Laser Tracking Interferometer

measurements to the component fiducials within 0.1 mm range. This automatic transmission and handling of measurements and alignment parameters largely excludes the usual risk of operational errors during routine work.

The Laser Tracker comes with a PC compatible computer system for computation, control, and data logging.

Sphere Mounts

Sphere mounts are magnetic sockets designed to hold the retro-reflector for the Laser Tracker. They can also accommodate more conventional instruments. These will be mounted on most of the detector and beam elements for referencing. They come in several varieties, samples of which are shown in Figure 9.3.7. The 2.25" heavy-duty sphere mount is the most economical ($57) and will probably suffice for most applications. It is machined to slightly lower centering tolerances than the standard 1.5" mount ($135) but the reproducibility is more important than the centering tolerance.

10/32 TAPPED HOLES
ON BACK SIDE
(2 PLACES)

(3) POINT NEST FOR
LOCATING SPHERICALLY
MOUNTED RETRO
REFLECTOR
STEEL, BLACK OXIDE
FINISH

CLEARANCE HOLE
FOR 10/32 SCREW

1.5000 DIAMETER
SMR REFERENCE

1.25 REFERENCE

2-1/4" ALUMINUM OUTSIDE
HOUSING

MAGNET

1.5 SPHERE MOUNT

(3) POINT NEST ON C/L OF "A"
DIAMETER WITHIN .0005

1.5000 DIAMETER
SMR REFERENCE

$1.000^{\pm.0005}$ TO
CENTERLINE
OF 1.500 SPHERE

MAGNET

"A" DIA.

+.0000
- .0005

Figure 9.3.7 Schematic of sphere mounts designed to hold corner reflectors for the

Section 10
Budget and Schedule

Presented in this section are the Budget and Schedule for the KTeV Beams Systems.

10.1   Budget

The budget in Table 10.1.1 provides costs for the following WBS Level 2 systems.

- · WBS 2.2   Primary Beam System
- · WBS 2.3   Beam Dump System
- · WBS 2.4   Secondary Beam System
- · WBS 2.8   Alignment System.

Costs for each system are broken down into Levels 3 and 4 in the following manner. Reading down, costs are listed in three columns identified as "Total Cost", "Existing", and "New". "New" identifies costs which we expect to incur during the 1994 and 1995 fiscal years. "Existing" accounts for existing plant costs and is not a new cost to be incurred. On any row these two costs, "Existing and "New" are summed under "Total Cost".

Totals for each of the columns marked "Total Cost", "Existing", and "New" are summed "above" on the preceding WBS Level row. So Level 4 costs for any column are summed above on the Level 3 row; Level 3 costs are summed above on the Level 2 row and the Level 2 costs are summed at the beginning of the document on the row identified as "BEAM SYSTEM TOTALS".

The date "Jan-94" heading the "New" column identifies the date from which costs are considered "New".

10.2 Schedule

The schedule is presented in Figure 10.2.1.

Items in the column "Name" are grouped roughly according to WBS Levels 2 and 3. The overall order roughly has items of the Primary beam System preceding items of the Beam Dump System which precede items of the Secondary Beam System. Each equivelent Level 3 item is then broken down into the constituent tasks required for completion.

Table 10.1.1

WBS	Item or System	Total Cost $k	Existing $k	Jan-94 New $k	Comments
	BEAM SYSTEMS TOTALS	3,436	2,032	1,405	Includes Secondary Beam Total and Alignment Total
2.2	Primary Beam Totals	1,109	892	217	
2.2.1	Pre-Target Area	834	834	0	
2.2.1.1	B2 Magnets	250	250		
2.2.1.2	Trims	24	24		
2.2.1.3	4Q120	280	280		
2.2.1.4	PS	280	280		
2.2.2	Instrumentation	100.4	58	42.4	
2.2.2.1	Micro SWIC	20	0	20	
2.2.2.2	Other SWIC's	12	12		
2.2.2.3	SWIC Scanners	33	33		
2.2.2.4	BPMs (including Electronics)	22.4		22.4	
2.2.2.5	SEM	13	13		

Table 1.1

WBS	Item or System	Total Cost	Jan-94 Existing	Jan-94 New	Comments
2.2	Primary Beam - Continued				
2.2.3	Installation	143	0	143	
2.2.3.1	Remove existing elements			20	Upstream & Downstream NM2 Hall Extensions
2.2.3.2	Electrical - Hard Bus			14	Purchase
2.2.3.3	Electrical Installation			84	Magnets and Power Supplies
2.2.3.4	Mechanical Installation			25	Magnets, Stands, LCW & Vacuum
2.2.4	Interlocks	31.9	0	31.9	Includes Primary, Secondary and Hall

Table 10.1.1

WBS	Item or System	Total Cost	Existing	Jan-94 New	Comments
2.3	**Beam Dump System Totals**	1,795	998	797	
2.3.1	Target Pile Magnet - NM2S1	181.1	160	21.1	
2.3.1.1	Magnet & Modify	113.6	100	13.6	
2.3.1.2	PS,Controls, Magnet Interlocks	61	60	1	
2.3.1.3	DC Cable & Install	2		2	
2.3.1.4	AC Cable & Install	2.5		2.5	
2.3.1.5	Rigging, Magnet & PS	2		2	
2.3.2	Dump	42.6	0	42.6	
2.3.2.1	Material & Fabrication	41.6		41.6	
2.3.2.2	Rigging	1		1	

Tab 2.1.1

WBS	Item or System	Total Cost	Existing	Jan-94 New	Comments
2.3	Beam Dump System - Continued				
2.3.3	E8/Hyperon Magnet - NM2S2	739.3	660	79.3	
2.3.3.1	Magnet (273 T)	600	600		
2.3.3.2	Fabricate and Install Insert	19		19	
2.3.3.3	PS,Controls, Magnet Interlocks	61	60	1	
2.3.3.4	DC Cables	4		4	
2.3.3.5	AC Cables	2.5		2.5	
2.3.3.6	Fabricate Support System	19.9		19.9	
2.3.3.7	Clean Up & Install Magnet	31.9		31.9	
2.3.3.8	Rigging , PS	1		1	
2.3.4	Target Pile Shielding	400	0	400	
		0			
2.3.4.2	Remove MC	170		170	
2.3.4.3	Remove Existing NM2 Target Pile	95		95	
2.3.4.4	Build New KTeV Target Pile	135		135	

Table 10.1.1

WBS	Item or System	Total Cost	Existing	Jan-94 New	Comments
2.3	**Beam Dump System - Continued**				
2.3.5	Mu-Sweep II - NM2S3	370.3	117.6	252.7	
2.3.5.1	Coil material	20		20	
2.3.5.2	Coil fabrication	115		115	
2.3.5.3	Steel	73.6	57.6	16	
2.3.5.4	Fabricate	24		24	
2.3.5.5	Support	21.5		21.5	
2.3.5.6	Rigging	51.2		51.2	
2.3.5.7	DC cabling	4		4	
2.3.5.8	AC Cabling	0			
2.3.5.9	PS,Controls, Magnet Interlocks	60	60		
2.3.5.10	Rigging, PS	1		1	
2.3.6	RAW	61.5	60	1.5	
2.3.6.1	Move & Re-connect	61.5	60	1.5	

Tabl .1.1

WBS	Item or System	Total Cost	Existing	Jan-94 New	Comments
2.4	**Secondary Beam Totals**	**407.1**	**142**	**265.1**	
2.4.1	Target and Absorbers	22	0	22	
2.4.1.1	Targets and Target Holder	5		5	
2.4.1.2	Target Drive Mechanism	10		10	
2.4.1.3	Absorber Materials	2		2	
2.4.1.4	Absorber Trays and Movers	5		5	
2.4.2	Primary Collimator	25.1	0	25.1	
2.4.2.1	New Steel Shield	12		12	
2.4.2.2	New Inner Block	2.4		2.4	
2.4.2.3	Assembly Labor	2.5		2.5	
2.4.2.4	Alignment Flippers	6.2		6.2	
2.4.2.5	Installation	2		2	
2.4.3	Slab Collimator	20	0	20	
2.4.3.1	Bellows	1		1	
2.4.3.2	Pipe and Slab Support	5		5	
2.4.3.3	Stands	2		2	
2.4.3.4	Jacks, Motors, Subframe	10		10	
2.4.3.5	Installation	2		2	

Table 10.1.1

WBS	Item or System	Total Cost	Jan-94 Existing	Jan-94 New	Comments
2.4	**Secondary Beam System - Continued**				
2.4.4	Defining Collimator	91	0	91	
2.4.4.1	Bellows	1		1	
2.4.4.2	Inserts (3)	21		21	
2.4.4.3	Vacuum Jacket	3		3	
2.4.4.4	Inner Iron Shielding	8		8	
2.4.4.5	Support x and y Motion	15.5		15.5	
2.4.4.6	Outer Shielding Support	26		26	
2.4.4.7	Alignment Flippers	10		10	
2.4.4.8	Installation	2		2	
2.4.4.9	Shield after Defining Material	3.5		3.5	
2.4.4.10	Installation of Shield	1		1	
2.4.5	Beam Profile Monitor	30	0	30	
2.4.5.1	W Convertor(s)	2		2	
2.4.5.2	in/out Motion	5		5	
2.4.5.3	Fixed Scintillators (12)	6		6	
2.4.5.4	Scanning Scintillators (14)	2		2	
2.4.5.5	Scanning Mover	15		15	

WBS	Item or System	Total Cost	Jan-94 Existing	Jan-94 New	Comments
2.4	Secondary Beam System - Continued				
2.4.6	Standard Existing Elements	219	142	77	
2.4.6.1	Rotator Magnet	81	57	24	
2.4.6.2	Beam Stop	39	35	4	
2.4.6.3	Jaw Collimator	27	20	7	
2.4.6.4	Final Sweeper	57	30	27	
2.4.6.5	Vacuum System	15		15	
2.8	Alignment	125	0	125	
2.8.1	Alignment Components	20		20	
2.8.2	Charged Labor	50		50	
2.8.3	Monitoring Systems	75		75	

FIGURE 10.2.1
4/8/94

FIGURE 10.2.1
4/8/94

FIGURE 10.2.1
4/8/94

Name	11/93		12/93		1/94		2/94		3/94		4/94		5/94		6/94		7/94		8/94		9/94		10/94		11/94		12/94		1/95		2/95		3/95		4/95		5/95		
	1	15	29	13	27	10	24	7	21	7	21	4	18	2	16	30	13	27	11	25	8	22	5	19	3	17	31	14	28	12	26	9	23	6	20	6	20	3	17	1	15	29
NM3S - REFURBISH											NM3S - REFURBISH																															
NM3S - INSTALL																																	NM3S - INSTALL									
NM2 INTERLOCK WORK COMPLETE																																			NM2 INTERLOCK WORK COMPLETE							
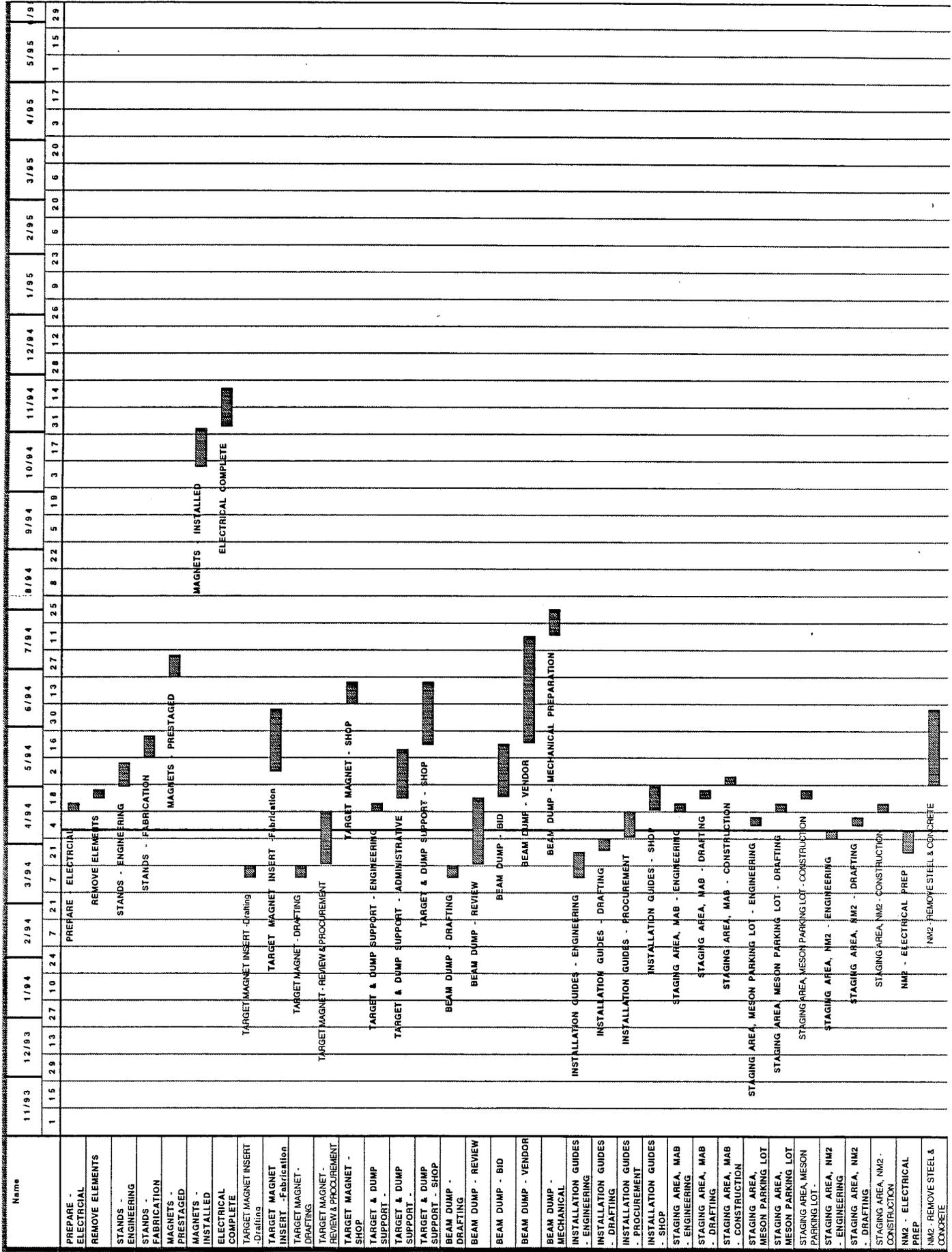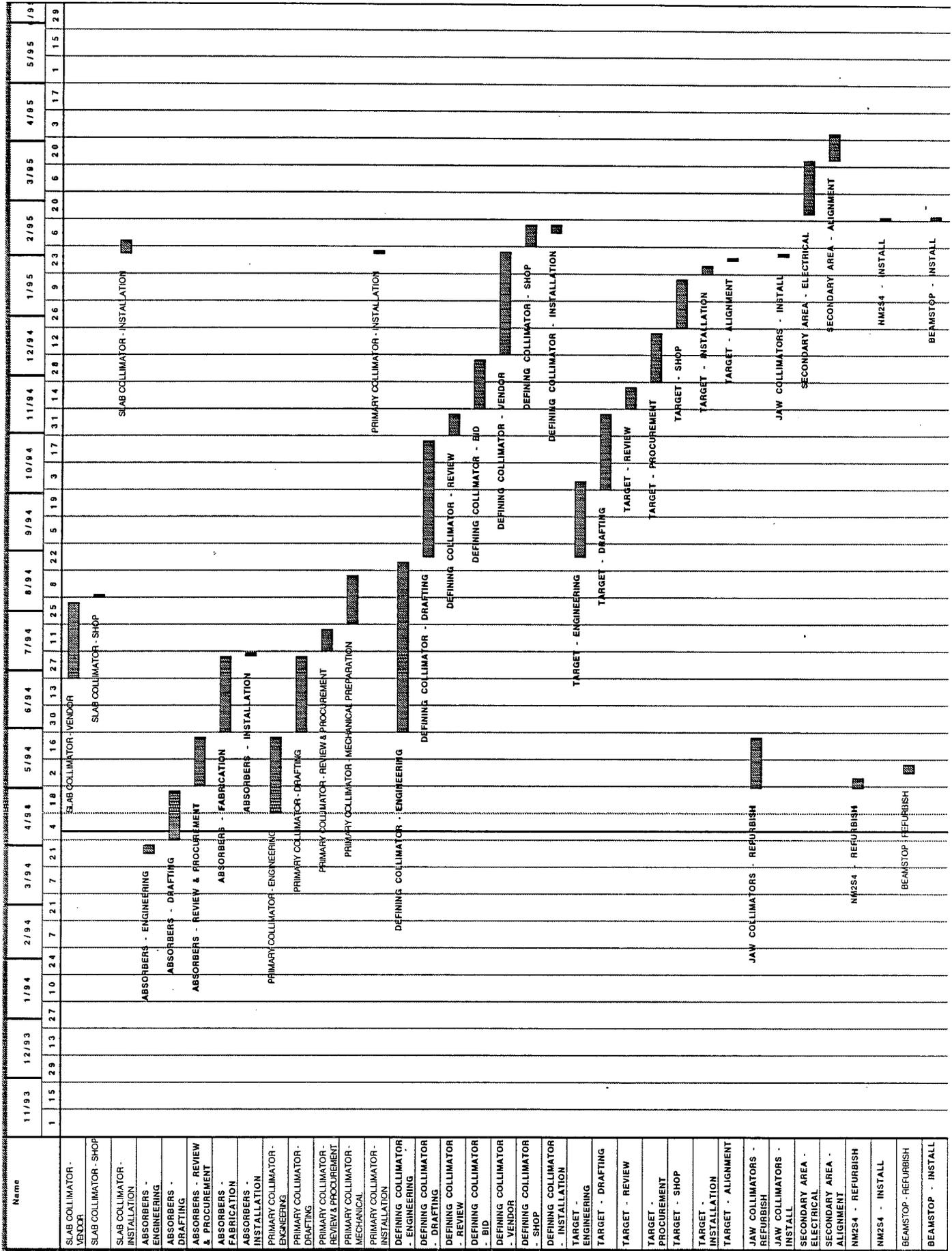
FIGURE 10.2.1
4/8/94

11. UNRESOLVED ISSUES / CONTINUING EFFORTS

Presented in this Section is a summary of issues and ongoing efforts which are as yet not fully specified in this KTeV Beam Systems Design Report. Some are in a queue status awaiting manpower (efforts), while a few need additional direction or inputs prior to the next steps (issues). This distinction is made in the presentation below. The listing is ordered by Design Report sections.

OVERVIEW OF KTEV BEAM SPECIFICATIONS

Specifications for stability requirements are in large measure determined, based on the KTeV physics goals. There will however remain the possibility of parameter tradeoffs due to better understanding of resource and technical issues as the construction of beam and detector systems continues.

PRIMARY BEAM

Significant continuing efforts are needed on several fronts:

i)   Development of software for beam motion and beam roll control. Control of beam instabilities or motion over a few or more spills is planned to be done using the RD EPICURE control system. This effort is to be done by the RD/Op. Beams Group. Compensation for beam roll during the spill can be done using existing detector and controls hardware with the AD ACNET system. This software development is an effort which will need to be done using this system.

ii)   ACNET - EPICURE communication link. Technical requirements for this were resolved during the previous Fixed Target run. Needed now are agreement between RD - AD staff of details for information which will pass between control systems, and putting this in place. Due to a difference in operational mode from previous running, this remains at some level an issue and requires continuing effort.

iii)   Improved understanding of detector muon rates due to halo associated with the primary beam transport. The current calculations need to be

268

benchmarked. We have partial indicators (only very qualitative so far) that the calculated muon rates from halo could be too high. If so, this makes this an easier issue re. beam cleanliness. Better understanding is needed. This work is to be done by the RD/Ops. Beams Group.

iv) New beam instrumentation. Development of a 100 micron wire spacing SEM is in progress by the AD/EE. Dept. A detailed schedule for this development, testing, and construction effort needs to be understood.

v) More beam instrumentation. Several BPM's of the AD/Switchyard design need to be built. This will be done either by the RD/EE. Dept., or subcontracted to the AD/MAD Dept. This needs to be understood, along with a detailed schedule.

vi) Final element design placement along with FRD identification, including spares. A continuing effort to get final element identification (from existing inventory), and final beam sheet which incorporates complete information re. magnet spacing due to flange lengths,etc.

CRITICAL DEVICES / INTERLOCKS

i) Acquiring the capability for as needed experimental hall access is an extremely important unresolved issue. This needs approval at higher than Division level prior to development of a detailed solution. The solution will require a significant effort by the Accelerator Division.

BEAM DUMP / MUON SWEEPING

i) Target pile shielding plan. The issue here is ensuring the capability to complete the target pile construction within fixed budget allocations. The steel projected to build the pile is to come from the existing NM2 and MCenter target piles. This is complicated by uncertainties in knowledge of some details of the existing MCenter target pile. Suitability of steel for use is determined both from geometry and residual radiation levels. Backup options for additional appropriately sized steel are being actively pursued.

SECONDARY BEAM

i)   Primary target engineering. This awaits RD/MSD engineering support.

ii)   Beam collimator alignment system. Details of function and design are currently being developed. Has a significant impact on collimator design also.

iii)   Primary and defining collimator. Once alignment system is fully specified, will be in queue for MSD engineering support.

iv)   Beam profile / alignment detector. Details of function and design are currently being developed.

ALIGNMENT AND STABILITY

i)   Final numbers for building sight risers and monuments. This is a balancing between available construction funds and alignment requirements. This will be determined using the alignment capability projections presented in this report.

ii)   A continuing effort for the comprehensive detector alignment plan.

iii)   Stability monitoring system. The final details of this system will be determined as better information is obtained re. resource requirements and projected building motions. This is not a critical path item for other project efforts.

Efforts above needing additional people resources are controlled by three competing factors:

a)   MSD engineering support. MSD currently allocates a considerable fraction of their staff for KTeV efforts. Here, internal KTeV priority ordering for these efforts by the available staff slows some beam system efforts. However, this is closely monitored for maintaining critical path efforts.

b)   RD/ Ops. Beams group support. Very considerable support from this group has been provided to reach current status. Division priorities for other efforts by this group will control the queue for some remaining tasks, especially for primary beam. Again, this is believed to be viable for schedule needs.

c)   AD beam system support. This is the most critical path not yet underway. Progress here is not realistically expected until this Division's efforts for the current collider run have achieved needed luminosities. This also controls the next Fixed Target run schedule. What is needed at this time is a commitment for the efforts needed, including particularly an effective solution for experimental hall access.

APPENDIX 2

KTEV PRIMARY BEAM SHEET

NM TRANSPORT   1-APR-94
0   1000 GEV

Z CENT.	X CENT	Y CENT.	POSITION CODE	ELEMENT CODE	POWER SUPPLY	B(KG) OR (KG/IN)
3184.00	-26.21	732.90	NMMUPT			
3185.74	-26.27	732.89	NM1BPM1			
3187.24	-26.31	732.89	NM1BPM2			
3188.49	-26.35	732.89	NM1WC			
3193.99	-26.51	732.88	NM1V-1	FRD11679 5-1.5-120 V-BEND	NM1U	18.688
3204.99	-26.84	732.87	NM1V-2	FRD11414 5-1.5-120 V-BEND	NM1U	18.688
3211.23	-27.02	732.87	NM1H	FRD11489 4-4-30 H-TRIM	NM1H	0.000
3620.01	-39.16	733.21	NM2USW	NM2 USTREAM WALL		
3620.57	-39.18	733.21	NM2USP	NM2 UPSTREAM PIPE		
3621.32	-39.20	733.22	NM2BPM1			
3622.82	-39.24	733.22	NM2BPM2			
3624.07	-39.28	733.22	NM2WC1			
3625.90	-39.33	733.22	NM2SEM			
3637.21	-39.68	733.24	NM2EU-1	B2	NM2EU	17.046
3658.20	-40.36	733.29	NM2EU-2	B2	NM2EU	17.046
3670.44	-40.78	733.33	NM2V-1	Vertical TRIM	NM2V	0.000
3677.69	-41.03	733.36	NM2Q1-1	4Q120	NM2Q1	4.879
3689.18	-41.43	733.40	NM2Q1-2	4Q120	NM2Q1	4.879
3700.68	-41.84	733.45	NM2Q1-3	4Q120	NM2Q1	4.879
3718.66	-42.47	733.52	NM2Q2-1	4Q120	NM2Q2	-5.005
3730.16	-42.87	733.57	NM2Q2-2	4Q120	NM2Q2	-5.005
3741.65	-43.27	733.61	NM2Q2-3	4Q120	NM2Q2	-5.005
3753.14	-43.68	733.66	NM2Q2-4	4Q120	NM2Q2	-5.005
3769.13	-44.24	733.71	NM2D1-1	B2	NM2D1	17.893
3790.12	-44.97	733.72	NM2D1-2	B2	NM2D1	17.893
3811.11	-45.71	733.67	NM2D2	B2	NM2D2	13.957
3823.35	-46.14	733.62	NM2V-2	Horizontal TRIM	NM2H	0.000
3825.60	-46.22	733.61	NM2WC2			
3836.09	-46.59	733.56	NM2WC3			
3838.09	-46.66	733.55	NM2TGT			
3838.09	-46.66	733.55	NMSEC			
4059.77	-54.43	733.51	NM2DSW			
4230.40	-60.41	733.47	NM3	3. 392.54782 'NM3' ;		

NAME	TYPE	FIRE DEPT	STATION	EASTING	NORTHING	HEIGHT	AZIMUTH	SLOPE	ROLL
1NM TRANSPORT	**1-APR-94**								
NMMUPT	DRIFT		39245.648	314.575	38207.941	8797.834	1 42 1	0 -8 17	0 0 -3
NM1BPM1	DRIFT		39257.648	314.931	38219.938	8797.806	1 42 1	0 -8 17	0 0 -3
NM1BPM1	DRIFT		39275.648	315.466	38237.930	8797.762	1 42 1	0 -8 17	0 0 -3
NM1BPM2	DRIFT		39275.648	315.466	38237.930	8797.762	1 42 1	0 -8 17	0 0 -3
NM1BPM2	DRIFT		39293.648	316.000	38255.922	8797.719	1 42 1	0 -8 17	0 0 -3
NM1WC	DRIFT		39293.648	316.000	38255.922	8797.719	1 42 1	0 -8 17	0 0 -3
NM1WC	DRIFT		39305.652	316.356	38267.914	8797.689	1 42 1	0 -8 17	0 0 -3
NM1V-1	5-1.5-120 11679		39305.652	316.356	38267.914	8797.689	1 42 1	0 -8 17	89 59 57
	SAGITTA CORRECT			316.356	38267.914	8797.686			
NM1V-1	5-1.5-120 11679		39425.648	319.917	38387.863	8797.503	1 42 1	0 -2 25	89 59 57
	SAGITTA CORRECT			319.917	38387.863	8797.499			
NM1V-2	5-1.5-120 11414		39437.648	320.273	38399.855	8797.495	1 42 1	0 -2 25	89 59 57
	SAGITTA CORRECT			320.273	38399.855	8797.491			
NM1V-2	5-1.5-120 11414		39557.648	323.833	38519.805	8797.513	1 42 1	0 3 27	89 59 57
	SAGITTA CORRECT			323.833	38519.805	8797.509			
NM1H	4-4-30 11489		39557.648	323.833	38519.805	8797.513	1 42 1	0 3 27	0 0 -3
	SAGITTA CORRECT			323.833	38519.805	8797.513			
NM1H	4-4-30 11489		39587.648	324.724	38549.789	8797.543	1 42 1	0 3 27	0 0 -3
	SAGITTA CORRECT			324.724	38549.789	8797.543			
NM2USW	DRIFT		44480.117	469.898	43440.102	8802.513	1 42 1	0 3 32	0 0 -3
NM2USP	DRIFT		44486.922	470.100	43446.898	8802.521	1 42 1	0 3 32	0 0 -3
NM2BPM1	DRIFT		44486.922	470.100	43446.898	8802.521	1 42 1	0 3 32	0 0 -3
NM2BPM1	DRIFT		44504.918	470.635	43464.895	8802.538	1 42 1	0 3 32	0 0 -3
NM2BPM2	DRIFT		44504.918	470.635	43464.895	8802.538	1 42 1	0 3 32	0 0 -3
NM2BPM2	DRIFT		44522.914	471.169	43482.887	8802.556	1 42 1	0 3 32	0 0 -3
NM2WC1	DRIFT		44522.914	471.169	43482.887	8802.556	1 42 1	0 3 32	0 0 -3
NM2WC1	DRIFT		44534.914	471.525	43494.883	8802.568	1 42 1	0 3 32	0 0 -3
NM2SEM	DRIFT		44534.914	471.525	43494.883	8802.568	1 42 1	0 3 32	0 0 -3
NM2SEM	DRIFT		44566.660	472.467	43526.609	8802.602	1 42 1	0 3 32	0 0 -3
NM2EU-1	BEND		44566.660	472.467	43526.609	8802.602	1 42 1	0 3 32	-30 24 3
	SAGITTA CORRECT			472.454	43526.609	8802.594			
NM2EU-1	BEND		44806.660	479.911	43766.492	8803.036	1 51 16	0 8 57	-30 24 2
	SAGITTA CORRECT			479.898	43766.492	8803.029			
NM2EU-2	BEND		44818.660	480.299	43778.492	8803.068	1 51 16	0 8 57	-30 24 2
	SAGITTA CORRECT			480.287	43778.492	8803.061			
NM2EU-2	BEND		45058.656	488.387	44018.352	8803.883	2 0 30	0 14 22	-30 24 0
	SAGITTA CORRECT			488.375	44018.352	8803.875			
NM2V-1	BEND		45070.656	488.808	44030.344	8803.933	2 0 30	0 14 22	89 59 60
	SAGITTA CORRECT			488.808	44030.344	8803.933			
NM2V-1	BEND		45100.656	489.859	44060.324	8804.058	2 0 30	0 14 22	89 59 60
	SAGITTA CORRECT			489.859	44060.324	8804.058			
NM2Q1-1	4Q120		45112.656	490.280	44072.316	8804.108	2 0 30	0 14 22	0 0 0
NM2Q1-1	4Q120		45232.656	494.485	44192.242	8804.609	2 0 30	0 14 22	0 0 0
NM2Q1-2	4Q120		45250.652	495.116	44210.230	8804.686	2 0 30	0 14 22	0 0 0
NM2Q1-2	4Q120		45370.652	499.321	44330.156	8805.187	2 0 30	0 14 23	0 0 0
NM2Q1-3	4Q120		45388.648	499.952	44348.145	8805.262	2 0 30	0 14 23	0 0 0
NM2Q1-3	4Q120		45508.648	504.157	44468.070	8805.764	2 0 30	0 14 23	0 0 0
NM2Q2-1	4Q120		45604.648	507.521	44564.012	8806.165	2 0 30	0 14 23	0 0 0
NM2Q2-1	4Q120		45724.648	511.727	44683.941	8806.667	2 0 30	0 14 23	0 0 0
NM2Q2-2	4Q120		45742.645	512.357	44701.930	8806.742	2 0 30	0 14 23	0 0 0
NM2Q2-2	4Q120		45862.645	516.563	44821.855	8807.244	2 0 30	0 14 23	0 0 0
NM2Q2-3	4Q120		45880.641	517.193	44839.844	8807.319	2 0 30	0 14 23	0 0 0
NM2Q2-3	4Q120		46000.641	521.399	44959.770	8807.821	2 0 30	0 14 23	0 0 0
NM2Q2-4	4Q120		46018.637	522.029	44977.758	8807.896	2 0 30	0 14 23	0 0 0
NM2Q2-4	4Q120		46138.637	526.235	45097.684	8808.399	2 0 30	0 14 23	0 0 0
NM2D1-1	BEND		46150.637	526.655	45109.676	8808.449	2 0 30	0 14 23	89 59 60
	SAGITTA CORRECT			526.655	45109.676	8808.464			
NM2D1-1	BEND		46390.637	535.066	45349.531	8809.061	2 0 30	0 3 9	89 59 60
	SAGITTA CORRECT			535.066	45349.531	8809.075			
NM2D1-2	BEND		46402.637	535.486	45361.520	8809.072	2 0 30	0 3 9	89 59 60
	SAGITTA CORRECT			535.486	45361.520	8809.087			
NM2D1-2	BEND		46642.633	543.897	45601.375	8808.900	2 0 30	0 -8 5	89 59 60
	SAGITTA CORRECT			543.897	45601.375	8808.915			
NM2D2	BEND		46654.637	544.318	45613.367	8808.872	2 0 30	0 -8 5	89 59 60

273

	SAGITTA CORRECT		544.318	45613.367	8808.884			
NM2D2	BEND	46894.633	552.728	45853.215	8808.001	2 0 30	0-16 51	89 59 60
	SAGITTA CORRECT		552.728	45853.215	8808.013			
NM2V-2	BEND	46906.633	553.149	45865.203	8807.941	2 0 30	0-16 51	0 0 0
	SAGITTA CORRECT		553.149	45865.203	8807.941			
NM2V-2	BEND	46936.633	554.200	45895.184	8807.795	2 0 30	0-16 51	0 0 0
	SAGITTA CORRECT		554.200	45895.184	8807.795			
NM2WC2	DRIFT	46948.633	554.620	45907.176	8807.735	2 0 30	0-16 51	0 0 0
NM2WC3	DRIFT	47074.633	559.036	46033.094	8807.118	2 0 30	0-16 51	0 0 0
NM2TGT	DRIFT	47098.633	559.877	46057.082	8807.001	2 0 30	0-16 51	0 0 0
NMSEC	DRIFT	47098.633	559.877	46057.082	8807.001	2 0 30	0 0 0	0 0 0
NM2DSW	DRIFT	49760.414	653.157	48717.223	8807.011	2 0 30	0 0 2	0 0 0
NM3	DRIFT	51809.211	724.956	50764.758	8807.037	2 0 30	0 0 4	0 0 0

Beam Sheet Program Version used in this job:

Machine: RDIV01   Version: RELEASE

Source File	Version
BSHEET	910820.143746
BSH	910820.143746
TRM	910820.143955
TRS	910524.113407
TRIN	910820.143901

APPENDIX 3

PRECLUDING DOWNSTREAM KTEV PRIMARY BEAM TRANSPORT

This appendix describes in more detail the methods used in setting the interlock presented in Section 3.1.1 to prevent the primary beam at 800 GeV from exiting the KTeV Target Pile. The precise values of the current interlocks depend on the final configuration of the Primary Beam line, but the methodology presented here is applicable in case this should change.

To prevent the beam from exiting the KTeV Target Pile, we specifically prevent an 800 GeV primary proton from entering the neutral beam aperture of NM2S2, the first major element downstream of the KTeV Target Pile. This will be done through current interlocks on NM2EU, NM2Q1, NM2Q2 and the AVB system, and careful alignment and configuration control including position "RED TAGS" on NM1U and NM2EU magnet strings.

The calculations for these interlocks were done to prevent a primary proton having the maximum possible deviation from the beam centerline from leaving NM2BD (the NM2 Beam Dump). The maximum allowed deviations from the primary beam centerline were determined by the positions and apertures of NM1U and NM2EU which act as fixed collimators to place a primary proton on the edge of the aperture of the Beam Dump. The horizontally sweeping NM2S1 magnet (the Target Sweeping Magnet) running at the nominal 5kG will not prevent beam from being horizontally steered into the neutral channel of the secondary beam, so the approach was to provide adequate protection by relying on the limits to vertical steering only. For a schematic of the apertures in NM1 and NM2 for the KTeV Primary Beam, see Figure A3.1 (This figure is present in Section 3.1.1 as Figure 3.1.1). The figure includes the extreme cases which defined the above interlocks. An elevation view of the KTeV Target Hall components is given in Figure A3.2. This Figure includes the minimum nominal primary beam centerline, and the most extreme trajectory allowed by the collimators that a beam particle can take in the NM2 Beam Dump aperture with the above proposed interlocks.

The angle from the target to the lower aperture edge on the upstream face of the NM2 Beam Dump is -2 mrad, but to accommodate major accidental deviations in

position and angle of incoming primary protons, we set the interlock on the AVB system to $I_{NM2D1} + 0.5*I_{NM2D2} \geq 4630$ amps, such that the primary beam is deflected by the AVB system to an angle of at least -4.0 mrad into the Beam Dump. This angle then defines the maximum excursion that a beam particle's position and angle is allowed to have before it enters the Beam Dump aperture. Any such change to place it greater than 0.512" above the primary beam centerline at the upstream face of the Beam Dump (20.3 feet from the target, 15 feet long) will place it into the aperture of the Beam Dump. Any trajectory change to put a +1.23" displacement to a particle at the downstream end of the Beam Dump would result in the proton exiting the dump through the aperture, entering the aperture of NM2S2, and possibly impacting in downstream enclosures. This trajectory will be precluded by the proposed interlocks.

The change in vertical beam position and angle at the downstream end of the Beam Dump is influenced by quadrupole steering in NM2. The position change from the nominal trajectory can be written as a transformation of the position and angle of the beam particle from NM2EU to the downstream end of the dump:

$$y_{Dump} = R_{33}y_{NM2} + R_{34}\dot{y}_{NM2}$$

Since the angle that a beam particle can take to get into the aperture of the Beam Dump ($\dot{y}_{Dump}$) can be limited by the aperture of NM2S1 (y_{NM2S1}), we can see if we need to limit the angle of the proton at NM2EU. We can then write:

$$\dot{y}_{NM2} = \frac{\dot{y}_{Dump} - R_{43}y_{NM2}}{R_{44}}$$

where:

$$\dot{y}_{Dump} = \frac{y_{NM2S1} - y_{Dump}}{36.45'}$$

with 36.45' the distance between the upstream end of NM2S1 and the Beam Dump.

We will use the NM2EU B2 dipole string as a collimator to limit y_{NM2} to be less than ±1.5" from the nominal trajectory. As can be seen in Figure 2.4.4, the beam at this point is expected to be about 0.6 cm at 1 sigma (0.557" full width at half maximum), giving ample of room for normal primary beam transport through the magnets. Within the upstream aperture limits of the Target Sweeping Magnet, y_{NM2S1} can be varied for given values of R_{43} and R_{44} until we find the largest value of y_{Dump}, as done in Figure

A3..3. The corresponding maximum $\dot{y}_{Dump}$ change is shown in Figure A3.4. This is the worst possible beam trajectory for this case of only controlling the configuration of NM2EU, NM2S1, and NM2BD. The values of R_{33} and R_{34} are found by varying the horizontal and vertical focal length of the NM2Q1-NM2Q2 quadrupole pair. We can change the currents of both magnets such that we vary the focal length of one plane and hold the focal length in the other plane constant, effectively decoupling the horizontal and vertical planes.

Looking at Figure A3.3, we can see that the maximum possible position change is not within the 1.23" distance to the lower edge of the aperture if the angles are limited only by the apertures of NM2EU and the Target Sweeping Magnet. Also, since the Primary Collimator is moveable in the vertical plane, it cannot be used as a trajectory-limiting aperture for safety purposes. NM2S3 would be the next downstream device that could be used to limit the primary beam trajectory. The trajectory of the beam passing through its aperture from the upstream end of the Target Pile will need to have a position change of more than +1.96" at the downstream of the NM2 Beam Dump, and an angle change more than +2.42 mrad, to allow it into NM3. As can be seen in Figures A3.2 and A3.3, the ranges for this case would allow this to happen. This possibility will be prevented by including current interlocks and the position "RED TAGS" on NM2 elements.

We also need to limit the angle of the beam entering the NM2 quadrupoles such that we can prevent beam from entering the aperture of NM2S2. The angle of the proton downstream of NM2EU will change due to current changes in the magnet current in NM2 and position changes at NM1 relative to position changes in NM2. We can write:

$$\dot{y}_{NM2} = \dot{y}_{NM2Mag} + (y_{NM1} - y_{NM2})/L$$

where L is the distance between the limiting aperture in NM1 and the limiting aperture in NM2.

We can change the angle due to magnet current changes in NM2 ($\dot{y}_{NM2Mag}$) through NM2V and NM2EU. Due to tuning requirements in the beam line, we need to have as much freedom as possible in changing the current in NM2V, a 4-4-30 trim with a maximum angle change ±0.14 mrad. If we interlock the NM2EU current such that it

can vary ±68 amps from the nominal value, the most that $\dot{y}_{NM2Mag}$ can change due to the change of NM2EU current is ±0.060 mrad. Therefore, the most that $\dot{y}_{NM2Mag}$ can change due to magnet current changes in NM2 is ±0.20 mrad.

We can also use the NM1U dipole string as a ±1.5″ collimator to limit the vertical position changes in NM1 (y_{NM1}) to be less than ±2″ (±1.5″ vertical aperture with a ±0.5″ alignment tolerance included), defining L=440' (13.4 cm/mrad). The magnets' tolerances of ±0.5″ in the vertical position relative to NM2EU provides an included safety margin of 0.10″ in the beam deviation from the nominal path at the downstream end of the Beam Dump. The use of NM1U and NM2EU as limiting apertures will require that the positions of these magnets must be "RED TAGGED", movable only though explicit instruction of the Radiation Safety Officer and Beam Line Physicist.

Then, for given values of R_{33} and R_{34}, we can vary y_{NM2}, y_{NM1}, and $\dot{y}_{NM2Mag}$ within the allowable limits until we find the largest value of y_{Dump}. This is the worst possible beam trajectory for this case with the proposed interlocks listed at the beginning of this section. Again, the values of R_{33} and R_{34} are found by varying the horizontal and vertical focal length of the NM2Q1-NM2Q2 quadrupole pair.

We can set the current limits on NM2Q1 and NM2Q2 by looking at the maximum position displacement for a primary proton at the end of the NM2 Beam Dump as a function of the inverse of the quadrupole pair's focal length (R_{43} transfer matrix element) in the vertical plane, taking into account displacement due to the bending magnets mentioned above. Using the distance to the aperture (1.23″) as the limit that we will allow the particle to travel, we set the quadrupoles' current limits as a linear combination of the two quadrupole string currents. Appropriate limits are set as shown on Figure A3.5, a plot of NM2Q2 field current vs. NM2Q1 field current for different vertical and horizontal inverse focal lengths.

The limits shown in Figure A3.5 are $0.217*I_{NM2Q1} + I_{NM2Q2} = -2.95 \pm 0.45$ kG/in @ 800 GeV (-567 ± 86 amps), where the -2.50 kG/in @ 800 GeV value is the upper limit on the R_{21} and R_{43} matrix element, and the -3.40 kG/in @ 800 GeV value is the lower limit. Placing a limit on the NM2Q1 power supply will prevent the proton from being directed into the aperture through quadrupole steering at high currents. The vertical dashed line shown in Figure A3.5 limiting I_{NM2Q1} is at 5.0 kG/in @ 800 GeV, or 1011 amps. Figure A3.6 shows these limits on a plot of maximum beam position change at

the downstream end of the Beam Dump vs. the inverse vertical focal length (R_{43}) at different horizontal focal lengths (R_{21}). The expected operating settings are at R_{21} = -0.217 mrad/cm and R_{43} = -0.557 mrad/cm, well within the allowed range shown on this graph.

The extreme position changes allowed with these interlocks are shown on Figures A3.1 and A3.2. Extrapolating the rays to the downstream end of NM2S3, we find that the maximum deviation allowed is 1.273" below the neutral beam centerline at that point. Since the magnet's vertical aperture is ±0.787", this puts the maximum position change 0.486" below the lower limiting aperture. This gives a 0.486" safety margin at the end of NM2S3 to prevent primary protons from impacting in NM3 and the KTeV Experimental Hall.

Beam pulses in which the beam activates the critical devices for that part of the beam line due to intensity or magnet interlock trips during a beam spill may occur as accident pulses. In the case of KTeV, the primary critical device protecting the beam line is MuLam, and the secondary device are the MuBends. We can safely say that the beam is lost in NM1U once the MuLam is below 4% of its set-to value, or 7.14 milliseconds using a time constant for MuLam of 0.175 seconds. MuLam splits the beam horizontally, so its tripping off has no bearing on the interlock system outlined above. However, if the trip is due to a magnet interlock outlined above, the time it takes to lose the beam upstream of NM2 does have a bearing on the safety of the system.

If NM2EU trips off, the beam will take a lower and more westward trajectory than nominal, putting the Primary beam lower at the Beam Dump. If NM2Q1 or NM2Q2 trip off, the magnet will be at 99.7% of the value it was running at before the trip when the beam is lost due to MuLam, using a time constant for the 4Q120s of 2.04 seconds. As can be seen in Figure A3.2, the primary beam may enter the aperture of NM2S2, but it will not exit the aperture of NM2S3 in this accident case.

If one of the magnet strings in the AVB system trip off, the beam will take a more upward trajectory while the magnet field is decaying. With the B2 magnets having a time constant of 0.75 seconds, in the 0.00714 seconds it will take for the beam to be lost upstream, the AVB system will bend 0.95% less than before the trip, which corresponds to a maximum upwardly angle change in the beam of 75 μrads. At the downstream end

of NM2S3, this is 0.134". Since the safety margin at this point for the shallowest allowed beam is 0.486", the beam will not enter the neutral beam line aperture.

Primary beam must not be transported through the neutral beam channel into the KTeV experimental hall since it is designed only to accept secondary beam of much lower energy and intensity. In addition beam line elements downstream of the targeting station within NM2 are not set to transport 800 GeV particles. Because of this, the introduction of primary beam into the neutral beam channel could result in higher than normal losses downstream of the targeting station. This could cause significant residual radiation dose rates, contamination, and increased air activation. Routine maintenance and unscheduled repairs would be more difficult. The goal to insure that the 800 GeV primary beam is confined to the well-shielded target station has been achieved in selecting the interlocks described in Section 3.1.1.

KTeV Primary Beamline Apertures - NM1 through NM2
Elevation view

NM1U NM1H

NM1U configuration controlled

Berm (not to scale)

Allowed Uncertainty for ±0.5" Between Enclosure Survey

410' long Beam Pipe

NM2EU NM2V NM2Q1

Case 1

Case 2

NM2EU interlocked to ±68 amps from nominal and configuration controlled

NM2Q2

Nominal Primary Beam Centerline

NM2 Quadrupoles interlocked to:
$0.217 \cdot I_{NM2Q1} + I_{NM2Q2} = -567 \pm 86$ amps
$I_{NM2Q1} \leq 1011$ amps

AVB Dipoles

TARGET

NM2H

1" 10'

AVB Dipoles interlocked to
$I_{NM2D1} + 0.5 \cdot I_{NM2D2} \leq 4630$ amps

NM2S1

NM2BD NM2S2

PRIMARY COLLIMATOR

NM2S3

Neutral Centerline

Figure A3.1: KTeV Primary Apertures. Shown here are the vertical apertures for the magnets from NM1 to the KTeV Target Hall, with the Nominal Primary Beam Centerline shown for the path of primary beam with the AVB system set to bend the beam to -4.00 mrads at the Target. The two extremes shown as thick solid lines are for beam entering NM2 at ±0.6629 mrads relative to the nominal beam trajectory, the beam paths from the lower aperture limit of either NM1U or NM2EU to the upper aperture limit of the other. The thick dashed lines are for beam entering at ±0.0947 mrad relative to the nominal beam trajectory, the beam path due to the allowed survey tolerance between enclosures, staying on the same side of the nominal beam along the edge of the NM1U and NM2EU apertures. The solid beam paths cross each other in the beam pipe region between NM1 and NM2. The magnets are set to produce the maximum allowed deviation from the nominal with these extremes at the downstream end of the Beam Dump.

Case 1 is for the NM2 quadrupoles set to R_{21}=-0.500 mrad/cm and R_{43}=-0.430 mrad/cm.

Case 2 is for the NM2 quadrupoles set to R_{21}=-0.500 mrad/cm and R_{43}=-0.687 mrad/cm.

For both cases, the AVB system is set to its minimum limit, and NM2EU & NM2V to their maximum upward bending limits. The range for allowable quadrupole current settings lie between these extremes. Note that the AVB and NM2S1 magnets are not configuration controlled in this scheme. An elevation view of the KTeV Target Hall components is given in Figure A3.2.

KTeV Target Hall Beam Dump System Apertures
Elevation view
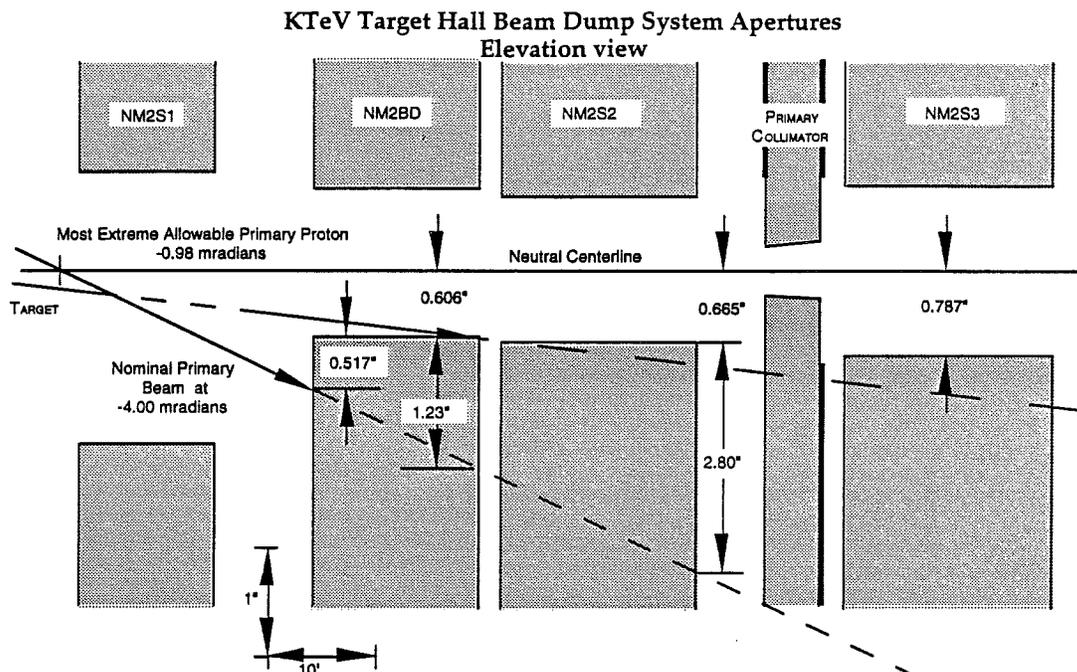
Figure A3.2: KTeV Target Hall Beam Dump System Apertures in the Elevation View. The KTeV Target Pile contains the NM2 Target, NM2S1, and NM2BD, with the upstream edge defined by the Target, and the downstream edge defined by the Beam Dump. This Figure also shows the minimum nominal primary beam path and the most extreme primary beam trajectory allowed by the interlocks described in the text.

Maximum Beam Position Change at Downstream of NM2BD
for Any Beam Particle Trajectory vs R43
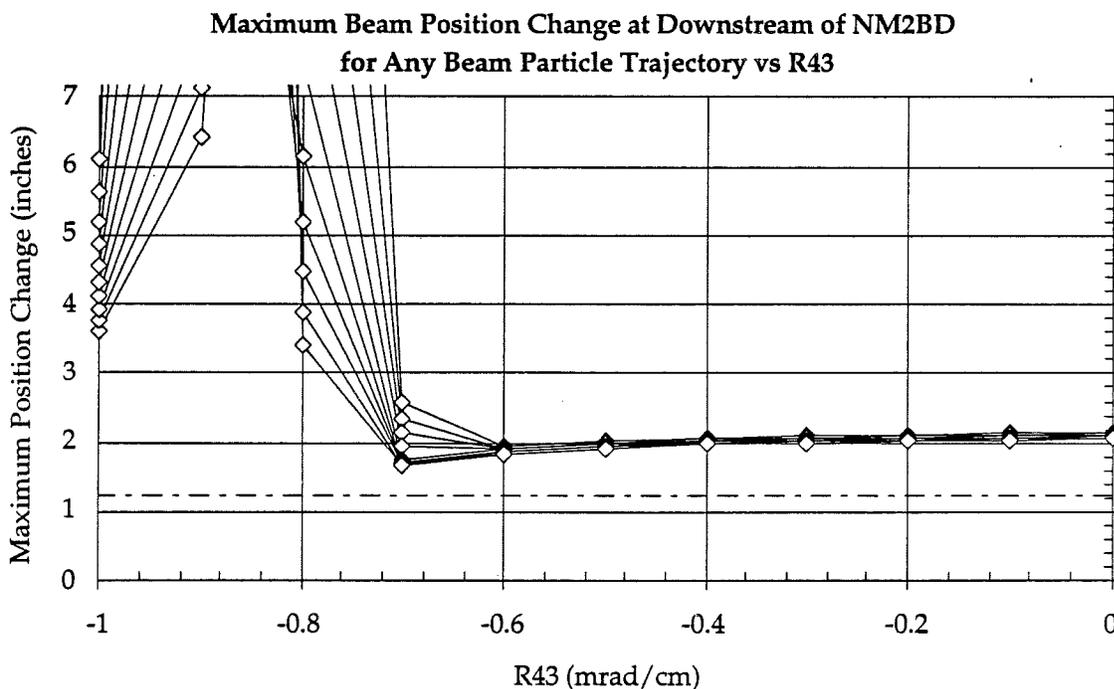
Figure A3.3: Maximum Beam Position Change at Downstream of NM2BD for Any Primary Beam Particle Trajectory vs. R_{43}. The dashed line signifies the farthest upward position change that a primary proton can have and still impact on the Beam Dump. The multiple lines show the result for various R_{21}, ranging from -0.050 mrad/cm along the upper track, and -0.50 mrad/cm along the lower track. The positions are limited only by the aperture restrictions on NM2EU, NM2S1, and NM2BD (see text).

Maximum Angle Change at Downstream of NM2BD
for Any Particle Trajectory vs R43
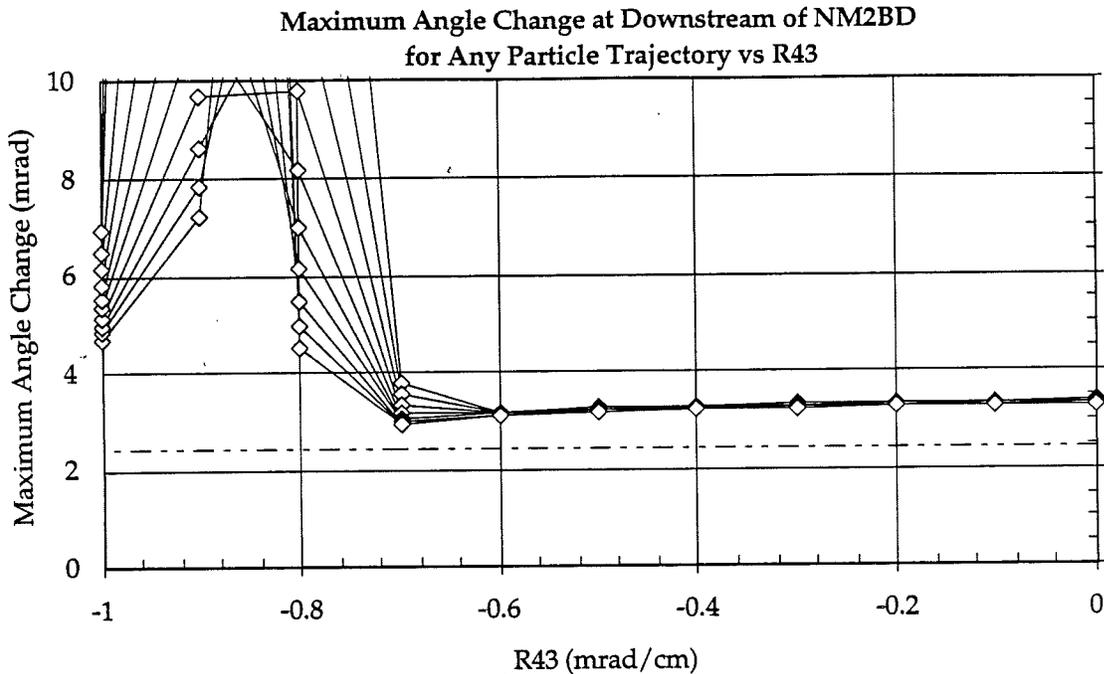
Figure A3.4: Maximum Beam Angle Change at Downstream of NM2BD for Any Primary Beam Particle Trajectory vs. R_{43}. The multiple lines show the result for various R_{21}, ranging from -0.050 mrad/cm along the upper track, and -0.50 mrad/cm along the lower track. The dashed line indicates the limit of a maximum 2.42 mrad angle change. The angles are limited only by the aperture restrictions on NM2EU, NM2S1, and NM2BD (see text).

## NM2Q2 Field vs. NM2Q1 Field (with Limits)
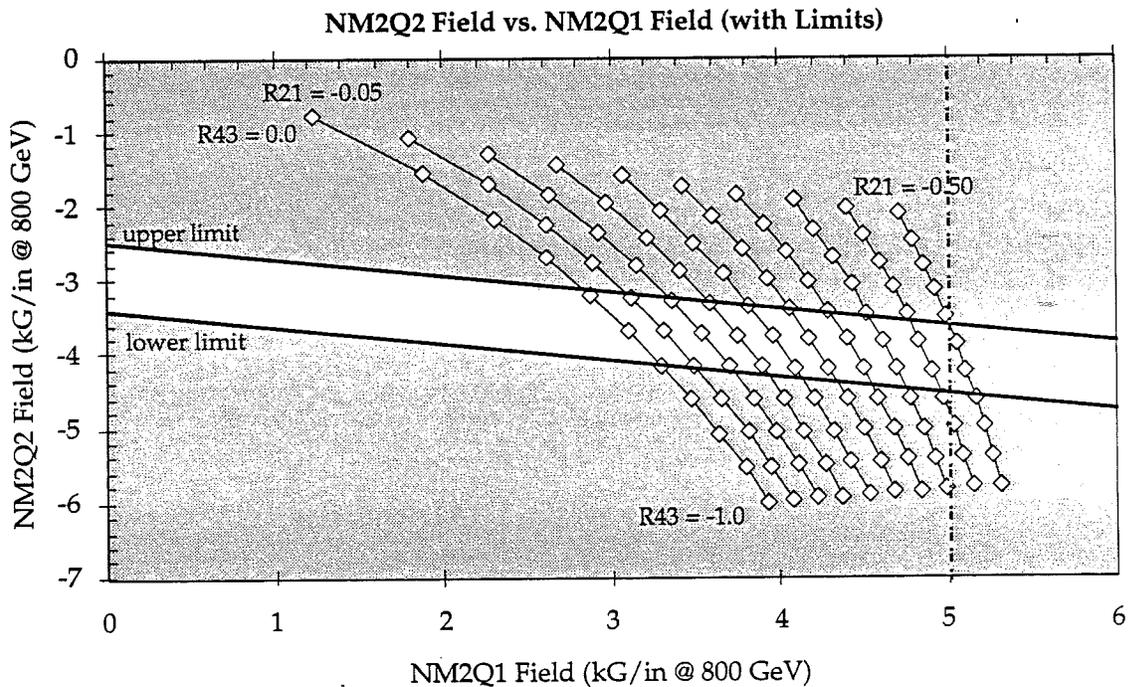
Figure A3.5: NM2Q2 Field vs. NM2Q1 Field (with Limits). Diagonal lines show limits at $0.217 * I_{NM2Q1} + I_{NM2Q2} = -2.95 \pm 0.45$ kG/in @ 800 GeV (-567 ± 86 amps). The dashed line is the current limit on NM2Q1 at 5.0 kG/in @ 800 GeV (1011 amps). The R_{21} and R_{43} values shown are in mrad/cm.

Maximum Beam Position Change at Downstream NM2BD vs R43
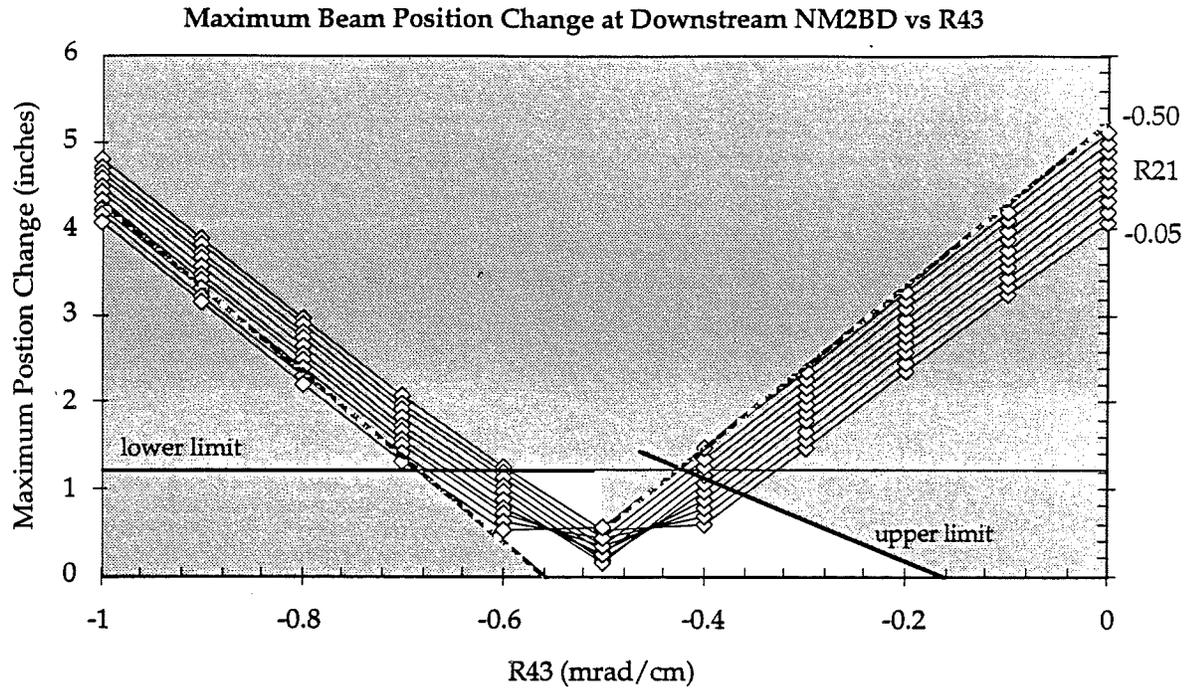
Figure A3.6: Maximum Beam Position Change at Downstream of NM2 Beam Dump vs. R_{43}. The 1.23" line signifies the farthest upward position change that a primary proton beam can travel and still impact on the Beam Dump. The upper and lower limits correspond to the limits on Figure A3.5, and the dashed line corresponds to the dashed line on Figure A3.5, showing the current limit on NM2Q1. The R_{21} values shown are in mrad/cm.